Appendix 1

Water Quality

Kodiak Airport EIS
Water Resources Technical Memorandum

Prepared for

The Federal Aviation Administration

Prepared by

VIGIL AGRIMIS
design professionals

819 SE Morrison Street, Suite 310
Portland, OR 97214

June 2008

Table of Contents

List of Tables

List of Photos

Appendices

1.0 Introduction

This Water Resources Technical Memorandum was completed by Vigil-Agrimis Inc. (VAI) to support the development of an Environmental Impact Statement (EIS) for proposed federal actions at Kodiak Airport. The purpose of the proposed federal actions at the Airport is to bring the runways into compliance with Federal Aviation Administration (FAA) Runway Safety Area (RSA) standards to the greatest extent practicable. The FAA requires that an airport such as Kodiak Airport have RSA, which serve as buffers if aircraft deviate from the runway during an accident or emergency. The required size standards of these RSA are based on the types of aircraft served at each runway. The existing runway safety areas at the Airport do not meet the current national standards for the types of aircraft being served. The EIS will evaluate the environmental consequences of enhancing runway safety areas at the Airport.

The runway system at Kodiak Airport consists of three runways: 07/25, 11/29 and 18/36. Runway 11/29 meets current FAA design standards, but Runways 7/25 and 18/36 falls short of the required safety area in both width and length. The FAA airport design standards for Runways 07/25 and 18/36 at Kodiak define the RSA as a rectangular area centered about the runway that is 500 feet wide along the length of the runway and extends 1,000 feet beyond each runway end.

1.1 Issues

In order to bring the existing runways into compliance with FAA standards, RSA would need to be added beyond the threshold of each deficient runway. Due to the topographic constraint of nearby Barometer Mountain, the addition on Runway 07/25 could only be met by extending the RSA into St. Paul Harbor. RSA deficiencies on Runway 18/36 would have to be met by extending the RSA either into St. Paul Harbor or into the mouth of the Buskin River. These marine and river resources support commercial, recreation and subsistence fisheries that are critically important to the Kodiak Island economy. These areas also provide important habitat for other aquatic organisms and wildlife. At the same time, the critical need to maintain operational criteria governing aircraft approach and departure procedures may limit alternatives that could otherwise minimize impacts to these sensitive areas.

1.2 Scope of Studies

The Kodiak Airport is located in a dynamic water resources setting where post glacial landforms, abundant precipitation and wide tidal fluctuations create and sustain a varied environment. This memorandum describes existing conditions for a number of water resources in the Kodiak Airport vicinity of interest to the EIS. The conditions described include:

- Stream hydrology,
- Stream geomorphology,
- Floodplains, and
- Fresh water quality.

The information in this document is based on review of existing data and reports as well as field investigations conducted in September 2007. Discussion of the methods, scope of study and findings for each of these resources follow.

2.0 Kodiak Island Geology and Climate

Kodiak Island is the second largest in the United Sates and is located approximately 250-miles south of Anchorage in the Gulf of Alaska, southwest of the Kenai Peninsula.

The Kodiak Island complex is a geologic extension of the Chugach Mountains, which are principally folded and faulted sedimentary rock. The island was connected to the mainland by a solid ice sheet during past glaciations. The varied contemporary topography on the island includes glaciated peaks, numerous fjords, and gradually sloping wide valleys. The island is still recovering from past glaciations and Sitka spruce are colonizing areas formerly dominated by permafrost (Nowacki et al, 2000).

Kodiak Island has a maritime climate (Hartman and Johnson, 1984). Weather is typically cloudy and cool with small temperature variations; strong winds; heavy precipitation; and high humidity, fog, and cloud cover. Many microclimates exist on the island due to the mountainous terrain.

3.0 Kodiak Airport Setting and Watershed Context

Kodiak Airport is located approximately five miles southwest of the City of Kodiak on the eastern side of Kodiak Island. The Airport is situated at the east end of the Buskin River watershed, where Louise Creek and Devil's Creek join the Buskin River. The Buskin River discharges into St. Paul Harbor, which is part of Chiniak Bay, at the northeast corner of the Airport adjacent to the Runway end 36 RSA. The lower reaches of the Buskin River are tidally influenced. **Figure 1** shows the location of the Airport. All figures are located in **Appendix A**.

Average annual precipitation at Kodiak Airport is 75.4 inches, with January being the wettest month and July being the driest (NOAA, 2006). Temperatures are typically between 20°F and 40°F from November to March, and between 30°F and 60°F from April to October (NOAA, 2006). The average annual temperature is 40.5°F at the Airport. Between 1973 and 2004 the highest recorded temperature at the Airport was 82°F, and the lowest recorded temperature was -16°F (ACRC, 2008). Snow is heavy and wet and averages 72 inches per year (ACRC, 2008). Peak flows in streams on Kodiak Island usually occur in early to mid summer when high temperatures cause increased snow melt and are coupled with heavy rain events.

Most of the surface water passing the Airport originates in the approximately 26-mi^2 Buskin River watershed (**Figure 2**). The Buskin River watershed ranges in elevation from sea level at St. Paul Harbor to nearly 2, 250 feet at Barometer Mountain. Buskin Lake is approximately four miles upstream from tide water. The entire watershed was previously glaciated and ranges from sections of steep, unvegetated bedrock to a wide, gently sloping valley. Sub-watersheds contributing flow to the river in the immediate vicinity of the Airport include Devil's Creek, and Louise Creek.

Devil's Creek enters the Buskin from the south (**Figure 2**). Barometer Mountain, west of the Airport, is on the boundary between the Buskin River and Devil's Creek Watersheds (~4 mi^2). Devil's Creek passes through the Airport and beneath Runway 07/25 before joining the Buskin River. The Devil's Creek watershed ranges in elevation from 26 feet to nearly 2,250 feet at Barometer Mountain.

The Louise Creek watershed (~2 -mi^2) drains to the Buskin River from the north, and is another notable tributary in the vicinity of the Airport. This stream has several lakes in its basin and approximately half the topographic relief of Devil's Creek. These characteristics suggest that its flow pattern is likely to be more steady than Devil's Creek, perhaps most important by contributing to base flows and not as critical to peak flows in the Buskin River.

Drury Gulch is another small watershed that drains to the United States Coast Guard (USCG) station where it terminates at a catch basin and is piped through the Airport stormwater system to St. Paul Harbor (**Figure 2**). This watershed (~0.15-mi^2) is a highly altered, intermittent stormwater-fed drainage. The watershed ranges in elevation from 45 feet to 900 feet at Old Women's Mountain.

The upper parts of the Buskin River and Devil's Creek watersheds are largely undeveloped. These areas are mainly covered with grasses and tundra vegetation at the higher elevations, with lower elevations dominated by a high-brush cover consisting of coastal alder thickets, willow, blueberry, raspberry, lingonberry, devil's club, grasses, ferns, lichens and mosses (Hogan & Nakanishi, 1995). Large Sitka spruce and cottonwood are found along the lower valley bottom.

The lower parts of the Buskin River and Devil's Creek watersheds and the Drury Gulch watershed are highly developed. These areas include the Airport runways, terminal and support buildings as well as the USCG Station. From the early 1940's to early 1970's most of the Buskin River and Drury Gulch watersheds were used for military purposes. Due to the land use practices of the time, several sites within these watersheds have been identified as having a potential risk to human health and the environment because of residual contamination.

Tides are an important influence at the lower end of the Buskin River watershed. The lower portion of the Buskin River in the vicinity of the Airport is tidally influenced. Tide elevations range from 9.53 feet at the mean higher high tide to 0.76 feet at the mean lower low tide. **Table 1** shows a diurnal tidal range of 8.77 feet.

Table 1. Tide Data for Kodiak Island, Women's Bay, Station 9457292, Epoch 1983-2001

Tide	Elevation (feet, NAVD88)
Extreme High Water (EHW) (December 31, 1986)	14.06
High Tide Line (HTL)	11.00
Mean Higher High Water (MHHW)	**9.53**
Mean High Water (MHW)	8.63
Mean Tide Level (MTL)	5.25
Mean Sea Level (MSL)	5.25
Mean Low Water (MLW)	1.87
Mean Lower Low Water (MLLW)	**0.76**
Extreme Low Water (ELW) (January 12, 2005)	-2.43

Source: DOWL, 2008 and Appendix B.

The most extensive wetland resources in the immediate vicinity of the Airport are those in the estuary of the Buskin River, just north of the Airport. These include both high marsh and low marsh communities as well as areas of unvegetated tidal flats. A handful of small wetlands exist on the Airport property in shallow topographic depressions and along drainage ways. The shoreline along St. Paul Harbor is also a regulated resource. **Appendix B**, *Kodiak Airport EIS*

Wetland Delineation Report, provides more information on area wetlands and non-wetland waters.

The following sections describe hydrology, fluvial geomorphology, tidal influence, and fresh water quality in the Kodiak Airport vicinity.

4.0 Hydrology and Fluvial Geomorphology

Hydrology describes the amount and spatial distribution of precipitation in a watershed and its pattern and rate of discharge into streams and Rivers. Hydrology is a key variable in defining the spatial extent of a river floodplain. The Buskin River flows next to the Airport so the hydrology assessment focused on the Buskin River watershed and select sub-watersheds, Devil's Creek and Louise Creek. Drury Gulch, a mapped solid waste management unit, is a small watershed that drains to the Airport. Hydrology was reviewed for this stream to better understand the likelihood that contaminants could enter surface water or groundwater in this location.

Fluvial geomorphology describes the process of stream or river channel evolution as well as the physical characteristics of channel form. Fluvial geomorphic processes are described based on inputs of discharge and the size and spatial distribution of sediment, and channel habitat feature forming large wood. Channel form is described based on measures of channel planform and slope as well as measures of geomorphic features such as pools and riffles, and channel cross section characteristics. RSA improvements are most likely to affect the Buskin River. Devil's Creek is less likely to be affected but may serve as a mitigation site should impacts to the Buskin River be unavoidable. Fluvial geomorphology assessment therefore focused on these streams.

The objectives of the hydrology and fluvial geomorphology assessment are to:

1. Develop a planning-level understanding of watershed hydrology for the Buskin River (including the Devil's Creek and Louise Creek sub-watersheds), and for Drury Gulch;
2. Develop an understanding of the fluvial geomorphologic processes governing the Buskin River, and Devil's Creek; and
3. Describe the channel characteristics and geomorphic features of the Buskin River and Devil's Creek.

4.1 Hydrology Methods

VAI reviewed existing data and documentation describing stream discharge in Kodiak Island watersheds to meet the hydrology objectives. Sources included:

- *Overview of Surface-Water Resources at the US Coast Guard Support Center Kodiak, Alaska*, 1987-89, USGS 1996;
- *Estimating the Magnitude and Frequency of Peak Streamflows for Ungaged Sites on Streams in Alaska and Conterminous Basins in Canada*, Water-Resources Investigations Report 03-4188, USGS, 2003;
- *Water Resources of the Kodiak-Shelikof Subregion, South-Central Alaska*; Surface Water Map, W78268, 1978; and
- *Precipitation Map of Alaska*, Alaska Geospatial Data Clearinghouse; 1997

None of the waters of interest in the study area have flow gages on them, so hydrologic analyses were conducted by using regional regression equations developed by Curran et al. (2003). These equations were used to calculate runoff for select recurrence interval flows for study area watersheds. Regional regression equations are based on gaged streams across southern coastal Alaska and have an average 40-percent standard error of prediction. Where possible these estimated discharges were compared to recorded discharges on gaged streams in similar Kodiak Island watersheds. Selected watersheds shared characteristics such as size, location, and landscape features.

4.2 Fluvial Geomorphology Methods

VAI conducted a field assessment from September 10 to14, 2007 to meet the fluvial geomorphology objectives. This investigation included:

- Observing the geomorphic features of the Buskin River, and Devil's Creek;
- Measuring seven cross sections and the longitudinal profile along Devil's Creek;
- Measuring 20 cross sections along the Buskin River;
- Measuring bridge structures and culverts on the Buskin River and Devil's Creek; and
- Sampling bulk sediment at five locations on the Buskin River.

Several other assessments were conducted in the office. These included:

- Combining the Buskin River cross section measurements with survey data collected by DOWL to establish a longitudinal profile,
- Reviewing historic and current air photos to measure channel sinuosity and planform change for the Buskin River and Devil's Creek, and
- Dividing the Buskin River into geomorphic reaches based on profile, sinuosity, entrenchment, bed material and field observations.

The Buskin River, Devil's Creek, and Drury Gulch are alluvial systems with varied flows and sediment transport patterns. These processes have formed the channel configurations, dimensions, and profiles that are visible today. Mathematical models for predicting potential channel changes do not exist, so an analysis of pattern, dimension, and profile with attention to bed and bank conditions is used as a surrogate to describe the potential for change in these systems. The findings from these evaluations are described below by stream.

4.3 Buskin River Hydrology and Fluvial Geomorphology

4.3.1 Hydrology

The Buskin River is fed by several unnamed tributaries along Barometer, Erskine, and Pyramid Mountains. A key feature of this approximately 26 mi^2 watershed is Buskin Lake. Buskin Lake is a feature that formed during glacial retreat in the region. Buskin Lake is located at the center of the Buskin River Valley. The Buskin River flows about four miles southeast across the valley from the lake to an estuary at its outlet into Chiniak Bay at St. Paul Harbor. Stream systems with storage features, such as extensive wetlands, or a lake in the case of the Buskin River, tend to not have as wide a range of flows between peak events and low flow events.

Peak events are important to understand when developing public infrastructure to avoid or reduce impacts to floodplain function and the damage that can occur to natural resources or human facilities during flood events. The magnitude of flood events is typically described by the event recurrence interval. A recurrence interval is the time between events equal or greater than a given magnitude as determined statistically. The recurrence interval familiar to most people is the 100-year flood, a flood that will statistically occur once in 100 years or has a one percent chance of occurring in any given year.

Regression equations for predicting peak discharge were used to determine flows for Buskin River in this study (**Table 2**). Regression equations typically use three to five parameters such as basin size, mean elevation, and rainfall to predict flows for ungaged streams based on flow information from nearby gaged streams. The regression equations used for these determinations were developed by the U.S. Geological Survey (Curran et al., 2003).

The reviewers completed a reasonableness review of the peak flow estimates developed from the USGS regression equations. They compared their results with independent estimates made by the USGS, measured flow rates from similar basins, and unit discharge analysis. These comparisons confirmed that the USGS regression equations provide reasonable estimates of peak flow rates from this planning-level EIS analysis.

Table 2. Buskin River Discharges Predicted Using Regression Equation

Stream	Contributing Drainage (mi^2)	Discharge (cfs)			
Recurrence Interval		**Q2**	**Q10**	**Q50**	**Q100**
Buskin River	25.7	1,700	2,870	3,990	4,480

4.3.2 Fluvial Geomorphology

Fluvial geomorphic assessment of the Buskin River focused on the section of stream between the Devil's Creek confluence and St. Paul Harbor. The development of military and airport facilities during the early 1940s confined this section of the Buskin River to the north side of the valley. Extensive filling and grading occurred along the lower river to create a level air field. The valley was filled and graded from the south side of the river to Upper Government Hill (just southwest of the taxiway along runways 11/29 and 18/36) and out to the St. Paul Harbor shoreline. In certain locations as much as 20 feet of fill was added over the natural alluvial plain (SAIC, 1995).

Within the assessment area, three manmade structures affect channel hydraulics and mobility: a bridge, a relic bridge embankment, and a seasonal fish weir.

The bridge (Bridge No. 2) was installed prior to 1951 and spans the Buskin River just northeast of Runway end 11 (**Figure 3**). It is a wood and steel span with 36 steel I-beam piles arraigned in rows of four (**Photo 1**). The bridge deck is in bad repair and it is closed to use. The bridge deck is approximately 18.5-feet above the deepest part of the channel (the thalweg) and provides good clearance for flood flows.

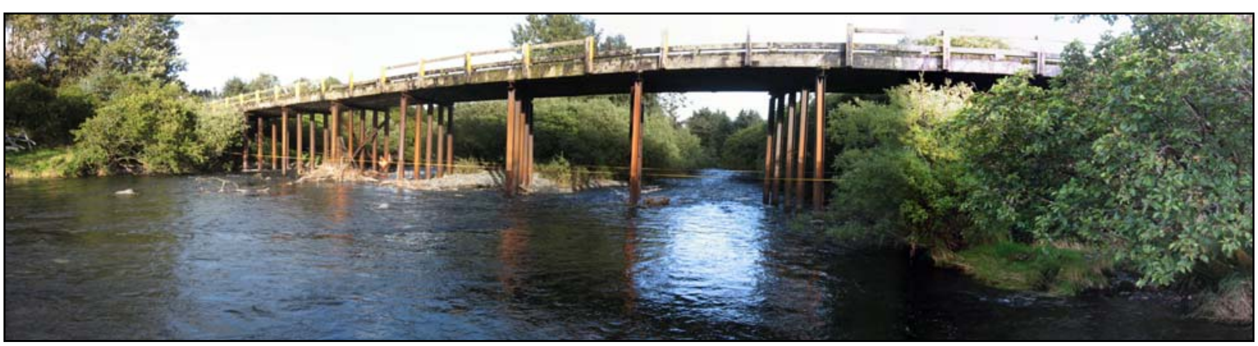

Photo 1: Bridge No. 2, Looking Downstream.

An embankment running south from the Buskin River State Recreation Area access road to the Buskin River (**Photo 2**) is all that remains of another bridge that once spanned the River (**Photo 5**). The embankment, in combination with a rocky bluff, controls the alignment of the River before it enters the estuary. The channel width remains about the same downstream of the embankment but the amount of land inundated at high tide and flood flows increases substantially on the ocean side of the embankment. This transition illustrates a lack of natural or man-made channel confinements downstream of the embankment as well as a change in hydraulics from a river to a tidal system.

Photo 2: Bridge Embankment Upstream of the Buskin River Estuary.

The seasonal fish weir, run by the Alaska Department of Fish and Game, is in place from mid May to early October. It spans the river just upstream of the existing bridge (**Photo 3**). The structure slows the flow of water through the reach but does not appear to have a significant affect on channel processes or mobility since this reach has been relatively stable over time.

Photo 3: Seasonal Fish Weir Just Upstream of Bridge No. 2.

4.3.3 Channel Sinuosity

Sinuosity is a measure of the degree of meander and is expressed as the ratio of channel length to valley length. Low sinuosity is in the range of 1.0 to 1.2, moderate sinuosity is in the range of 1.2 to 1.5, and high sinuosity is in the range of 1.5 to 4.0 (Rosgen, 1996). Based on the most recently available aerial photography, from 2004, the sinuosity of the Buskin River downstream of the Chiniak Highway is low – approximately 1.2. **Figure 3** illustrates the 2004 alignment used to assess sinuosity. Similar reaches in unaltered river systems typically have a moderate to high sinuosity such as the reach between Buskin Lake and the Highway. The confinement of the Buskin River by the Airport has shortened and simplified the channel planform reducing the sinuosity ratio to 1.2. The loss of channel sinuosity/length means that less channel friction is provided to dissipate energy during peak flows resulting in fewer and lower-quality habitat features.

4.3.4 Channel Planform Change

Lateral channel migration in the vicinity of the Airport was analyzed using aerial photos from 1951, 1967, 1990 and 2004. **Figure 3** depicts the approximate centerlines of these historical channel alignments. The upper reach of the Buskin River appears to be relatively stable with minor channel adjustments occurring upstream of the embankment where the river has several channels. However, within the estuary reach, the areas of estuary and channel outlet locations have drastically changed. The estuary is not visible in the 1951 aerial photograph (**Photo 4**). The month, day and time of this aerial photo as well as the river flow and tide level at the time it was taken are unknown. However, it does appear that upland vegetation is growing across what is now estuary. Additionally, a dark area is visible just north of the channel (**Photo 4**), that could be an excavated borrow area. The next available aerial photograph is 1967. In this image the estuary area is plainly visible (**Photo 5**). There are at least two possible explanations for this change:

1. *Transformation primarily due to the Good Friday Earthquake*: The magnitude 8.4 earthquake (March 27, 1964) was centered in the Prince William Sound region of Alaska. The earthquake resulted in significant subsidence on Kodiak Island. This was due to both soil liquefaction and the downward movement of the tectonic plate. The earthquake was followed by a tsunami that struck the coastline at Kodiak with a recorded single amplitude wave height of 18 feet (Sokolowski, 2008). The combination of these two forces – earthquake and tsunami – could have created the estuary and changed the form of the channel mouth.

2. *Transformation due to reconstruction after the Good Friday Earthquake*: The Good Friday Earthquake cause approximately $31 million in damages in the town of Kodiak and over $10 million in damages in Women’s Bay (Sokolowski, 2008). An unknown amount of destruction occurred at the Airport and Coast Guard Base Center. The current estuary area could have been formed by borrow excavation to repair damage though no documentation was found to support this theory.

In either case, the river mouth appears to have dramatically changed its alignment from its location adjacent to the Airport. Given the photos before and since this relocation, the river does not appear to regularly scroll back and forth across the barrier bar. River mouths are highly mobile locations, and are constantly adjusting to changes in river and ocean hydraulic conditions. Additionally, Alaska is prone to earthquakes and the subsidence and tsunamis they sometimes produce. Though earthquakes of this magnitude do not happen often, if another large earthquake were to strike, the estuary could again be prone to dramatic changes.

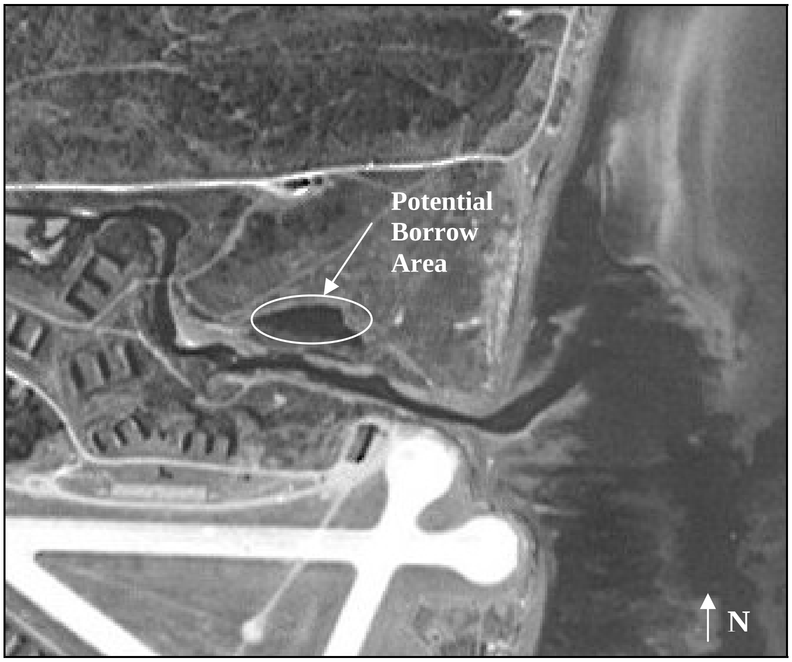

Photo 4: Buskin River Mouth (1951).

Photo 5: Buskin River Mouth (1967).

4.3.5 Channel Longitudinal Profile and Reach Breaks

Figure 4 plots the Buskin River profile, along the thalweg, from its confluence with Devil's Creek to its outlet into St. Paul Harbor. Profiles typically alternate between steeper/shallower channel features that correspond to riffles and flatter/deeper features that correspond to pools.

Transitions link riffles and pools and typically have slopes that match the mean channel slope. Glides are generally flat uniformly deep areas with little surface water disturbance.

The Buskin River can be broken into two main sections based on dominant hydraulic process – the fluvial section and the tidal section **(Figure 3)**.

The thalweg slope of the fluvial section is approximately 0.3 percent. This section can be broken into four reaches based on slope, entrenchment, bed material and channel form as indicated in **Figure 4**. The two upstream reaches are confined by bedrock. At high flows, water moves quickly through this area transporting bed material. The third reach is less confined and shows evidence of the deposition and reorganization of transported material. The fourth reach is somewhat confined by both bedrock outcroppings and fill and channel revetments adjacent to the Airport. From upstream to downstream these reaches are:

1. *Upper pool and riffle reach*: This reach is characterized by long riffles followed by deep pools. The deepest part of the Buskin River study area is in this reach. The form of the channel in this reach is due to channel entrenchment by large bedrock formations along both banks. The north bank is steep throughout this reach due to these bedrock formations (**Photo 6**) and natural topography. In the upstream end of the reach Devil's Creek and Louise Creek flow into the Buskin River. The confluence of Louise Creak, along the north bank, is fixed between two large bedrock formations. Along the southern bank an alluvial fan has developed at the Devil's Creek confluence. It transitions into a large point bar. Downstream, the point bar shifts into a gently sloping bank with a narrow floodplain which is constrained by a steep cliff face. The cliff face eventually intersects the channel and transitions to a steep bank throughout the rest of this reach. Many pools in this reach are scoured to bedrock and riffles are formed by boulders. This material is evidence of relatively fast flows that can transport smaller material downstream.

Photo 6: Rock Outcropping on North Bank of the Upper Pool and Riffle Reach.

2. *Glide reach*: This reach consists of a long deep and straight zone where the channel is uniformly deep. Natural topographical features have created steeper banks throughout this reach. Within this reach the channel appears to be stable and the bed is armored. Armoring is the winnowing away of finer particles to leave a deposit of the coarse fraction along the surface of the channel (Leopold, 1994). Bed material consists of large to small cobbles mixed with small boulders. The channel is uniformly scoured and water in this reach is relatively deep. The channel form and bed material indicate that smaller material is transported downstream. This reach terminates at the fish weir that may have been placed here to take advantage of this natural transition.

3. *Multi-channel reach*: This reach consists of two to three steeper channels that pass through and around islands, and minor pools and riffles have formed. The islands are heavily vegetated and provide roughness and velocity dissipation during high flows. The location and shape of these islands is relatively stable over time. The north bank is steeper in the upper part of this reach then it transitions to a gently sloping bank with a wide floodplain along the Buskin River State Park day use area. Just downstream of the day use area a bedrock formation protrudes into the channel from the north and the bank transitions back to a steep slope. The southern bank along the Airport is relatively steep throughout this reach. Multi-channel streams are typically found in sediment deposition zones. Bed material in this reach consists of coarse gravels to small cobbles. Material from upstream is deposited in this reach as slopes decrease. This material is periodically reorganized during high river flows.

4. *Lower pool and riffle reach*: This reach is characterized by a series of deep pools and riffles in an area of moderate sinuosity where the channel meanders around the historic bridge embankment. Channel banks are relatively steep along the north bank due to the bridge embankment and natural topography. Along the south bank the topography transitions from a shallow sloping point bar at the upstream end of the sub-reach to a steep bank at the downstream end. In the upper section of this sub-reach an armored mid-channel bar has formed of mixed cobbles and coarse gravels. Bed material in this reach is variable and includes smaller material (fine gravels to small cobles) mixed with small boulders. This material has contributed to the long cascade-like riffles in this reach.

The tidal section consists of one geomorphic reach, the estuary reach. It is characterized by a wide meandering channel with a thalweg slope of approximately 0.1 percent. Bed material in this reach is characterized by fine silts and sands with small cobles in areas of moving water such as the channel. The embankment controls the landward extent of tidal influence on the Buskin River.

The head of tide is considered the furthest upstream distance at which flows are influenced by tidal hydraulics. No published data defining the head of tide for the Buskin River was found. Therefore, the location of the head of tide was determined in the field based on observations of changes in stream bed material and vegetation. Based on these observations the head of tide was determined to be upstream of the embankment at the transition from the multi-channel reach to the lower pool and riffle reach (**Figure 3**).

4.3.6 Sediment Sampling

Bedload transport occurs along the stream bed when particles are moved by a combination of sliding, rolling, and saltation (short hops with temporary rests). The gradation of sediment samples taken within the channel provides information on current channel hydraulics. Generally, larger material settles out in areas of higher velocity and smaller materials settle in areas of lower velocity. Bulk bedload sampling was conducted at five locations along the Buskin River and the barrier bar shown in **Figure 5**. The purpose of the grain size sampling was to develop a general understanding of the size and spatial distribution of bed material found throughout the system. This information helps to describe the velocity and sediment transport capacity of water flowing through the stream system.

On September 14, 2007 samples were collected, placed in 5-gallon buckets, and sent to a laboratory for sieve analysis. Sieve analysis quantifies the size of a very wide range of particle sizes, including those particles that are too small to be measured with a particle size analyzer in the field.

Table 3 summarizes the results of the sieve analysis of these samples. Samples 1 and 2 represent the change in sediment gradation along the barrier bar. Sample 3 represents the gradation within the estuary area and Samples 4 and 5 represent the gradation within the upper reach of the Buskin River. In the locations where Samples 4 and 5 where taken, the bed appeared to be armored. The results of this sieve analysis are indicative of the higher velocities within the narrower upper channel reach and lower velocities within the tidally influenced estuary area.

Table 3: Grain Size Distribution of Bed Load Samples.

Percent Finer*	Grain Size (mm)				
	Sample 1	Sample 2	Sample 3	Sample 4	Sample 5
D5	0.18	2	0.84	0.84	1.5
D16	0.2	5	2.3	3	4.5
D50	2.5	15	12.5	24.5	37
D84	8	37.5	37	52	110
D95	16	100	51	75	-

* Percent Finer is the percent of material less than a specific grain size. Sample 2 for example, has a D50 of 15 and a D95 of 100. So 50-percent of the material is smaller that 15 mm and 95-percent of the material is smaller than 100 mm.

4.3.7 10- and 100-Year Floodplain

The Federal Emergency Management Agency (FEMA) is responsible for mapping regulatory floodplain boundaries in the U.S. No FEMA mapping is available for the Buskin River. Vigil-Agrimis, Inc. modeled existing hydraulic conditions for the Buskin River. The existing conditions model was completed early in the project to provide an understanding of the relationship between hydrologic processes and geomorphic conditions in the Buskin River in the vicinity of the Kodiak Airport. Of particular interest was the relationship between flood flows and the geomorphology of the barrier bar. The model was also used to produce a 10- and 100-year recurrence interval floodplain boundary in the project area.

These boundaries will be used to avoid or minimize impacts to regulated floodplains as RSA improvement plans are developed. The *DRAFT HEC-RAS Existing Conditions Model Technical Memorandum* is included in **Appendix C** of this report. It includes a description of the methods used to create the model. Proposed conditions modeling will be conducted later in the project when the RSA improvement alternatives have been developed.

The Ordinary High Water (OHW) boundary and the 10- and 100-year floodplain boundaries are illustrated in **Figure 6**. The floodplain boundaries illustrate a high tide condition, consistent with FEMA coastal floodplain guidelines.

The 10-year floodplain is similar in form but narrower that the 100-year floodplain. Generally the boundary lines are close to the same position in areas where the floodplain is bounded by either a natural or man-made feature that stops flood flows. These include rock wall faces downstream of the Devil's Creek confluence and filled areas such as the old bridge embankment and portions of the Airport. The area within the floodplain boundaries downstream of the embankment is regularly inundated under higher high tide conditions.

The 100-year floodplain encompasses the Buskin River riparian corridor and the Buskin River estuary, although the estuary is dominated more by tidal processes than fluvial processes. With the exception of the tip of the barrier bar at the mouth of the Buskin River, the top of the bar is not inundated during the 100-year flood. With the exception of the estuary, which is broad and flat, the 100-year floodplain ranges from about 60 to 470 feet in width and is confined within the relatively narrow valley bottom upstream of the old bridge embankment. Downstream of the constriction and within the estuary, the 100-year floodplain is up to 1,100 feet wide in places. The existing Airport infrastructure is outside of the 100-year floodplain.

4.4 Devils Creek Hydrology and Fluvial Geomorphology

4.4.1 Hydrology

Devil's Creek discharge is dominated by surface water runoff from adjacent land. Flows originate along the south side of Erskine and Barometer Mountains and the north side of Old Women's Mountain. The Creek flows about five miles from the southwest to the northeast before its confluence with the Buskin River. Several unnamed tributaries, originating along the south side of Barometer and Erskine Mountains, contribute flows to the Creek.

Devil's Creek was analyzed in a similar manner as the Buskin River in terms of peak flows. Regression equations developed by the U.S. Geological Survey were used to determine the peak flows.

A unit discharge analysis was also used as a reasonableness or robustness check for Devil's Creek. Myrtle Creek was selected for comparison to Devil's Creek. Myrtle Creek is approximately the same size, has a similar basin orientation, and receives about the same precipitation as Devil's Creek. The USGS installed a gage on Myrtle Creek in 1963, and has monitored that gage since. Peak flows typically occur in May and June and low flows in March and April.

Table 4 describes Devil's Creek hydrology and discharges based on regression equations and unit discharges for Myrtle Creek. Select calculated discharges are included for comparison.

Table 4. Devil's Creek – Myrtle Creek Peak Flow Comparison

Stream	Contributing Drainage (mi^2)	Discharge (cfs)			
		Q2	Q10	Q50	Q100
Devil's Creek	4.1	370	630	880	990

There was more variance between the regression determined and the unit discharge determined flows for Devil's Creek than on the Buskin River. The regression equations were used to predict flows for Devil's Creek to be consistent with the analysis for the Buskin River.

4.4.2 Fluvial Geomorphology

The development of the military facilities in the lower Buskin River valley required major alterations to Devil's Creek. The lower reach of the channel from the Buskin River to just upstream of the Chiniak Highway was channelized (**Figure 3**) and sections were diverted through three culverts and under two bridges.

The first culvert is approximately 300 feet upstream from the Buskin River. In this location, two 60-foot long – 12-foot diameter corrugated metal pipe (CMP) culverts convey Devil's Creek under the Airport access road (**Photo 7**).

Photo 7: Outlet of 12-foot Diameter Culverts below the Airport Access Road on Devil's Creek.

The second culvert is under the runway and taxiway. During construction of the Airport, the creek was diverted into a 500-feet long culvert in this location (SAIC, 1995). Between 1951 and 1967 the Airport facilities were expanded. Runway 7/29 was lengthened and a taxiway was installed to parallel the runway. At this time the original culvert was replaced with a 750-foot long concrete box culvert that is approximately 6-feet high by 10-feet wide (**Photo 8**).

The third culvert is just outside of the Airport boundary where Devil's Creek crosses beneath the Chiniak Highway. This culvert is a 120-foot long CMP culvert.

Photo 8: Concrete Box Culvert Inlet on Devil's Creek under the Runway and Taxiway.

Two derelict bridges also cross Devil's Creek. One is illustrated in **Figure 3**. All of the features are located on the channel profile for reference in **Figure 7**.

The vertical adjustments made to the channel when it was straightened are unknown. The channel banks are steep and are either heavily vegetated with willows or are lined with riprap. Approximately 500 feet of the channel is lined with wood along the bed and banks; the intent of this structure is unknown (**Photo 9**). The transition from the wood-lined channel to a natural bed is almost not evident in the field. No bed scour was observed upstream or downstream of the wood lined section indicating that the stream bed is vertically stable at this transition.

Photo 9: Wood Lined Channel on Devil's Creek.

4.4.3 Sinuosity

The channelization of Devil's Creek is apparent when looking at its sinuosity. From approximately 1,500 feet upstream of the Chiniak Highway to its outlet with the Buskin River, the sinuosity of Devil's Creek is roughly 1.0 based on aerial photography from 2004. **Figure 3** shows portions of the 2004 alignment used in the sinuosity assessment. This low sinuosity is not typical for a low gradient reach in a wide valley.

4.4.4 Profile

Figure 7 is a plot of the Devil's Creek profile, along the thalweg, from approximately 850 feet upstream of the Chiniak Highway to its confluence with the Buskin River. A bedrock formation upstream of the Buskin River is a noticeable knick point and obstructs fish passage. The channel has formed an 11 foot waterfall at this bedrock outcrop (**Photo 10**). Just downstream of the waterfall, over 200 feet of the channel is scoured down to bedrock. The channel slope upstream of the waterfall is approximately 1.5 percent and the channel slope downstream of the waterfall is approximately 1.9 percent.

Photo 10: 11-foot Waterfall in Downstream Section of Devil's Creek.

4.5 Channel Geometry for the Buskin River and Devil's Creek

Channel cross sectional dimensions, entrenchment, and slope describe channel geometry within a given reach. Channel cross sectional dimensions vary in width, depth and flow area along the stream corridor as the channel transitions through pool and riffle zones. Dimensions also vary based on channel slope, large woody debris, riparian area disturbances, and other factors.

Empirical studies by Leopold (1994) and Rosgen (1996) specify several stream channel indices that can be calculated using ratios of stream channel dimensions. The width to depth ratio and the entrenchment ratio are two indices that can be applied to the Buskin River and Devil's Creek. The width to depth ratio indicates the level of channel incision, and is calculated as the bankfull width divided by the bankfull depth. Incised channels have width to depth ratios less than 12. The entrenchment ratio is a measure of the horizontal confinement of the stream and it is calculated as the floodprone width divided by the bankfull width. The floodprone width for this analysis was estimated to be the width of the channel at twice the bankfull depth. Entrenchment ratios less then 1.4 are considered entrenched, ratios between 1.4 and 2.2 are considered moderately entrenched, and ratios greater than 2.2 are slightly entrenched (Rosgen, 1996). **Table 5** summarizes the average cross-section geometry within the Buskin River within the study areas. Cross section data for the fluvial section is from all available transition cross sections.

Table 5: Summary of Channel Characteristics of the Buskin River.

Channel Characteristic	**Buskin River**					
	Tidal Section			*Fluvial Section*		
	Min	Max	Average	Min	Max	Average
Bankfull Width (ft):	-	-	-	74	94	86
MHW Width (ft):	71	1031	359	-	-	-
Bankfull Depth (ft):	-	-	-	3.2	5.5	4
MHW Depth (ft):	4.5	8.5	6.3	-	-	-
Floodprone Width (ft):	-	-	-	84	340	156
Width/Depth Ratio:			-			22
Entrenchment Ratio(Wfp/Wbkf):			-			1.8
Reach Length (ft):			4650			4860

The Buskin River channel characteristic geometry measurements were divided into two sections based on their governing geomorphic processes: Tidal and Fluvial. The tidal section is characterized by a wide deep channel that does not show any signs of incision. The fluvial section is approximately one-third the width and half the depth of the tidal section. The fluvial section, which has experienced historical filling of its floodplain, does not show signs of incision and has an average width to depth ratio of 22. On average this section is considered to be moderately entrenched at a ratio of 1.8. To better understand entrenchment in specific reaches representative transition cross sections were selected for analysis.

The fluvial section of the Buskin River includes four reaches. Stream types for each reach were determined based on the Rosgen Stream Classification System (Rosgen, 1996) and are shown in **Table 6**. Both the glide and upper pool and riffle reaches are horizontally confined by bedrock features which cause small floodprone widths and are considered to be entrenched, though the glide reach is only slightly above the width-to-depth incision threshold with a ratio of 14.8. The multi-channel and lower pool and riffle reaches are less confined by natural topography and have wider floodprone widths. However, the lower pool and riffle reach is considered to be moderately entrenched at a ratio of 1.6.

Table 6: Buskin River Channel Geometry by Reach.

Buskin River Reach	**Slope (%)**	**Bankfull Width (Wbkf)(ft)**	**Bankfull Depth (Dbkf)(ft)**	**Floodprone Width (Wf) (ft)**	**Width to Depth Ratio (Wbkf/Dbkf)**	**Entrenchment Ratio (Wfp/Wbkf)**	**Dominant Bed Material**	**Stream Type**
Upper Pool/Riffle	0.64	70	4	88	17.5	1.3	Bedrock/ Alluvial	B3a
Glide	0.32	74	5	90	14.8	1.2	Alluvial	F3
Multi-Channel	0.33	-	4	190	-	-	Alluvial	D4
Lower Pool/Riffle	0.24	94	4	153	23.5	1.6	Alluvial	C4

Devil's Creek has been highly altered by humans and is a moderately entrenched stream. Because this system is altered the empirical methods may not produce meaningful results. Field data describing the stream was included to characterize existing conditions. **Table 7** describes the channel characteristic geometry of the stream. This system does not appear to be changing rapidly, most likely because of the channel lining and armoring along the creek.

Table 7. Summary of Channel Characteristics Geometry of Devil's Creek.

Channel Characteristic	Devil's Creek		
	Min	Max	Average
Bankfull Width (ft):	32	47	38
Bankfull Depth (ft):	1.7	3.7	2.5
Width/Depth Ratio:			15
Reach Length (ft):			3887

4.6 Drury Gulch and Louise Creek Hydrology

Drury Gulch originates along the northeast tip of Old Women's Mountain and drains a narrow strip of the Coast Guard Base. The channel flows from the southwest to the northeast, 0.8 miles before it flows into catch basin just south of the Airport property line. Flows are then piped another 0.8 mi across the Airport stormwater system which outlets into St. Paul Harbor at Runway end 29. A large portion of the watershed is owned by the USCG and is developed.

Louise Creek originates at Lake Louise which is connected to Lake Catherine. This upper lake is fed by a couple of unnamed stream draining the southwest flanks of Pillar Mountain.

Gaged Kodiak Island watersheds with similar size, location, and landscape features where not found for comparison to Drury Gulch or Louise Creek. **Table 8** summarizes the calculated discharges for these watersheds.

Table 8. Calculated Discharge for Select Recurrence Intervals in Drury Gulch and Louise Creek

Stream	Contributing Drainage (mi^2)	Discharge (cfs)			
		Q2	**Q10**	**Q50**	**Q100**
Drury Gulch	0.15	25	40	55	65
Louise Creek	1.7	170	290	410	460

Drury Gulch and Louise Creek contribute a small percentage of the discharge to the Buskin River; therefore, computed recurrence interval flows are sufficient for planning level analysis.

Flow was not observed in Drury Gulch during the field assessment on September 14, 2007 despite heavy rains the previous three days. A historic metal dump is located on Drury Gulch and the site was identified in the Resource Conservation Recovery Act Facilities Investigation of the Coast Guard Base. This site is discussed in more detail in Section 5.2.2. As a corrective measure, contaminated material will be removed. About 2,000 feet of the Drury Gulch channel will be filled and relocated to a parallel drainage (ADEC, 2008). Due to planned alterations to this drainage way a fluvial-geomorphic analysis was not conducted.

5.0 Fresh Water Quality

The quality of water is defined by its physical, chemical, and biological characteristics. These characteristics help determine the appropriateness for various beneficial uses of both surface water and groundwater. VAI evaluated existing surface water and groundwater quality conditions near the Airport by reviewing available documentation and performing limited field reviews.

The water quality evaluation focused on water bodies that might be affected by proposed changes to RSA in the Airport vicinity, though the Buskin River watershed is also discussed to provide a context for site specific information. Primary fresh water resources are the Buskin River and Devil's Creek. Drury Gulch is also included as it is a known hazardous material site in the Airport vicinity (see Section 5.2.2).

5.1 Methods

VAI reviewed the following key documents:

- Stormwater Pollution Prevention Plan (SWPPP) for the Kodiak Airport, Shannon and Wilson Inc; May 2000
- Stormwater Pollution Prevention Plan (SWPPP) for USCG Integrated Support Command Kodiak; November 2001
- Hydrologic and Water-Quality Data for USCG Support Center Kodiak, Alaska, 1987-89; USGS, 1996
- Final RFI/CMS Report Volume 1 Introduction and Facility-Wide Information USCG Support Center Kodiak, Kodiak Alaska, Science Applications International Corporation; February 1995
- Total Environmental Restoration Contract, Final Decision Document Drury Gulch, Kodiak Alaska; July 2003
- 18 AAC 70 Water Quality Standards; Alaska Department of Environmental Conservation, March 2006
- Alaska Department of Environmental Conservation (ADEC) Contaminated Sites Database, last accessed 5/2/08 at http://www.dec.state.ak.us/SPAR/CSP/db_search.htm
- NPDES Multi-Sector General Permit for Storm Water Discharge Associated with Industrial Activities, US EPA Federal Register Volume 65 No. 210, October 30th, 2000
- Comprehensive Site Compliance Evaluation Integrated Support Command Kodiak; Naval Facilities Engineering Command Northwest; December 2006

Additionally, VAI conducted field reviews from September 10-14, 2007. These reviews included observing site conditions and stormwater drainage patterns throughout the Airport, and measuring specific conductance and salinity in the Buskin River estuary.

The documents used to review groundwater are cited in that section of the text. No field reviews were conducted to evaluate groundwater chemistry.

5.2 Surface Water

Surface water is an important resource to the people of Kodiak Island because it is their main source of potable water, and it helps to sustain the resource-driven economy of the island. The principal drinking water sources for the Coast Guard Base, which supplies the Airport, are three surface water intakes at the southern end of Buskin Lake. This surface water is treated in a water treatment facility located at the mouth of Buskin Lake, where it is filtered and chlorinated at a pump house before being piped to users. Water testing from this source is discussed in the water quality conditions section 5.3 of this report.

5.2.1 Beneficial Uses and Water Quality Standards

The U.S. Environmental Protection Agency (EPA) and Alaska Department of Environmental Conservation (ADEC) regulate the quality of waters in the State of Alaska by defining "beneficial uses" for each water body and setting appropriate water quality standards for these uses, as required by the Federal Clean Water Act. Beneficial uses are the purposes that a water body is intended to provide, such as for drinking water or the growth and propagation of fish, shellfish, and other aquatic life, or recreation, for example. Water bodies can and often do support a number of different beneficial uses. **Table 9** is a summary of the beneficial uses for the key water bodies of interest to this study.

Alaska's water quality standards (AWQS) require that all "waters of the state" be regulated for all freshwater beneficial uses unless they have been reclassified and are exempt from these regulations (Jim Powell, ADEC, pers. comm., 2008). Water bodies that do not meet water quality standards are termed "water quality limited." There are currently 25 water quality limited water bodies in Alaska (ADEC, 2006). The Buskin River and Devil's Creek are not classified as water quality limited (EPA, 2004).

Water quality standards are the reference levels (or acceptable characteristics) for individual water quality parameters that must be met in order to support the recognized beneficial uses for a waterway. For example, in order to protect the beneficial use of aquatic life, waters used by anadromous and resident fish must typically contain dissolved oxygen (DO) concentrations of more than 7 milligrams per liter (mg/L). **Table 10** is a summary of the AWQS for conventional water quality parameters for fresh water.

Table 9: Beneficial Uses of Water Bodies of Interest at the Kodiak Airport (18 AAC 70).

Beneficial Uses	**Buskin River**	**Devil's Creek**	**Drury Gulch**
(1) FRESH WATER USES			
(A) **Water Supply**	X	X	X
(i) drinking, culinary, and food processing			
(ii) agriculture, including irrigation and stock watering			
(iii) aquaculture			
(iv) industrial			
(B) **Water Recreation**	X	X	X
(i) contact recreation			
(ii) secondary recreation			
(C) **Growth and Propagation of Fish, Shellfish, Other Aquatic Life, and Wildlife**	X	X	X
(2) MARINE WATER USES			
(A) **Water Supply**	X*	X*	X*
(i) aquaculture			
(ii) seafood processing			
(iii) industrial			
(B) **Water Recreation**	X*	X*	X*
(i) contact recreation			
(ii) secondary recreation			
(C) **Growth and Propagation of Fish, Shellfish, Other Aquatic Life, and Wildlife**	X*	X*	X*
(D) **Harvesting for Consumption of Raw Mollusks or Other Raw Aquatic Life**	--	--	--

* Alaska Water Quality Standards 18 AAC 70.040(3) state that "...in estuaries, where the fresh and marine water quality criteria differ within the same use class, the standard will be determined on the basis of salinity…"

Table 10: AWQS for Conventional Water Quality Parameters for Fresh Water (18 AAC 70).

Parameter	Applicable Water Quality Standard	Most Restrictive "Beneficial Use" for Parameter
Fecal coliform bacteria	Mean may not exceed 20 FC/100 ml, and not more than 10% of the samples may exceed 40 FC/100 ml. For groundwater, the FC concentration must be less than 1 FC/100 ml, using the fecal coliform Membrane Filter Technique, or less than 3 FC/100 ml, using the fecal coliform most probable number (MPN) technique.	water supply*
Dissolved gas	D.O. must be greater than 7 mg/L in waters used by anadromous and resident fish. In no case may D.O. be less than 5 mg/l to a depth of 20 cm in the interstitial waters of gravel used by anadromous or resident fish for spawning. For waters not used by anadromous or resident fish, D.O. must be greater than or equal to 5 mg/l. In no case may D.O. be greater than 17 mg/l. The concentration of D.O. may not exceed 110% of saturation at any point of sample collection.	aquatic life
pH	May not be less than 6.5 or greater than 8.5. If the natural condition pH is outside this range, substances may not be added that cause an increase in the buffering capacity of the water.	recreation (primary contact)
Turbidity	May not exceed 5 nephelometric turbidity units (NTU) above natural conditions when the natural turbidity is 50 NTU or less, and may not have more than 10% increase in turbidity when the natural turbidity is more than 50 NTU, not to exceed a maximum increase of 25 NTU.	Water supply*
Temperature	May not exceed 20ºC at any time. The following maximum temperatures may not be exceeded, where applicable: -Migration routes 15ºC, -Spawning areas 13ºC, -Rearing areas 15ºC, -Egg & fry incubation 13ºC For all other waters, the weekly average temperature may not exceed site-specific requirements needed to preserve normal species diversity or to prevent appearance of nuisance organisms.	Aquaculture & Aquatic Life
Dissolved inorganic substances	Total dissolved solids (TDS) from all sources may not exceed 500 mg/l. Neither chlorides nor sulfates may exceed 250 mg/l.	Water supply*
Sediment	The percent accumulation of fine sediment in the range of 0.1 mm to 4.0 mm in the gravel bed of waters used by anadromous or resident fish for spawning may not be increased more than 5% by weight above natural conditions (as shown from grain size accumulation graph). In no case may the 0.1 mm to 4.0 mm fine sediment range in those gravel beds exceed a maximum of 30% by weight (as shown from grain size accumulation graph). In all other surface waters no sediment loads (suspended or deposited) that can cause adverse effects on aquatic animal or plant life, their reproduction or habitat may be present.	Aquatic life
Toxics and other deliterious (organic and inorganic substances)	The concentration of substances in water may not exceed the criteria shown in Table I or in Table V, column A of the *Alaska Water Quality Criteria Manual.* Substance concentration in water may not exceed any chronic and acute criteria established in this chapter, for a toxic pollutant of concern to protect sensitive and biologically important life stages of resident species of this state. there may be no concentration of toxic substances in water or in shoreline or bottom sediments that, singly or in combination, cause or reasonably can be expected to cause, adverse effects on aquatic life or produce undesirable or nuisance aquatic life, except as authorized by this chapter. Substances may not be present in concentrations that individually or in combination impart undesirable odor or taste to fish or other aquatic organisms, as determined by either bioassay or organoleptic tests.	Water supply* & Aquatic life
Color	May not exceed 15 color units or the natural condition, whichever is greater. Color or apparent color may not reduce the depth of the compensation point for photosynthetic activity by more than 10% from the seasonally established norm for aquatic life.	Water supply* & Aquatic life
Petroleum hydrocarbons, oils, and grease	Total aqueous hydrocarbons (TAqH) in the water column may not exceed 15 μg/l. Total aromatic hydrocarbons (TAH) in the water column may not exceed 10 μg/l. There may be no concentrations of petroleum hydrocarbons, animal fats, or vegetable oils in shoreline or bottom sediments that cause deleterious effects to aquatic life. Surface waters and adjoining shorelines must be virtually free from floating oil, film, sheen, or discoloration.	Aquaculture
Radioactivity	May not exceed the concentrations specified in Table 1 of the Alaska Water Quality Criteria Manual for radioactive contaminants and may not exceed limits specified in 10 C.F.R. 20 and National Bureau of Standards, Handbook 69.	Water supply* & Aquatic life
Residues (floating solids, debris, sludge, deposits, foam, scum, or other residues)	May not, alone or in combination with other substances or wastes, make the water unfit or unsafe for the use, or cause acute or chronic problem levels as determined by bioassay or other appropriate methods. May not, alone or in combination with other substances, cause a film, sheen, or discoloration on the surface of the water or adjoining shorelines, or cause leaching of toxic or deleterious substances, or cause a sludge, solid, or emulsion to be deposited beneath or upon the surface of the water, within the water column, on the bottom, or upon adjoining shorelines.	Aquatic life

5.2.2 Resource Conservation Recovery Act (RCRA) Sites

Historical land uses in the Buskin and Drury Gulch watersheds may affect the future water quality of these systems and their receiving waters. From the early 1940's to early 1970's most of the Buskin River and Drury Gulch watersheds were used for military purposes. A naval submarine base and air station were constructed at Women's Bay and an army outpost was established near the Buskin River. Several sites within the watersheds were identified as having a potential risk to human health and the environment because they may contain contaminants, presumably related to the military activities. These sites were identified in a Resource Conservation Recovery Act (RCRA) Facility Investigation (RFI) and Corrective Measures Study (CMS) analyses conducted during 1993 and 1994. A map of the identified RCRA sites is included in **Figure 8**.

Open RCRA sites within the watersheds of interest include:

- Site 1 – Coast guard landfill
- Site 2 – Navy landfill
- Site 5 – Historic fire training area
- Site 12 – Buskin Lake Drum Disposal No. 1
- Site 16 – Historic Airport staging area
- Site 18 – Historic metal dump at Drury Gulch
- Site 22 – AKDOT maintenance building
- Site 27B – Historic Site of the advanced underwater weapons shop
- Site 34 – Former army ordinance shop, current AKDOT building
- Site 35 – Historic Site of the fire training pit.

The USCG landfill (Site 1) covers approximately 10 acres and is located within the Buskin River watershed, approximately 1 mile north of the Airport (**Figure 8**). It consists of predominantly domestic refuse. However, several thousand gallons of paint may have been disposed of and fuel-contaminated soils were reportedly used as cover material (Glass, 1996). The reviewers were not able to determine if this landfill contained a bottom liner. Historically this landfill had two leachate streams: one that discharged directly to the Buskin River and another that discharged to Lake Louise and drains into the Buskin River (USCG, 1986). The landfill was closed in 1987 and a combination leachate collection and runoff diversion system was installed. The leachate collection system discharges into the sanitary sewer system and the USCG sewage treatment plant. During high flow events, this system can be diverted to open ditches via manually opened valves. During the summer of 2000, the landfill was covered with a clay liner (USCG, 2001).

The Navy landfill (Site 2) covers approximately 15 acres. It is located within the Buskin River watershed approximately 3/4 of a mile north of the Airport (**Figure 8**). The landfill was operational from the 1940's to the early 1970's and during that time it contained a lead waste pile that is considered to be clean and closed. The predominant type of refuse at this site is unknown; the landfill may contain domestic refuse as well as petroleum-based products such as solvents, degreasers, and paints (Glass, 1996). The reviewers were not able to determine if this landfill contained a bottom liner. The landfill is adjacent to a pond called Red Lake; the Lake is considered water quality limited due to high concentrations of iron and manganese. Drainage from Red Lake travels approximately 400 yards before it discharges into the Buskin River (ADEC, 2008). Vinyl chloride was detected in surface water obtained from a ditch near the landfill in concentrations exceeding Maximum Contaminant Levels (MCL) for drinking water (Glass, 1996). During the summer of 2000 this landfill was capped (USCG, 2001).

Buskin Lake drum disposal Number 1 (Site 12) is an area west of the lake (**Figure 8**) where approximately 3,000 55-gallon drums were discarded. The contents of these drums are unknown; they were found to be rusted and all are empty. Manganese was detected in well and surface water samples taken near the site. Soil samples had detectable concentrations of lead (0.3 to 8.4 mg/kg) (Glass, 1996). The drums were removed in 1994, and contaminated soils were excavated in 1999 and 2001. In 2007 the site was planned for conditional closure; however, as of the writing of this report the Site is listed as open (ADEC, 2008).

The USCG airport staging area (Site 16) is composed of several individual sites including the advanced underwater weapons shop (Site 27B), three underground storage tanks (USTs), and the historic Fire Training Pit (Site 35). All of these sites are contaminated with diesel range organics (DRO). Site 35 contains the most contamination, with flammable materials being sprayed on the ground and ignited for fire training throughout the 1950's and 1960's (ADEC, 2008). Site 35 is also contaminated with low level volatile organic carbons (VOC). In 2001 approximately 20,000 cubic yards of contaminated soils were removed from the Fire training Pit source area (ADEC, 2008). Remedial investigation conducted in 2005 determined a smear zone originating at the fire training pit and extending for about 700 feet towards the Buskin River. A smear zone is an area that has been contaminated due to water table movement. The smear zone at Site 35 is 2 to 4 feet thick and appears to have stopped spreading and is in a state of equilibrium (ADEC, 2008). A remedial investigation, feasibility study, and treatabilty study were performed at Site 35 in 2005-2006. A remediation pilot study was started during 2006-2007.

The Drury Gulch metal dump (Site 18) is located to the southeast of the Airport (**Figure 8**). This historic metal dump at Drury Gulch is approximately 3,600 feet long and covers and area of approximately 6 acres. For an unknown period of time between 1939 and 1975 the Navy stored or disposed of a variety of metal and wood debris in Drury Gulch (USACE, 2003). This debris includes electric transformers containing polychlorinated biphenyls (PCBs) that were stored, emptied, burned, and buried along the Gulch (Glass, 1996). In the Mid 1970's to 1980's the majority of this waste was removed from the site or buried onsite and the surface was re-graded. Investigations throughout the 1990's indicated elevated levels of PCBs. Contamination levels were as high as 897 mg/kg in the upper one foot of soil in the lower gulch area (USACE, 2003). Additionally, lead and 1,2-dichloroethane were detected in concentrations in the groundwater exceeding their respective MCLs. Aluminum and manganese were found in concentration in the groundwater equaling or exceeding their secondary MCLs. In 2000 and 2004, remediation efforts removed large portions of contaminated soil at this site. During the 2004 effort, soil and sediment with PCB concentrations of 10 mg/kg and greater were excavated and soils with levels of PCB that were less than 10mg/kg were backfilled with clean material (USACE, 2003). An additional 2 to 3 inches of clean topcover was placed over the backfill.

Little or no existing information was available for Sites 5, 22, and 34. The fire training area (Site 5) is contaminated with petroleum. Site 22 is contaminated with petroleum, solvent and paint as a result of releases and spills from a tanker truck and two drum storage areas. Additional RCRA sites and further discussions of contaminant levels are included in the groundwater section of this report.

5.2.3 Airport Operations and Maintenance

The airport is permitted to discharge stormwater under the NPDES Multi-Sector General Permit for Storm Water Discharge Associated with Industrial Activities (MSGP). Subpart S of this permit pertains to stormwater discharges associated with runway and aircraft de-icing operations; aircraft servicing; aircraft, ground vehicle, and equipment maintenance; and material storage areas. Under Subpart S of this permit the Airport is required to prepare and implement a stormwater pollution and prevention plan (SWPPP). The SWPPP identifies potential sources of stormwater pollution and ensures implementation of measures to minimize and control pollutants. The SWPPP prepared for the Airport identifies these sources and provides best management practices (BMPs) to reduce contamination (Shannon & Wilson Inc., 2000). They include:

- *Equipment maintenance operations*: Minor maintenance of snow removal equipment is conducted inside the operations and maintenance building along Taxiway C, while major repairs are conducted inside the ADOT&PF road maintenance facility building. Snow removal equipment is washed next to the operations and maintenance building on a flat gravel surface without a drainage system. Potential contaminants include oil, grease, anti-freeze, solvents, and fuel. To reduce contaminant contact with stormwater, the Airport SWPPP recommends that the following best management practices (BMPs) be implemented or continued:
    - Perform equipment washing in a designated wash area or wash bay. Collect wash water for discharge to the sanitary sewer system or an isolated detention area.
    - Prevent wash water from entering the storm drain system using temporary blockages, dikes, or berms. Collect wash water for discharge to a sanitary sewer system.
    - Conduct maintenance activities inside a building.

- *Equipment fueling operations*: Equipment and vehicle fueling is conducted at the operations and maintenance building. Fuel is stored behind the building in above ground storage tanks. The surrounding ground cover is gravel and the diesel and gas are stored in 1,000 and 1,100 gallon tanks, respectively. To reduce contaminant contact with stormwater, the Airport SWPPP recommends that the following key BMP's be implemented or continued:
    - Develop a spill prevention, control, and countermeasure (SPCC) plan for the facility. Follow the procedures and recommendations in the SPCC plan during all fuel transfer operations.
    - Require facility personnel to observe all fuel transfer operations.
    - Equip fuel pumps and tanks with overflow and automatic shut-off devices.

- *Runway de-icing*: Runway and taxiway de-icing are normally performed at the Airport by using palletized urea and sand. The three-year average usage of urea at the Airport is approximately 80 tons. Urea and sand are both stored in a building east of the operations and maintenance building away from precipitation. Dissolved oxygen deficits and other water quality concerns can occur when deicing chemicals are able to drain directly into streams and other waters. A detailed evaluation of the effect of runway de-icing on water quality is outside the scope of this review. However, several best management practices are in place to reduce stormwater contact with urea. The Airport SWPPP requires the following BMP's:

    - Maintaining a monthly inventory of the type and amount of de-icing chemicals used.
    - Inspecting de-icing equipment and de-icing areas weekly during periods of de-icing application.

- *Runway maintenance*: Maintenance activities include annual repainting of the runway markings and periodic sealing of stress cracks in the asphalt. These maintenance procedures are conducted in accordance with ADOT&PF and are conducted in dry weather conditions. Potential contaminants include paints and solvents. To reduce contaminant contact with stormwater, the Airport SWPPP recommends that the following key BMP's be implemented or continued:
    - Perform maintenance activities during dry weather.
    - Use a high efficiency, airless painting system.
    - Collect and recycle paints and solvents.

- *Exposed material*: Any materials used for equipment maintenance that could potentially be exposed to precipitation during use or loading and unloading activities may be a source of water pollution. Potential contaminants include diesel fuel, gasoline, and heating oil. To reduce contaminant contact with stormwater, the Airport SWPPP recommends that the following key BMP's be implemented or continued:
    - Storing materials indoors.
    - When materials are stored outside, cover the materials with an awning, roof, or tarp and store containers off the ground surface.
    - Develop a SPCC plan for the facility and follow the procedures and recommendations within it during all fuel transfer operations.

- *Sediment and erosion control*: Sand is used for de-icing along the apron areas of the Kodiak Airport. The apron areas are those paved areas set aside for loading, unloading or maintaining aircraft. The de-icing sand can contribute sediment to stormwater runoff. The Airport SWPPP recommends that the following BMP's be implemented:
    - Route storm water runoff to a detention area to reduce sediment loading.
    - Use erosion control techniques such as mulching, filter fences, straw bales, or diversion terracing.

A separate SWPPP was also developed by the USCG in 2001 for the entire Coast Guard Base and associated Airport activities. This document lists additional BMPs that are to be utilized to reduce stormwater contamination for each operations and maintenance procedure.

5.2.4 Stormwater

The Airport stormwater drainage system is described in both the SWPPP for the Kodiak Airport (Shannon and Wilson Inc, 2000) and the SWPPP for the Coast Guard Base (USCG, 2001). Both reports include similar drainage maps.

For the purposes of this NEPA review, the investigators divided the majority of the Airport property into 17 drainage basins, as shown in **Figure 9**. The existing conditions for each of these stormwater drainage basins are summarized in **Table 11**. The estimated stormwater runoff flows are from Airport property only and are based on the fifty-year, one-hour storm event. Offsite drainage onto the Airport was not quantified. However, offsite drainage inflow locations are shown in **Figure 8.**

The delineated basins drain directly into the receiving waters listed below.

- Buskin River
- Devil's Creek
- Louise Creek
- St. Paul Harbor

The entire watershed of Drury Gulch is outside of the Airport property. It drains into a catch basin just south of the property line; from there it is believed to drain into the Airport stormwater system and discharge into St. Paul Harbor.

Table 11: Kodiak Airport Stormwater Status.

Basin ID	Estimated Area (Acres)	% Impervious	% Pervious	% Open Water	Estimated 50Yr-1hr Storm Runoff Volume (Acre-Ft)*	Receiving Water	Open RCRA Site (Refer to Figure 8)
1	15.6	34%	66%	0%	0.6	Buskin River	14 & 34
2	8.4	4%	96%	0%	0.2	Buskin River	-
3	19.5	2%	95%	4%	0.4	Louise Creek	-
4	17.9	0%	100%	0%	0.4	Buskin River	-
5	70.4	40%	60%	0%	2.7	Buskin River	16
6	17.8	10%	86%	3%	0.4	Devil's Creek	16
7	20.5	2%	98%	0%	0.5	Buskin River	16
8	57.9	26%	74%	0%	1.9	Buskin River	16
9	52.4	10%	90%	0%	1.3	Buskin River	16, 27A, 27B, 35
10	6	38%	62%	0%	0.2	St. Paul Harbor	
11	92.5	39%	61%	0%	3.5	St. Paul Harbor	16
12	26.4	32%	68%	0%	0.9	St. Paul Harbor	
13	33.7	18%	82%	0%	1.0	St. Paul Harbor	
14	12	4%	91%	5%	0.3	Devil's Creek	16
15	57	14%	86%	0%	1.5	St. Paul Harbor	16
16	10.9	0%	100%	0%	0.2	St. Paul Harbor	
17	2.8	50%	50%	0%	0.1	St. Paul Harbor	
Totals:	521.7	23%	77%	0%	16.1		
Buskin River	243.1	22%	78%	0%	7.5		
Devil's Creek	29.8	8%	78%	4%	0.7		
Louise Creek	19.5	2%	88%	4%	0.4		
St. Paul Hbr.	229.3	27%	95%	0%	7.5		

* Volume estimated using the Rational Method with $C_{impervious}$=0.90 $C_{pervious}$=.3 Rainfall Intensity = 0.85 in/hr

Twenty-three percent of the Airport has been classified as impervious to stormwater infiltration and 77 percent of the land has been identified as pervious. The total volume of stormwater discharged from the Airport property during the fifty-year, one-hour storm event was estimated to be 16 acre-feet, with the Buskin River and the St. Paul Harbor receiving the majority of the stormwater.

The Buskin River receives 7.5 acre-ft of stormwater runoff directly from seven Airport drainage basins which cover an area of approximately 243 acres. This area includes Basins 1, 2, 4, 5, 7, 8, and 9. Twenty-two percent of this area has been identified as impervious and 78 percent has been identified as pervious. RCRA sites within these drainage basins are Sites 16, 27B, 34, and 35. Devil's Creek and Louise Creek both discharge into the Buskin River thus it receives the stormwater runoff from the Airport captured by these water bodies.

Devil's Creek receives 0.7 acre-feet of stormwater runoff from Airport drainage basins 6 and 14, which comprise an area of approximately 30 acres. Eight percent of this area has been identified as impervious and 88 percent has been identified as pervious. The sole RCRA site within the Devil's Creek drainage basins is Site 16 the Airport Staging Area.

Louise Creek receives 0.4 acre-ft of stormwater runoff from Drainage Basin 3 which comprises approximately 19.5 acres. Two percent of this area has been identified as impervious and 95 percent has been identified as pervious. No RCRA sites exist in Basin 3.

St. Paul Harbor receives 7.5 acre-feet of stormwater runoff directly from 7 drainage basins that comprise approximately 230 acres. These drainage basins include Basins 10, 11, 12, 13, 15, 16, and 17. Twenty-seven percent of this area has been identified as impervious and 73 percent has been identified as pervious. The sole RCRA site within the St. Paul Harbor drainage basins is Site 16 the Airport Staging Area. Site 5 is just outside of the Airport property and St. Paul Harbor also receives stormwater flow from this site and other RCRA sites along the Nyman Peninsula.

Existing Airport activities or land uses that could potentially affect water quality were evaluated in 5 categories for each drainage basin (**Table 12**):

- *Equipment maintenance operations area*: Areas where equipment maintenance operations are conducted and hazardous materials are stored.
- *Equipment fueling operations area:* Areas where equipment and vehicle fueling is conducted.
- *Runway and taxiway area:* Areas where typical runway maintenance and urea application takes place.
- *Sediment and erosion control areas:* Areas where sand is applied for de-icing purposes.
- *Gravel parking areas:* Areas where gravel parking lots exist and vehicle fluid leaks could occur.

Approximately twenty-two percent of the study area contains airport operations and land use practices that could affect the water quality of adjacent streams if stormwater is not adequately managed.

Table 12. Airport Operations and Land Use Practices that Could Affect Water Quality.

Basin ID	Receiving Water	Area of Potential Water Quality Issues				
		Equipment Maintenance Operations (Acres)	Equipment Fueling Operations (Acres)	Runway/ Taxiway Areas * (Acres)	Sediment and Erosion Control Areas (Acres)	Gravel Parking Areas (Acres)
1	Buskin River	-	-	-	-	5.7
2	Buskin River	-	-	-	-	1.0
3	Louise Creek	-	-	-	-	0.8
4	Buskin River	-	-	-	-	0.2
5	Buskin River	-	-	4.8	15.2	3.2
6	Devil's Creek	-	-	0.61	1.7	0.2
7	Buskin River	-	-	-	-	0.2
8	Buskin River	-	-	14.7	-	-
9	Buskin River	-	-	4.8	-	-
10	St. Paul Harbor	-	-	2.3	-	-
11	St. Paul Harbor	-	-	36.2	-	-
12	St. Paul Harbor	-	-	8.5	-	-
13	St. Paul Harbor	-	-	6	-	-
14	Devil's Creek	-	-	0.5	-	-
15	St. Paul Harbor	3.1	0.1	7.4	-	1
16	St. Paul Harbor	-	-	-	-	-
17	St. Paul Harbor					
	Totals:	**3.1**	**0.1**	**85.8**	**16.9**	**12.2**
	Buskin River	0	0	24.3	15.2	10.21
	Devil's Creek	0	0	1.11	1.7	0.24
	Louise Creek	0	0	0	0	0.75
	St. Paul Harbor	3.1	0.09	60.4	0	1

* Includes typical runway maintenance and urea application

5.3 Water Quality Conditions

Only a limited amount of information is available on existing surface water quality conditions in the area. However, test results from the USCG water treatment plant and historic stormwater sampling provide insight into the existing water quality conditions of the Buskin River. The USCG water treatment plant withdraws surface water from east end of Buskin Lake. **Table 13** summarizes the ADEC required water quality test results from the treated water at the USCG water treatment plant during 2007 (USCG, 2007). The maximum contaminant level (MCL) is the highest level of a contaminant that is allowed in drinking water. The action level is the concentration of a contaminant that, if exceeded, triggers additional treatment.

Table 13: 2007 annual summary of treated water testing at the USCG Water Treatment Plant (Reproduced from USCG, 2007)

Contaminant (Sampling Interval)	**Units**	**Level Detected**	**MCL**	**Major Source in Water**
Turbidity (Daily)	NTU	0.27*	0.3	Soil runoff
Fluoride (Daily)	ppm	1.48	4	Erosion of natural deposits and added to water
Nitrate (Every year)	ppm	0.334	10	Runoff from fertilizer use, leaching from septic tanks, and erosion of natural deposits
TTHMs	ppb	23.88**	80	By product of drinking water chlorination
HAA5s	ppb	16.4**	60	By product of drinking water chlorination
Other Contaminants			**Action Level**	
Lead (2006)	ppb	9.19	15	Corrosion of household plumbing, erosion of natural deposits
Copper (2006)	ppm	0.165	1.3	Corrosion of household plumbing, erosion of natural deposits

* Single highest measurement (measured every 4 hours when pumps are running)
** Annual average
TTHMs=Trihalomethanes – Boroform, Bromodichloromethane, Chloroform and Dibromochloromethane
HAA5s=Haloacetic acids NTU=Nephelometric Turbidity Unit ppm= Parts per million
ppb=Parts per billion

Surface water sources have a high susceptibility to contamination. However, the treated water is within all MCL and action level standards, indicating that the water source is in good condition.

The MSGP requires that benchmark monitoring of stormwater be conducted for ammonia, biochemical oxygen demand (BOD), chemical oxygen demand (COD) and pH. Benchmark monitoring is used to determine how effective the SWPPP is at controlling the discharge of pollutants into receiving waters (EPA, 2000). Specific numeric values for benchmark monitoring are set in the MSGP. Exceedance of these values does not, in and of itself, constitute a violation of a water quality standard; instead it indicates that changes to the SWPPP may be needed.

Benchmark monitoring at airport stormwater discharge locations for Basins 5 and 11 (**Figure 9**) were conducted from February 2005 to August of 2006 (NAVFAC, 2006). Stormwater samples from Basin 5 were below benchmark monitoring limits for ammonia and pH, but exceeded the benchmark monitoring limits for BOD and COD. The benchmark limit for BOD is 30 milligrams per liter (mg/l) and the highest BOD result was 247 mg/l. The COD benchmark limit is 120 mg/l, however the exceeded values for COD were not available. This Basin drains most of the airport terminal area and discharges directly into the Buskin River. Urea is applied to approximately seven percent of Basin 5 for de-icing purposes. The high levels of BOD and COD in this area may be attributed to application of urea. When benchmark values are exceeded, it is the responsibility of the permittee to modify activities in order to achieve monitoring levels below these values. Benchmark monitoring samples taken at the same time at

Basin 11 were all below benchmark values. Urea is applied to approximately 39 percent of Basin 11 which drains most of runway 7/25.

A comprehensive review of de-icing is beyond the scope for this analysis. De-icing is regulated on a federal level for all airports.

5.3.1 Tidal Influence

During high tides, marine water from St. Paul Harbor flows up the Buskin River and mixes with fresh water causing brackish conditions. The transition zone, where water mixes and shifts from brackish to freshwater, is an important habitat for salmonids. To create a general understanding of this transition zone within the estuary, specific conductance, salinity, and temperature measurements where taken during a high tide cycle on September 12, 2007. Measurements were taken between 2:15 p.m. and 4:30 p.m. during a 7.39-foot high tide (NAVD88 datum) that occurred at 3:24 p.m. (NOAA, 2007). Measurements where taken at nine locations throughout the estuary and vicinity. These locations are shown in **Figure 9** and recorded values are summarized in **Table 14**.

During high tides, the salinity associated with tidal waters from St. Paul Harbor increases the concentration of dissolved ions in the lower reach of the Buskin River. This effect is reflected in the conductance data (which measures dissolved ions and salinity in the water column). The specific conductance of the River near the mouth of the estuary before high tide was 2865 microsemens (µs), reflecting brackish water conditions. Values in the range of 30 to 50 µs reflect fresh water conditions. The slightly elevated specific conductance values at Site E likely reflect stagnant water conditions where small amounts of unmixed brackish water remained after tide reversal.

Table 14: Buskin River Water Measurements Taken During the 7.39-foot High Tide Cycle.

Measurement Location	Time	Specific Conductance (µs)	Temp (^{o}C)
A	14:15	249	11.8
B	14:25	2865	11.8
C	15:00	53	11.7
D	15:10	38	12.2
E	15:20	117	13.1
F	15:30	42	11.8
G	15:35	32	11.7
H	15:40	32	11.7
I	15:45	32	11.7
H	15:50	32	11.7
G	16:00	32	11.7
F	16:05	33	11.8
E	16:10	121	13.5
D	16:15	46	13.1
C	16:25	45	12.2
B	16:35	10900	11.8
A	16:30	501	12.2

Based on these measurements, the salinity transition zone during this high tide extended to approximately Site A, near the mouth of the river. These measurements were taken during the lower of the two daily high tides, at a tidal elevation of approximately 7.39 feet. For comparison, the mean higher high water (MHHW) elevation is 9.53 feet. Because field conditions did not reflect maximum daily tide elevations, this measurement does not show the full upstream extent of the transition zone. **Table 15** shows the range of tidal elevations at Kodiak Island.

Table 15: Range of Tide Levels for Kodiak Island (NOAA, 2007)

Tide Level	Project Survey (Feet-NAVD88)
Extreme High Water (EHW)	14.0
Mean Higher High Water (MHHW)	9.5
Mean High Water (MHW)	8.6
Mean Lower Low Water (MLLW)	0.8
Extreme Low Water (ELW)	-2.4

Vegetation can also be used as a salinity indicator in the field. Tidal marsh ecology is closely related to tidal elevations and inundation. Eelgrass beds occur from MLLW to MHW. Low salt marsh vegetation extends from MHW to MHHW where tidal inundation occurs on most days. High salt marsh colonizes areas above MHHW where land is inundated by tides but with less than daily frequency (Weinmann et al, 1984). Vegetation within the estuary coincides with the documented tide levels. The extent of the vegetation indicates that the transition zone extends to measurement location F, at the downstream end of the old bridge embankment.

5.4 Groundwater

5.4.1 Groundwater System in the Vicinity of the Kodiak Airport

An aquifer is a geologic formation that is sufficiently saturated to allow the movement of economic quantities of water to wells or springs. No major aquifers underlie the Kodiak Airport (SAIC, 1995). However, many of the surficial and near-surface unconsolidated materials may yield water to wells locally (Hogan and Nakanishi, 1995).

Most groundwater flow near the Kodiak Airport is within the surficial and near-surface unconsolidated sediments rather than in the underlying marine sedimentary bedrock. Surficial geology near the Kodiak Airport is complex and variable and affects groundwater presence and movement. The unconsolidated sediments include varying thicknesses of artificial fill, glacial till, gravel, and sand; all of which range in thickness from zero feet (exposed bedrock) to 46 feet (Hogan and Nakanishi, 1995). These unconsolidated sediments are generally covered by a layer of volcanic ash from the 1912 eruption of Novarupta (Mt. Katmai) and organic-rich soils. The thickest sediments include stream, estuarine, and lake sediments near Buskin Lake and the Buskin River valley. The sediments with the highest hydraulic conductivity are the river sediments near the Buskin River. The primary water-bearing units are gravel and sand, while glacial till and bedrock act as barriers to vertical and horizontal groundwater flow (Hogan and Nakanishi, 1995).

The bedrock units underlying the majority of Kodiak Island are almost impermeable allowing little groundwater movement (Hogan and Nakanishi, 1995). However, in the vicinity of the

USCG Station, secondary fracturing in the bedrock may allow water flow due to interconnecting fractures (Brown, 1989).

Groundwater recharge in the vicinity of the Airport is primarily due to precipitation infiltrating from the surface (SAIC, 1995). Recharge is related to the amount and type of precipitation, topography, soils, and vegetation. Water elevations in wells measured in 1988-1989 ranged from 0.3 to 2.0 feet below the land surface during periods of heavy precipitation, while water levels dropped to 4.9 to 40.0 feet below the land surface during extensive dry spells (Hogan and Nakanishi, 1995).

Groundwater on Kodiak Island travels through a number of pathways to streams, rivers, springs, seeps, and to the atmosphere (SAIC, 1995). The general direction of groundwater flow in the Airport vicinity is towards St. Paul Harbor to the east and the Buskin River to the north (P.J. Still, U.S. Geological Survey, unpublished data, 1990, as cited in Hogan and Nakanishi, 1995). Women's Bay ultimately receives all groundwater that hasn't been lost to evapotranspiration.

5.4.2 Freshwater/Saltwater Interface

The location of the freshwater/saltwater interface in groundwater has not been determined at the Kodiak Airport. However, it may be approximated using the Ghyben-Herzberg principle, which suggests that in unconfined coastal aquifers, the depth to which the fresh water lens extends below sea level is approximately 40 times the height of the water table above sea level. In the vicinity of the Kodiak Airport, up to 180 meters of freshwater may overlie the freshwater-saltwater interface (J.O. Brunett and M.R. Carr, U.S. Geological Survey, unpublished data, 1990, as cited in Hogan and Nakanishi, 1995).

5.4.3 Sources of Local Groundwater Pollution

Historical waste-disposal practices and spills from decades of military and aviation uses in the vicinity of the Kodiak Airport have created concerns for existing and future groundwater quality. The USGS, at the request of the Coast Guard in February 1987 initiated a study of the hydrologic and geologic conditions at the Coast Guard Base and adjacent areas. Eighteen areas of potential contamination were studied, over 100 monitoring wells were sampled, and numerous surface water and soils samples were analyzed. Published reports from this investigation include: Allely (1989), Brown (1989), Carr (1996), Combellick (1989), Glass (1996), Solie and Reifenstuhl (1989), and Solin (1996).

Of the 19 sites studied in Glass (1996), five potentially contaminated sites located closest to the runways and two landfills near the Buskin River are discussed here because of their proximity to the runways and the Buskin River (**Figure 8**). The general conditions of these RCRA sites are described in the surface water quality section of this report. All groundwater and site characteristics discussed below are from Glass (1996). The Site reference numbers (for example, "Site 1" are from Glass (1996).

Water quality described in this section refers to Maximum Contaminant Level Goals (MCLG), Maximum Contaminant Levels (MCL) and Secondary Maximum Contaminant Levels (SMCL). The MCL is the maximum allowable level of a contaminant in drinking water which is delivered to any user of a public water system. MCLG is a concentration of a drinking-water contaminant that is protective of adverse human health effects and allows an adequate margin of safety. The U.S. Environmental Protection Agency (USEPA) sets an MCLG at zero for probable or known human cancer-causing compounds (carcinogens). An SMCL provides a guideline for public-water suppliers and is a goal for drinking-water quality.

Site 1 is the former Coast Guard Landfill. Concentrations of all constituents measured in the groundwater at this location were lower than the MCLs for drinking water. At this location, the MCLG standard was exceeded for arsenic, lead, 1,2-dichloroethane, vinyl chloride, and chloroform and the SMCL was exceeded for aluminum, iron, and manganese.

Site 2 is the former U.S. Navy Landfill. Concentrations of all constituents measured in the groundwater at this location were lower than the MCLs for drinking water. Arsenic, 1,2-dichloroethane, and vinyl chloride were detected in groundwater samples at this location in concentrations exceeding MCLG and aluminum, iron, and manganese were detected in groundwater samples at this location in concentrations exceeding SMCL.

Site 5 is a former fire-fighting training area located between Women's Bay and the Airport's north-south runway. Fuels and other flammable liquids were burned sporadically in an unlined pit from around 1979 through 1987. No tested contaminants exceeded MCLs for drinking water; arsenic, lead, and 1,2-dichloroethane were found in groundwater at this location in concentrations exceeding the MCLG. In addition, aluminum, iron, and manganese were found in groundwater at this location in concentrations exceeding the SMCL.

Site 14 is a former quartermaster gas station located near the intersection of Old Tom Stiles Road and Anton Larsen Bay Road northwest of where Kodiak Island Highway crosses the Buskin River. Underground storage tanks may still exist at this location. No contaminants were detected at concentrations exceeding MCLs and two contaminants (Chloroform and 1,2-dichloroethane) were detected in groundwater at levels exceeding MCLG.

Site 15 is a former gas station on G Avenue near the Petersen Elementary School. Underground storage tanks were removed from this location. No contaminants were detected at concentrations exceeding MCLs at this location. Chloroform and 1,2-dichloroethane were detected at levels exceeding MCLG and aluminum and manganese were detected at levels exceeding SMCL in the groundwater at this location.

Site 16 is the Airport staging area and occupies a large proportion of the Airport, excluding the former fire-fighting training area (Area 5) and a few other locations. Over time, various fuels have been spilled or leaked on the property. The locations of some buried fuel tanks are unknown. Lead and cadmium were detected at a concentration exceeding the MCL for drinking water. Cadmium, lead, and 1,2-dichloroethane were detected in the groundwater at concentrations exceeding the MCLG. Aluminum, iron, and manganese were detected at concentrations exceeding the SMCL. Toluene was also detected in one well at a concentration of 6.5 micrograms/liter.

5.4.4 Users of Groundwater

The only groundwater source that is used by the Coast Guard or Airport is for a recreational beach house owned and operated by the Coast Guard located north of the mouth of the Buskin River. The water-supply well for the beach house is over 100 feet deep.

There are no injection wells at ISC Kodiak.

References

ACRC, 2008, Climatological Data – Kodiak Airport, Alaska Climate Research Center website, accessed 5/5/2008 http://climate.gi.alaska.edu/Climate/Location/Southcentral/ Kodiak.html

ADEC, 2006; Water Quality Standards 18 AAC 70; Alaska Department of Environmental Conservation; March 23, 2006

ADEC, 2008, Contaminated Sites Program Database Search. ADEC Division of Spill Prevention and Response website, accessed 5/2/2008 at http://www.dec.state.ak.us/spar/csp/db_search.html

ADT&PF, 1995. Alaska Highway Drainage Manual; Alaska Department of Transportation and Public Facilities; June 1995.

ADT&PF, January 2004. Kodiak Airport Master Plan. AKSAS Project No. 54009, Alaska Department of Transportation and Public Facilities and HDR Alaska Inc, January 2004

Allely, R.D., 1989. Shallow seismic-refraction profiling of the U.S. Coast Guard Reservation, Kodiak, Alaska: Alaska Department of Natural Resources, Division of Geological and Geophysical Survey's Public Data File 89-8C, 73 p.

Brown, J.M., 1989. Bedrock geotechnical properties affecting ground-water movement in the U.S. Coast Guard Reservation, Kodiak Alaska: Alaska Division of Geological and Geophysical Surveys Public Data File 89-8D, 32 p.

Carr, M.R., 1996. Description of wells drilled at the U.S. Coast Guard Support Center Kodiak, Alaska, 1988-89: U.S. Geological Survey Open-File Report 96-134, 233 p.

Christensen, Doug, 2002. The Great Alaska Earthquake of 1964. Alaska Earthquake Information Center, Geophysical Institute, University of Alaska Fairbanks. http://www.aeic.alaska.edu /quakes/Alaska_1964_earthquake.html, November 2002, accessed 3/24/2007.

Combellick, R.A., 1989, Surficial geology of the U.S. Coast Guard Reservation, Kodiak, Alaska. Public Data File 89-8B, Alaska Division of Geological and Geophysical Surveys, Fairbanks, Alaska, 54 p.

Curran, J.H., Meyer, D.F., and Tasker, G.D., 2003, Estimating the magnitude and frequency of peak streamflows for ungaged sites on streams in Alaska and conterminous basins in Canada: U.S. Geological Survey Water-Resources Investigations Report 03-4188.

DOWL Engineers, 2008. *Topographic survey of the Kodiak Airport*. Created for the Kodiak Airport EIS, January 2008, from field surveys in autumn 2007.

EPA, 2000; NPDES Multi-Sector General Permit for Storm Water Discharge Associated with Industrial Activities; United States Environmental Protection Agency; Federal Register Vol 65 No 210; Monday October 30, 2000

EPA, 2004; Assessment Data for Alaska, Kodiak-Afognak Islands Watershed, Year 2004. United States Environmental Protection Agency National Assessment Database.

http://iaspub.epa.gov/tmdl/w305b_report_V4.huc?p_huc=19020701&p_state=AK, 2004, accessed 3/21/08

Fleming, M. (USGS) and Torre Jorgenson (ABRI).ADEC, 2003; Alaska Water Quality Criteria Manual for Toxic and Other Deleterious Organic and Inorganic Substances; Alaska Department of Environmental Conservation; May 15, 2003

Glass, Roy L, 1996. Hydrologic and Water-Quality Data for U.S. Coast Guard Support Center Kodiak, Alaska 1987-89. US Geological Survey, Open-File Report 96-498.

Hartman, C.W., and Johnson, P.R., 1984, Environmental atlas of Alaska: University of Alaska Fairbanks, Institute of Water Resources/Engineering Experiment Station, 95 p.

Hogan, E.V. and Nakanishi, S., 1995. Overview of environmental and hydrogeologic conditions near Kodiak, Alaska. U.S. Geological Survey, Anchorage, Alaska, Open-File Report 95-406, 14 p. plus appendices.

Leopold, Luna; 1994. A View of the River; Harvard University Press.

McGee, D.L., 1972. Kodiak Island and vicinity. State of Alaska Department of Natural Resources, Division of Geological and Geophysical Survey, Alaska Geology and Mineral Resources, Alaska Open File Report 31, 7 p.

NAVFAC, 2006; Comprehensive Site Compliance Evaluation Integrated Support Command Kodiak; Naval Facilities Engineering Command Northwest; December 2006

NOAA, 2006. National Climatic Data Center (NCDC), Climatography of the United States No. 84, 1971-2000, accessed 12/19/2006 <http://www5.ncdc.noaa.gov/cgibin/climatenormals /climatenormals.pl>

NOAA, 2007. Tide Data: Kodiak Island, Alaska Station ID: 9457292, National Oceanic and Atmospheric Administration, Raw Data from < http://tidesandcurrents.noaa.gov/ data_menu.shtml?stn=9457292%20Kodiak%20Island,%20AK&type=Tide%20Data>, accessed 3/24/2007

Nowacki, G. (USFS), P. Spencer (NPS), T. Brock (USFS). 2000. Narrative Descriptions for the Ecoregions of Alaska and Neighboring Territories. U.S. Geological Survey agdcftp1.wr.usgs.gov/pub/projects/fhm/ecounify.doc

Powell, Jim. Alaska Department of Environmental Conservation, Juneau, Alaska. Personal communication with Mauria Pappagallo (Vigil-Agrimis Inc) regarding water quality standards. January 11, 2008

Rosgen, Dave. 1996. Applied River Morphology. Wildland Hydrology, Pagosa Springs, CO.

SAIC, 1995. Final RFI/CMS Report Volume 1 Introduction and facility-wide information, U.S. Coast Guard Support Center Kodiak, Kodiak, Alaska. Prepared for U.S. Coast Guard Facilities Design and Construction Center, Seattle, Washington by Science Applications International Corporation, Olympia, Washington, 125 p. plus appendices.

Shannon & Wilson Inc, 2000. Stormwater Pollution Prevention Plan (SWPPP) Kodiak Airport, Alaska Department of Transportation and Public Facilities Anchorage, Alaska, May 2000.

Sokolowski, Thomas J, 2008. The Great Alaskan Earthquake and Tsunamis of 1964; West Coast and Alaska Tsunami Warning Center, Palmer Alaska. Accessed at: <http://wcatwc.arh.noaa.gov/about/64quake.htm> on 4/4/2008

Solie, D.N. and Reifenstuhl, R.R., 1989. Bedrock Geology of the U.S. Coast Guard Reservation, Kodiak, Alaska. Public Data File 89-8A, Alaska Division of Geological and Geophysical Surveys, Fairbanks, Alaska, 32 p.

Solin, Gary, 1996. Overview of Surface-Water Resources at the U.S. Coast Guard Support Center Kodiak, Alaska. USGS. Anchorage, Alaska.

USACE, 2003; Drury Gulch Kodiak Island, Alaska; USACE and Jacobs Engineering Group Inc, Total Environmental Restoration Contract No. DACA 85-95-D-0018; July 2003.

USCG, 1986. Support Center Kodiak Land Use Plan; United States Coast Guard.

USCG, 2001. Storm Water Pollution Prevention Plan for USCG Integrated Support Command Kodiak. November 2001.

USCG, 2007. Annual Water Quality Report 2007. Integrated Support Command, Kodiak.

USGS, 1978. Water Resources of the Kodiak-Shelikof Subregion, South-Central Alaska; Surface Water Map, W78268

USGS, 1997. Precipitation Map of Alaska, Alaska Geospatial Data Clearinghouse; accessed at <http://agdc.usgs.gov/data/usgs/water/metadata/ak_precip.html> 3/10/2008

Weinmann, Fred, Marc Boule, Ken Brunner, John Malek and Vic Yoshino. 1984. Wetland Plants of the Pacific Northwest. U.S. Army Corps of Engineers. Seattle District.

Appendix A: Figures

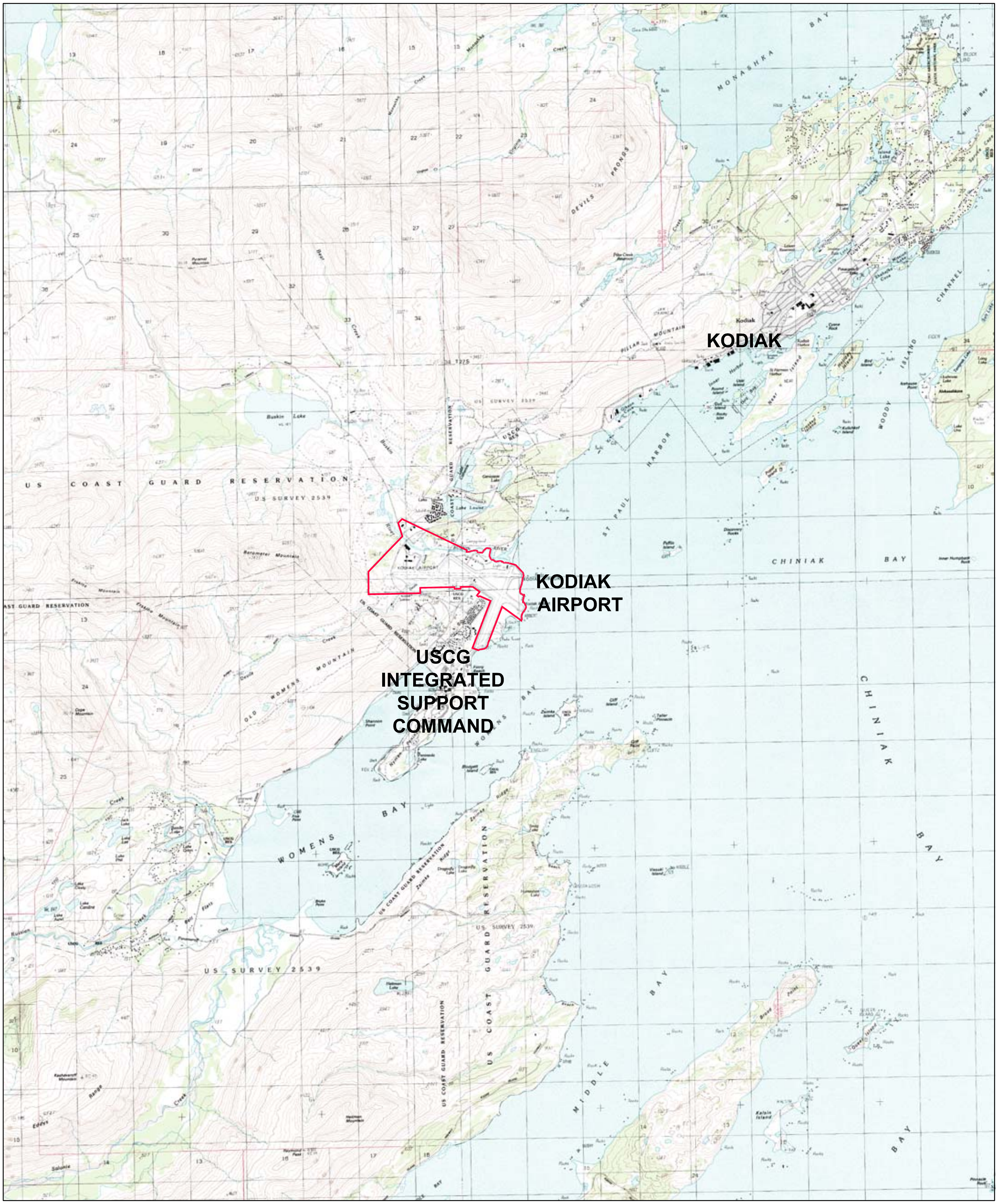

DWG: Y:\BARND001\PHASE 2\CAD\PLOT DWGS\WR-Tech-Memo\Figure_1-VICINITY.dwg USER: mpappagallo
DATE: May 15, 2008 4:41pm XREFS:TB_Figure_8x11-port BARND001_GIS

FIGURE 1
KODIAK AIRPORT VICINITY

0 2000 4000 8000 16000

SCALE: 1"=8000'

Kodiak Airport EIS - *Water Resources Technical Memorandum*

VIGIL AGRIMIS
design professionals

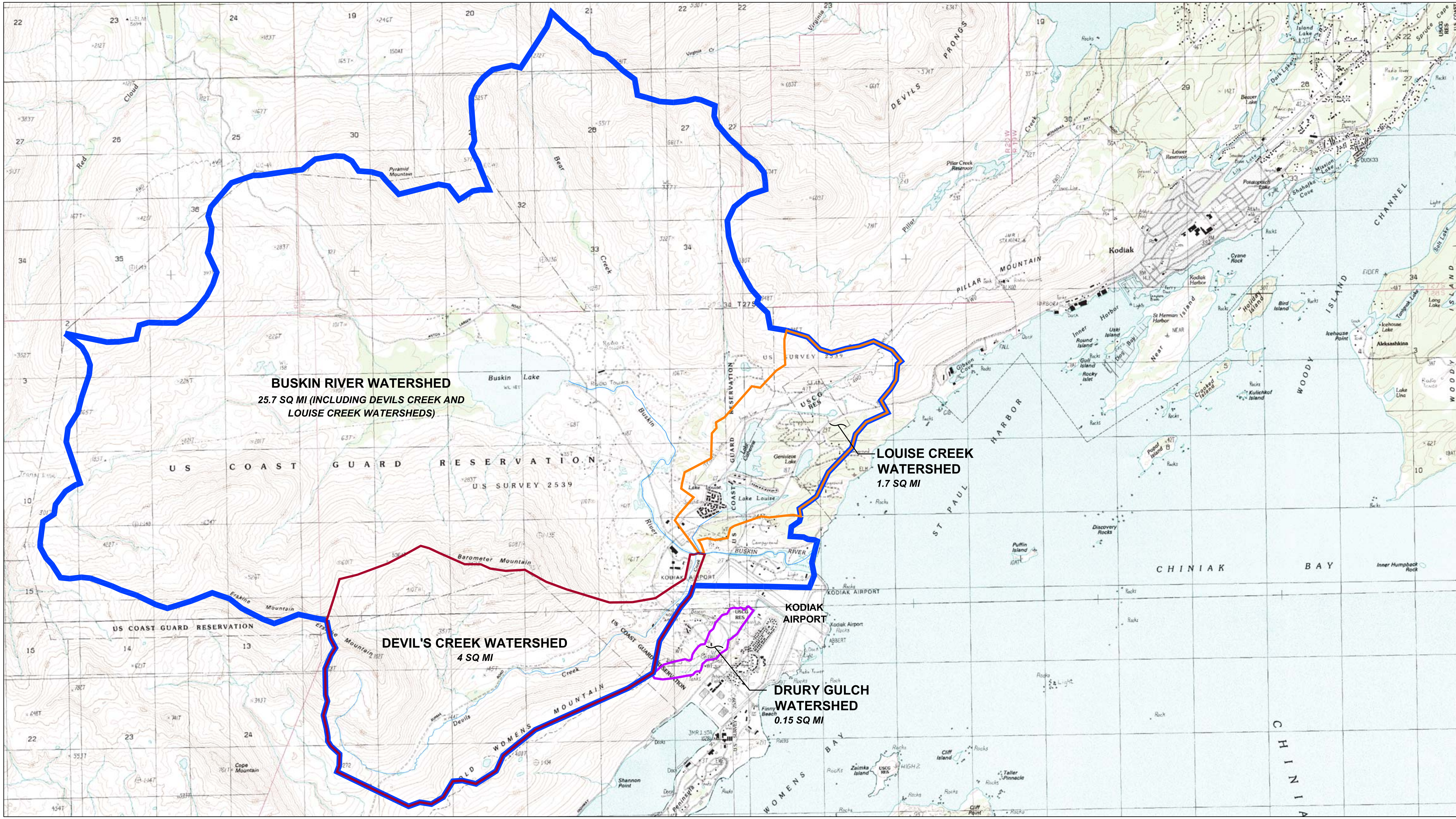

DWG: Y:\BARND001\PHASE 2\CAD\PLOT DWGS\WR-Tech-Memo\Figure_2-Watersheds.dwg USER: mpappagallo
DATE: May 15, 2008 4:27pm XREFS:TB_Figure_11x17 BARND001_GIS

FIGURE 2
WATERSHEDS OF INTEREST SURROUNDING THE KODIAK AIRPORT

CONTOURS IN METERS

0 1250 2500 5000 10000

SCALE = 1"=5000'

Kodiak Airport EIS - *Water Resources Technical Memorandum*

VIGIL AGRIMIS design professionals

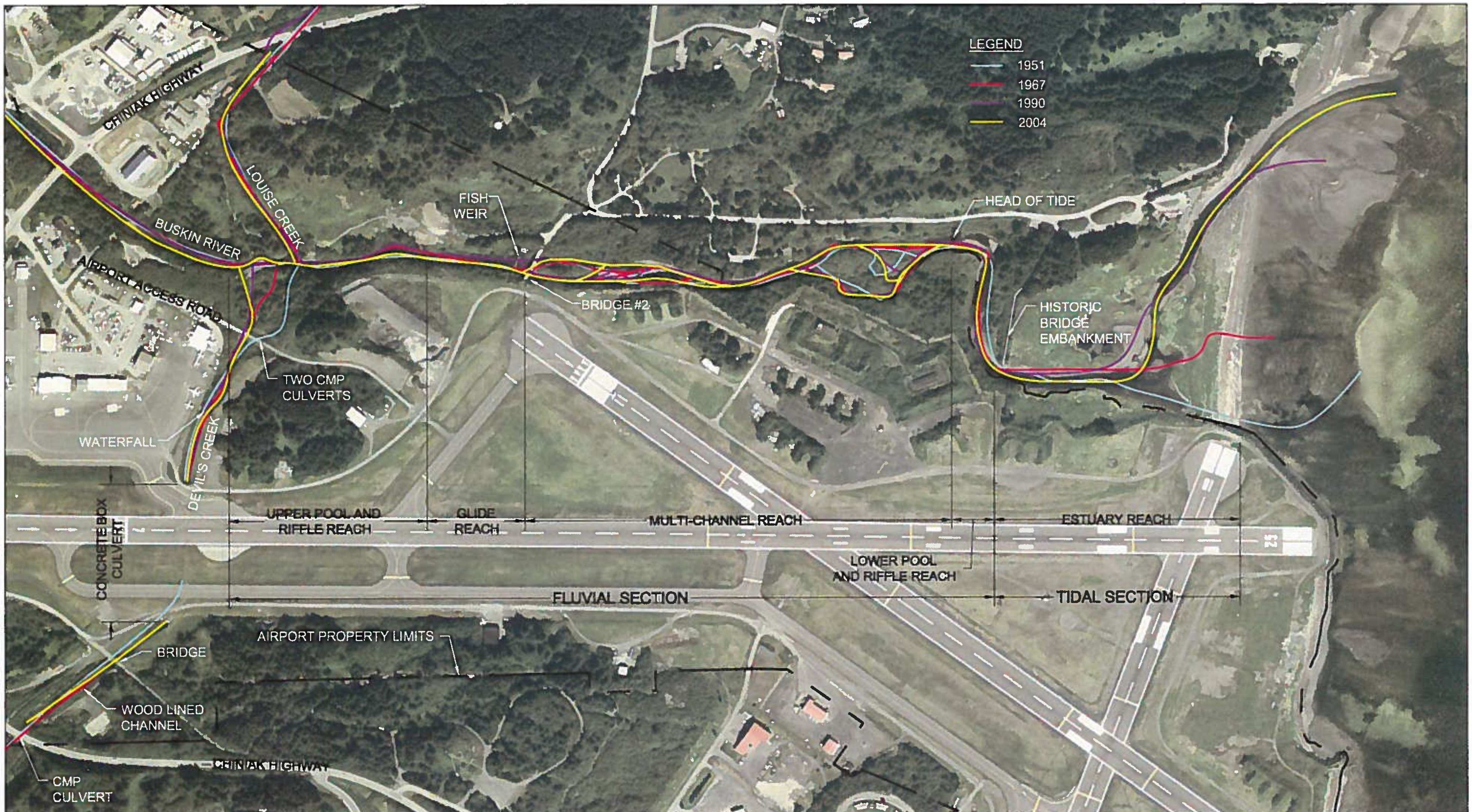

2004 AERIAL PHOTO

FIGURE 3
CHANNEL PLANFORM COMPARISON 1951 TO 2004

0 125 250 500 1000
SCALE 1" = 500'

Kodiak Airport EIS - *Water Resources Technical Memorandum*

VIGIL AGRIMIS
design professionals

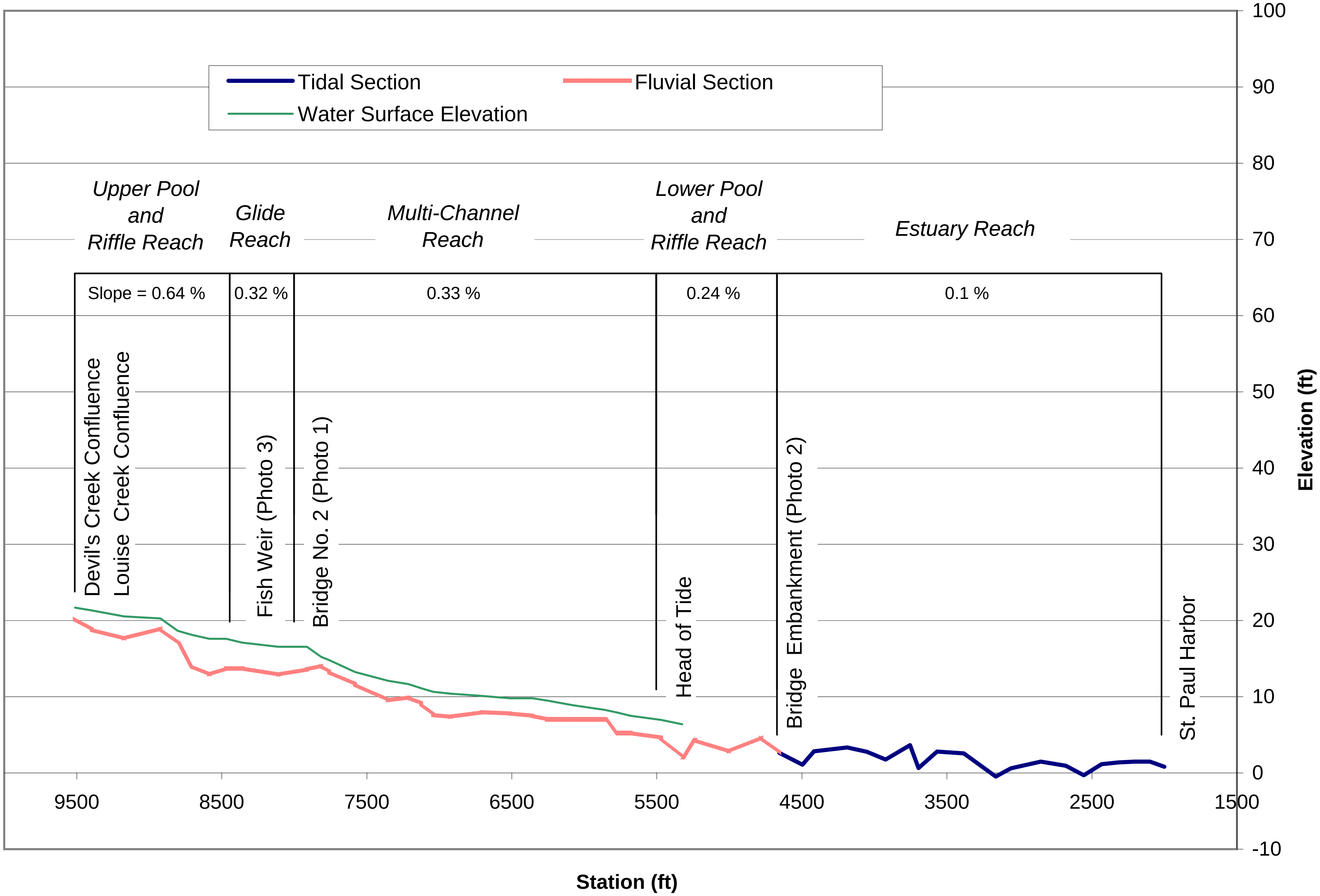

FIGURE 4
BUSKIN RIVER PROFILE THROUGH THE PROJECT AREA
Kodiak Airport EIS - *Water Resources Technical Memorandum*

Y:\BARND001\PHASE 2\4-Stream Assessment\Buskin-Profile.xls

VIGIL AGRIMIS design professionals

FIGURE 5
BUSKIN RIVER SEDIMENT SAMPLING LOCATIONS

Kodiak Airport EIS - *Water Resources Technical Memorandum*

VIGIL AGRIMIS
design professionals

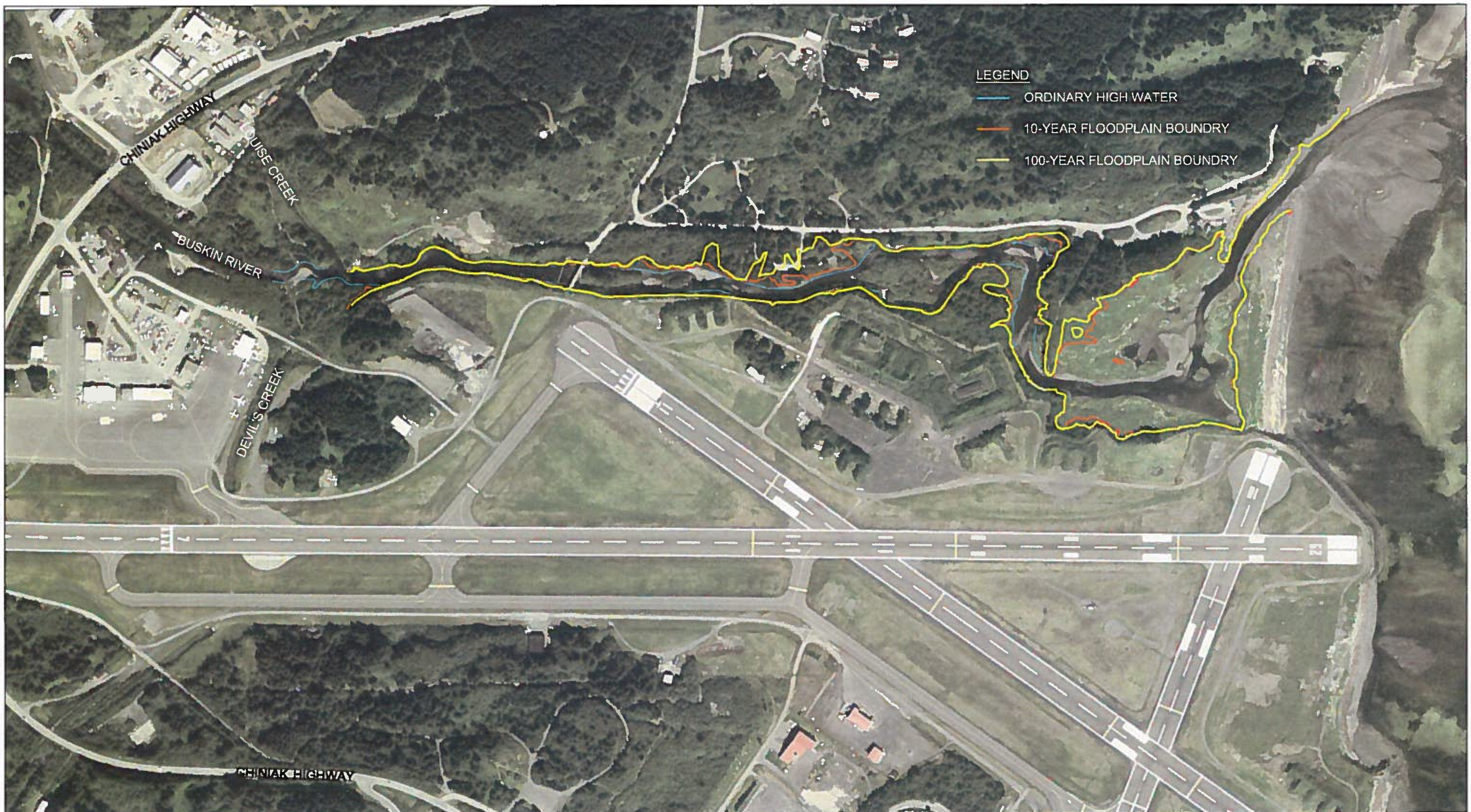

FIGURE 6
BUSKIN RIVER ORDINARY HIGH WATER AND FLOODPLAIN BOUNDRY MAP

0 125 250 500 1000
SCALE 1"=500'

Kodiak Airport EIS - *Water Resources Technical Memorandum*

VIGIL AGRIMIS
design professionals

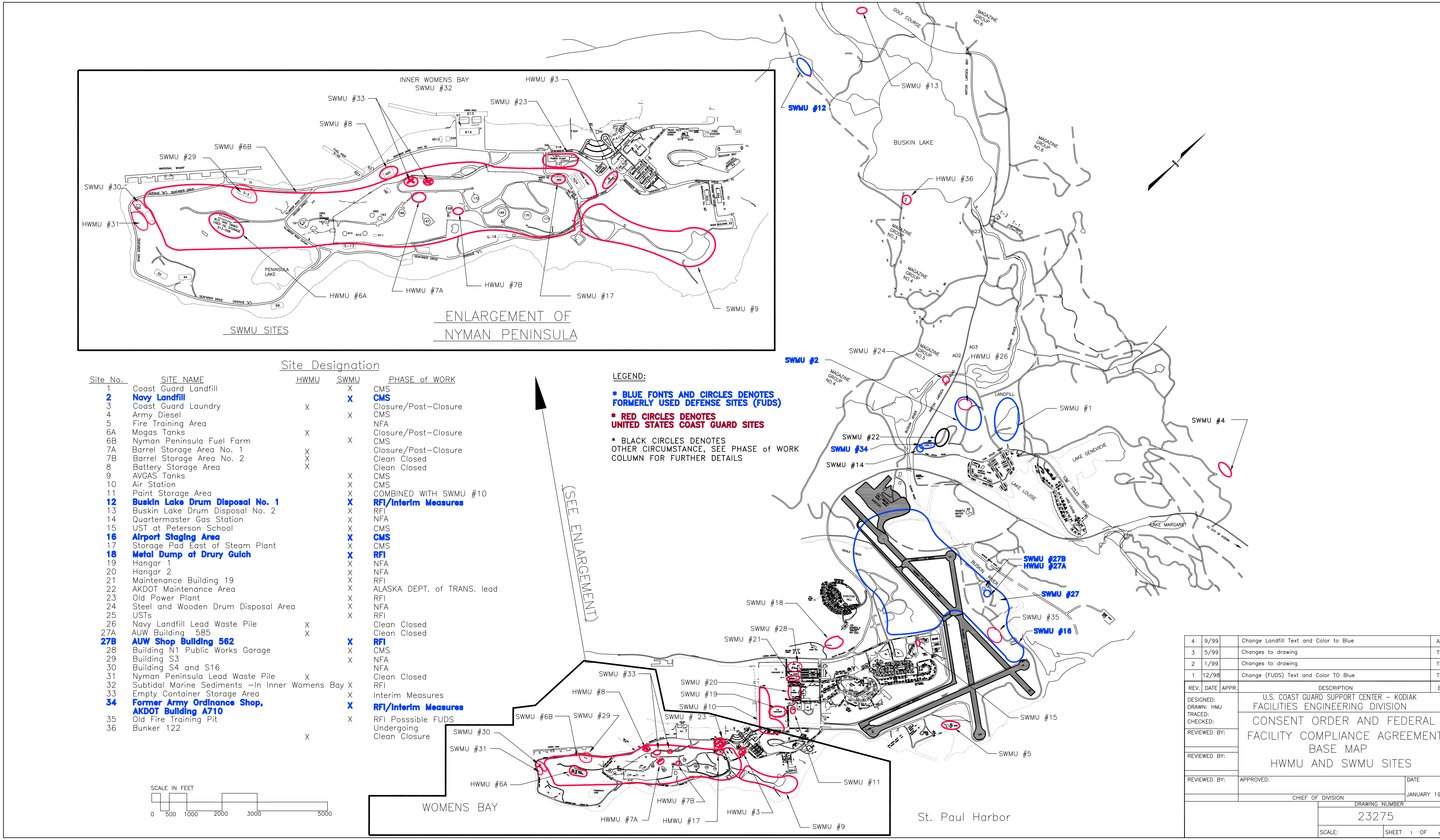

Site Designation

Site No.	SITE NAME	HWMU	SWMU	PHASE of WORK
1	Coast Guard Landfill		X	CMS
2	**Navy Landfill**		**X**	**CMS**
3	Coast Guard Laundry	X		Closure/Post–Closure
4	Army Diesel		X	CMS
5	Fire Training Area			NFA
6A	Mogas Tanks	X		Closure/Post–Closure
6B	Nyman Peninsula Fuel Farm		X	CMS
7A	Barrel Storage Area No. 1	X		Closure/Post–Closure
7B	Barrel Storage Area No. 2	X		Clean Closed
8	Battery Storage Area	X		Clean Closed
9	AVGAS Tanks		X	CMS
10	Air Station		X	CMS
11	Paint Storage Area		X	COMBINED WITH SWMU #10
12	**Buskin Lake Drum Disposal No. 1**		**X**	**RFI/Interim Measures**
13	Buskin Lake Drum Disposal No. 2		X	RFI
14	Quartermaster Gas Station		X	NFA
15	UST at Peterson School		X	CMS
16	**Airport Staging Area**		**X**	**CMS**
17	Storage Pad East of Steam Plant		X	CMS
18	**Metal Dump at Drury Gulch**		**X**	**RFI**
19	Hangar 1		X	NFA
20	Hangar 2		X	NFA
21	Maintenance Building 19		X	RFI
22	AKDOT Maintenance Area		X	ALASKA DEPT. of TRANS. lead
23	Old Power Plant		X	RFI
24	Steel and Wooden Drum Disposal Area		X	NFA
25	USTs		X	RFI
26	Navy Landfill Lead Waste Pile	X		Clean Closed
27A	AUW Building 585	X		Clean Closed
27B	**AUW Shop Building 562**		**X**	**RFI**
28	Building N1 Public Works Garage		X	CMS
29	Building S3		X	NFA
30	Building S4 and S16			NFA
31	Nyman Peninsula Lead Waste Pile	X		Clean Closed
32	Subtidal Marine Sediments –In Inner Womens Bay		X	RFI
33	Empty Container Storage Area		X	Interim Measures
34	**Former Army Ordinance Shop, AKDOT Building A710**		**X**	**RFI/Interim Measures**
35	Old Fire Training Pit		X	RFI Posssible FUDS
36	Bunker 122	X		Undergoing Clean Closure

LEGEND:

*** BLUE FONTS AND CIRCLES DENOTES FORMERLY USED DEFENSE SITES (FUDS)**

*** RED CIRCLES DENOTES UNITED STATES COAST GUARD SITES**

* BLACK CIRCLES DENOTES OTHER CIRCUMSTANCE, SEE PHASE of WORK COLUMN FOR FURTHER DETAILS

REV.	DATE	APPR.	DESCRIPTION	BY
4	9/99		Change Landfill Text and Color to Blue	AR
3	5/99		Changes to drawing	TM
2	1/99		Changes to drawing	TM
1	12/98		Change (FUDS) Text and Color TO Blue	TM

DESIGNED:
DRAWN: HMJ
TRACED:
CHECKED:
REVIEWED BY:
REVIEWED BY:
REVIEWED BY:

U.S. COAST GUARD SUPPORT CENTER – KODIAK
FACILITIES ENGINEERING DIVISION

CONSENT ORDER AND FEDERAL FACILITY COMPLIANCE AGREEMENT
BASE MAP
HWMU AND SWMU SITES

APPROVED:
CHIEF OF DIVISION
DATE JANUARY 1995
DRAWING NUMBER 23275
SCALE:
SHEET 1 OF 1

DWG: Y:\BARND001\PHASE 2\CAD\PLOT DWGS\WR-Tech-Memo\Figure_8-RCRA.dwg USER: mpappagallo
DATE: May 15, 2008 3:22pm XREFS:TB_Figure_11x17 23275smu BASE MAP HWMU SWMU SITE MJP

FIGURE 8
USCG RCRA SITE LOCATIONS

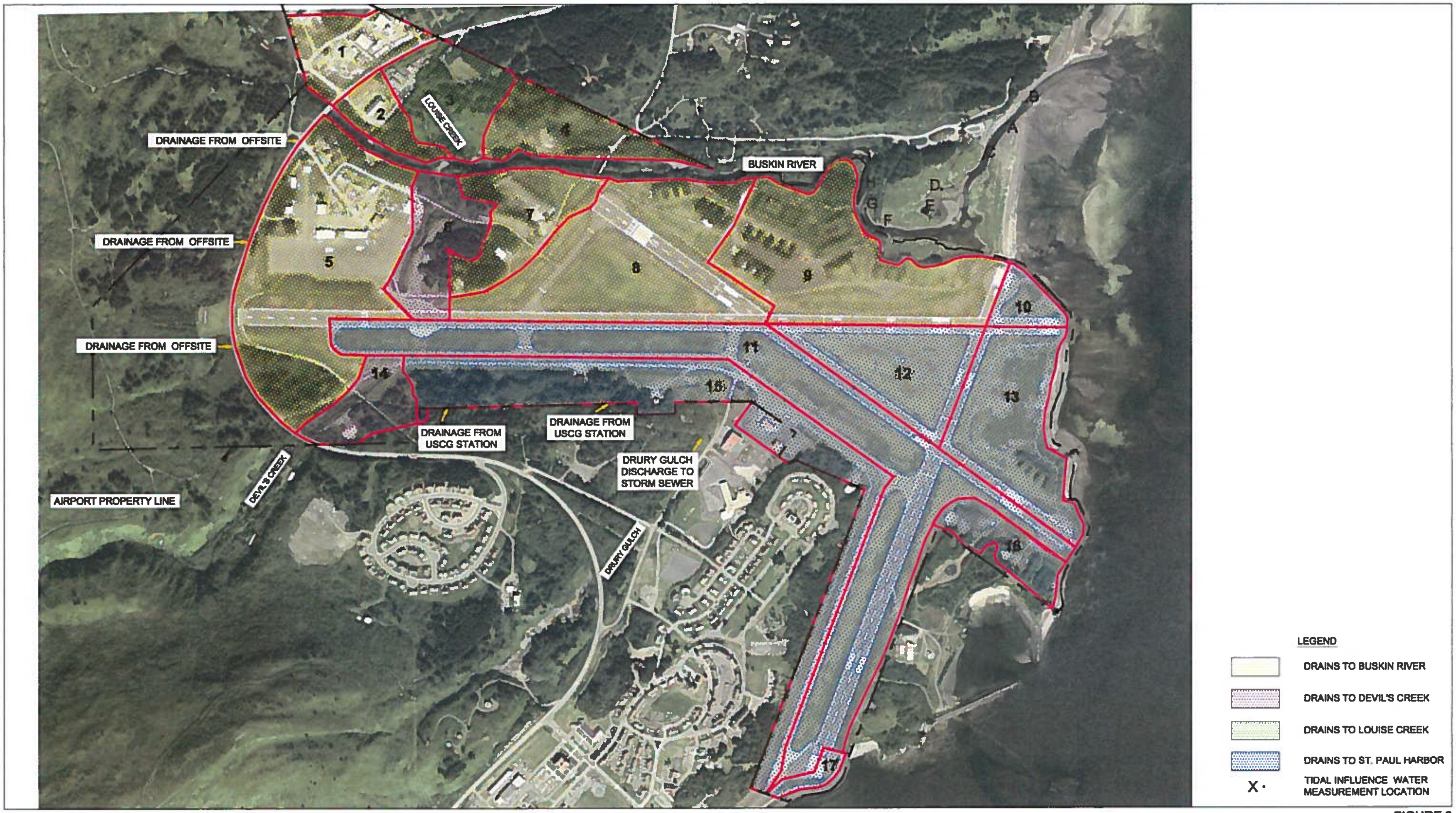

FIGURE 9
STORMWATER DRAINAGE BASINS AT THE KODIAK AIRPORT

Kodiak Airport EIS - *Water Resources Technical Memorandum*

VIGIL AGRIMIS design professionals

Appendix B: Wetland Delineation Report

Appendix C: Hydraulics Technical Memorandum

TECHNICAL REPORT-DRAFT

RUNWAY SAFETY AREA IMPROVEMENT ALTERNATIVES STUDY

INCLUDES

COASTAL AND NEAR-SHORE PROCESS DESCRIPTION CIRCULATION AND WATER QUALITY MODELING, AND WAVE MODELING

Prepared for

DOWL ENGINEERS

Prepared by

COASTLINE ENGINEERING

And

Dynamic Solutions-International, LLC

May 2009

TABLE OF CONTENTS

List of Tables

List of Figures

Executive Summary

This report describes the coastal and near-shore processes occurring in portions Chiniak Bay, St. Paul Harbor and Womens Bay near the Kodiak Airport in Kodiak, Alaska. In addition, this report presents the results of circulation, water quality and wave modeling for existing conditions and for various Runway Safety Area (RSA) improvement alternatives proposed at the airport in the Kodiak Airport RSA Improvement EIS.

Kodiak has a maritime climate that is generally dominated by weather patterns of the North Pacific. At times, particularly in the winter, it is strongly influenced by mainland Alaska weather

The majority of its shorelines consist of narrow (in some cases nonexistent) beaches backed by steep bluffs of rock outcrops. Very little longshore transport occurs in the area, as there is minor sediment input into the system. Sediments are being delivered to the shoreline by several small streams at the head of Womens Bay and by the Buskin River.

The Buskin River area does exhibit typical longshore and onshore/off shore transport processes, but it is diminished by lack of sediment supply and minor longshore transport energy.

The circulation and water quality characteristics were modeled using a two-dimensional, vertically averaged, finite difference model that was calibrated using real tidal heights, water velocities and airport winds.

The tides and current data were collected from Acoustic Doppler Current Profilers at four locations within the western end of Chiniak Bay for the entire month of October, 2007. Subsequent analysis demonstrated that this period was representative of the distribution of wind speeds and directions for the entire average year.

The modeling demonstrated the following existing conditions:

- The project area was controlled by very low water currents and a large, slow-moving eddy whose southern boundary generally coincided with the mouth of the Buskin River.
- Tidal flows in this area were limited to just a few centimeters per second (cps).
- Wind were a more dominant factor than the tides and often increased surface currents to 20-25 cps.
- Wave-induced bed shear stresses exceed those caused by the currents, which were only strong enough to initiate movement of very fine sediments.
- Even though waves were responsible for stronger shear stresses, they dissipated rapidly as they encountered the shallow waters of the western portion of Chiniak Bay and St. Paul Harbor. The shallow water also refracted these waves so that

they approached nearly parallel to the shorelines which reduced the longshore transport wave energy.
- The Buskin River fresh water plume moved towards the south under certain wind conditions.

Modeling of the proposed RSA extensions showed the following:
- The RSA extensions could provide shoreline protection from waves resulting in a further lowering of an already minimal amount of sediment transport energy.
- The structures could bury or isolate sediment sources that currently may be used in part to assist in the northward migration of the mouth of the Buskin River.
- The RSA extension on Runway 07/25 could alter the southward flow of the Buskin River freshwater plume, as the flow would be forced into deeper waters with increased velocities.
- The RSA extension of Runway 18/36 would completely cover much of the existing sandy beach along the barrier bar just seaward of the river.

1. INTRODUCTION

FAA is in the process of conducting a Runway Safety Area Improvement Alternatives Study (RSAIAS) to bring the Kodiak Airport (ADQ) into compliance with FAA regulations. As part of that process an Environmental Impact Statement (EIS) is required. Several alternatives are being considered to modify the airport runways. Any of these alternatives, if constructed, could have impacts on the region around the airport. Obviously, not all the impacts will have the same effect or zone of influence. This technical report will address the coastal and near-shore oceanographic effects to the physical environment.

Specifically this report will address the coastal engineering, coastal processes and the numerical modeling that was done to describe the existing conditions in the affected area. Later additions will address the specific changes that each of the alternatives will make. It will provide descriptions of the affected area and relevant processes that continue to change that area. Weather, general circulation, tides, waves, coastal processes, and water exchange within the area will be addressed in an attempt to provide a baseline for accessing changes that might occur from any of the alternatives. This report describes the results of literature research, field investigations, engineering analysis and numerical modeling directed toward a better understanding of what is occurring within the affected area.

2. KODIAK PHYSICAL CONDITIONS

2.1 Geographic Setting

The City of Kodiak is located on the eastern side of Kodiak Island and is 250 miles south-southwest of Anchorage and 100 miles SSW off the southern tip of the Kenai Peninsula. Its nearest distance to the Alaska mainland is 70 miles to the WSW (Figure 1). Kodiak Island is the largest island in the Kodiak Archipelago and the second largest island in the United States. This archipelago is composed of several islands whose coasts are crenulated with numerous bays and inlets and its terrain has been highly modified by both tectonic and glacial forces. The City of Kodiak is located on the northeast corner of Kodiak Island in St. Paul Harbor, one of several bays inside Chiniak Bay.

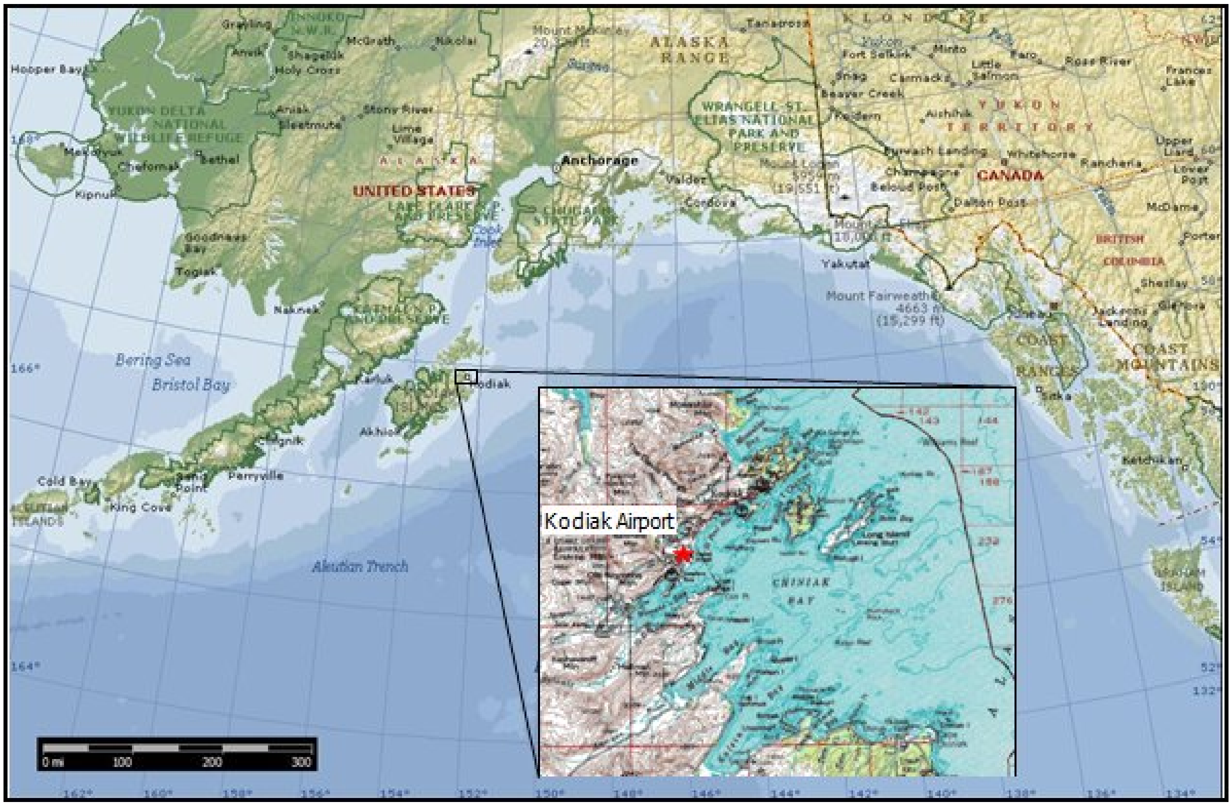

Figure 1 Kodiak Airport location map.

Chiniak Bay is the major water body to which the affected area is a part. It forms an indentation in the northeastern Kodiak Island shoreline between Spruce Cape north of the City of Kodiak and Cape Chiniak[1] about 14 naut. miles to the south-southeast. It contains both Near and Long Islands and numerous smaller islands. The bay is totally exposed on its east to the Gulf of Alaska and bounded on the west by the Kodiak shoreline (Figure 2).

Its westward extension into the affected area includes St. Paul Harbor on the northwest and Womens Bay on the southwest. These two contiguous water bodies are somewhat isolated from and protected by a series of islands and shoals that severely restrict Gulf of Alaska wave activity inside the affected area. Outside the protected area, the wave activity can be extreme. This protection plus additional sheltering from natural projections and indentations in the shoreline within the affected area result in it being either moderately or well protected.

The airport is located between St. Paul Harbor and Womens Bay almost 4 miles southwest of the city and immediately south of the Buskin River delta. The Buskin River

[1] NOAA Chart 16580

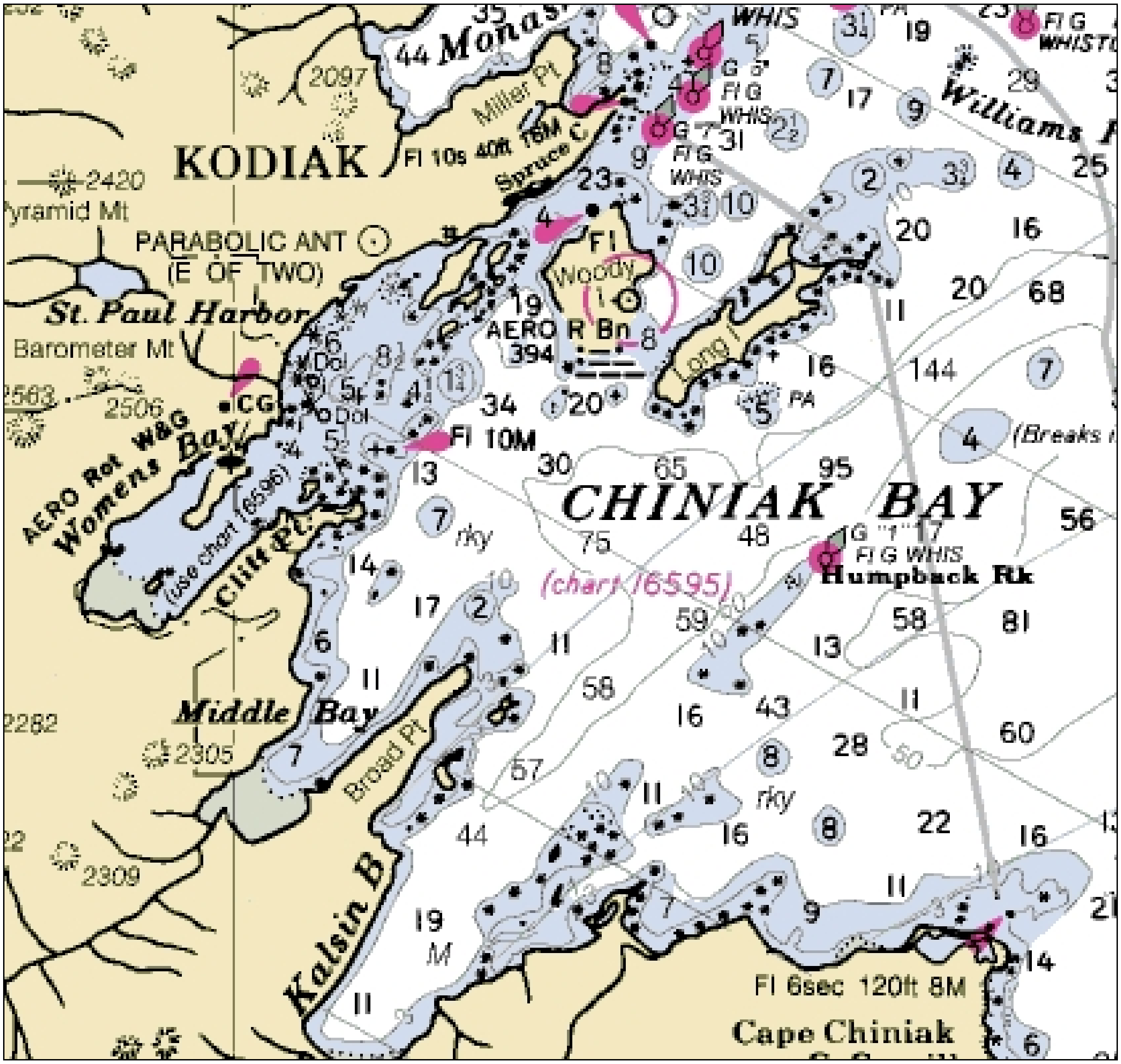

Figure 2 Chiniak Bay (NOAA Chart 16580).

flows from Buskin Lake about 3 miles to the northwest. The runway is on the site of the former Naval Air Station Kodiak. The Naval Station was closed in 1950 and the airport property was turned over to the Coast Guard in 1971. The State of Alaska leases the property for the airport that includes three runways (Figure 3). The existing runways were constructed of fill and apparently required diverting the Buskin River channel to the north to acquire sufficient land for the facilities. This was done about 1939-40. Presumably, much of the river's delta was also incorporated into the fill project. All of the runways are paved and two are possibly upgrade candidates as part of the current EIS.

Figure 3 Kodiak Airport.

Water depths in excess of 60 feet occur just seaward of the small islands that separate Womens Bay and St. Paul Harbor from the more exposed part of Chiniak Bay. Depths of 500 feet and greater occur on the eastern side of the bay.

Inside the protective islands, the water shoals considerably although two deep spots of 60 feet (one in Womens Bay and another in St. Paul Harbor) do occur (Figure 4). The shoaling seems to be the result of deposition mainly from the Buskin River and at the head of Womens Bay.

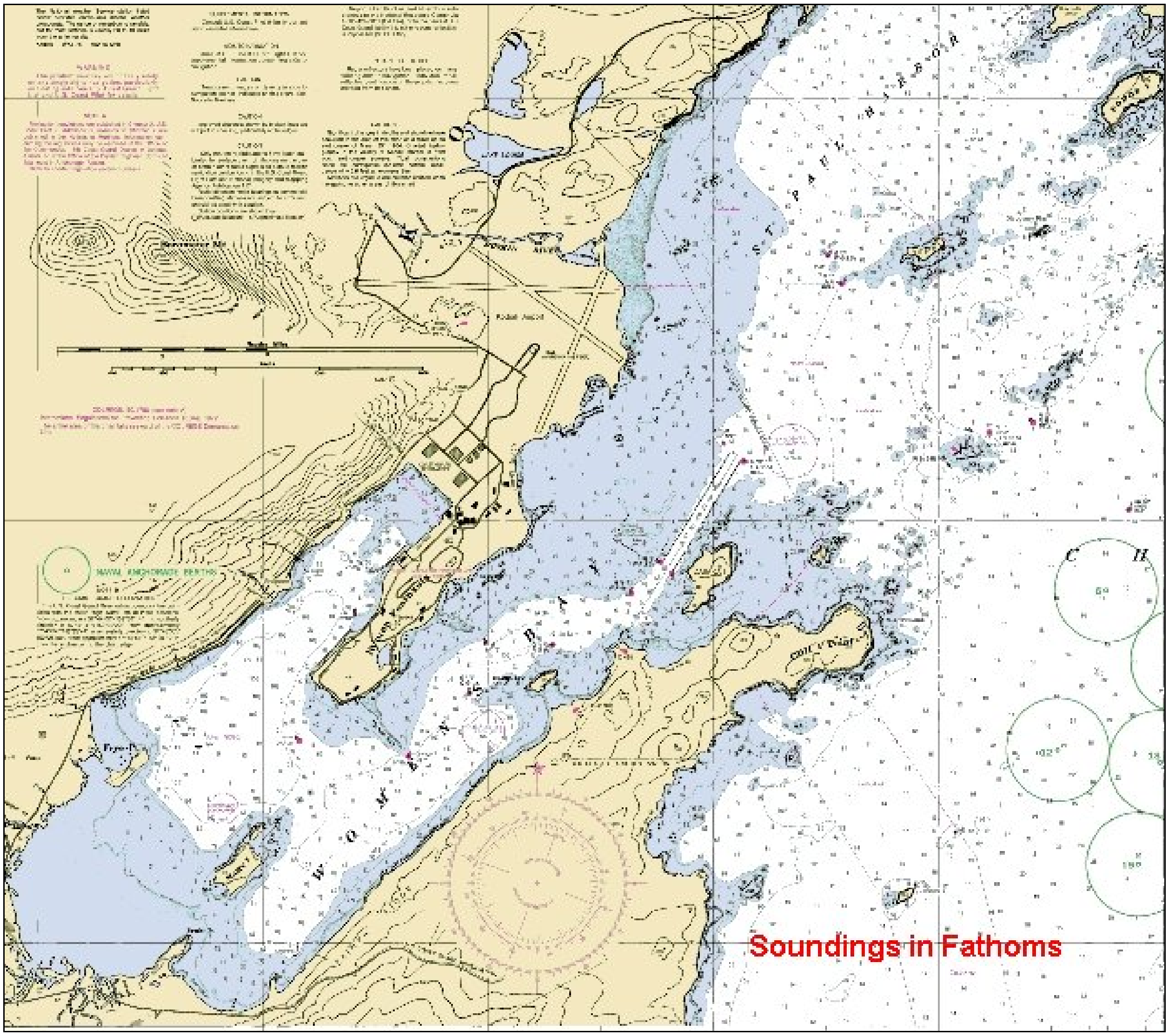

Figure 4 Project area (NOAA Chart 16595).

2.2 Kodiak Climate

The climate of Kodiak is summarized in Table 2.1. It has a typical maritime climate that includes above average precipitation and has more moderate temperatures than found on the Alaska mainland away from the coast. Summers are cooler and winters are warmer than the mainland.

Table 2-1 **General Climate for Kodiak Airport (1973-2007)**[2]

	Jan	Feb	Mar	Apr	May	Jun	Jul	Aug	Sep	Oct	Nov	Dec	Annual
Avg. Max Temp (°F)	35.7	36.0	38.8	43.7	50.1	55.8	60.4	62.0	56.3	47.2	39.8	36.5	46.9
Avg. Min Temp (°F)	26.4	25.7	27.8	32.6	38.7	44.4	49.1	49.0	43.4	34.8	29.1	25.9	35.6
Avg. Mean Temp (°F)	31.2	30.9	33.2	38.2	44.4	50.1	54.8	55.5	49.9	41.0	34.5	31.2	41.2
Record High Mean Temp (°F)	53	55	53	69	76	82	82	79	73	62	54	56	66.2
Record Low Mean Temp (°F)	-16	-8	1	7	24	31	38	34	26	10	2	-2	12.3
Avg. Total Precipitation (in)	8.72	6.01	5.20	5.61	5.85	5.59	4.43	4.58	7.43	8.54	6.81	8.26	6.4
Max Total Precipitation (in)	16.4	12.4	12.7	12.6	12.7	16.9	10.2	11.1	19.4	17.1	15.9	19.8	14.8
Min Total Precipitation (in)	0.31	1.44	0.67	0.29	1.53	0.67	0.84	0.65	1.20	3.15	0.68	1.21	1.1
Avg. Total Snowfall (in)[3]	12.7	12.7	13.5	5.8	0.4	0	0	0	0	2.0	4.9	11.2	5.3

Daylight hours range from as few as eight hours at winter solstice to more than 20 at summer solstice. Summer temperatures average 65°F, but can be as warm as the mid-70s on occasion or as cool at the mid-50s during the day. The average range of winter temperatures is 10-35 degrees.

2.3 Tsunami Potential

The tsunami (seismic sea wave) threat is greater in Alaska than any other place in the United States. The 1964 Earthquake generated the most destructive tsunami ever recorded in Alaska. It caused loss of life or destruction of property or both in nearly all coastal regions of south-central Alaska, along the west coast of Canada and the U.S. and in Hawaii. The impact in Kodiak was severe with eight lives lost, 158 houses destroyed and a total of $31 million worth of damage.

Since then the Alaska Earthquake Information Center has prepared maps of anticipated earthquake flooding limits for a number of earthquake scenarios which include both a variety of magnitudes and different source functions. An example of the impacts found in the affected area can be seen in Figures 5a and 5b.

[2] Source: Western Region Climate Center
[3] For 1931-1971

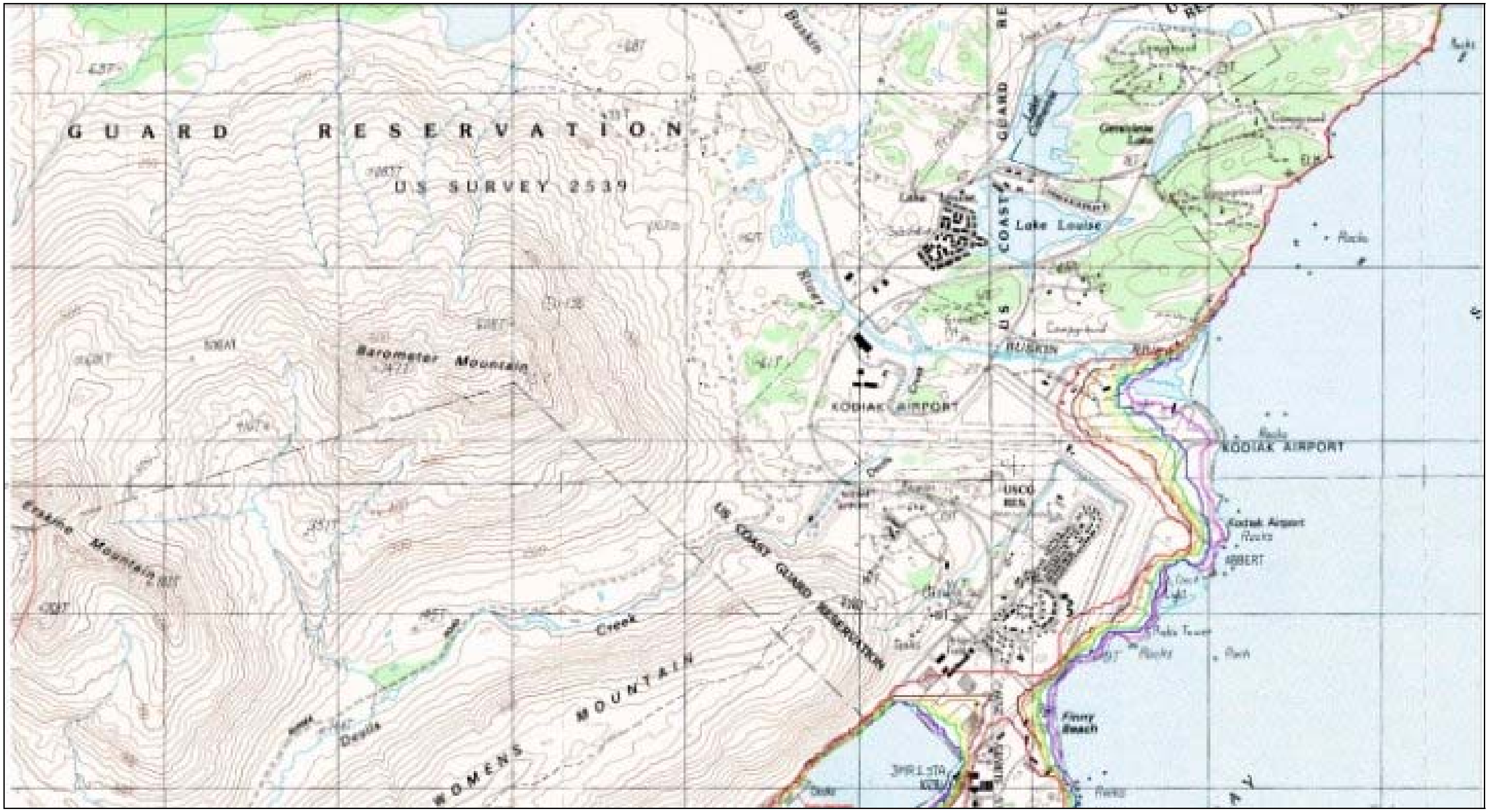

Figure 5a **Tsunami inundation map (northern area).**

Figure 5b Tsunami inundation map (southern area).

The lines drawn over the affected area represent the shoreward limits of flooding for various earthquake scenarios. The shore-most red line represents the probable limits of the 1964 earthquake with 17 sub-faults creating the seismic sea wave. This is assumed to be the worst that could occur. The limits were the results of computer simulations for the given scenarios.

A tsunami in Kodiak will more than likely behave like a short period tide rather than like a breaking wave that tends to attract surfers. As a result the effect will be to cause a rapid rise in sea level and serious flooding. It appears that the project and a good portion of the Buskin River mouth and near-shore region would likely be flooded. Other than damage from the actual earthquake, it is likely that runway facilities could resume service relatively soon after a tsunami impacted the affected area. The runway could receive extensive drift debris.

2.4 General Oceanography

2.4.1 Regional Circulation

There are relatively large-scale current systems on both the east and west side of Kodiak Island (Reed and Schumacher, 1987). On the west side is the strong Alaska Coastal Current that may develop as far away as along the coast of British Columbia and follow the coast north along southeastern Alaska and then west along south-central Alaska (Figure 6). It gains strength and size as the freshwater coastal drainage continues to reinforce it. Some and perhaps all of this current may enter Prince William Sound, and upon exiting the sound it resumes its journey west (Weingartner, 2005) passing the mouth of Cook Inlet. The majority continues to the west-southwest.

The current system on the east side of Kodiak is made up primarily from a portion of the eastward flowing North Pacific that breaks off forming the northward directed Alaska Current on the east side of the Gulf of Alaska (Reed and Schumacher, *op. cit*.). It continues on a counter-clockwise path and just north of Kodiak it narrows to about half its previous width and becomes the Alaska Stream as it passes Kodiak and continues west-southwestward. It may merge with a portion of the Alaska Coastal Current near the mouth of Cook Inlet.

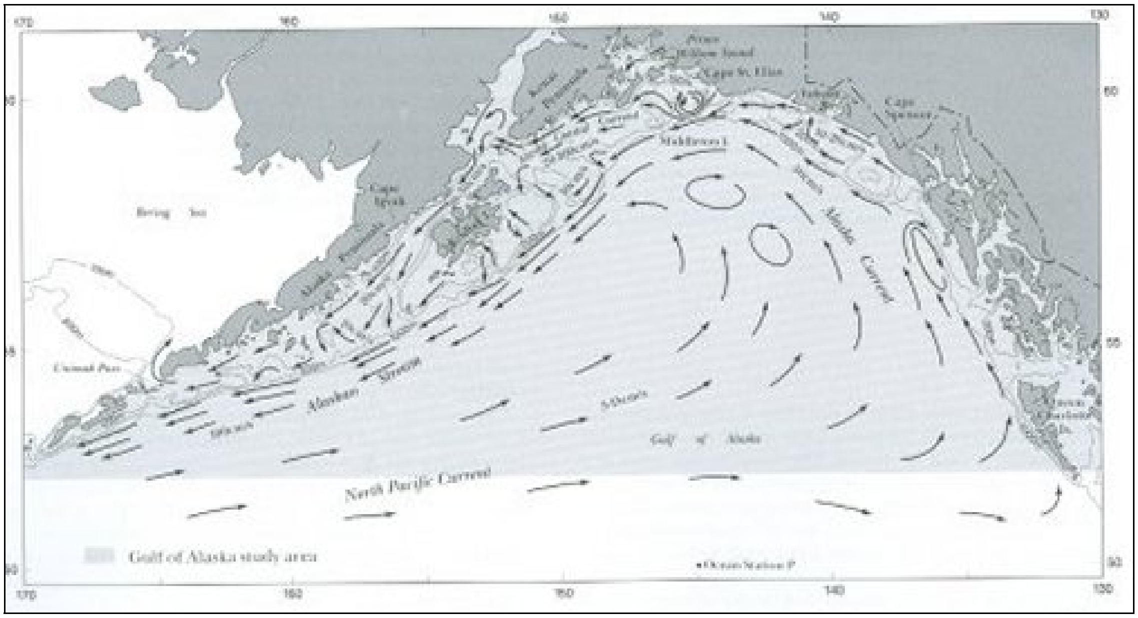

Figure 6 Ocean currents in the Gulf of Alaska.

While the Alaska Stream does pass Kodiak, its western boundary seems to be 50 miles or so east of the island. Therefore it may have relatively little influence on the circulation in Chiniak Bay or the area directly affected by the project. Circulation here seems more a result of local tides, depth and geographic configuration; winds generate surface currents.

2.4.2 Local Currents

The currents in the affected area are driven primarily by local tides. The mean tidal ranges in the affected area is less than 9 feet (see next section) and given the openness of the area large tidal currents would not be likely. The most probable location for high tide currents would be in the channel between Woody and Kodiak Islands near the city center. Local data were collected for a limited time as part of the data collection program for this EIS.

Primarily in support of the computer circulation modeling that will be described in a later section, data were collected at four locations during a one-month period and at two additional locations for a second month. The reason for the second deployment was to insure that enough data would be available in case an error occurred in any of the initial deployments. All meters seemed to function well and the data from the second deployment was not needed to calibrate the computer model. These data will be discussed in greater detail in the computer modeling section.

Pertinent details of the deployment for the first four meters are provided in Table 2.2. They were all Acoustic Doppler Current Profilers (ADCPs) and were capable of measuring the two horizontal components of the current at multiple elevations between the bottom and the surface of the water column. The measurements were collected between October 3rd and November 4th of 2007.

Table 2-2 Kodiak Airport ADCP Current Stations

STATION	Seabed Elevation Feet (MLLW) [Meters]	North Lat	West Long
Women's Bay	-50.5 (-15.4)	57° 43.515563'	152° 29.391658'
Airport	-23.6 (-7.2)	57° 44.755945'	152° 28.013994'
Cliff Point.	-82 (-25.0)	57° 44.053485'	152° 25.694903'
Woody Island.	-113.8 (-34.7)	57° 48.095493'	152° 20.261667'

Figure 7 presents part of NOAA Chart 16595 with the locations of the four instrument packages. An example of a typical instrument ensemble used to collect the data can be seen in Figure 8. This view is from the top looking down on the frame and instruments; the bottom is sitting on a grating that is part of the boat deck. The blue-topped instrument with the four red circles is the ADCP. The cylindrical object below is the acoustic release that facilitates recovery of the equipment after deployment, the red spherical device is the "pop-up" float for the release and the white object to its right and below is the line storage canister for the release.

Figure 9 presents a short current speed record (about four tidal cycles) from the four instruments. The current speeds for the three more southerly locations suggest a low flow regime relative to the Woody Island site. This could certainly suggest that flushing in the affected area and in particular Womens Bay could be limited. This will be examined in greater detail in the discussion of the modeling results.

2.4.3 Tides and Tidal Datums

Like most places in Alaska, Kodiak tides are semi-diurnal mixed tides. They are "semi-diurnal" because they are driven by astronomical motions with a period of about 12 hours. There is also a diurnal inequality in the two daily tides with one of the highs being significantly higher than the other, and, conversely, there is one low tide that is lower than the other. This inequality is the reason they are "mixed" and is due to influences from motions with periods of about 24 hours. The following table (Table 2.3) presents the key benchmarks gleaned from the tidal record. Until 1994 tide measurements were acquired from a NOAA reference station located along the city docks near downtown Kodiak. Then the tide recorder was moved to the Coast Guard Base and is located in Womens Bay on the northwestern shoreline of the Nyman

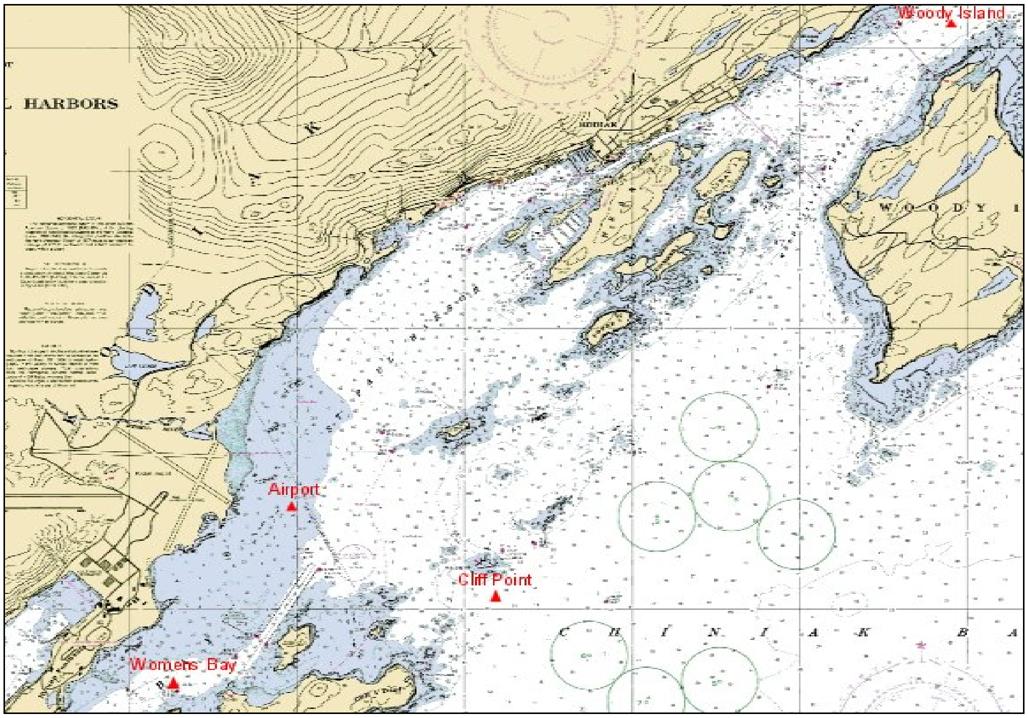

Figure 7 Location of the four Acoustic Doppler Current Profilers (ADCP).

Figure 8 Typical instrument ensemble including ACDP and release.

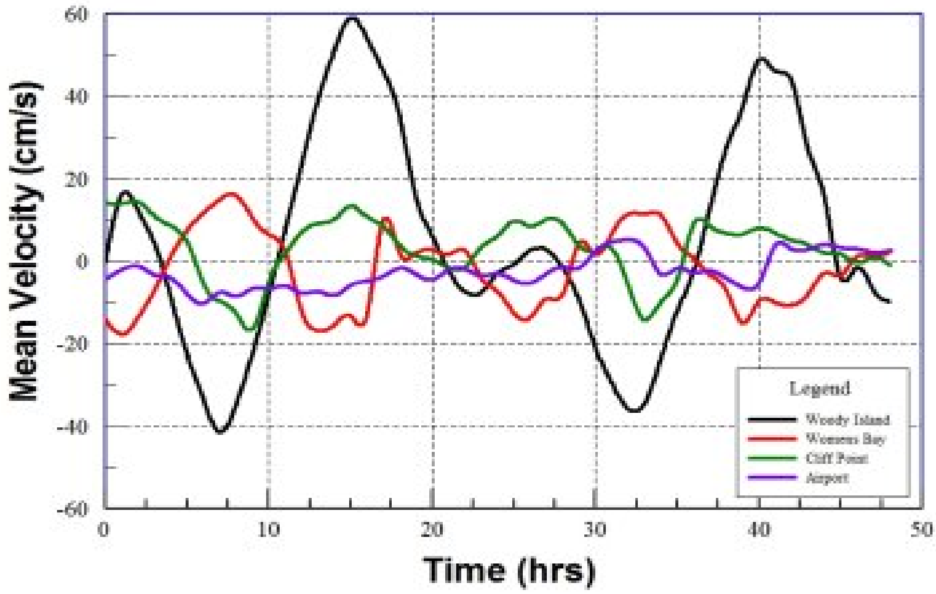

Figure 9 Short ADCP records for each instrument (about 4 tidal cycles).

Table 2-3 Kodiak, AK Tidal Datums[4]	
Datum	**Elevation (ft)**
Highest Observed Water Level (12/31/1986)	13.09
Mean Higher High Water (MHHW)	8.76
Mean High Water (MHW)	7.87
Mean Sea Level (MSL)	4.50
Mean Tide Level (MTL)	4.48
Mean Low Water (MLW)	1.09
Mean Lower Low Water (MLLW)	0.00
Lowest Observed Water Level (02/06/1989)	-3.32
Notes: Length of Series: 5 YEARS Time Period: January 1994 - December 1998 Tidal Epoch: 1960-1978	

[4] From NOAA, NOS published tidal datum information for Station ID: 9457292

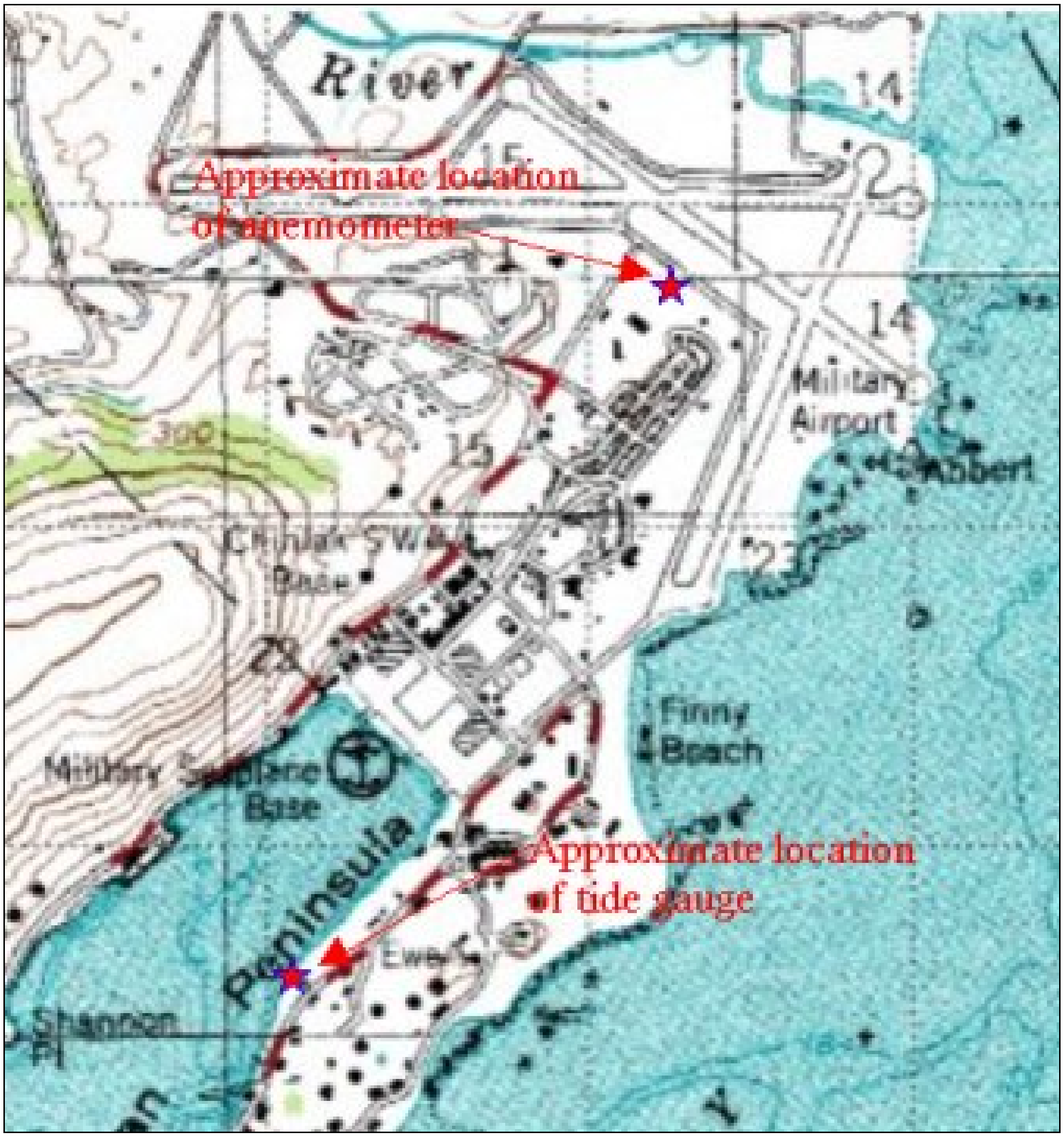

Figure 10 Approximate location of Tide Gage (Womens Bay) and anemometer (airport).

Peninsula (Figure 10). According to the NOAA website, Kodiak is experiencing anomalous changes in relative sea level trends and has therefore opted not to use the entire epoch to calculate standard benchmarks. That is why only the five-year period of 1994-1998 was used for the tabled values.

In structure design in the marine environment, an important parameter is the design water level. It is based on several factors but tide height is one of the most significant. It is important to know the amount of time the tide is above or below certain values. The following table provides that information.

Table 2.4 was created from analyzing 20 years of predicted tidal data and does not account for any storm surge or wave set-up.

Table 2-4 Percent of the time the water level is less than given elevation

Elevation	Percent
11 ft.	99.98 %
10	99.40
9	96.90
8	90.89
7	81.02
6	69.03
5	56.03
4	44.24
3	31.97
2	20.94
1	11.83
0	5.37
-1	1.64
-2	0.23

2.5 Winds

2.5.1 General

The highs and lows that form in the North Pacific Ocean and Gulf of Alaska strongly influence the winds and overall climate in the affected area. In the summer the North Pacific High tends to stabilize the weather producing rather mild and moist but relatively calm conditions. Fog is also common during this time. The stability is in part due to the difference in heating between the ocean and the land. As the land warms more than the water, the lower pressures become associated with the warming land and higher pressures with the water. The summer temperature differences between land and water are not as great as winter differentials and so summer conditions are more stable than those in the winter.

In the fall and winter the lows move into the GOA and produce a much more unsettled condition. Large temperature differentials can occur in the winter and the lows now associated with the warmer sea water can become very strong producing severe winds in the affected area. Counter-clockwise rotation is associated with the low pressure centers and as they move into the eastern GOA, winds in Kodiak become northerly. This brings colder air out of south and central Alaska and can cause significant snowfalls and cold weather in the affected area.

2.5.2 Gulf of Alaska Winds

A second long-term wind record is available from the NOAA Buoy 46001 located at 56°18'N latitude 148°1.3'W longitude. This is about 140 miles southeast of the affected area. Although another buoy (Buoy 46078) is within 70 miles of the affected area, it has been collecting data only since 2004 and even then the data reliability has been much lower than Buoy 46001. Figure 11 is an example of the type of buoy at this location. The buoy shown in the figure is at anchor under ideal sea conditions.

These data are presented as a wind rose in Figure 12 and the frequencies as a function of speed and direction are present in Table 2.5. The wind rose demonstrates a significant difference from the airport winds. In addition to being stronger, the wind direction increases from a minimum for north winds clockwise to be a maximum for west winds. They do not exhibit the topographic control that is apparent in on-island winds. The buoy wind data for this period demonstrated a reliability of about 80 percent.

Figure 11 Typical buoy like the one used at Station 46001

Table 2-5 Wind Frequency for NOAA Buoy 46001										
Wind Dir (°T)	**Wind Speed (mph)**									
	0 -5	**<5-10**	**<10-15**	**<15-20**	**<20-25**	**<25-30**	**<30-35**	**<35-40**	**<40-45**	**Totals**
0	0.15%	0.33%	0.45%	0.41%	0.21%	0.11%	0.03%	0.02%	0.00%	**1.71%**
10	0.12	0.32	0.31	0.28	0.17	0.09	0.03	0.00	0.01	**1.33**
20	0.16	0.33	0.31	0.23	0.16	0.10	0.02	0.01	0.00	**1.32**
30	0.12	0.28	0.32	0.23	0.19	0.09	0.04	0.01	0.00	**1.28**
40	0.13	0.27	0.32	0.31	0.22	0.12	0.04	0.02	0.00	**1.43**
50	0.11	0.28	0.40	0.30	0.26	0.13	0.05	0.02	0.00	**1.55**
60	0.12	0.30	0.45	0.35	0.26	0.14	0.07	0.02	0.00	**1.71**
70	0.12	0.33	0.44	0.44	0.31	0.19	0.09	0.05	0.01	**1.98**
80	0.13	0.30	0.48	0.5	0.37	0.22	0.15	0.04	0.01	**2.20**
90	0.14	0.36	0.53	0.56	0.55	0.34	0.20	0.06	0.02	**2.76**
100	0.14	0.35	0.51	0.58	0.52	0.35	0.21	0.06	0.01	**2.73**
110	0.16	0.37	0.53	0.64	0.57	0.38	0.20	0.06	0.02	**2.93**
120	0.14	0.38	0.59	0.61	0.54	0.35	0.15	0.06	0.01	**2.83**
130	0.16	0.40	0.61	0.61	0.51	0.32	0.14	0.04	0.01	**2.8**
140	0.15	0.42	0.66	0.71	0.57	0.36	0.12	0.03	0.00	**3.02**
150	0.15	0.39	0.64	0.72	0.53	0.26	0.10	0.02	0.01	**2.82**
160	0.17	0.44	0.67	0.79	0.59	0.31	0.13	0.03	0.00	**3.13**
170	0.15	0.41	0.73	0.78	0.57	0.28	0.12	0.02	0.00	**3.06**
180	0.16	0.48	0.86	0.82	0.53	0.26	0.06	0.00	0.00	**3.17**
190	0.19	0.49	0.88	0.84	0.51	0.26	0.07	0.01	0.00	**3.25**
200	0.19	0.53	0.92	0.92	0.56	0.24	0.08	0.01	0.00	**3.45**
210	0.19	0.53	0.98	0.92	0.55	0.24	0.07	0.03	0.01	**3.52**
220	0.17	0.55	0.94	0.98	0.56	0.28	0.07	0.02	0.01	**3.58**
230	0.19	0.56	1.05	1.03	0.67	0.33	0.08	0.02	0.01	**3.94**
240	0.17	0.57	1.09	1.24	0.76	0.39	0.12	0.03	0.01	**4.37**
250	0.16	0.57	1.25	1.37	0.88	0.40	0.15	0.04	0.01	**4.83**
260	0.14	0.56	1.29	1.35	0.90	0.52	0.22	0.06	0.01	**5.05**
270	0.17	0.61	1.16	1.25	0.90	0.55	0.29	0.08	0.02	**5.03**
280	0.15	0.51	0.89	0.82	0.64	0.34	0.15	0.05	0.01	**3.56**
290	0.17	0.44	0.7	0.69	0.54	0.30	0.16	0.08	0.01	**3.09**
300	0.14	0.46	0.64	0.58	0.46	0.35	0.21	0.09	0.03	**2.96**
310	0.13	0.36	0.56	0.49	0.45	0.37	0.20	0.09	0.03	**2.68**
320	0.16	0.38	0.50	0.42	0.36	0.30	0.14	0.06	0.01	**2.33**
330	0.13	0.30	0.39	0.34	0.27	0.16	0.08	0.02	0.01	**1.70**
340	0.14	0.30	0.40	0.29	0.22	0.10	0.03	0.01	0.00	**1.49**
350	0.12	0.29	0.34	0.26	0.16	0.08	0.03	0.01	0.00	**1.29**
Totals	**5.38**	**14.75**	**23.79**	**23.66**	**17.02**	**9.61**	**4.10**	**1.28**	**0.29**	**99.88**

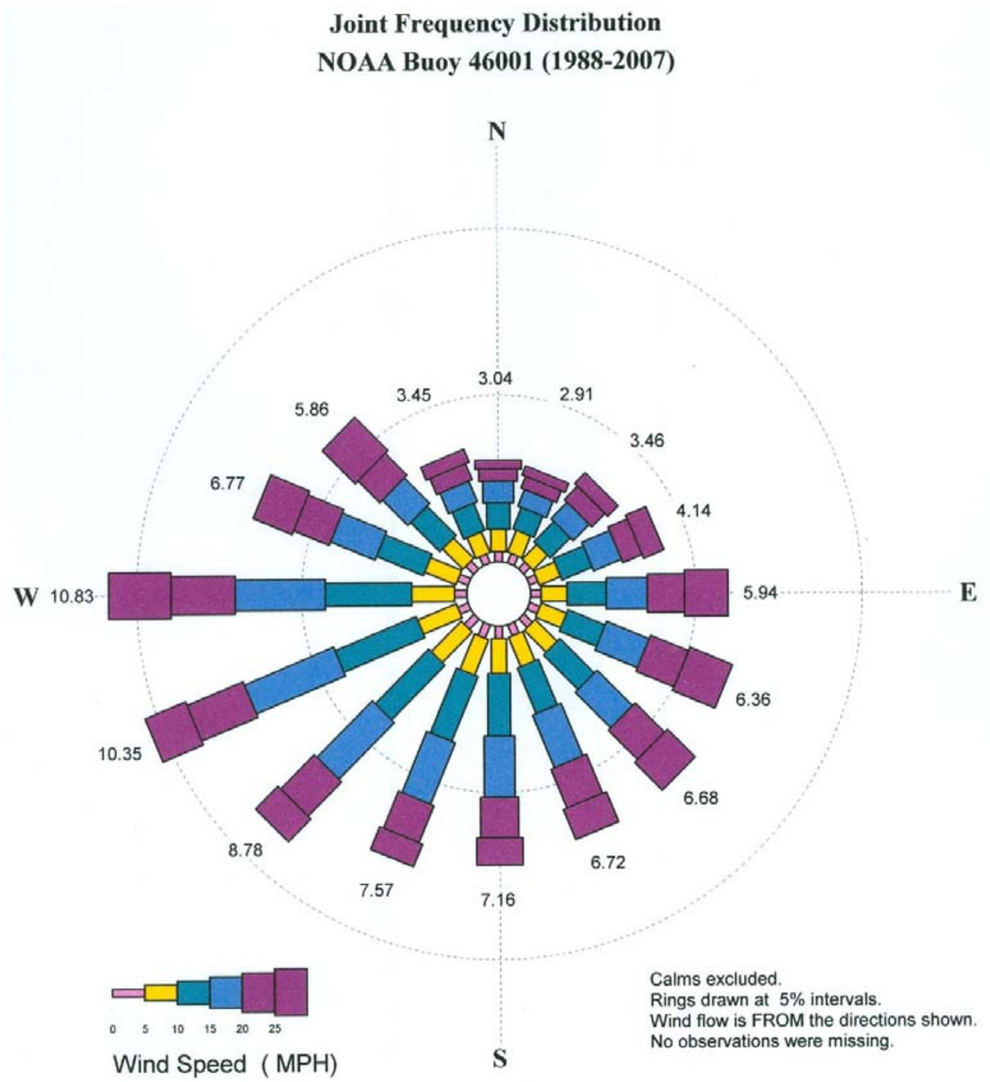

Figure 12 Wind rose for NOAA Buoy 46001 (1988-2007).

2.5.3 Local Winds

Archived winds for the Kodiak airport are available since 1945. The current location of the anemometer can also be seen in Figure 10. Twenty years of data (1988-2007) have been acquired and processed. These can be seen in Figure 13 that is a wind rose for these data. The directions indicated refer to the direction from which the winds come.

From this figure, two predominant wind directions are evident and make up about 75 percent of the wind occurrences. The first is east sector represented from northeast to southeast (roughly 110°) and accounts for about 44 percent of the winds. The airport is totally exposed from that direction. Just over 30 percent come out of the much narrower sector (about 45°) from west-northwest to northwest. Within this sector are the two major valleys separated by Barometer Mountain. The Buskin River flows out of the more northerly aligned of these two valleys.

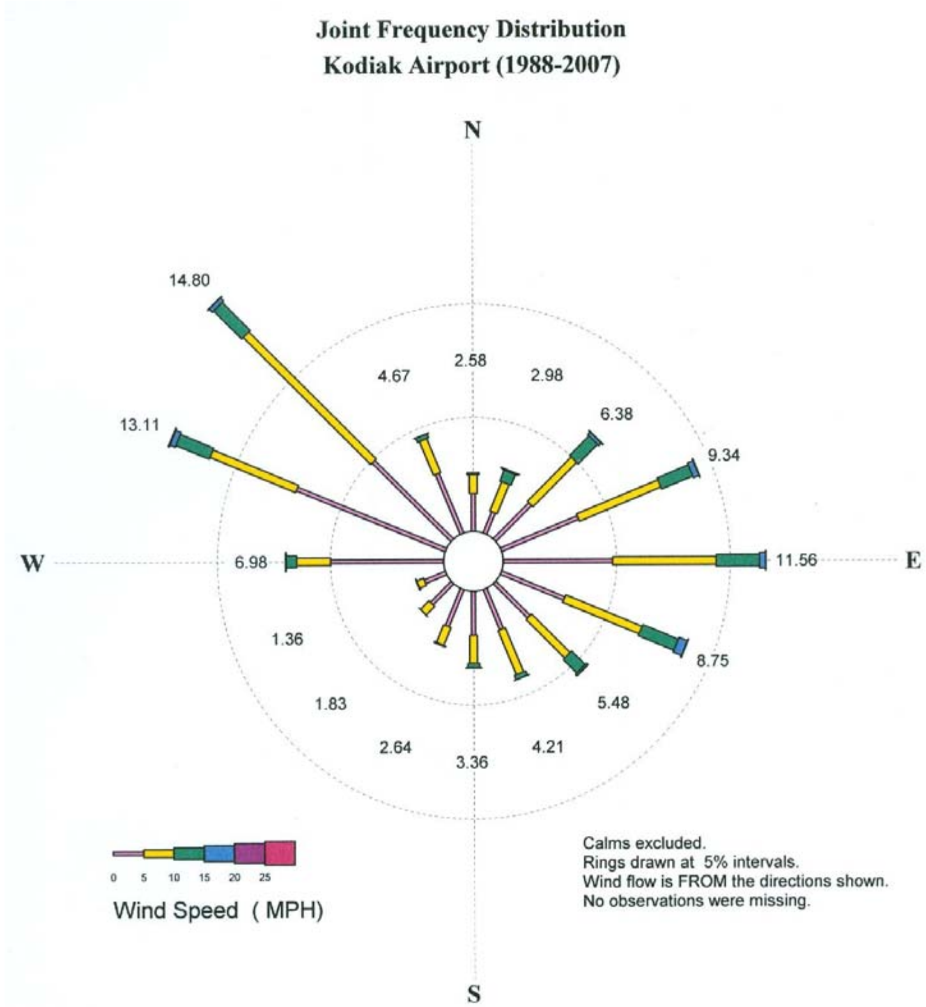

Figure 13 Wind rose for Kodiak Airport (1988-2007).

A tabulation of the wind frequency for given speeds and directions can be found in Table 2.6. There was about 93 percent of usable data for the 20-year period.

Table 2-6 Wind Frequency for Kodiak Airport						
Wind Dir (°T)	**Wind Speed (mph)**					
	0 -5	**<5-10**	**<10-15**	**<15-20**	**<20-25**	**Totals**
0	0.53%	0.2%	0.01%	0%	0.00	**0.74%**
10	0.51	0.32	0.03	0.00	0.00	**0.86**
20	0.53	0.59	0.09	0.00	0.00	**1.21**
30	0.58	0.74	0.25	0.03	0.00	**1.60**
40	0.86	0.96	0.37	0.05	0.00	**2.24**
50	1.57	1.84	0.43	0.03	0.00	**3.87**
60	2.19	2.23	0.55	0.05	0.00	**5.02**
70	1.88	1.53	0.52	0.04	0.00	**3.97**
80	1.78	1.54	0.44	0.03	0.00	**3.79**
90	1.78	1.7	0.47	0.06	0.00	**4.01**
100	1.61	1.61	0.49	0.05	0.00	**3.76**
110	1.82	1.87	0.53	0.07	0.00	**4.29**
120	1.76	1.99	0.58	0.07	0.00	**4.40**
130	1.38	1.49	0.31	0.02	0.00	**3.20**
140	1.18	0.86	0.14	0.01	0.00	**2.19**
150	1.17	0.94	0.06	0.00	0.00	**2.17**
160	1.08	0.76	0.02	0.00	0.00	**1.86**
170	0.85	0.51	0.04	0.00	0.00	**1.40**
180	0.74	0.26	0.02	0.00	0.00	**1.02**
190	0.67	0.21	0.00	0.00	0.00	**0.88**
200	0.92	0.34	0.01	0.00	0.00	**1.27**
210	1.01	0.36	0.00	0.00	0.00	**1.37**
220	0.9	0.31	0.00	0.00	0.00	**1.21**
230	0.85	0.25	0.01	0.00	0.00	**1.11**
240	0.72	0.17	0.01	0.00	0.00	**0.90**
250	0.71	0.18	0.01	0.00	0.00	**0.90**
260	0.91	0.25	0.03	0.00	0.00	**1.19**
270	1.62	0.45	0.07	0.00	0.00	**2.14**
280	2.77	0.77	0.16	0.02	0.00	**3.72**
290	4.28	1.55	0.38	0.05	0.01	**6.27**
300	3.36	3.08	0.76	0.12	0.02	**7.34**
310	2.98	4.70	0.87	0.09	0.01	**8.65**
320	2.78	3.11	0.29	0.01	0.00	**6.19**
330	1.83	1.16	0.09	0.00	0.00	**3.08**
340	1.03	0.35	0.02	0.00	0.00	**1.40**
350	0.61	0.19	0.01	0.00	0.00	**0.81**
Totals	**51.75**	**39.37**	**8.07**	**0.80**	**0.04**	**100.03**

2.6 Wave Climate

2.6.1 General

Most waves are generated by the action of wind drag on the water's surface. In deep water, wave growth is controlled by the wind speed, wind duration and size of the generating area (fetch). In the Gulf of Alaska, the strong, nearly steady lows that develop in the winter provide superb generating conditions and huge waves can be produced with systems lasting many hours or days. These can spread out in nearly all directions from the generating area experiencing only small reduction until they begin to make land fall and are affected by shoaling water.

No long-term wave measurements have been made in the affected area but the NOAA buoys described above also collect wave data. Due to their behavior to persist and propagate nearly unaltered, it is reasonable to predict wave character in the affected area from wave conditions offshore. The offshore conditions will be described first.

2.6.2 Gulf of Alaska Waves

Wave data were also collected by the NOAA Buoy 46001 located southeast of Kodiak. A frequency distribution for significant[5] wave heights and peak[6] periods is presented on

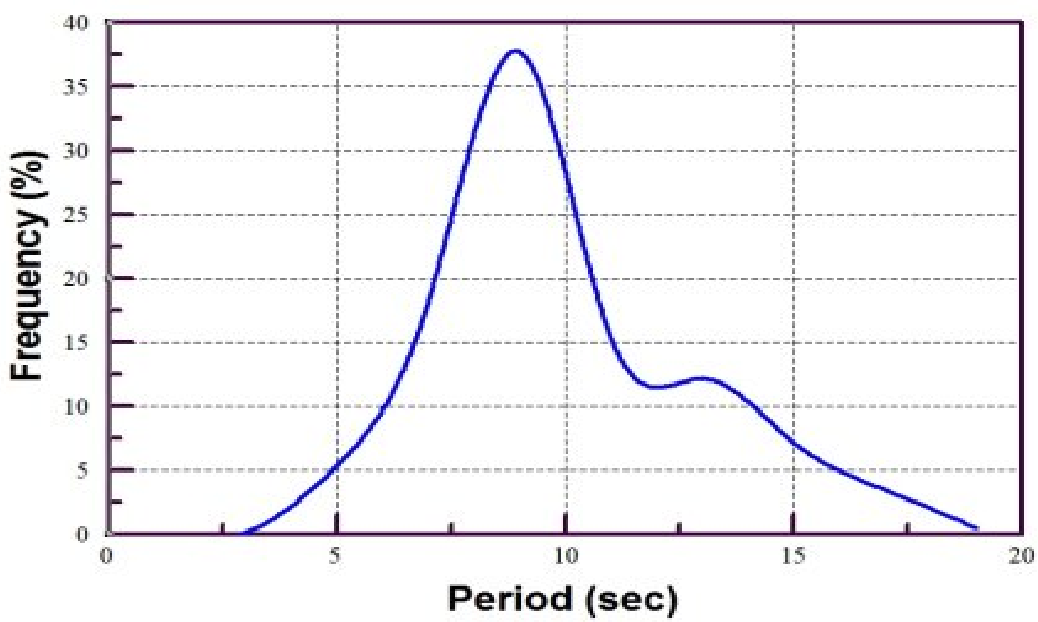

Figure 14 Wave period frequencies for NOAA Buoy 46001 (1988-2007).

[5] The significant wave is the average of the highest third of the wave heights.
[6] Peak period is the period corresponding to the period which contributes the maximum energy. It is close to the significant period (see definition for the significant wave height).

Table 2.7 for twenty years of data (1988-2007). The data were quite reliable with an 89 percent of usable data being collected during that period. A plot of the frequency of wave periods is shown in Figure 14. The maximum number occurs with a period of 8 to 10 seconds.

2.6.3 Local Waves

Waves were recorded at each of the ADCPs deployed as part of the current monitoring program for the circulation modeling calibration and verification. However due to the lack of severe weather during the recording period, those data were not processed. The waves in the affected area are investigated only as they will relate to the design conditions of the alternatives that will ultimately be selected for further consideration.

Table 2-7 Frequency for Wave Heights and Periods for NOAA Buoy 46001

Height Range (ft)	Period Ranges (s)										
	0-2	>2-4	>4-6	>6-8	>8-10	>10-12	>12-14	>14-16	>16-18	>18-20	Totals
0-2	0%	0%	0.01%	0.02%	0.02%	0.01%	0.06%	0.08%	0.04%	0.01%	0.25%
>2-4	0.00	0.11	1.39	2.29	1.69	0.32	0.74	2.14	1.4	0.11	10.19
>4-6	0.00	0.02	2.74	6.33	7.05	1.31	0.76	0.67	0.69	0.07	19.64
>6-8	0.00	0.00	1.00	5.20	8.63	2.46	1.36	0.41	0.16	0.05	19.27
>8-10	0.00	0.00	0.18	2.89	7.85	2.89	1.80	0.57	0.14	0.05	16.37
>10-12	0.00	0.00	0.01	1.09	5.63	2.40	1.88	0.63	0.14	0.04	11.82
>12-14	0.00	0.00	0.00	0.31	3.61	2.02	1.52	0.69	0.15	0.04	8.34
>14-16	0.00	0.00	0.00	0.04	1.91	1.53	1.25	0.55	0.17	0.03	5.48
>16-18	0.00	0.00	0.00	0.00	0.86	1.05	0.95	0.45	0.13	0.02	3.46
>18-20	0.00	0.00	0.00	0.00	0.35	0.69	0.68	0.32	0.12	0.02	2.18
>20-22	0.00	0.00	0.00	0.00	0.09	0.42	0.50	0.23	0.09	0.02	1.35
>22-24	0.00	0.00	0.00	0.00	0.02	0.17	0.31	0.16	0.07	0.01	0.74
>24-26	0.00	0.00	0.00	0.00	0.00	0.05	0.18	0.12	0.06	0.01	0.42
>26-28	0.00	0.00	0.00	0.00	0.00	0.01	0.11	0.08	0.04	0.00	0.24
>28-30	0.00	0.00	0.00	0.00	0.00	0.01	0.04	0.04	0.02	0.00	0.11
>30-32	0.00	0.00	0.00	0.00	0.00	0.00	0.01	0.03	0.02	0.00	0.06
>32-34	0.00	0.00	0.00	0.00	0.00	0.00	0.01	0.01	0.01	0.00	0.03
Totals	0.00	0.13	5.33	18.17	37.71	15.34	12.16	7.18	3.46	0.48	99.96

We have chosen to investigate larger-wave behavior as these will influence certain aspects of the design. The locally-generated waves due to winds within the affected area have neither the fetch nor water depth to produce waves that will have any design significance.

2.7 Coastal Geomorphology and Longshore Transport

2.7.1 General

The shoreline in the vicinity of the affected area consisting of Womens Bay and the southern portion of St. Paul Harbor consists of bedrock outcrops with intervening pocket beaches and with two rather major floodplains. One floodplain occurs at the head of Womens Bay and the other is associated with the Buskin River. Both floodplains represent the seaward extension of one or more mountain valleys whose cross-valley profiles have the typical U-shaped form caused by over-steepening due to glaciations.

The NOAA Chart 16595 (Kodiak and St. Paul Harbors) provides interesting and useful information about the near-shore waters in the affected area. With few exceptions, the depths are less than 18 feet deep (MLLW) within the affected area. In St. Paul Harbor to the north and in Womens Bay to the south, the depths exceed 60 feet in places.

The bottom seems to be composed of a variety of materials including bedrock, boulders, cobbles, gravel and sands. The two areas mentioned above stand out as relatively major sedimentation zones. Those at the head of Womens Bay probably constitute some of the finest-sized sediments in the affected area. The second major depositional area is located off the east end of the airport. Its northern limit is nearly to Gibson Cove and extends southward to just south of the tip of Nyman Peninsula in Womens Bay. Sediments in this deposit consist of coarse sands with some gravels and cobbles. This deposit is clearly dynamic and responds to wave activity on a regular basis. These are undoubtedly deposits from the present and former location of the mouth of the Buskin River. The river was manually displaced to the north to reclaim property for the runways.

In deeper water there are probably ample occurrences of bedrock outcrops and larger boulders that may have been deposited during past glaciations. The deeper portions within the affected area are likely to be veneered by medium to fine sand that has been transported from the deposits described above. The deeper portions off Womens Bay probably contain significant quantities of fine sand and silt.

There is a clear demarcation between the affected area and deeper portions of Chiniak Bay to the east. (Chiniak Bay may be part of the affected area for some impacts.) This separation is established by the northward peninsular extension terminating with Cliff Point and includes the series of shoals (some going dry on lower tidal stands) and small islets between Cliff Point and Popov Island 2.5 naut. miles to the northwest. These shoals and small islands provide effective protection from Gulf of Alaska waves.

The shoreline can be generally classified as erosional as opposed to depositional. Tectonic activity has resulted in bedrock to be at or near the surface in many areas. Those that are at the shoreline are continually attacked by waves and tides and gradually degrade into smaller material. This appears to be a young shoreline with a highly irregular (crenulated) shape. Irregular shorelines tend to become straighter or more regular as they age. The bedrock outcrops along the shore are not continuous but are broken up by more easily eroded beaches. This creates indentations in the shoreline where the material eroded from the adjacent headlands settles forming pocket beaches. These features are quite characteristic of the entire shoreline.

The shorelines in the affected area will be described using a narrative and photographs. Much of this description is from the ShoreZone Mapping program[7] sponsored by several organizations[8] including the Exxon Valdez Oil Spill Recovery Council, the Cook Inlet Region Citizen's Advisory Council, UAF, U.S. F&WS, and NOAA. Information was also taken from the NOAA Chart 16595. The area described is from just southwest of Cliff Point, along the shoreline of Womens Bay, around the southern end of the Nyman Peninsula, and then north to the entrance into Gibson Cove.

2.7.2 Description of Affected Area Shorelines

This discussion is accompanied by Figure 15 which is a composite of U.S.G.S. Quad maps with lines drawn to designate the areas being described and are identified with capital letters. Hard-rock headland outcrops, many from low vertical cliffs and some that project seaward of the shoreline, are abundant along the southeast shoreline of Womens Bay particularly in the vicinity of Zaimka Island south to onshore of Blodgett Island (Figure 16, A on Figure 15). Narrow pocket beaches lie between the headlands that project onto the beach and are composed of sediments with a variety of sizes. Abutting the outcrops, the sediments are coarser—boulders and cobbles. These may grade into cobbles and pebbles further from the outcrops. The amount of sand matrix increases with distance from the headlands.

The sediments appear angular indicative of minor displacements from their source or from being at a lower state of wave activity. Occasionally there are small delta deposits from small streams that empty onto the beach. Although not obvious from this figure, the beach deposit on the right hand side of this photograph is partially a delta deposit.

[7] Dr. John Harper and Mary Morris of Coastal and Ocean Resources, Inc of Sidney, B.C., Canada conducted the field work for the ShoreZone Mapping program.
[8] Other sponsors included the Park Service and the Coastal Impact Assistance Program.

Figure 15 The project area with letters to designate locations shown in subsequent figures (16-27).

Further south from about Blodgett Island to the head of Womens Bay, the beach becomes somewhat straighter (Figure 17, B on Fig. 15). The rocky outcrops have become vegetated and in places are hardly discernable. They can be recognized by slight protrusions of vegetation with larger boulders often on the beach in front of them. The overall size of the material becomes finer and there appears to be several active or relic delta deposits; there is even what appears to be a major slump just off one of the beach locations.

Several streams—Solonie, Russian and Sargent Creeks being the largest—form a major depositional feature as a system of coalescing deltas at the head of Womens Bay

Figure 16 Pocket beach development near Zaimka Island. Looking south into Womens Bay.

(Figure 18, C on Fig. 15). Two hard-rock features that extend well beyond the shoreline break up this nearly continuous delta feature. The first projection is Bruhn Point that appears to extend subsurface out to Mary Island. Fine material including sand and silt are entering the bay on this delta which is an extension of the onshore wetland and will eventually become part of future wetlands.

This depositional environment appears to come to an end at Fyre Point (Figure 19, D on Fig. 15), the second of two hard-rock extensions. Here a tombolo-like[9] deposit connects the island to the shoreline with its seaward side making a shoreline change from the depositional delta features to the narrow, coarse sand-pebble-cobble beaches more indicative of erosional shorelines.

[9] A tombolo is a depositional feature that develops as an offshore structure (natural or manmade islands for example) causes a reduction in wave energy between it and the shoreline. This reduction in wave energy causes sediments being transported along the beach as littoral drift to become deposited creating a connection between the beach and island.

Figure 17 Looking southwest from a point about 0.4 miles south of Blodgett Island.

Figure 18 Looking across the deltas for Solonie and Panamaroff Creeks at the head of Womens Bay. The base of Bruhn Pt. is on the left center of photograph.

These are occasionally interrupted by eroding hard-rock headlands extending to the waterline and beyond in places. There is a considerable amount of man-made facilities located along this beach including placed riprap used for road protection. The beaches are 30-40 feet wide landward from the Mean-Lower-Low-Water (MLLW). At least one of the hard-rock headlands has been leveled and is being used for storage (Figure 20, E on Fig. 15). A sheet-pile dock has been constructed about halfway into the embayment between Old Womens Mountain and the inside of Nyman Peninsula. This dock is over 1,200 feet long and at places is over 200 feet wide.

Figure 19 A view across Frye Point. The beach has formed due to sediment transport on the tombolo.

The Coast Guard base marine facilities are located on the north and eastern side of the peninsula. The northern end has been squared off with riprap-protected fill and is the site of three seaplanes ramps that no longer appear to be in service.

Along the west side of the peninsula, the Coast Guard has two working docks, a berthing dock and just south of that a petroleum dock. The remains of an old wooden dock is present between the petroleum dock and the southern tip of the peninsula. It is no longer in service. Most of the backshore area has been filled and portions of it protected with riprap. It is hard to discern the natural from all the man-made features along portions of this shoreline. Just north of the berthing dock, the beach appears to be nearly 100 feet wide—the widest beaches encountered in the affected area.

Figure 20 Man-made facilities on the northwest side of Womens Bay. Storage in the foreground and sheet-dock beyond.

The backshore fill continues around the southwest tip of the peninsula. The beach here is somewhat wider than most of those encountered (40-60 feet) except for the beach just north of the berthing dock which may have been widened due to man's intervention. Beginning just north of this corner of the peninsula and then continuing to the west and along the east side of the peninsula, there are several Conex storage containers apparently used for petroleum spill boom storage.

Along the east side of the peninsula the beaches again become narrower. Proceeding north, two coves are encountered each about 1,500 feet long and bounded by eroding headlands (Figure 21, F on Fig. 15). Pocket beaches have developed in both coves with the most extensive development in the southernmost cove. The beaches consist of pebble-cobble over sand and cobble-boulder over sand with the latter being closer to the headlands. Flattened, hard-rock shoals extend seaward of the beach in places. About one-half mile north of the northern cove is a major headland feature with very narrow beaches of cobbles and boulders. This headland terminates with an extension offshore and then grades into a wider (75 feet) sand-pebble beach with some cobbles—Finny Beach (Figure 22, G on Fig. 15). The beach is 2,000 feet long. An abandoned outfall extends offshore at the northern end of the beach which in turn grades into a

Figure 21 A view up the shoreline from the southeast side of the Nyman Peninsula.

Figure 22 Rock outcrop transitioning into Finny Beach.

riprap fill—part of the southern end of Runway 18/36; just beyond that is a major headland.

A few hundred feet north, the headland gives way to a small cove whose opening is protected on both ends with riprap breakwaters that enhanced its use as a former small-boat-harbor (Figure 23, H on Fig 15). It appears to have been usable only during the higher part of the tide cycle but appears to be no longer used for that purpose. An active storm drain outfall extends seaward from the southern breakwater. The shoreline just north of this harbor consists of a small sand-pebble beach about 200 feet long. This merges into riprap armor use to protect the eastern end of Runway 11/29 (Figure 24, I on Fig. 15).

A natural sand-pebble beach with a small amount of cobbles is present between this runway end and the eastern end of Runway 07/25. Also present is a large sand-pebble near-shore shoal (Figure 25, J on Fig. 15) which appears to become increasingly more exposed from about mid-tide to low tide. This appears to be a sedimentary delta feature, probably the former site of the Buskin River delta.

Starting just north of the northern end of Runway 18/36 begins the present Buskin River barrier bar and delta feature (Figure 26, K on Fig. 15). This is an extensive depositional (given the limited size of the river) deltaic formation manifest in the near-shore by shoals of sand and pebbles. The barrier bar fronting the Buskin River is offset well to the north indicating a sediment transport direction from the south. Grasses growing along nearly the entire length of the bar from the end of the runway to its terminus over 1,000 feet to the north attest to the probability that the bar migrates slowly to the north; a more active beach growth and breakout cycle would preclude establishing so much vegetation.

The probable progression of the bar/river feature is that after reaching some distance to the north, the river mouth probably resets to a more southern location near the base of the riprap slope protecting Runway 18/36. The building process to the north is again initiated. This resetting probably occurs suddenly with a breakout in the new location during a storm/high tide event. The present location of the mouth is considerably to the north (Figure 27, L on Fig. 15). This process is discussed in the next section.

Seaward of the grasses, the sediments transition from cobble veneers over a sand-pebble matrix to a sand-pebble mix near the waterline. While the trend is for the sediments to get smaller seaward to the waterline, there are amounts of large pebbles/small cobbles nearly everywhere below the beach surface.

River deposits extend for a distance to about 2,500 feet north of the end of the runway both on the beach and in the near-shore. These deposits continue in the

Figure 23 Small boat harbor near the east end of runway 11/29.

Figure 24 Riprap protection for seaward end of runway 11/29.

Figure 25 Near-shore shoal at the east end of Runway 07/25. Site of the former Buskin River delta.

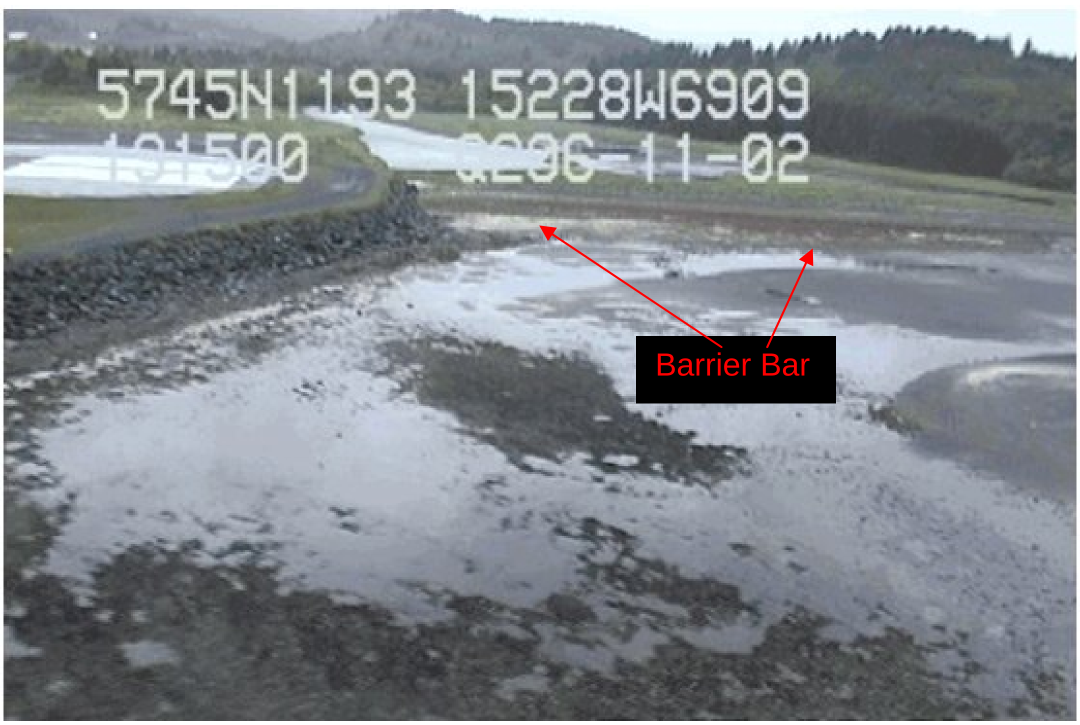

Figure 26 The southern end of the Buskin River barrier bar system adjacent to the northern end of Runway 18/36.

Figure 27 A view of the northern end of the Buskin River barrier bar. The river's mouth is on the far right.

near-shore even after the back-shore transitions into the higher vertical cliffs that begin at the base of the Buskin River overlook. The cliffs continue north with occasional breaks where small pocket beaches form. The beach composition—arising from the eroding cliffs—appears to be quite different from the offshore material. The beach is composed of sand-pebble-cobble-boulders while the offshore remains the finer material from the Buskin River runoff. There is a noticeable break in the slope between these two materials. The beach is much steeper indicative of the coarser composition.

The pattern of vertical eroding cliffs interspersed with small pocket beaches continues northward with decreasing amounts of river deposits offshore. About 3,000 feet north of the river, the fine deposits disappear from the near-shore region.

These nearly continuous eroding vertical cliffs continue to the entrance of Gibson Cove with only a single small pocket beach just south of the cove. The very narrow beaches off the cliffs are composed of cobble-boulders, many of which appear not to have moved once they dropped from the cliffs.

2.7.3 The Buskin River

The location of the mouth of the Buskin River is a function of several factors:

- The direction and quantity of sediments that are transported from adjacent coastal and near-shore areas,
- The amount of sediment being supplied by the river,
- The river's peak flows (or near peak flows), and
- The timing of large tides especially large tides occurring during storm events.

The situation at the mouth of the Buskin is fairly typical of rivers and inlets that enter into larger bodies of water. Sediment tends to be deposited on the up-drift shoulder of the entrance. This is due to the loss of longshore current speed as it begins to cross the out-flowing current of the river or inlet.

This current which has been moving and carrying sediment parallel to the shore from the up-drift direction begins to deposit its sediment load (littoral drift or transport) as it approaches the deeper water. It also becomes directed offshore with the outflow.

It might be helpful to refer to the end of the beach on the up-drift side of the river as the up-drift shoulder and, conversely, the beginning of the beach on the down-drift side as the down-drift shoulder. The reduction in the longshore current upon reaching the river causes deposition and initiates the formation of a bar at the up-drift shoulder. This bar is directed generally parallel to the beach but can also be oriented slightly offshore. The rate of bar growth due to the deposited sediments depends on the quantity of sediments being deposited and on the velocity of the outgoing stream.

Simultaneously, erosion begins on the down-drift shoulder of the river as the longshore current begins to reform after being completely eliminated on entering the stream. This deposition on the up-drift shoulder and erosion on the down-drift shoulder causes the stream mouth to migrate down-drift with the up-drift bar following along. The entire river, in turn, continues to form a path parallel (or nearly parallel) to the shoreline.

At the same time that the new beach bar is developing, some of the longshore sediments that are not deposited on this newly-forming beach can be carried offshore to and through the breaker zone. This sediment may get finer in the offshore direction. This more-offshore shoal occasionally can form on the down-drift side of the river depending on the direction of the prevailing near-shore currents (these currents are distinct from the longshore current which always moves in response to the wave direction).

At some point the ever-lengthening stream, which is now directed parallel or nearly parallel to the shoreline, becomes hydrologically inefficient due to increased friction. As a result, the elevation of the stream's surface assumes a greater slope near the mouth to overcome this friction and maintain the flow. When this increased head is accompanied by high flood flows and perhaps high tides and even a storm (with a surge and high waves), the barrier bar can become very saturated and lose its strength. This is when a river break-out is likely to occur somewhere along the bar. Often this is at the initial bend where it changes direction to become parallel to the beach, but this location is sometimes controlled by other factors and it is possible to occur anywhere along the bar.

The sediments for the bar at the Buskin River probably come directly from the transport of the former delta to the south of the river and from re-transportation of river deposits that are first deposited offshore and then eventually get incorporated into the longshore transport.

It appears that the Buskin River may not have experienced a complete cycle as yet. That is, since the river was established at its present course in 1940, its migration may have continued to the north until the present without a single breakout. Sometimes these cycles can be quite long and other times they can occur nearly annually. Also sometimes that bar can be several miles long. An example of this in Cook Inlet is the bar associated with the Starisky Creek north of Anchor Point.

3. DESCRIPTION OF NO ACTION ALTERNATIVE

The no action alternative is tantamount to not implementing any of the alternatives and to keep the runways as they currently exist (Figure 28). The runways would continue to be degraded during some storms that occur during high tides when considerable debris are thrown onto the seaward ends of both runways 11/29 and 07/250. Flight operations may be delayed as this material is cleaned up. The armor seems to be adequate to protect the seaward side of the airport property. As the waves continue to impact the armor, the fill will erode at a slow pace as water permeates between the primary and secondary armor. This will tend to degrade the armor over time and it will require periodic maintenance.

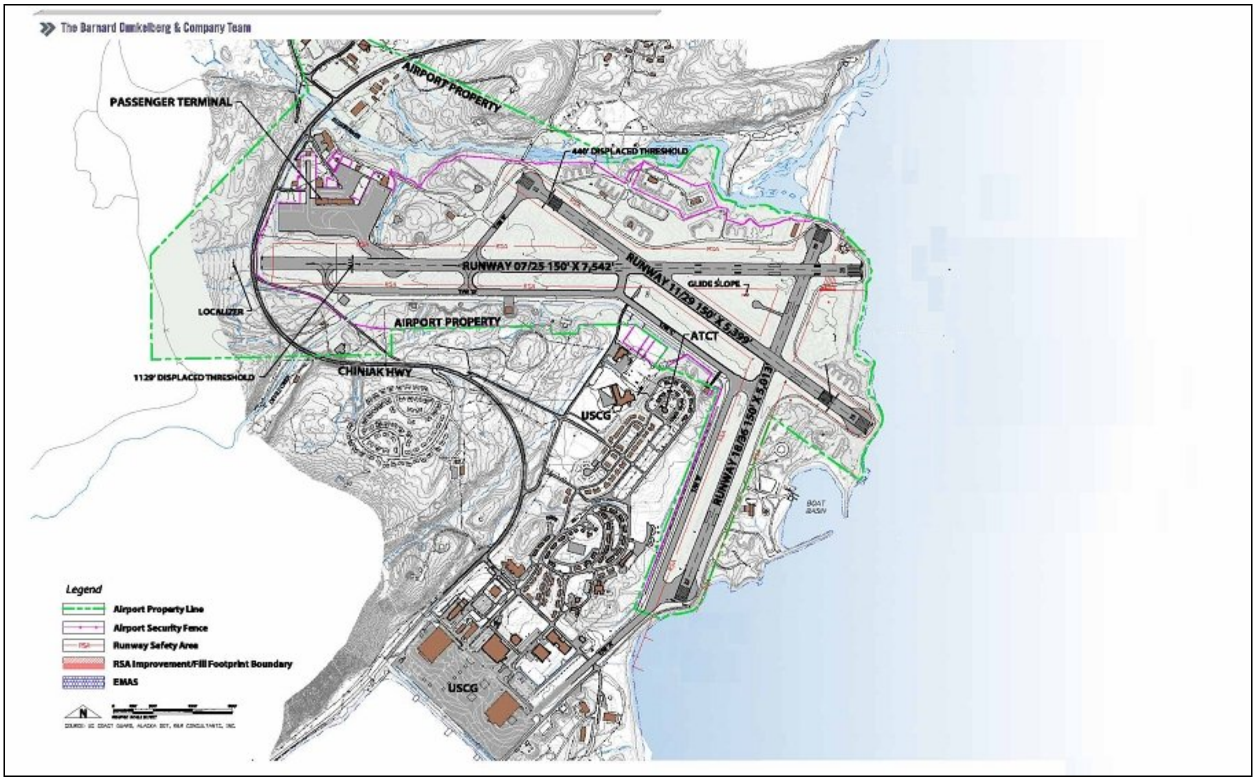

Figure 28 Kodiak Airport- Existing Condition (No Action Alternative).

4. COASTAL HYDRODYNAMIC PROCESS MODELING

4.1 EFDC-Explorer Modeling System

Hydrodynamic models account for the movement of surface waters where water motion is influenced by cross-sectional area, depth and bottom slope of the water body, freshwater inflows, water surface elevation and physical processes such as bottom friction, winds, turbulent mixing and vertical stratification induced by water temperature and salt content (i.e., density).

4.1.1 Overview of EFDC

The Environmental Fluid Dynamics Code (EFDC) is a general-purpose modeling package for simulating three-dimensional flow, transport, and biogeochemical processes in surface water systems including: rivers, lakes, estuaries, reservoirs, wetlands, and near shore to shelf scale coastal regions. The public domain EFDC model was originally developed at the Virginia Institute of Marine Science for estuarine and coastal applications. In addition to hydrodynamic and salinity and temperature transport simulation capabilities, EFDC includes sub-models to simulate sediment transport, eutrophication[10], and the transport and fate of toxic contaminants in the water and sediment bed. EFDC is unique among advanced surface water models since it uses a single source code to interface hydrodynamics (Hamrick, 1992) with sediment transport (Tetra Tech, 2000), toxic chemicals (Tetra Tech, 1999) and eutrophication (Park et al., 1995) within a single source code (Hamrick, 1996). The code is widely used by Federal agencies, including the Army Corps of Engineers, EPA and the USGS.

4.1.2 Governing Physics of EFDC

The EFDC hydrodynamic model is a variable density, unsteady flow model that uses the Boussinesq approximation[11], hydrostatic pressure field and internal solutions of vertical eddy viscosity and diffusivity. The EFDC model solves the vertically hydrostatic, free-surface, turbulent-averaged equations of motions for a variable density fluid.

Dynamically coupled transport equations for turbulent kinetic energy, turbulent length scale, salinity, and temperature are solved. The two turbulence parameter transport equations implement the Mellor-Yamada level ‘2.5’ turbulence closure scheme (Mellor and Yamada, 1982; Galperin et al., 1988). The bottom stress formulation for friction, accounting for the rate of momentum loss at the sediment bed/water interface, is

[10] The process of oxygen deficiency caused principally by algae growth due to excessive concentrations of inorganic nutrients.
[11] The terms involving differences in density of variable fluids are only important in the buoyancy term, i.e., those terms multiplied by gravity.

represented using a turbulent boundary layer formulation based on a quadratic function of near-bottom velocity. Water temperature is solved as an integral part of the hydrodynamic model with heat transport simulated using the atmospheric heat exchange model developed by Rosati and Miyakoda (1988) in which solar radiation at the water surface is reduced as a function of depth in the water column.

The state equations and numerical solution methods used in the EFDC hydrodynamic model are given in Hamrick (1992; 1996), Blumberg and Mellor (1987) and Martin and McCutcheon (1999). The interested reader is referred to these sources since the equations of the model are not presented in this technical report.

4.1.3 Numerical Solution Schemes of EFDC

The spatial domain of a water body can be represented in EFDC using (a) either Cartesian, or curvilinear orthogonal, coordinates in the horizontal (x,y) domain; and (b) a stretched, or sigma, coordinate scheme in the vertical (z) domain. The numerical scheme used in EFDC to solve the equations of motion uses a second-order accurate, spatial finite difference scheme on a staggered or C grid. The model's time integration uses a second-order accurate, two time-level, finite difference scheme with an internal/external mode splitting procedure to separate the internal shear, from the external free surface gravity wave. The external mode solution is semi-implicit, and simultaneously computes the two-dimensional surface elevation field by a preconditioned conjugate gradient procedure. The external solution is completed by the calculation of the depth averaged velocities using the new surface elevation field. The model's semi-implicit external solution allows large time steps that are constrained only by the stability criteria of the explicit central difference or high-order upwind advection scheme (Smolarkiewicz and Margolin, 1993) used for the nonlinear accelerations.

Horizontal boundary conditions for the external mode solution include options for simultaneously specifying the surface elevation only, the characteristic of an incoming wave (Bennett and McIntosh, 1982), free radiation of an outgoing wave (Bennett, 1976; Blumberg and Kantha, 1985), or the normal volumetric flux on arbitrary portions of the boundary. The EFDC model's internal momentum equation solution, at the same time step as the external, is implicit with respect to vertical diffusion. The internal solution for the momentum equations is in terms of the vertical profile of shear stress and velocity shear. Time splitting inherent in the two time-level scheme is controlled by periodic insertion of a second-order accurate two-time level trapezoidal step. In addition to the general 3-dimensional (x,y,z) spatial domain, the EFDC model can also be readily configured as a two-dimensional model in either the horizontal (2D: x,y) or vertical (2D: x,z) planes.

The EFDC model implements a second-order accurate in space and time, mass conservation fractional-step solution scheme for the Eulerian transport equations for salinity, temperature, suspended sediment, water quality constituents, and toxic contaminants. The transport equations are temporally integrated at the same time step or twice the time step of the momentum equation solution (Smolarkiewicz and Margolin, 1993). The advective step of the transport solution uses either the central difference scheme used in the Blumberg-Mellor (1987) model or a hierarchy of positive definite upwind difference schemes. The highest accuracy upwind scheme, second-order accurate in space and time, is based on a flux-corrected transport version of Smolarkiewicz's multidimensional positive definite advection transport algorithm (Smolarkiewicz and Clark, 1986; Smolarkiewicz and Grabowski, 1990) which is monotonic and minimizes numerical diffusion. The horizontal diffusion step, if required, is explicit in time, while the vertical diffusion step is implicit. Horizontal boundary conditions include time variable material inflow concentrations, upwind outflow, and a damping relaxation specification of climatological boundary concentration.

4.1.4 Enhancements to EFDC

The Dynamic Solutions, LLC version of EFDC (EFDC-DS) has a number of enhancements that have been made to the EPA-supported EFDC code maintained by Tetra Tech, Inc. Enhancements have been made to EFDC to assist model development and application. Key enhancements to the EFDC code include the following:

- Dynamic memory allocation allows the user to use the same executable code for applications to different water bodies. Dynamic allocation eliminates the need to re-compile the EFDC code for different applications because of different maximum array sizes required to specify the computational grid domain and time series input data sets. Dynamic allocation also helps prevent inadvertent errors and provides better traceability for source code development.
- Enhanced heat exchange options that use equilibrium temperatures for the water and atmospheric interface and spatially variable sediment bed temperatures.
- New output snapshot controls for targeting specific periods for high frequency output within the standard regular output frequency.
- Streamlining the code for quicker execution times.
- Customizing linkage of model results for the Windows-based EFDC-Explorer graphical pre- and post-processor for EFDC.
- Ability to customize the linkage of any 2D or 3D EFDC output variable for the EFDC-Explorer post-processor.

4.1.5 State Variables and Computed Output Variables of EFDC

Hydrodynamic models simulate velocity and transport fields, elevation of the free water surface; and bottom stress. The state variables of EFDC include: stage height or free water surface elevation; salinity, water temperature and velocity. A three-dimensional application of EFDC simulates velocity in three-dimensions (x,y,z) as the 'u' and 'v' horizontal (x,y) components and the 'w' vertical (z) component. Turbulent kinetic energy and turbulent macroscale length scale parameters are also included as state variables in EFDC. Water density is computed in EFDC as a function of water temperature and salinity. EFDC computes horizontal diffusivity as an output variable of the model from horizontal turbulent closure methods. EFDC also computes vertical eddy viscosity and vertical eddy diffusivity from vertical turbulence closure schemes as output variables of the model.

4.1.6 EFDC-Explorer Description

Critical to the cost effective and successful setup, calibration and application of an EFDC model is the availability and capabilities of pre- and post-processing tools. Dynamic Solutions originally developed the EFDC-Explorer (EE) software in response to its own internal needs to efficiently build and calibrate EFDC models. Currently, the EFDC-Explorer pre- and post-processor is a Windows-based GUI public-domain software designed to support model set-up, Cartesian and curvilinear grid generation, testing, calibration, and data visualization, including plots and animation, of model results (Craig, 2003). EE currently supports the following EFDC applications:

- Hydrodynamics,
- Density dependent flow state variables: Salinity/Temperature,
- Sediment Transport (Including the latest SEDFlume implementation),
- Toxics,
- Water Quality with Sediment Diagenesis, and
- Tracers.

EFDC-Explorer is currently being used by EPA, USGS, US Army Corps of Engineers, Oklahoma Department of Environmental Quality, Texas Commission on Environmental Quality, Suwanee River Water Management District and private consulting firms in the US and other countries.

4.2 Model Development and Calibration

An Environmental Fluid Dynamic Code (EFDC) (Hamrick, 1996) coastal hydrodynamic model was set-up, refined, calibrated, and validated to available observed data. The EFDC pre- and post-processing utility used for this study is EFDC-Explorer (Craig, 2004).

Grid development is a critical component of any hydrodynamic modeling study. A model grid is the result of a balance of spatial resolution, site conceptual model and modeling objectives against the computational time and resources. High resolution grids can produce great horizontal and vertical detail but if the run times are excessive then the modeling study will fail due to the inability to produce enough runs to obtain good calibration, verification and target scenarios.

To meet the objective of the Kodiak Airport RSAIAS, two models were needed. A coarse grid model was developed first followed by a finer nested grid model of the coastal region near the airport. This two grid approach was required to be able to set physically meaningful boundary conditions in Woody Island Channel and Chiniak Bay but still allow a detailed assessment of the velocities and bed shear stress in the areas of the proposed runway extensions. A description of each of these models is discussed in the following sections.

Both Kodiak models were two-dimensional, depth averaged models. Wind surface stress was included in the models to simulate the wind effects on water surface elevations and currents. Density effects due to salinity and temperature were not included. Wave generated shear stresses and mixing due to waves were also not included.

This report addresses the model development, calibration and application to the current conditions of the Kodiak coastal region. The simulation period focused on the 31 day time period of October 2 to November 3, 2007. This period was selected to coincide with the ADCP data collection period. Once the models were calibrated to the data, an analysis of the model results for that period provided the baseline for the No Action Alternative analysis.

4.2.1 Bathymetry

Bathymetric data are required to build the Kodiak Airport coastal hydrodynamic model. The bathymetry of a system has significant impacts on the simulation results. Bathymetric data were obtained from the NOAA NOS bathymetry data web repository (www.ngdc.noaa.gov) for the model domain. These data were obtained and converted to common horizontal (UTM NAD83 meters) and vertical (mean lower low water (MLLW) in meters) datums. Figure 29 shows the composite data, with over 77,400 points, for the model domain. Each XYZ data point was plotted as a small colored symbol. The color of the symbol represents the elevation of the data point. The same bathymetric data were used in the development of both models.

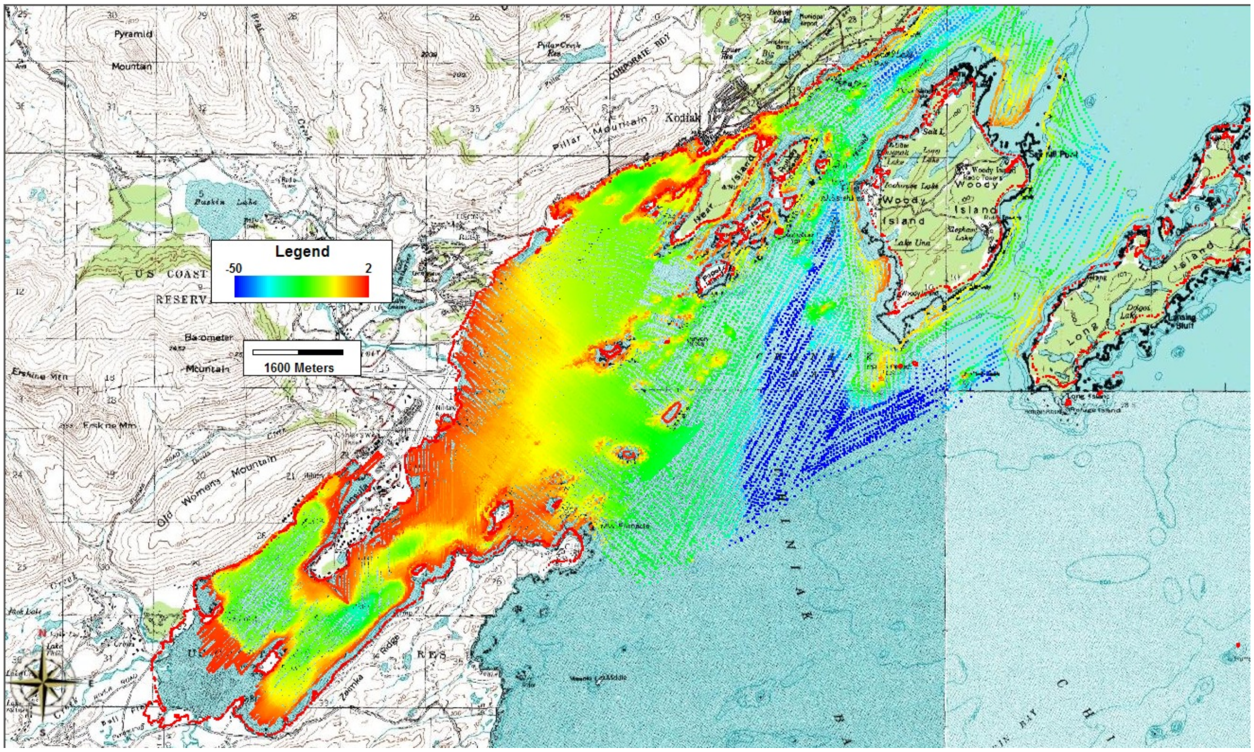

Figure 29 NOAA bathymetric data in meters relative to MLLW.

4.2.2 Winds

The Kodiak Airport meteorological data for the period of the simulation were provided. These data were processed into the format required by EFDC. A wind rose summary of these data is shown in Figure 30. It can be seen from this plot that there is a dominant on-shore wind to the West and West-Northwest during the calibration period.

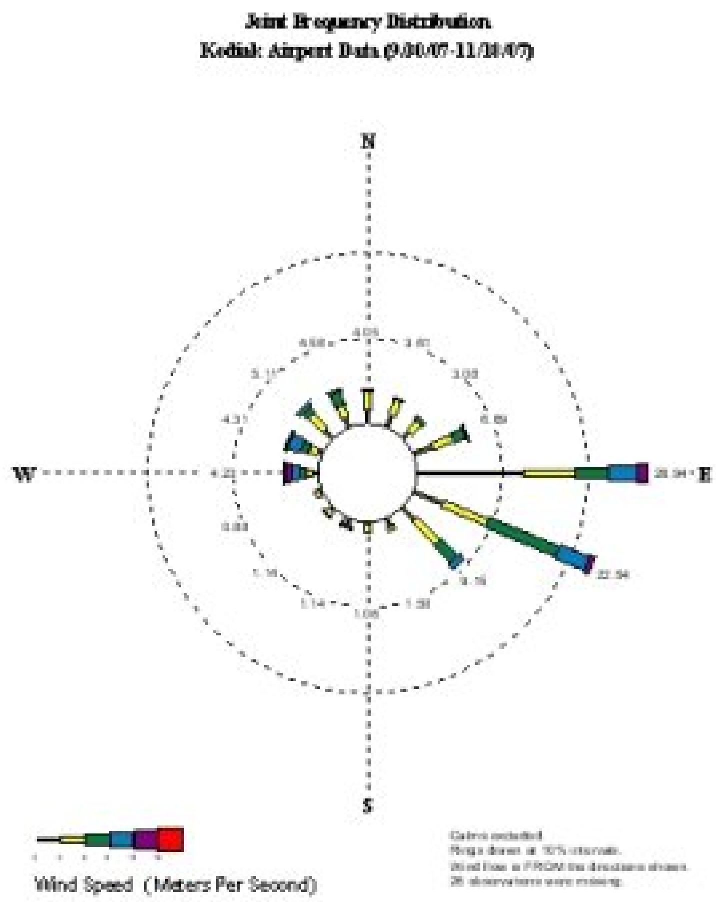

Figure 30 Kodiak Airport wind rose for the calibration period.

4.2.3 Flow Boundary Conditions

From a review of the USGS maps and discussions with the team, it was determined that there was only one significant freshwater source in the model domain, Buskin River. This river flows adjacent to the airport and discharges into the ocean in an area that may be impacted by the runway extensions.

At the current time, there are no time series data, measured or simulated, available for the river discharge. A single discharge estimate was provided of 6.3 m^3/s (221 ft^3/s). This was used as a constant discharge for all of the models. This flow rate is near the estimated mean annual flow (MAF) of the Buskin River, which is 6.1 m^3/s (215 ft^3/s).

4.2.4 Coarse Grid Model

4.2.4.1 Grid Development

A curvilinear grid was developed using the Delft RGFGrid (Delft, 2006) program for the Coarse Grid Model (CGM). The RGFGrid was configured for EFDC by importing the GRD file into EFDC-Explorer. Final minor editing to the grid was performed using EFDC-Explorer. The grid contained 3115 curvilinear horizontal grid cells. Figure 31 provides a plot for the coarse grid Kodiak coastal hydrodynamic EFDC model. This figure also shows a few of the indices for illustration.

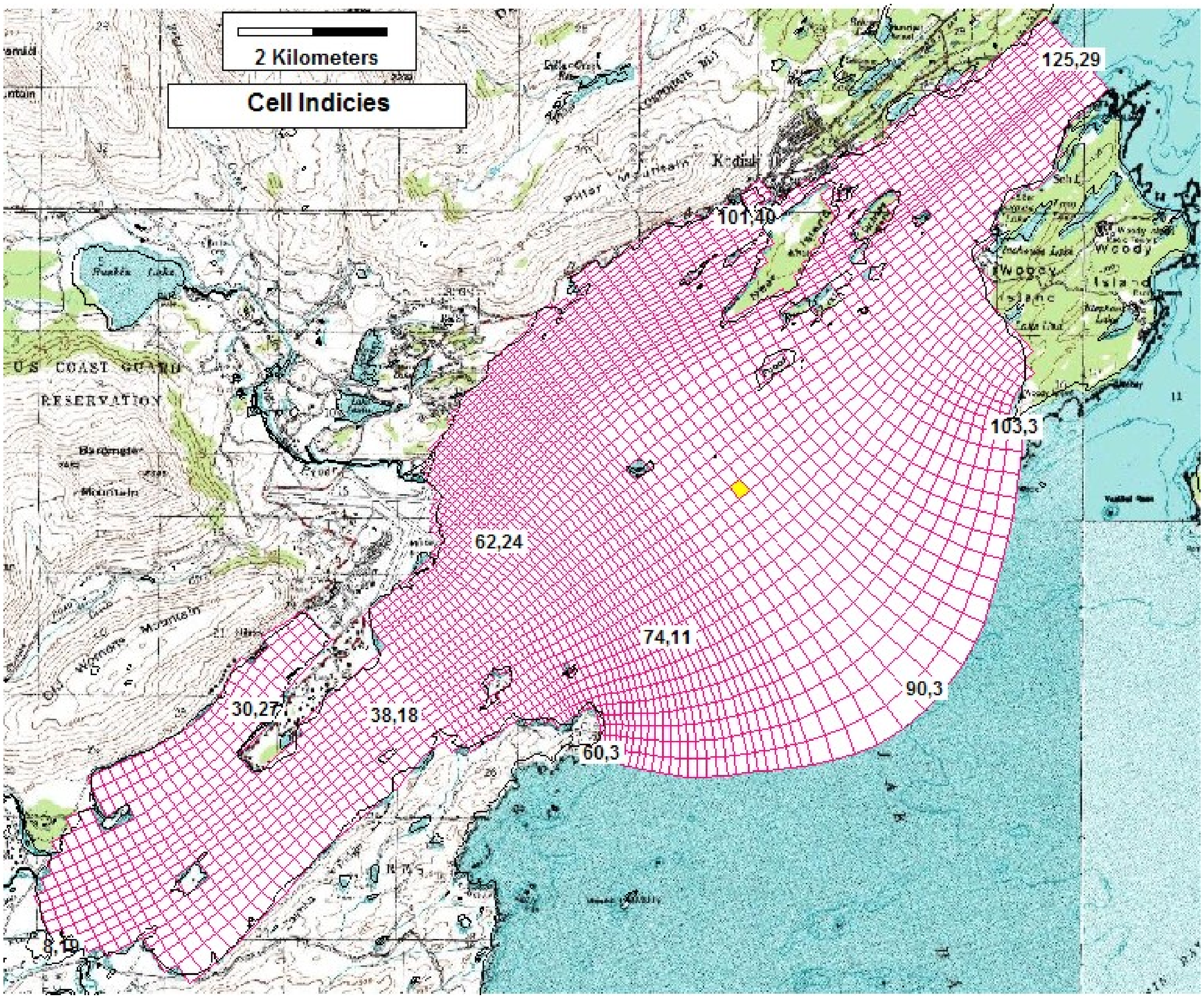

Figure 31 Kodiak Airport coastal hydrodynamic EFDC model grid (CGM).

Using the grid shown in Figure 31 and the bathymetric data shown in Figure 29, the model bathymetry for each cell was assigned. Figure 32 shows the coarse Kodiak grid with the final bathymetry. The actual deepest part of the model is -96.9 meters but the color range was set to -50 meters to show better resolution in the shallower regions. Thus all elevations at or less than -50 meters share the deep-blue color.

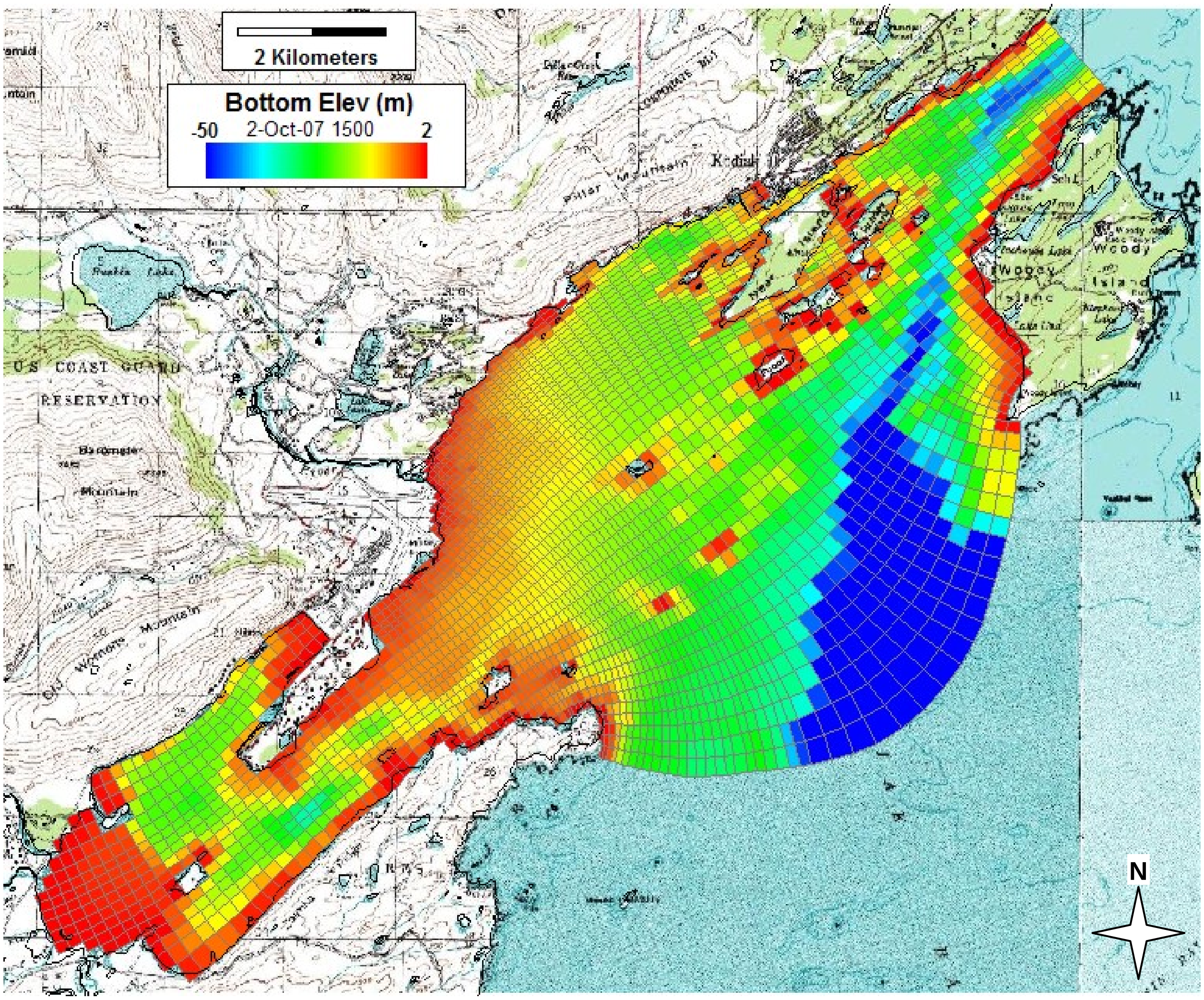

Figure 32 Kodiak Airport model bathymetry (MLLW, CGM).

4.2.4.2 Boundary Conditions

Once the final grid and bathymetry were determined, the boundary conditions were assigned to the appropriate grid cells based on location and type. The model used two types of boundaries; open boundary used for tidal forcings and an inflow boundary. Open boundaries were assigned to at the Chiniak Bay boundary (named the "SE" boundary) and in the Woody Island Channel (named the "NE" boundary). An inflow boundary was assigned to two cells where the Buskin River discharges into St. Paul Harbor. Figure 33 shows the EFDC model grid with the boundary condition locations identified and labeled by boundary group. An EFDC boundary group is defined as a collection of one or more EFDC model cells that comprise one logical inflow/forcing.

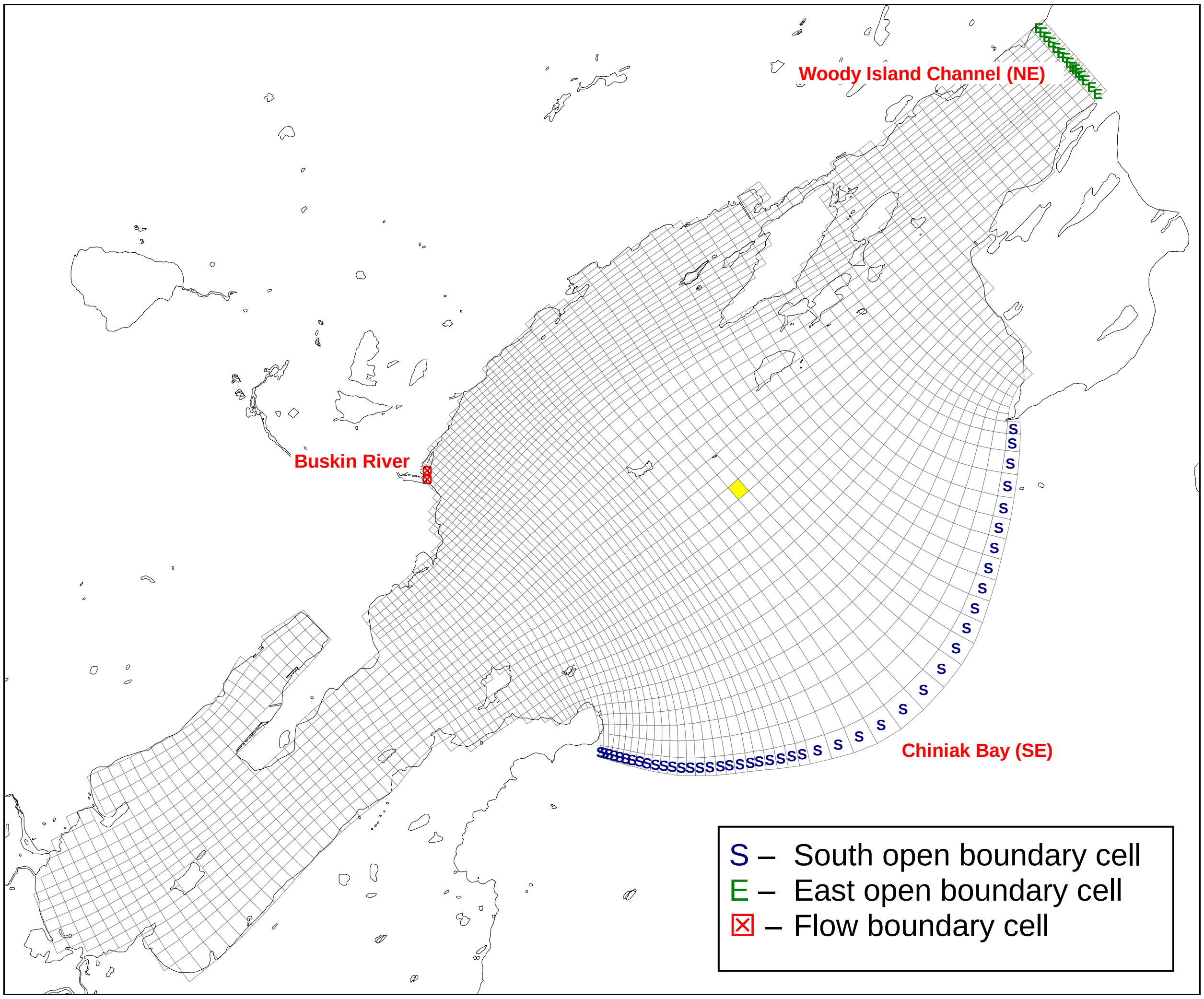

Figure 33 Boundary condition map (CGM).

Flow Boundary

An early estimate for the Buskin River was a mean annual discharge of 3.5 m^3/s (125 ft^3/s) (Solin, 1996). This was later updated by the Kodiak EIS team hydrologists to 6.1 m^3/s (215 ft^3/s). It is our understanding that this calculation was made by comparing a discharge measurement on the Buskin River to data from a similar USGS gauged stream. For the circulation modeling, a Buskin River discharge of 6.3 m^3/s for the Buskin River was used.

Open Boundary

The open boundaries were set using data from the ADCP data collection program. In addition to the vertical 3D velocity data measured by the ADCP's, the water depths were also recorded. These data were processed into water level series. Figure 34 shows the processed water surface elevation data for each of the ADCP units. These data were normalized to at 0.0 mean tide level by subtracting each unit's average depth. The data were then converted to the MLLW datum. However, given that the ADCP levels were not tied into a common vertical datum, small adjustments were needed in the tide levels to obtain calibration to the velocity data. The ADCP sites of Cliff Point and Woody Island were used to set the open boundary pressure series of Chiniak Bay (SE) and Woody Island Channel (NE), respectively.

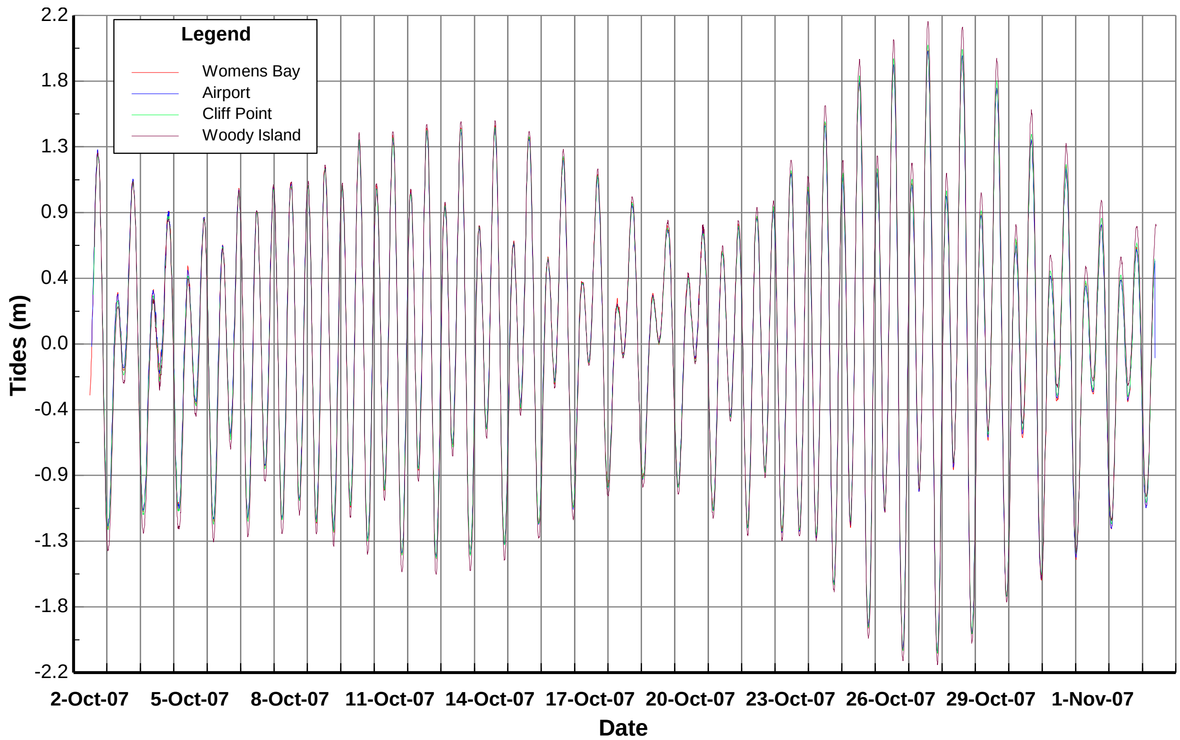

Figure 34 ADCP derived water surface elevations, normalized to mean depth.

4.2.4.3 Calibration Results

Using the model as described above, a series of model runs were made to obtain calibration. The primary calibration parameter adjusted was the tide levels for the Woody Island Channel. This boundary in combination with the Chiniak Bay levels causes relatively large currents in the channel. The primary calibration comparisons were the model versus ADCP velocity data comparisons. As the model is depth averaged, the ADCP velocity data were post-processed into their depth averaged values. Since the Woody Island and Cliff Point ADCP units were used to set the boundary conditions, only the Womens Bay and airport data was available for calibration.

The comparisons of model versus ADCP data velocity magnitudes for the airport and Womens Bay sites are shown in Figures 35 and 36, respectively. It can be seen that the velocities at the airport site are significantly lower than at the Womens Bay site. Figure 37 shows a 2-dimensional plan view of the model versus data comparisons for the depth averaged velocities during the ebb and flood tides on October 9, 2007.

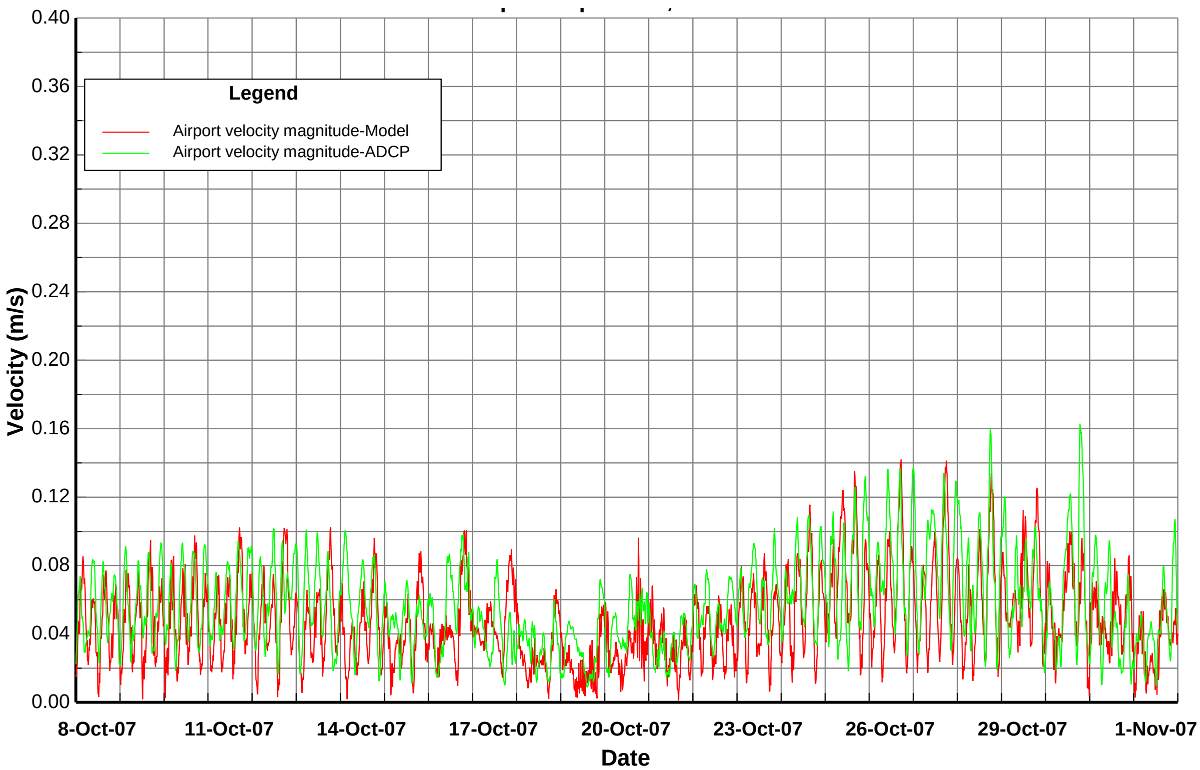

Figure 35 Velocity magnitude comparison of model versus data for the airport.

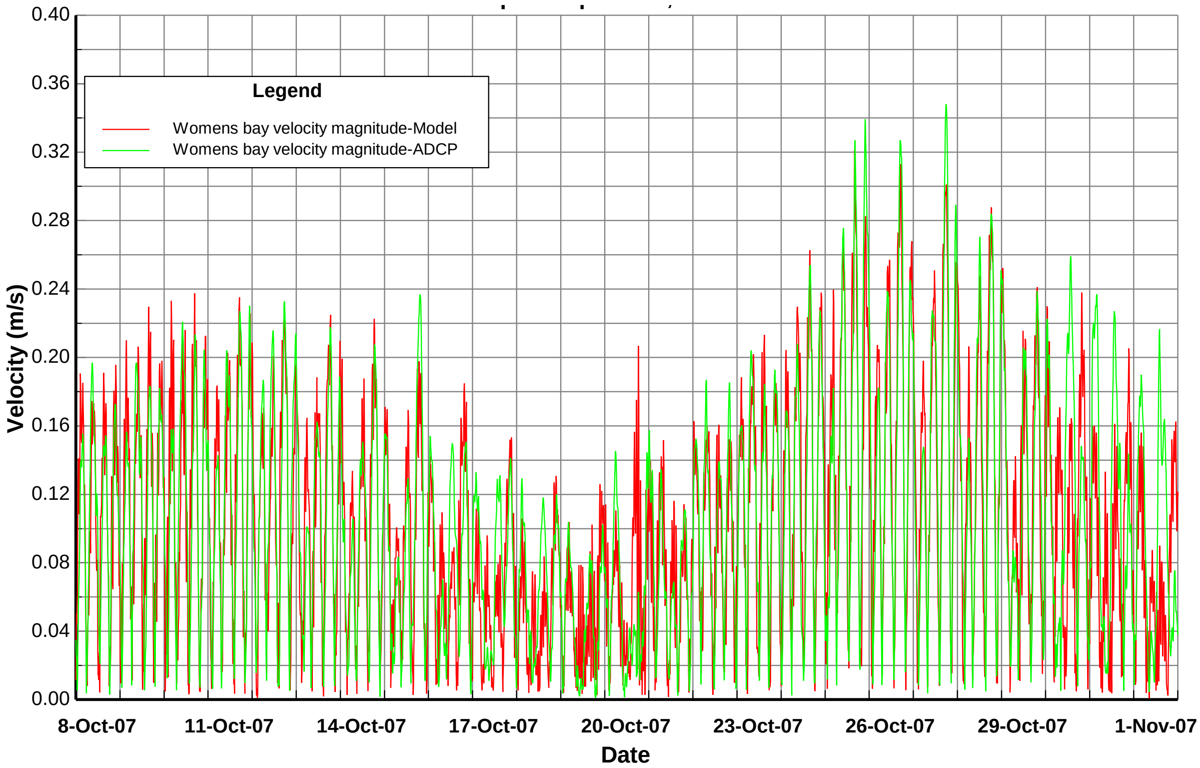

Figure 36 Velocity magnitude comparison of model versus data for the Womens Bay site.

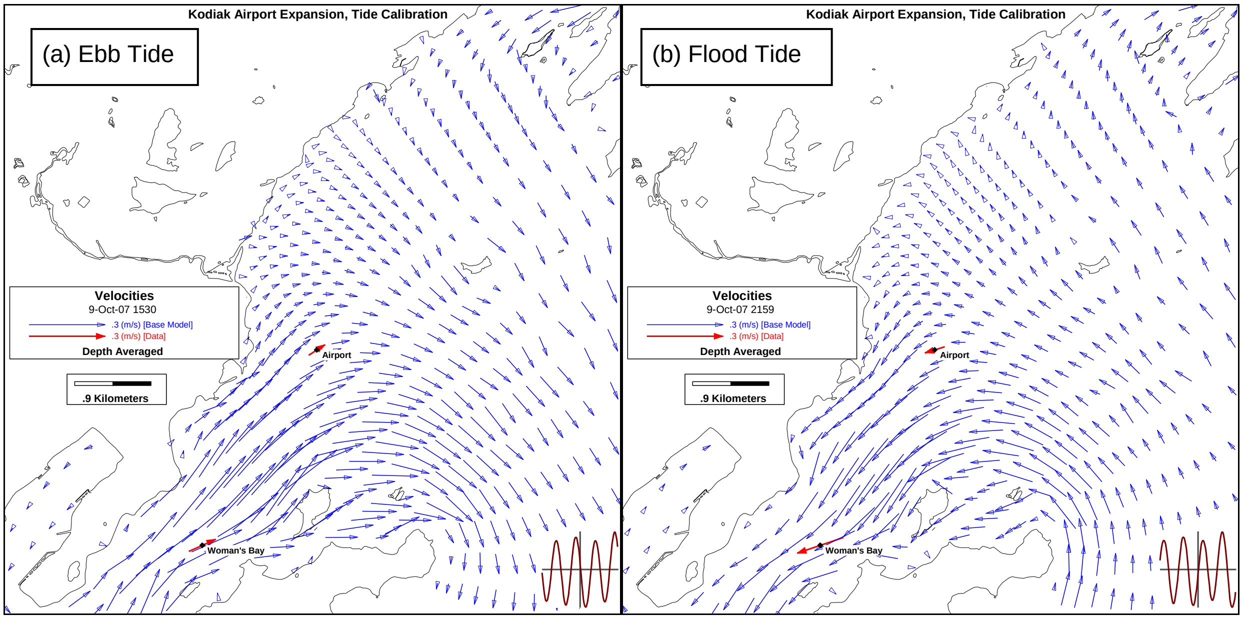

Figure 37 Velocity comparison of model versus data for (a) ebb tide and (b) flood tide conditions on October 9.

4.2.5 Nested Grid Model

Once the CGM was calibrated the Nested Grid Model (NGM) was developed. The primary differences between the two models were the grids and the boundary conditions.

4.2.5.1 Grid Development

The NGM grid is shown in Figure 38. This model has 3,788 active cells and covers 1,860 ha (7.2 mi^2). Figure 39 shows the NGM domain overlaid on the CGM model domain for reference.

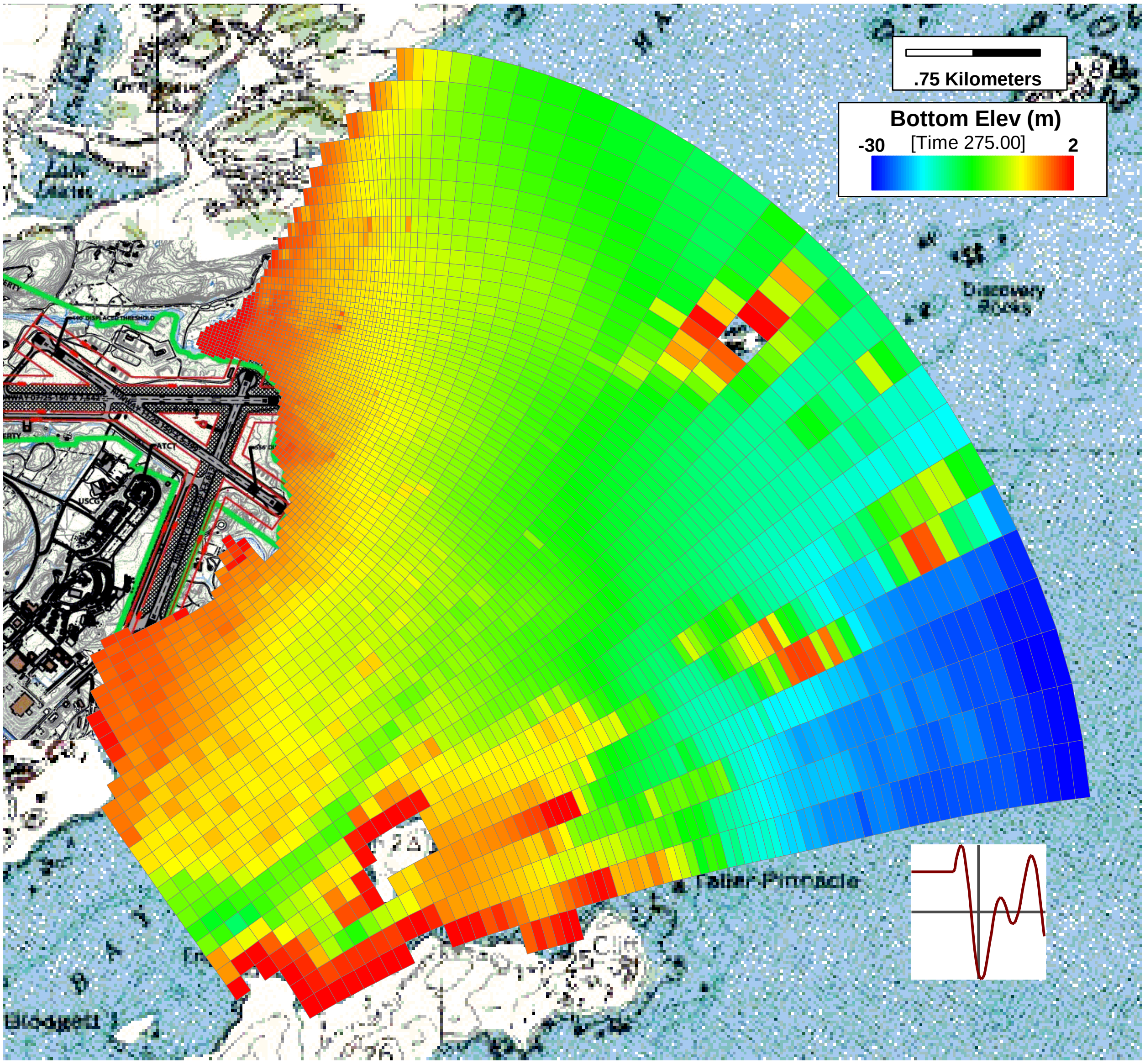

Figure 38 Kodiak Airport bathymetry and grid (MLLW, NGM).

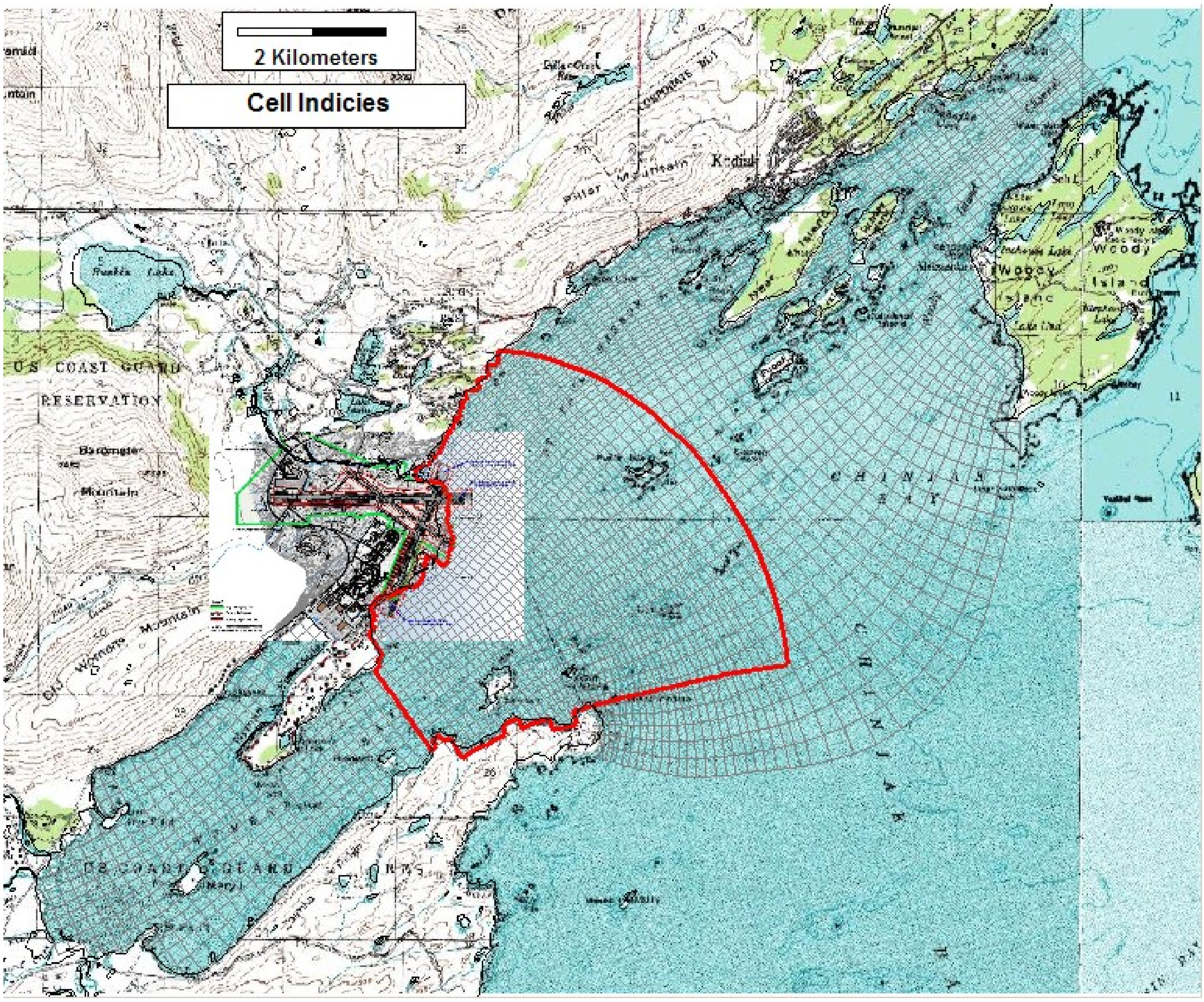

Figure 39 Nested Grid Model domain overlaid on the Coarse Grid Model.

4.2.5.2 Boundary Conditions

Figure 40 provides a plot of the NG model domain with the location, type and name of each boundary condition group.

The boundary conditions for the NGM model were extracted from the CGM. For the east and south boundaries in Chiniak Bay and St Paul Harbor, the CGM water levels were used to set the NGM boundaries. For each CGM cell corresponding to an NGM cell, the CGM water levels were extracted from the calibrated model and assigned as a boundary time series for the NGM cell.

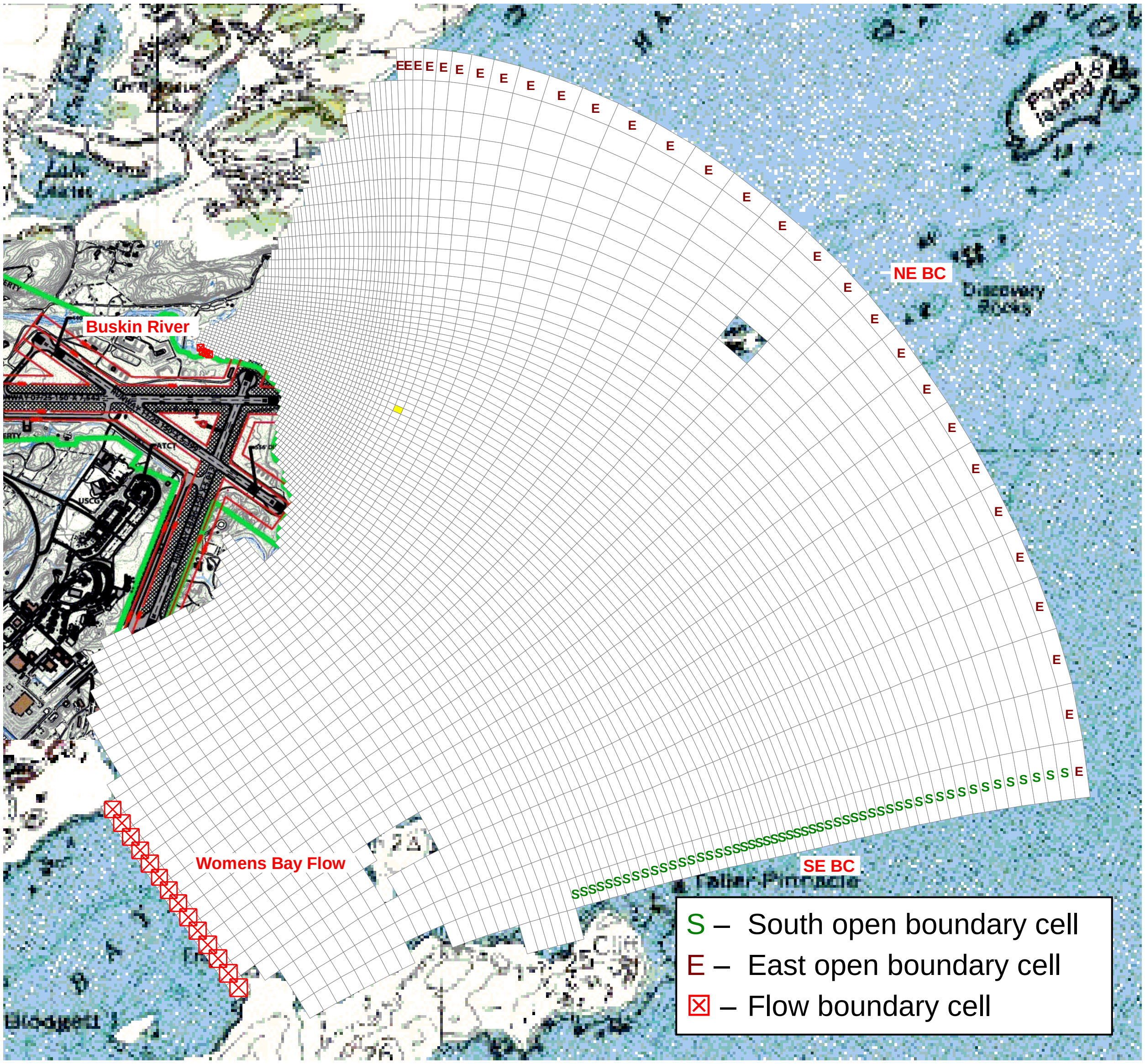

Figure 40 Boundary condition map (NGM).

For the boundary connecting at Womens Bay, a flow boundary was used. The time series of flows across the location of the NGM boundary were extracted from the CG model. Figure 41 shows the computed flows from the CGM model. These flows were assigned as the boundary condition for the NGM.

The flow boundary for Buskin River used the same approach as used for the CG model. A constant flow of 6.3 m^3/s was split among the four cells located near the mouth of the Buskin River.

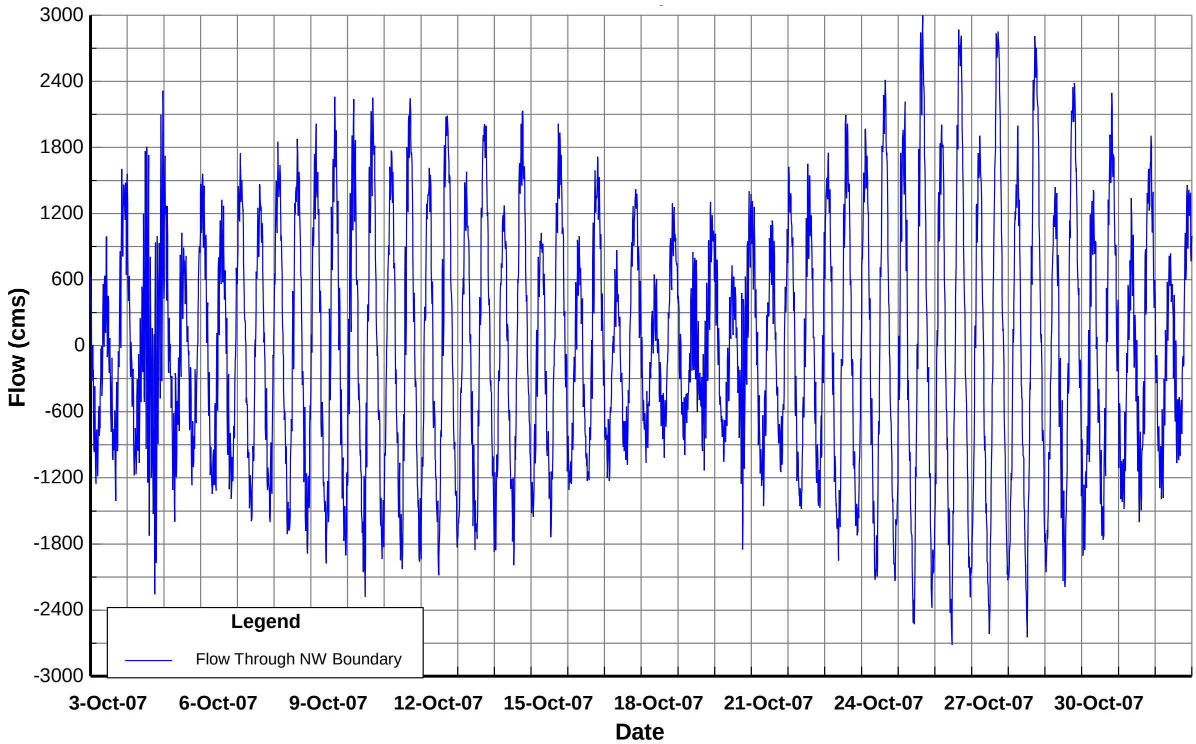

Figure 41 Flow in the CGM model at the NGM Womens Bay boundary section.

4.2.5.3 Calibration Results

The NG model was calibrated to the velocity magnitudes and directions from the Airport ADCP site. Figure 42 shows the results of the velocity magnitude comparison with the data. The model magnitudes matched the Airport ADCP data reasonable well given the lack of strong forcing tidal flows.

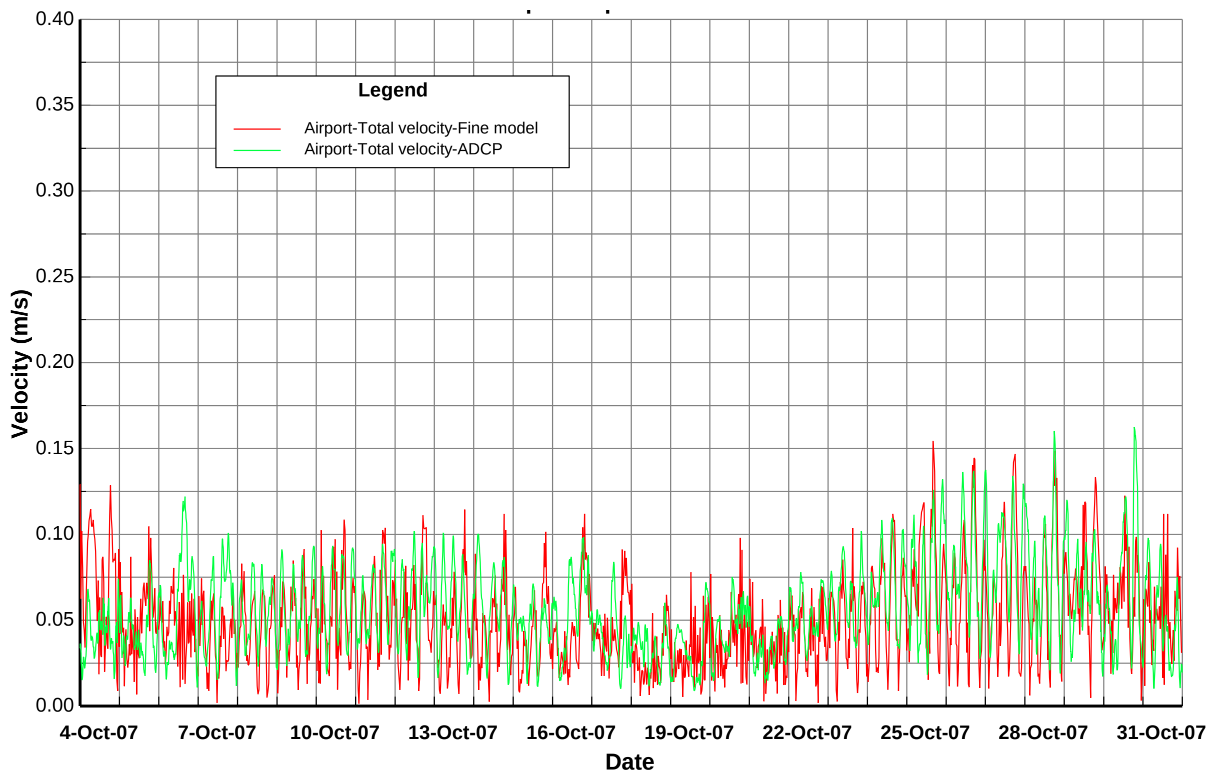

Figure 42 Velocity magnitude comparison of model versus data for the airport site (NGM).

4.3 Existing Conditions

After the CGM and NGM models were calibrated, the models were used to evaluate the existing currents, bed shear stresses and mixing patterns.

Figure 43 shows several snapshots in time during a typical tidal cycle. The period shown is for October 9, 10am to 10:30pm. Without the effect of waves, the near shore region around the airport is nearly a backwater area. The tidal currents are small. For this period, the region just east of the airport is essentially a large eddy during the tide cycle.

This can be illustrated two ways. First, using the CGM model, dye with a concentration of 100 mg/l was added to the Buskin River flows. The model computed the dye distribution in St. Paul Harbor. Figure 44 summarizes the dye concentrations at various times during the simulation period. It can be seen that the Buskin River waters tend to hug the coastline but are very influenced by the winds. During the first period of time until October 20th there was a strong on-shore wind which held the Buskin waters close to shore (Figure 44(b)). Then the winds shifted to come out of the west and northwest.

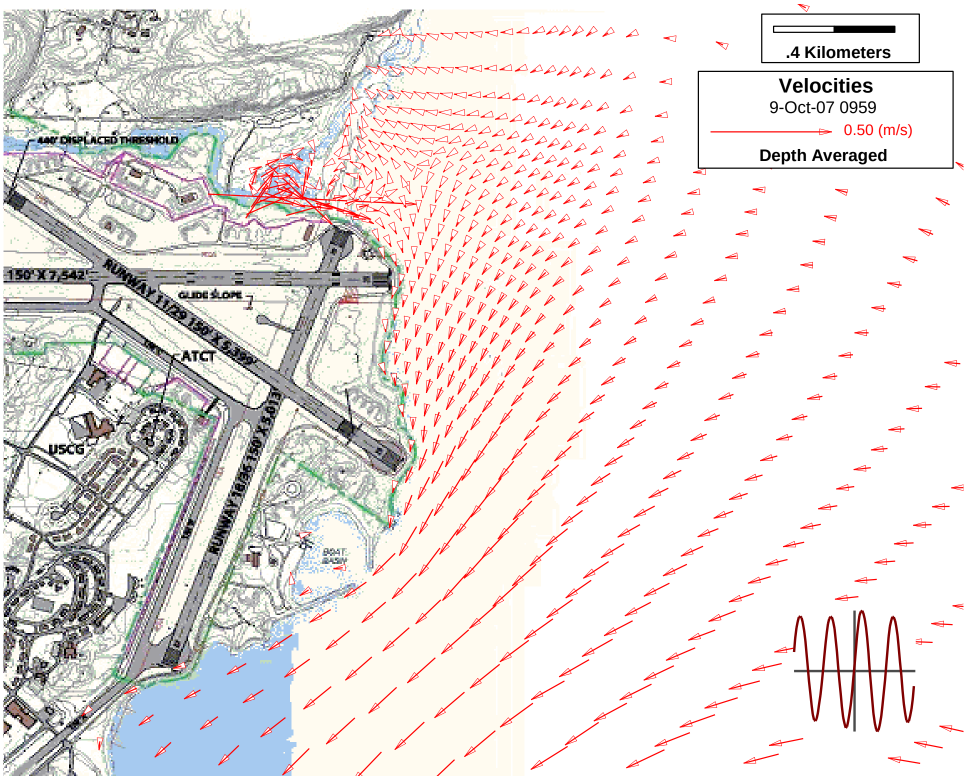

Figure 43a Typical current pattern during a tide cycle (NGM).

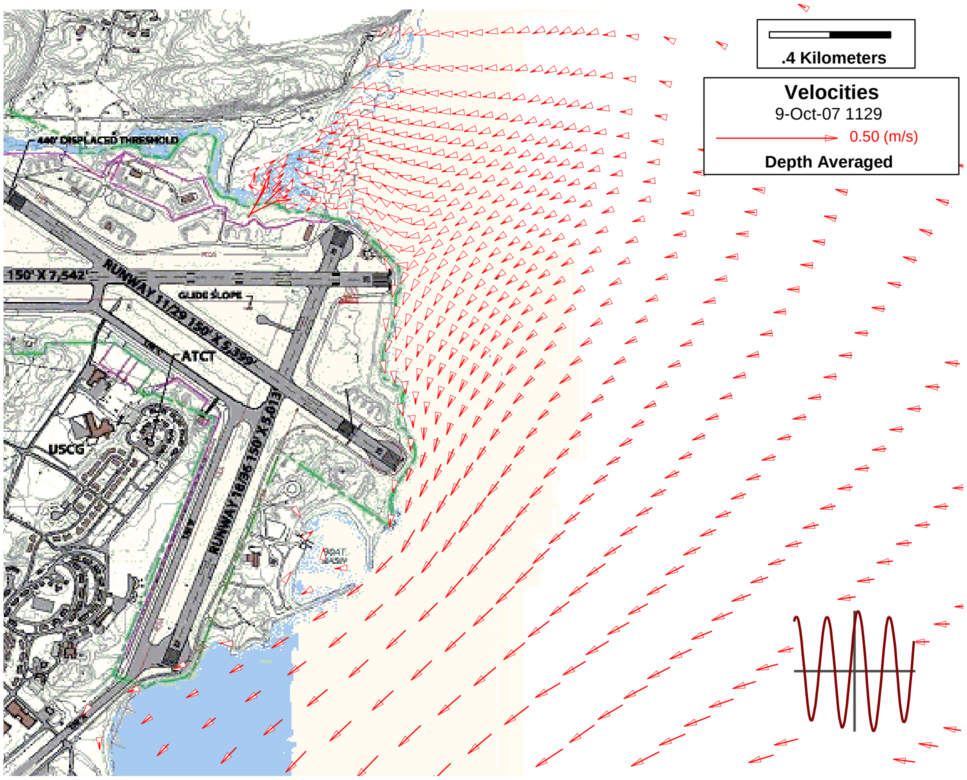

Figure 43b Typical current pattern during a tide cycle (NGM).

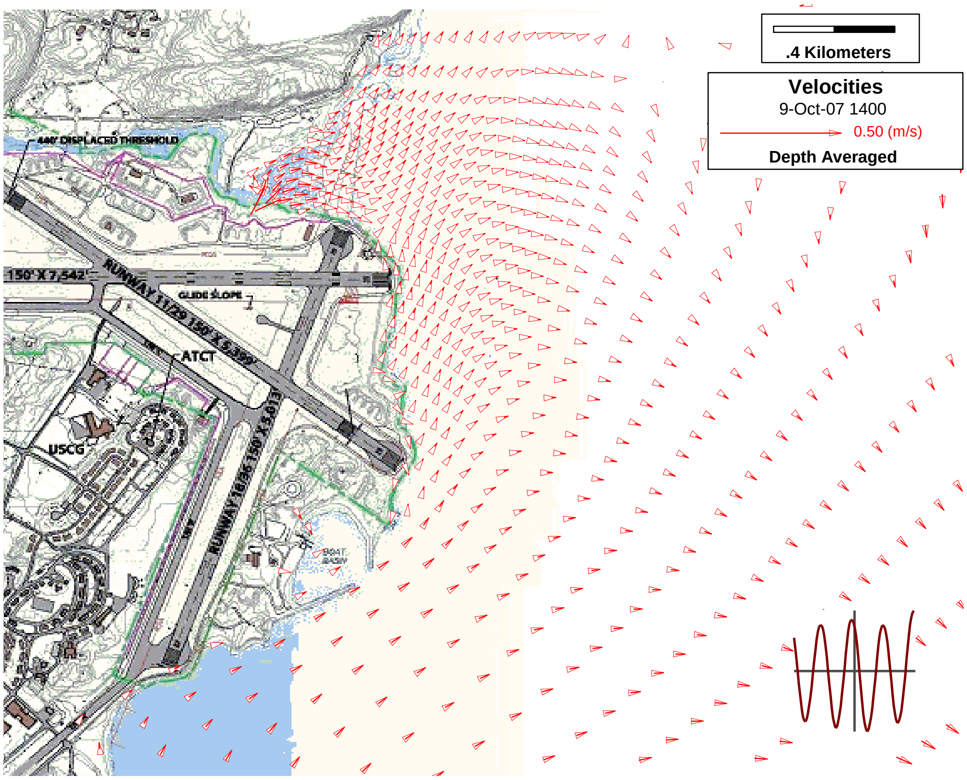

Figure 43c Typical current pattern during a tide cycle (NGM).

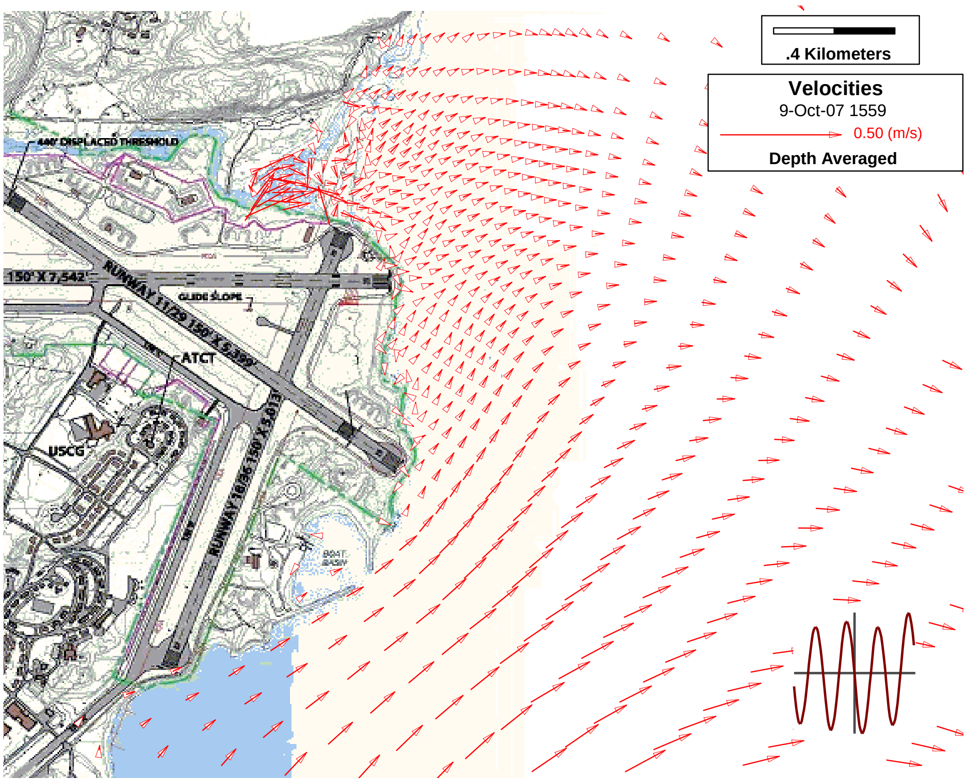

Figure 43d Typical current pattern during a tide cycle (NGM).

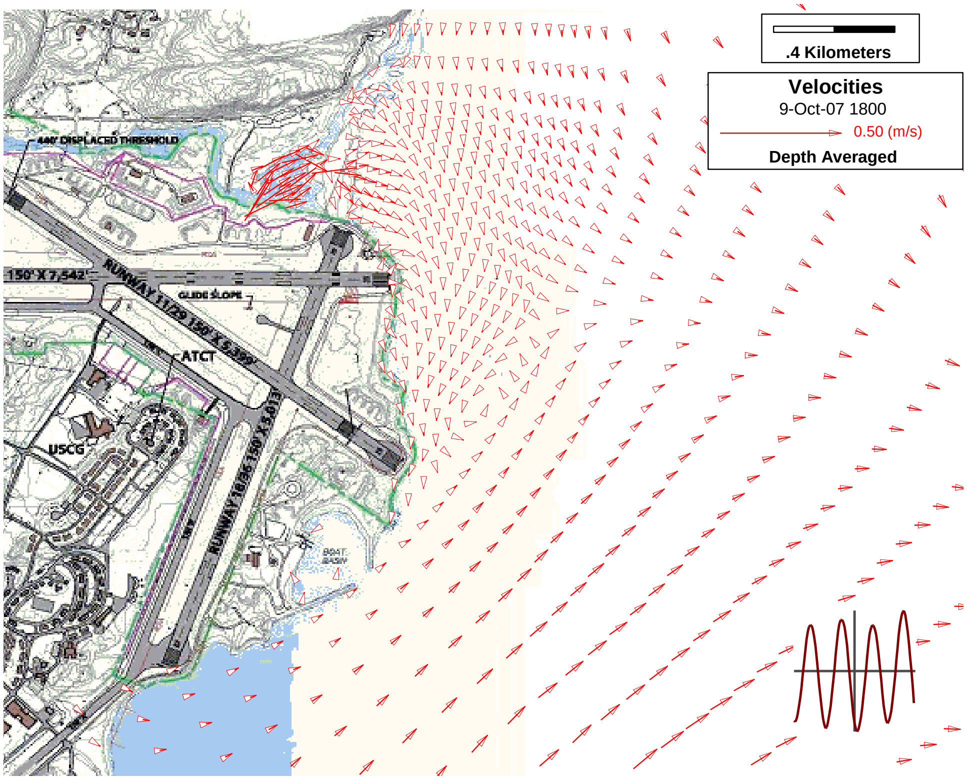

Figure 43e Typical current pattern during a tide cycle (NGM).

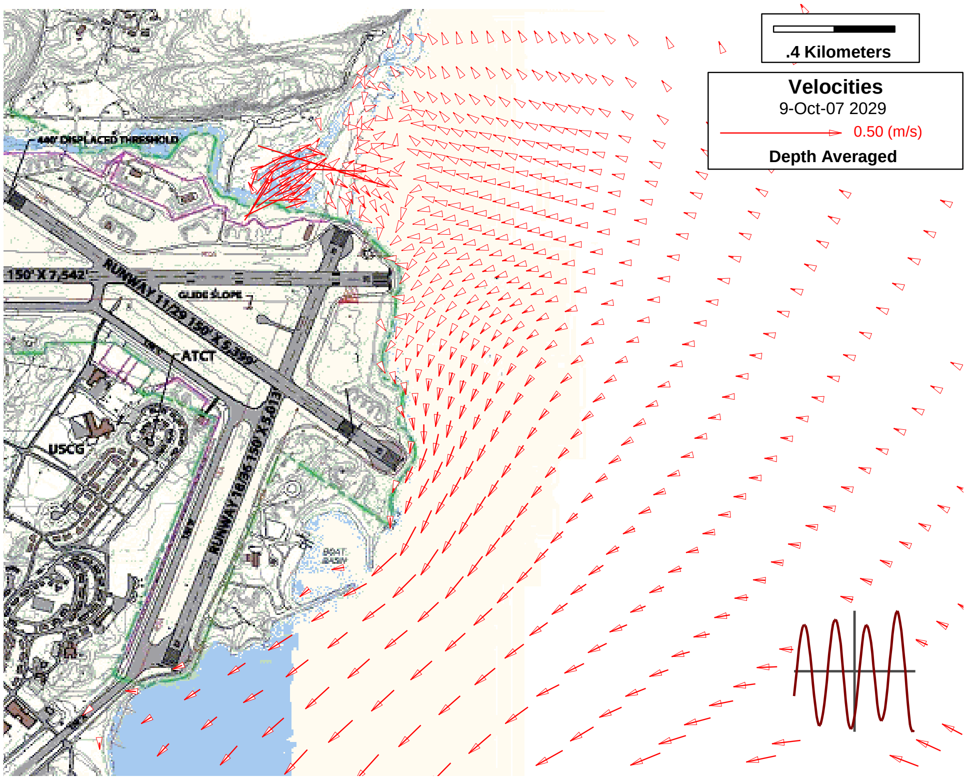

Figure 43f Typical current pattern during a tide cycle (NGM).

This pushed the Buskin waters off shore (Figures 44(c) and 44(d)). The wind indicator in each of the panels shows the "wind to" direction. This method demonstrates that the net transport of the waters near the airport are dominated by wind driven currents more than tides.

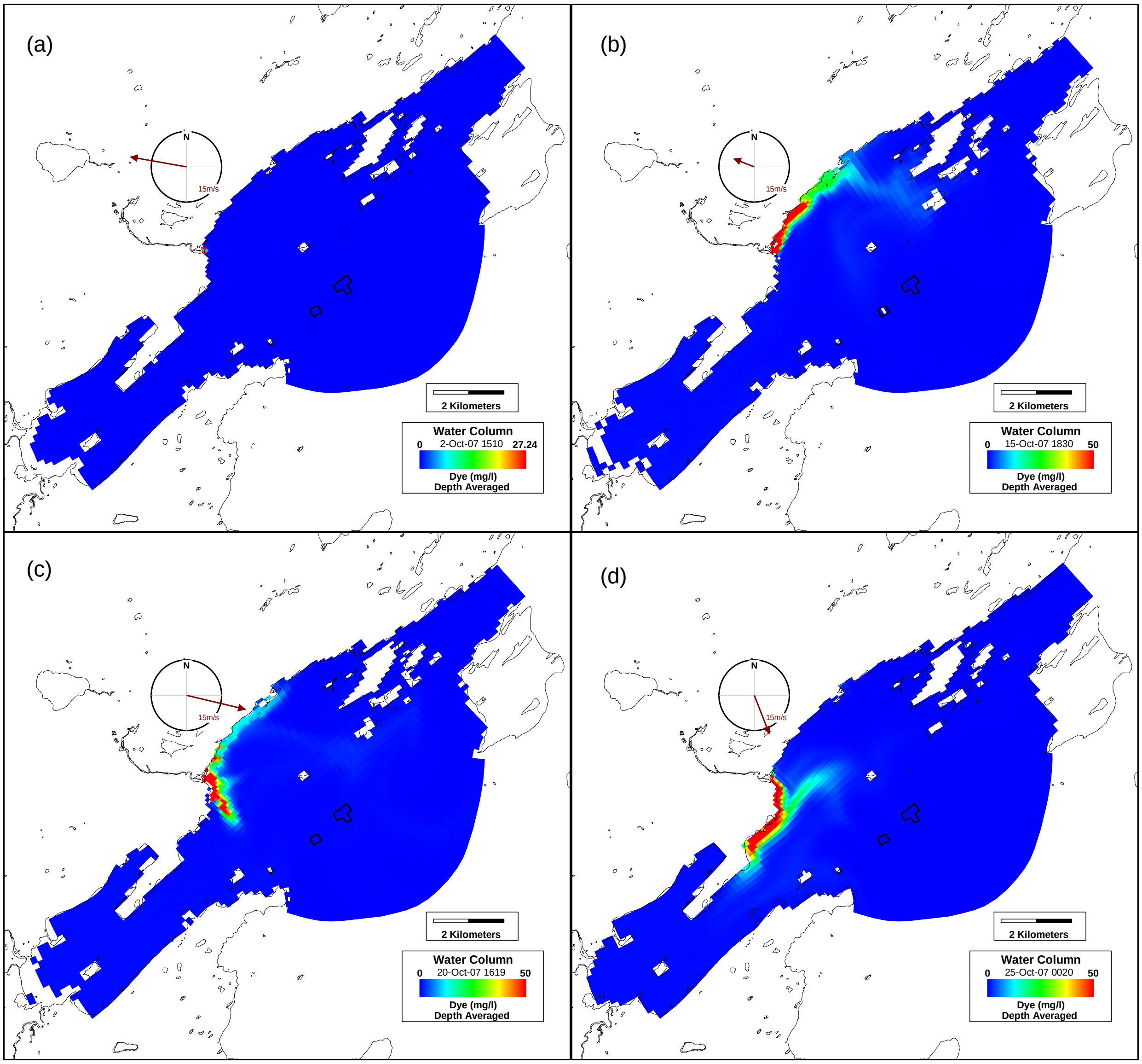

Figure 44 Buskin River flow mixing analysis.

The second method is by using the model to compute “Age of Water.” The CG model is used to compute the current residence time of a packet of water. As the model progresses, the water is “aged,” advected and dispersed due to tides and winds. At the beginning of the run, all of the water has an “age” of 0.0. All of the boundary conditions have an “age” of zero assigned. At the end of the 31 day simulation, the maximum “age” of any water would be 31 days. Figure 45 summarizes the residence time analysis. At the beginning of the run, the water age is 0.0, Figure 45(a). Later as the water “ages,” the older water is mainly in St. Paul Harbor and Womens Bay (Figures 45(b) and 45(c)). Near the end of the simulation period, it can be seen that Womens Bay has had relatively little exchange with water from a boundary and the waters in St. Paul Harbor are older (Figure 45(d)).

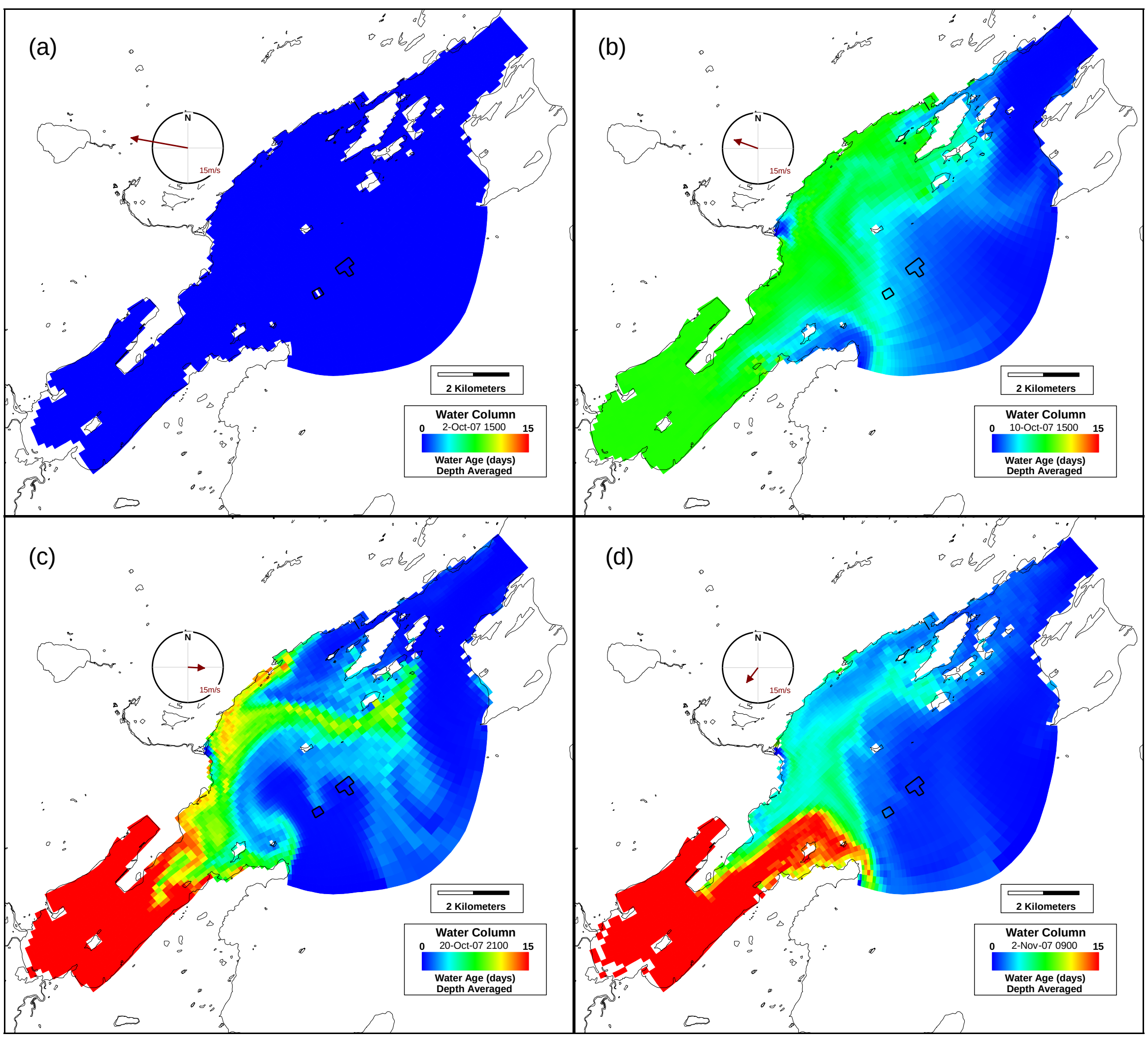

Figure 45 Coarse Grid Model residence time analysis.

Sediment transport was not simulated. However, to address the question of sediment scour and deposition, bed shear stresses were computed for both the CGM and the NGM models. Figure 46 shows the bed shear stress in Newtons/m^2 (N/m^2) when the ebb flow is near a maximum for the NG model. These bed shear stresses are small and would result in little to no scour. With a maximum shear stress of about 1 N/m^2, only fine silts and unconsolidated clays would be scoured and/or resuspended. Since the velocities were relatively low, these low bed shear stresses should be expected. This analysis should be tempered with an understanding that storm events and wave generated turbulence were not treated.

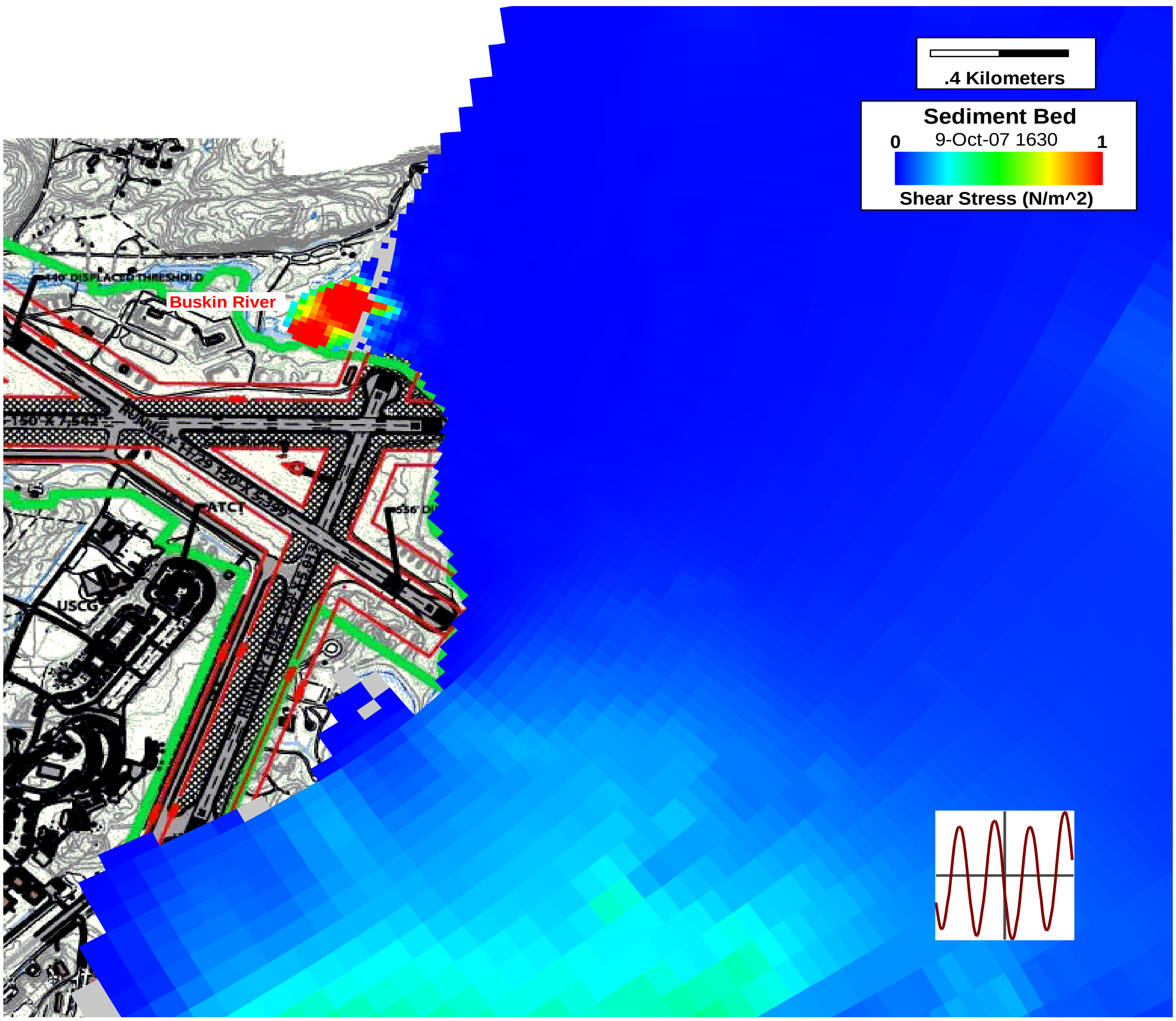

Figure 46 Near airport bed shear during maximum ebb flow (NGM).

4.4 Hydrodynamic Modeling of Alternatives

To analyze the hydrodynamic responses to the runway extension alternatives, the fine grid model presented in Section 4.2.5 was used as the base case scenario. To address the various runway extension alternatives, this base case model was modified by deactivating the cells in the areas of the runway extensions thereby representing the filled/dry land areas while keeping the remaining grid identical. All other boundary and initial conditions were kept the same as the base case model. The period used for the alternatives analysis was October 2007.

The following alternatives were modeled:

- Runway 18/36 RSA Alternative 2-Extend RSA on both Runway ends by 400 feet and use declared distance.
- Runway 8/36 RSA Alternative 3-Extend runway end 18 by 1200 feet and use declared distance.
- Runway 07/25 RSA Alternative 2-Extend Runway end 25 by 800 feet.
- Combined Alternatives: Runway 18/36 RSA- extend runway end 18 by 1,200 feet; Runway 18/36 RSA-extend runway end 36 by 600 feet; and Runway 07/25 RSA-extend runway end 25 RSA by 800 feet.

The model results for each alternative were then compared with the base case for analysis of velocity patterns, flow, mixing of the Buskin River flows and bed shear stress.

4.4.1 Models Development

4.4.1.1 Grid Development

The Base Case grid is shown in Figure 47. This model has 13533 active cells and covers 1860 ha (7.2 mi^2). The cells in the model domain near the airport are the most refined with the smallest grid size of 12x12m. Away from the airport ,the grid sizes increase to a maximum size of the cells of about 80x80m.

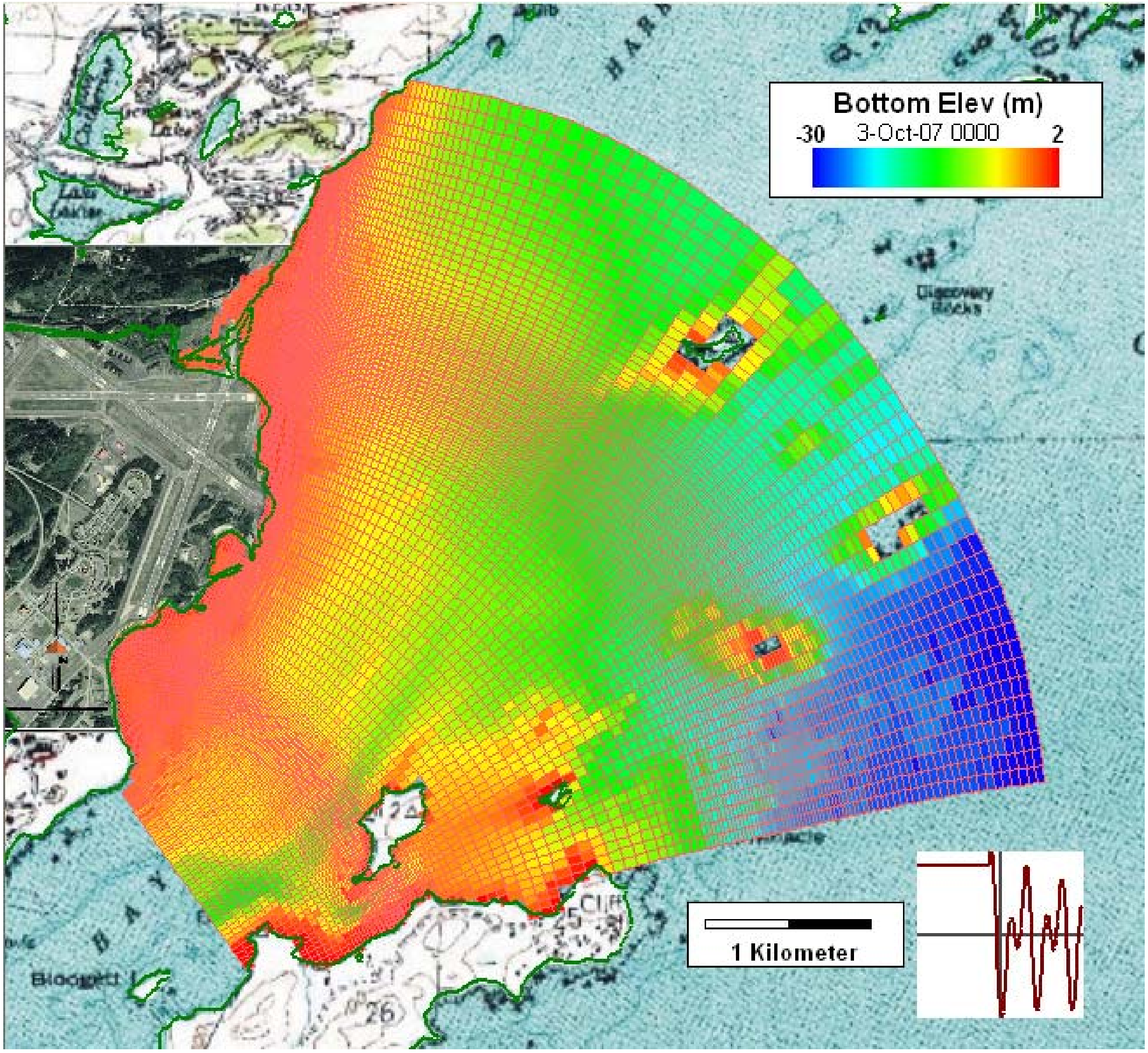

Figure 47 Kodiak Airport bathymetry and grid (Base Case Model).

4.4.1.2 Boundary Conditions

Figure 48 provides a plot of the Base Case model domain with the location, type and name of each boundary condition group. The boundary conditions for the base case and all the alternative models were kept the same. These boundary conditions were the same as was used in the nested grid model.

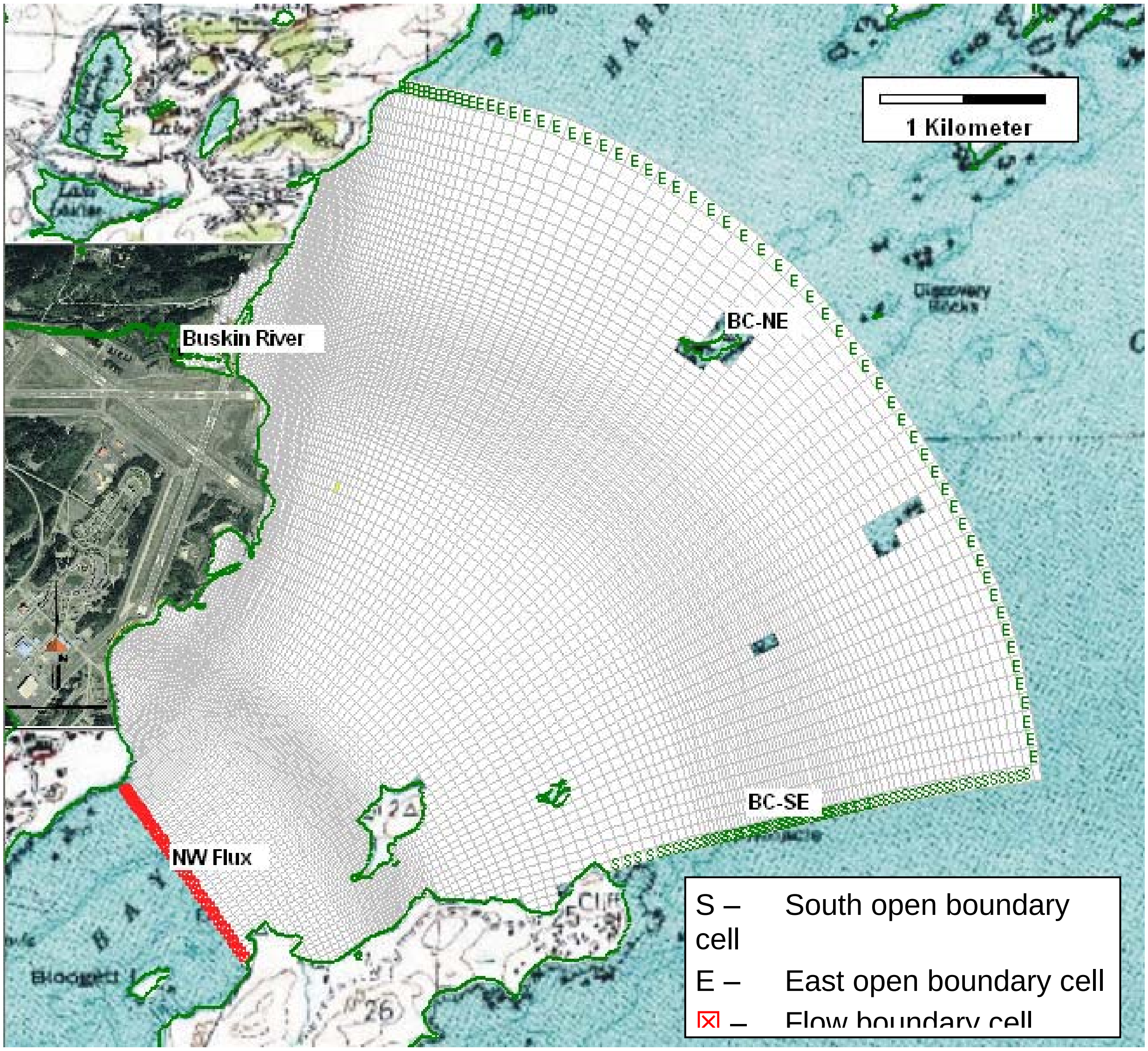

Figure 48 Base Case boundary condition map.

The flow boundary for the Buskin River used the same approach as was used for the CG and NG models. A constant flow of 6.3 m^3/s was split between the two cells located near the mouth of the Buskin River. In association with the Buskin flow, a concentration of 100mg/l of a dye was added to the river flow to illustrate mixing and river water distribution in St. Paul Harbor.

4.4.2 Base Case

The Figure 49 shows the close up of the grid near the airport for the Base Case. This figure shows the fine grid spacing along the shoreline and in the areas of the proposed runaway extensions.

The Base Case model was calibrated to the velocity magnitudes and directions from the Airport ADCP site. Figure 50 shows the results of the velocity magnitude comparison with the data. The model magnitudes matched the Airport ADCP data reasonable well given the lack of strong forcing tidal flows.

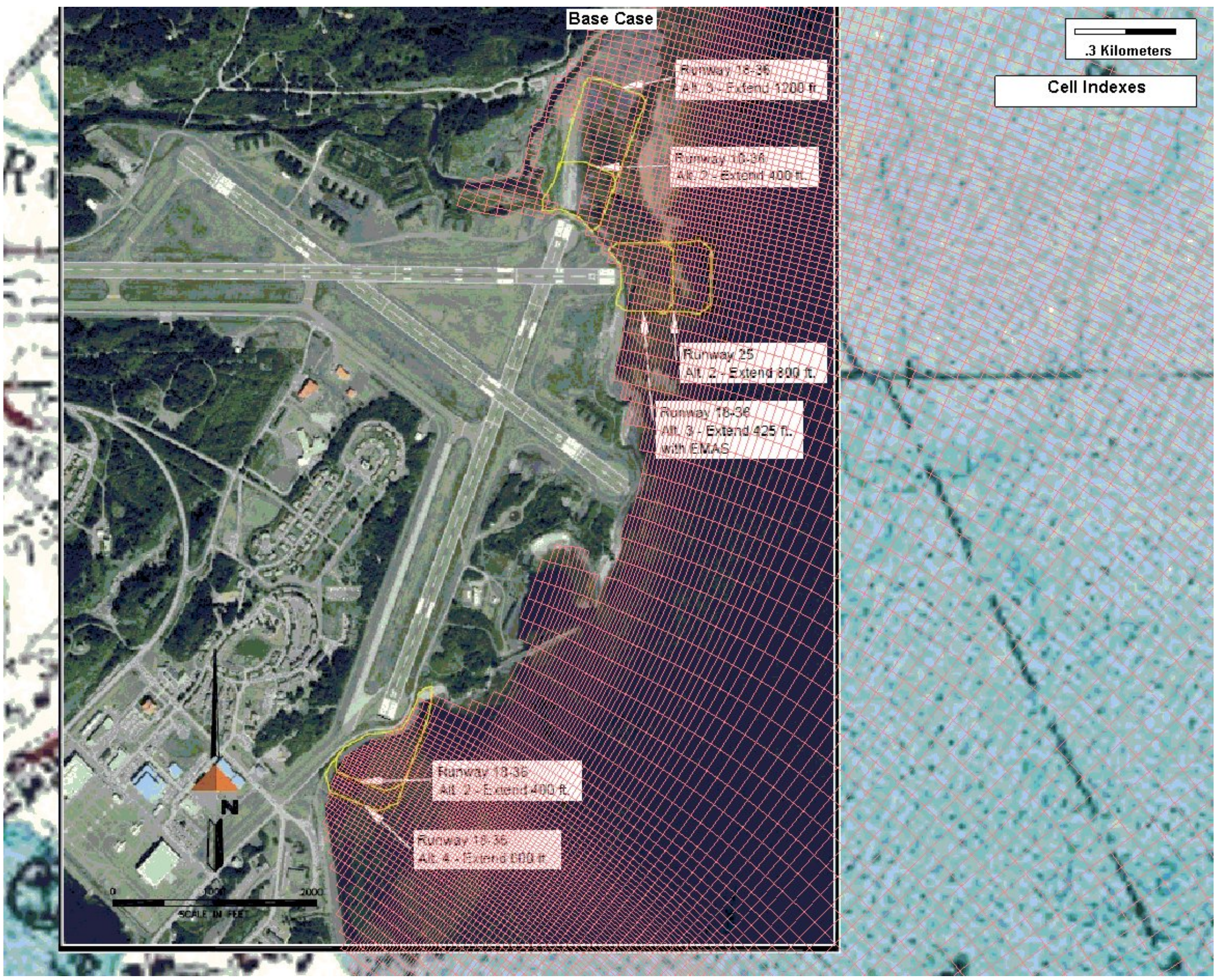

Figure 49 Base Case model grid near Kodiak Airport.

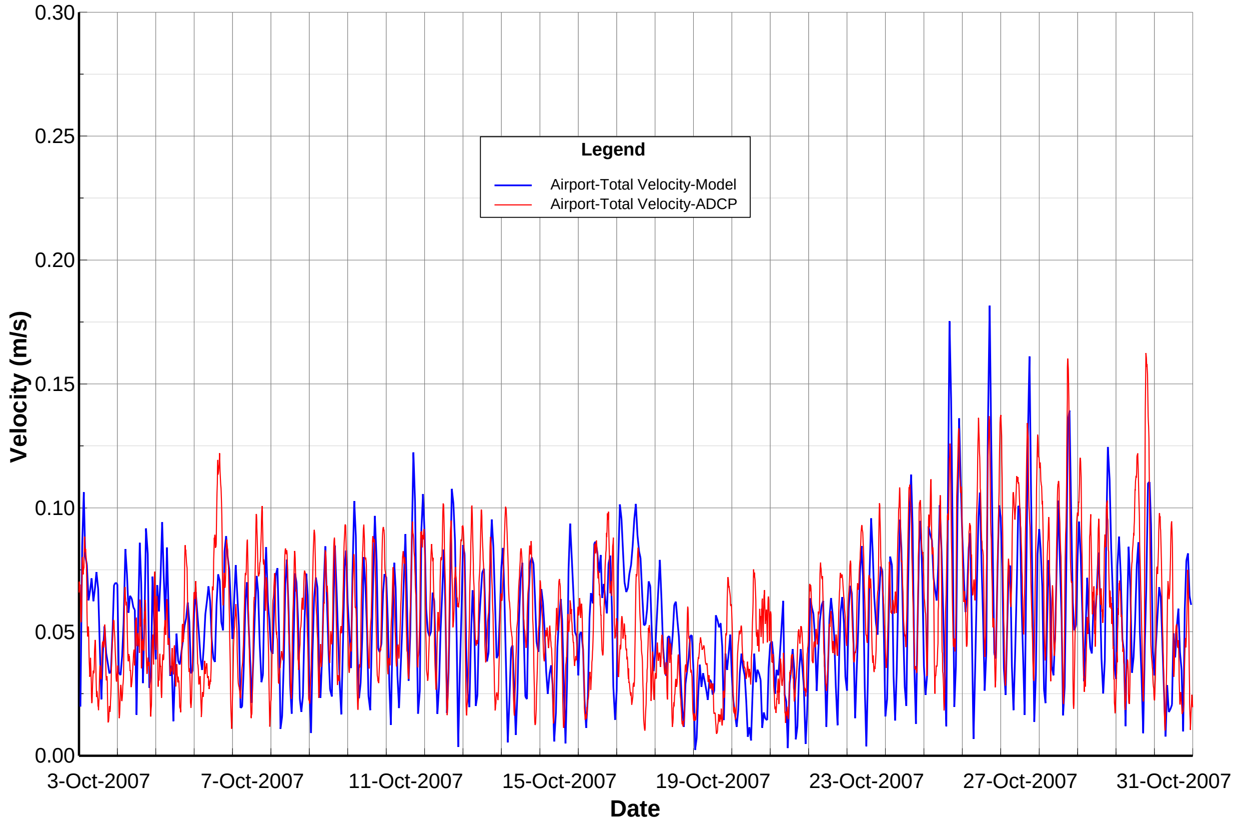

Figure 50 Velocity magnitude comparison of model versus data for the airport site (Base Case model).

Figure 51 illustrates a typical velocity field for the Base Case during two snapshots in time. Figure 51a shows the velocities during a ebb flow condition and Figure 51b shows a typical flood tide condition. Given the shape of the harbor and the position of the airport in the harbor, flows induced by surface wind shears are as important as tidally induced velocities.

Figure 52 summarizes the dye concentrations representing the Buskin River water mixing at various times during the simulation period. The Buskin River waters tend to hug the shoreline during any onshore winds but then get swept out into St Paul Harbor during times when the winds shift offshore. Figure 53 shows the bed shear stress in Newtons/m^2 (N/m^2) for the corresponding times.

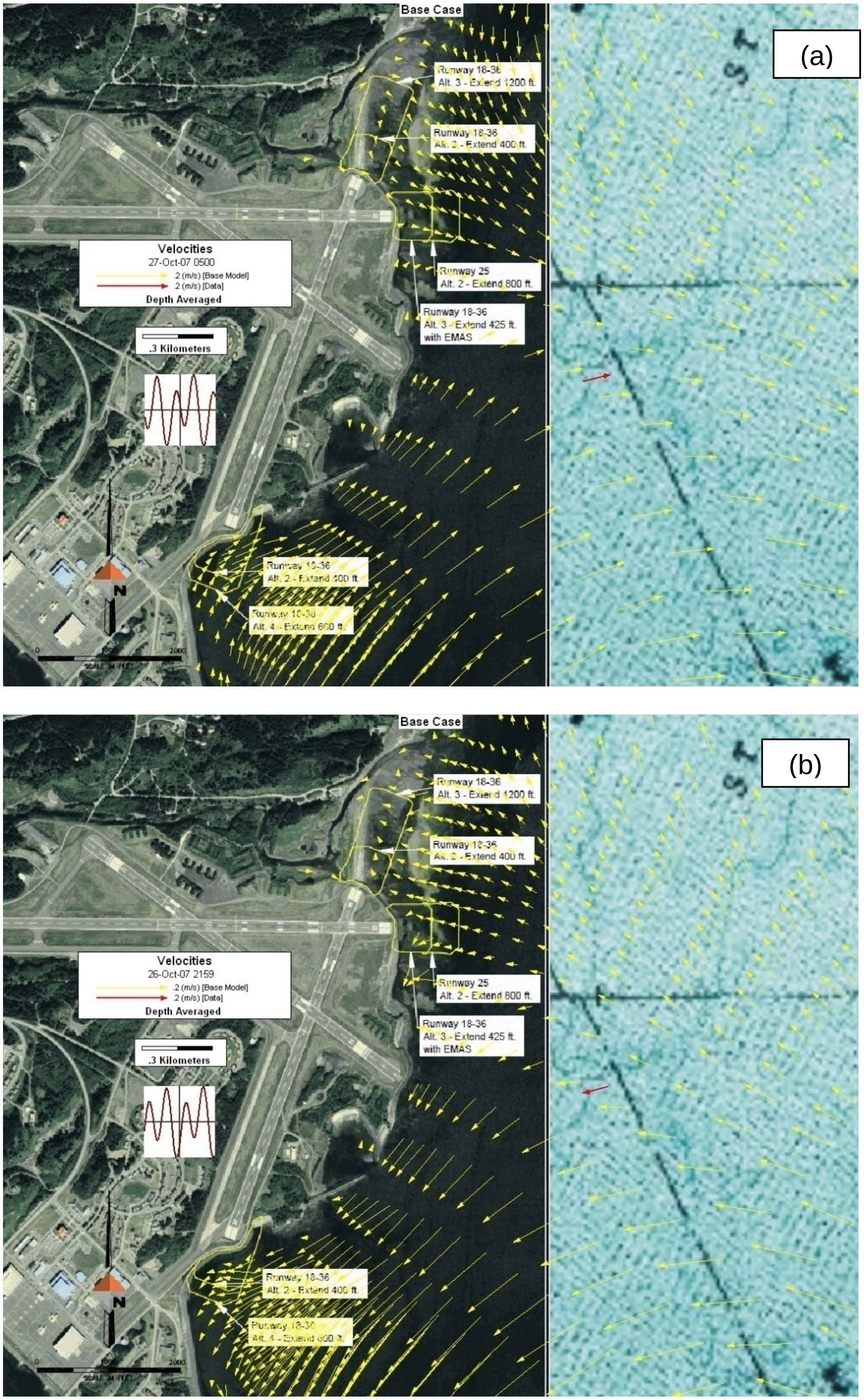

Figure 51 Base Case: Typical velocity patterns during tide (a) ebb tide and (b) flood tide.

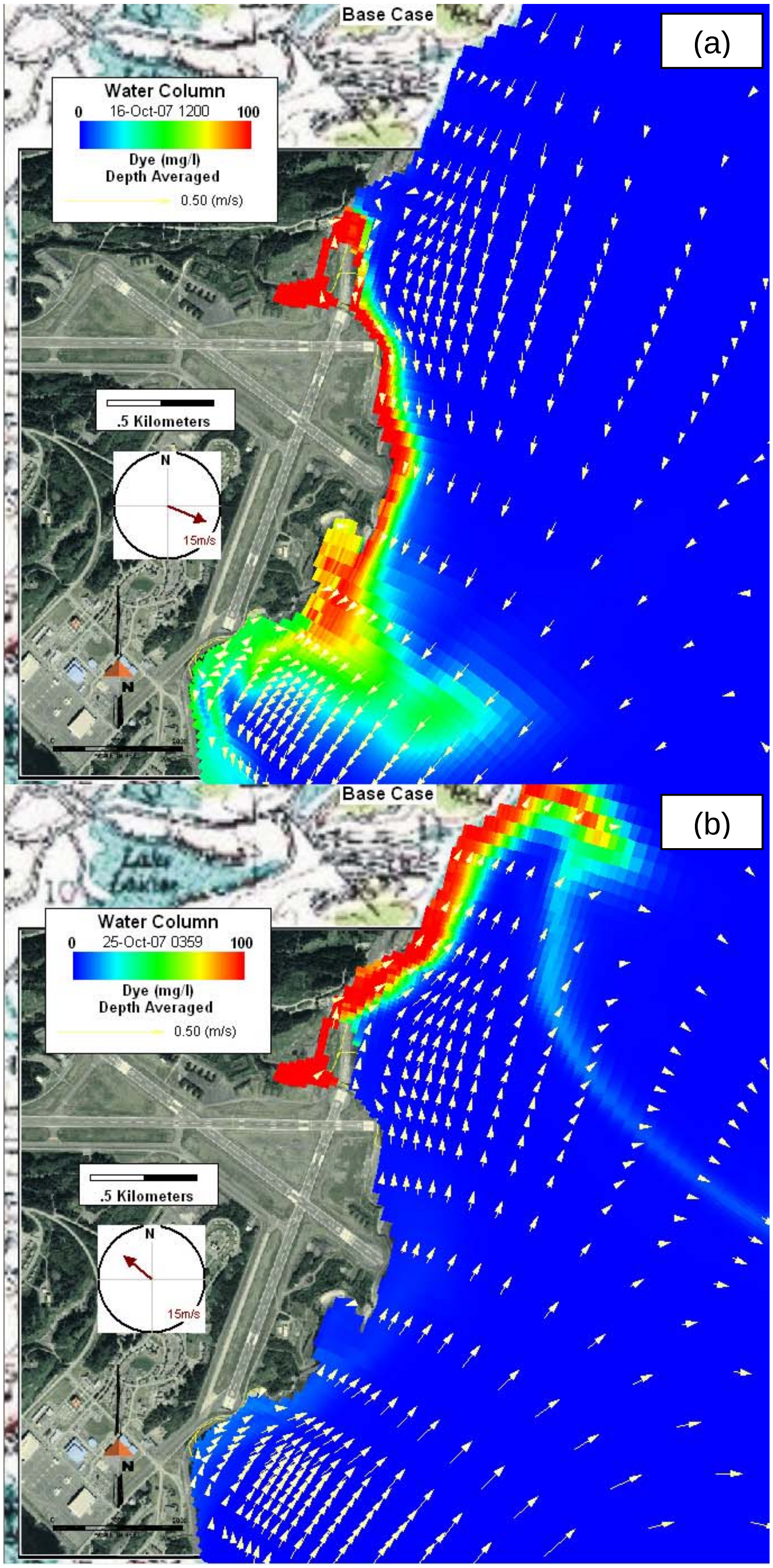

Figure 52 Base Case: Typical dye concentration patterns for (a) offshore winds and (b) onshore winds.

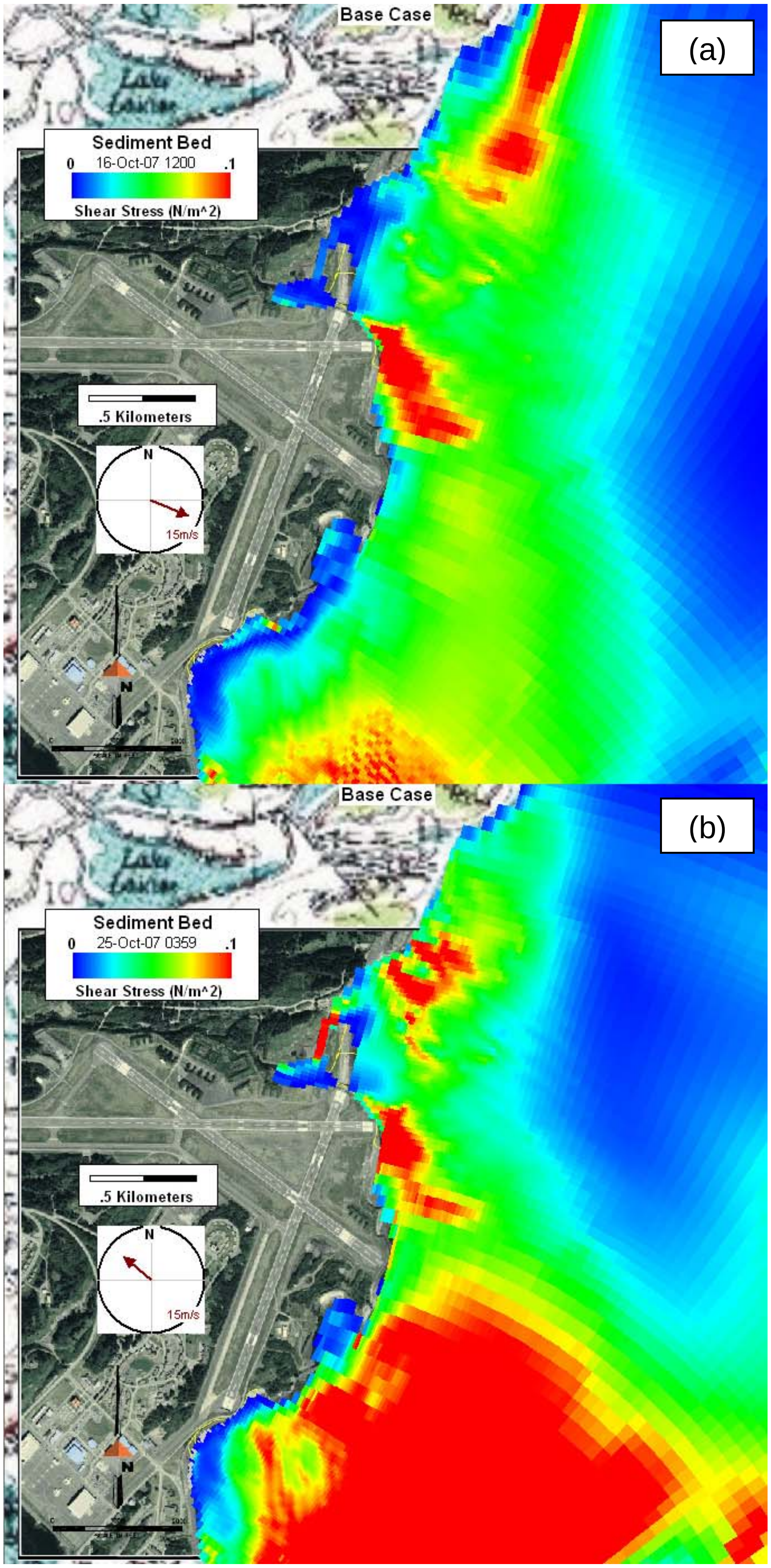

Figure 53 Base Case: Typical bed shear stress for (a) offshore winds and (b) onshore winds.

4.4.3 Runway 18/36 RSA Alternative 2

The *Runway 18/36 RSA Alternative 2* proposed to extend the RSA on both ends of Runway 18/36 by 400 feet. In the areas of the extension, a number of cells were deactivated to represent the filled areas. The depth of the water, the elevation of the runway and the slope of the embankments were used to estimate the extents of the cells to deactivate. The Figure 54 shows the resulting grid for the area near the airport for Runway 18/36 RSA Alternative 2.

The revised model was run for the same time period as the Base Case model. Figure 55 shows the dye concentrations for this alternative for the same times as shown in Figure 52 for the Base Case. Figure 56 shows the differences between the dye concentration for Runway 18/36 Alternative 2 Case and the Base Case. The red areas show where the Buskin River water will have a higher concentration relative to the Base Case. The blue areas would have less river water mixed in to harbor waters.

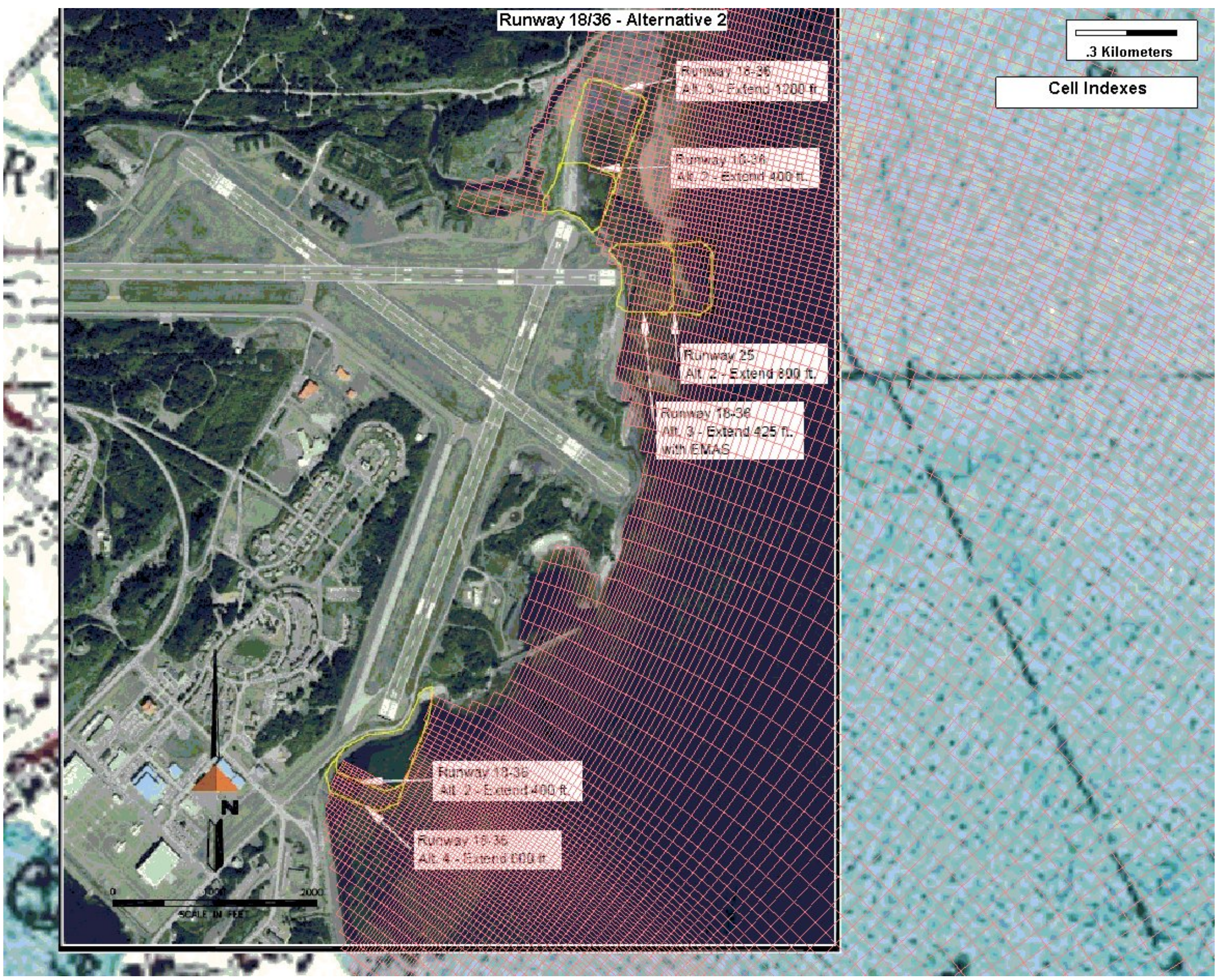

Figure 54 Runway 18/36 Alternative 2 model grid.

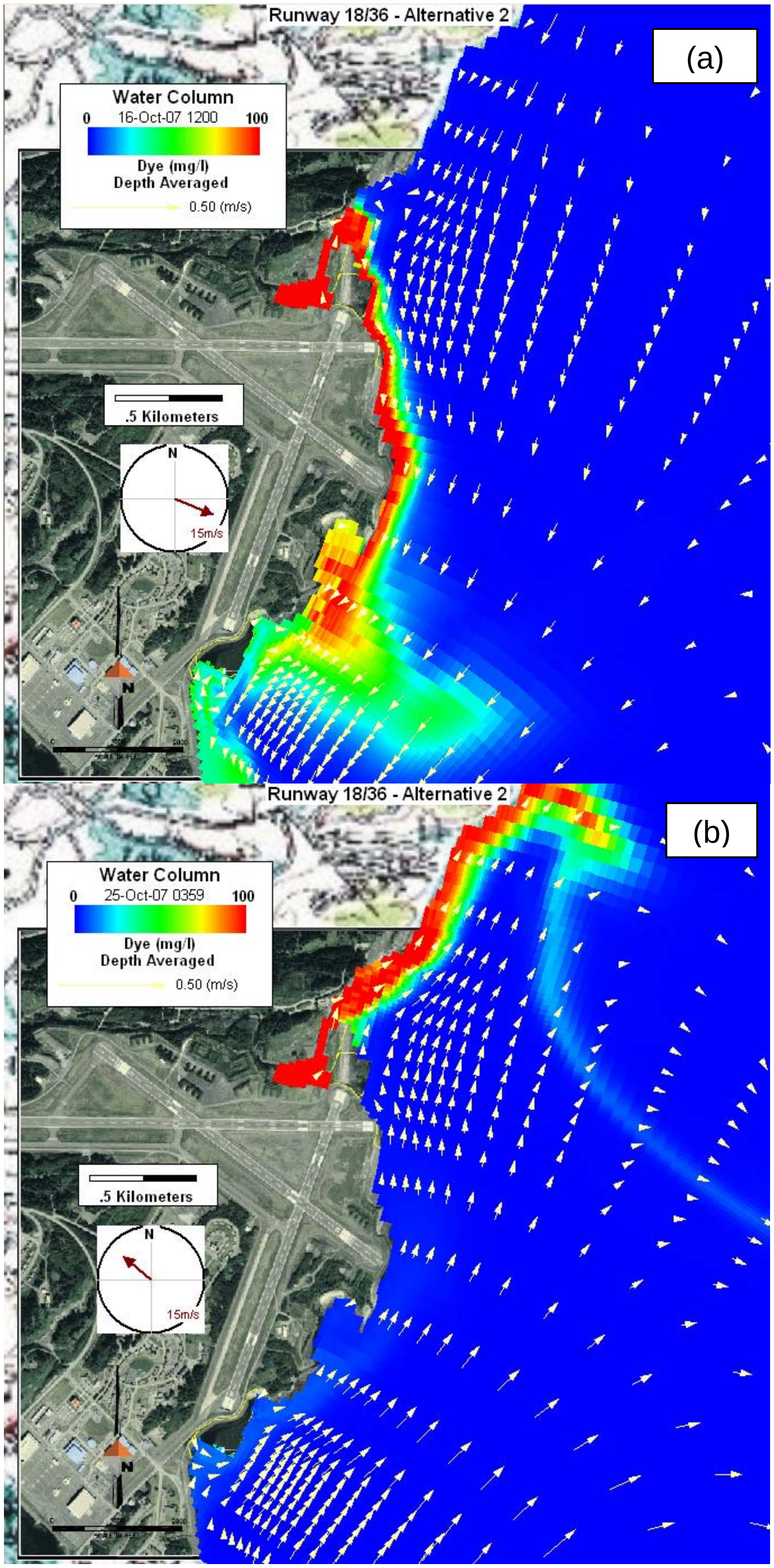

Figure 55 Runway 18/36 Alternative 2; Typical dye concentration patterns for (a) offshore winds and (b) onshore winds.

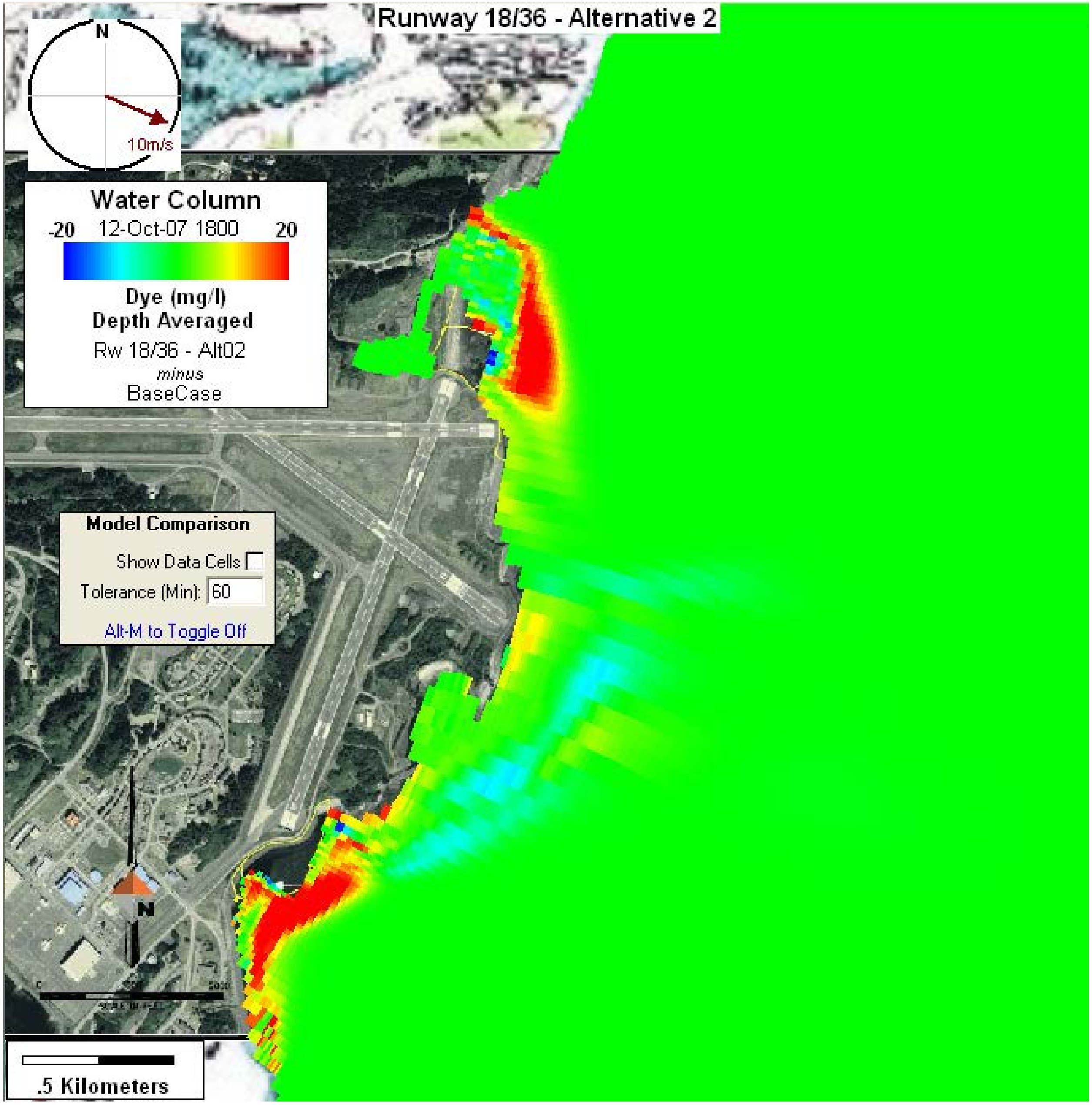

Figure 56 Runway 18/36 Alternative 2; Difference between dye concentrations of Alternative and Base Case.

Figure 57 shows the bed shear stress for the same times as shown for the Base Case in Figure 53. Figure 58 shows the differences between the bed shear stress for Runway 18/36 Alternative 2 Case and the Base Case. Red areas show where the bed shear stresses are higher than the Base Case. Blue areas would have lower bed shear stresses than the Base Case.

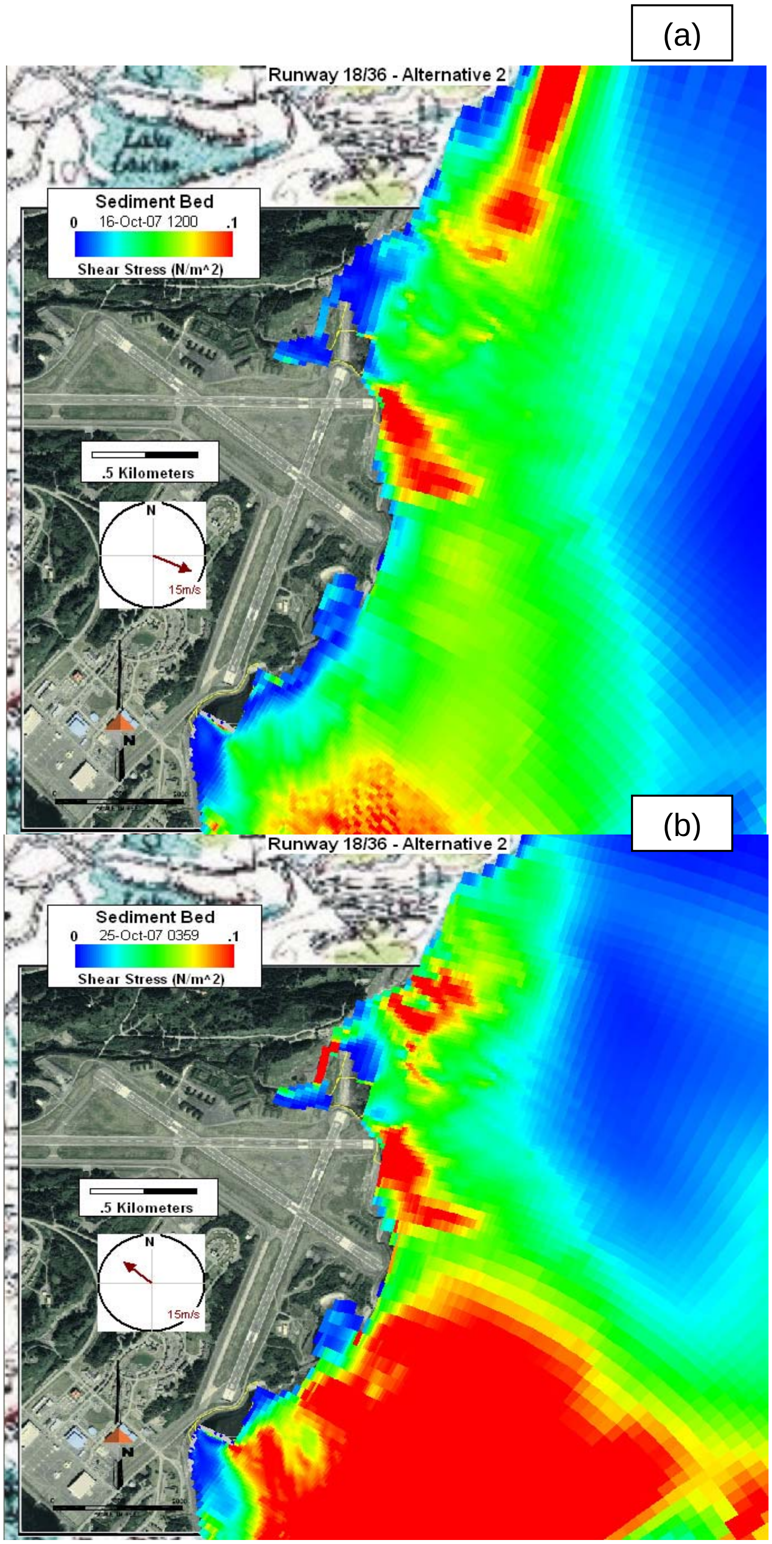

Figure 57 Runway 18/36 Alternative 2; Typical bed shear stress for (a) offshore winds and (b) onshore winds.

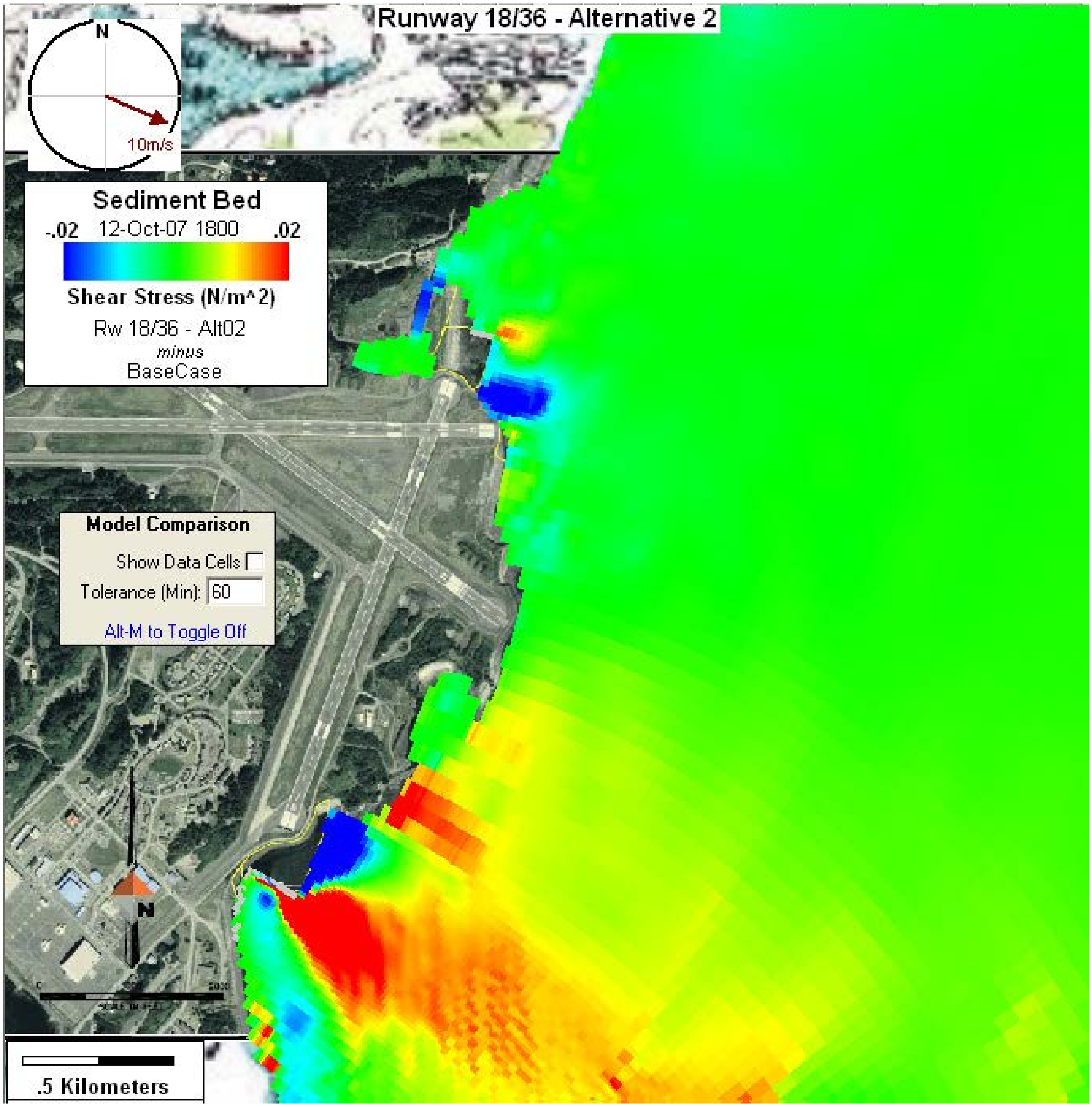

Figure 58 Runway 18/36 Alternative 2; Difference between bed shear stresses of Alternative and Base Case.

4.4.4 Runway 18/36 RSA Alternative 3

The *Runway 18/36 RSA Alternative 3* proposed to extend the Runway 18/36 RSA by 1,200 feet. In the areas of the extension, a number of cells were deactivated to represent the filled areas. The depth of the water, the elevation of the runway and the slope of the embankments were used to estimate the extents of the cells to deactivate. The Figure 59 shows the resulting grid for the area near the airport for *Runway 18/36 RSA Alternative 3.*

The revised model was run for the same time period as the Base Case model. Figure 60 shows the dye concentrations for this alternative for the same times as shown in Figure 52 for the Base Case. Figure 61 shows the differences in the dye concentrations between the Runway 18/36 Alternative 3 Case and the Base Case. Red areas show where the Buskin River waters will have a higher concentration relative to the Base Case. Blue areas would have less Buskin River waters mixed in to harbor waters.

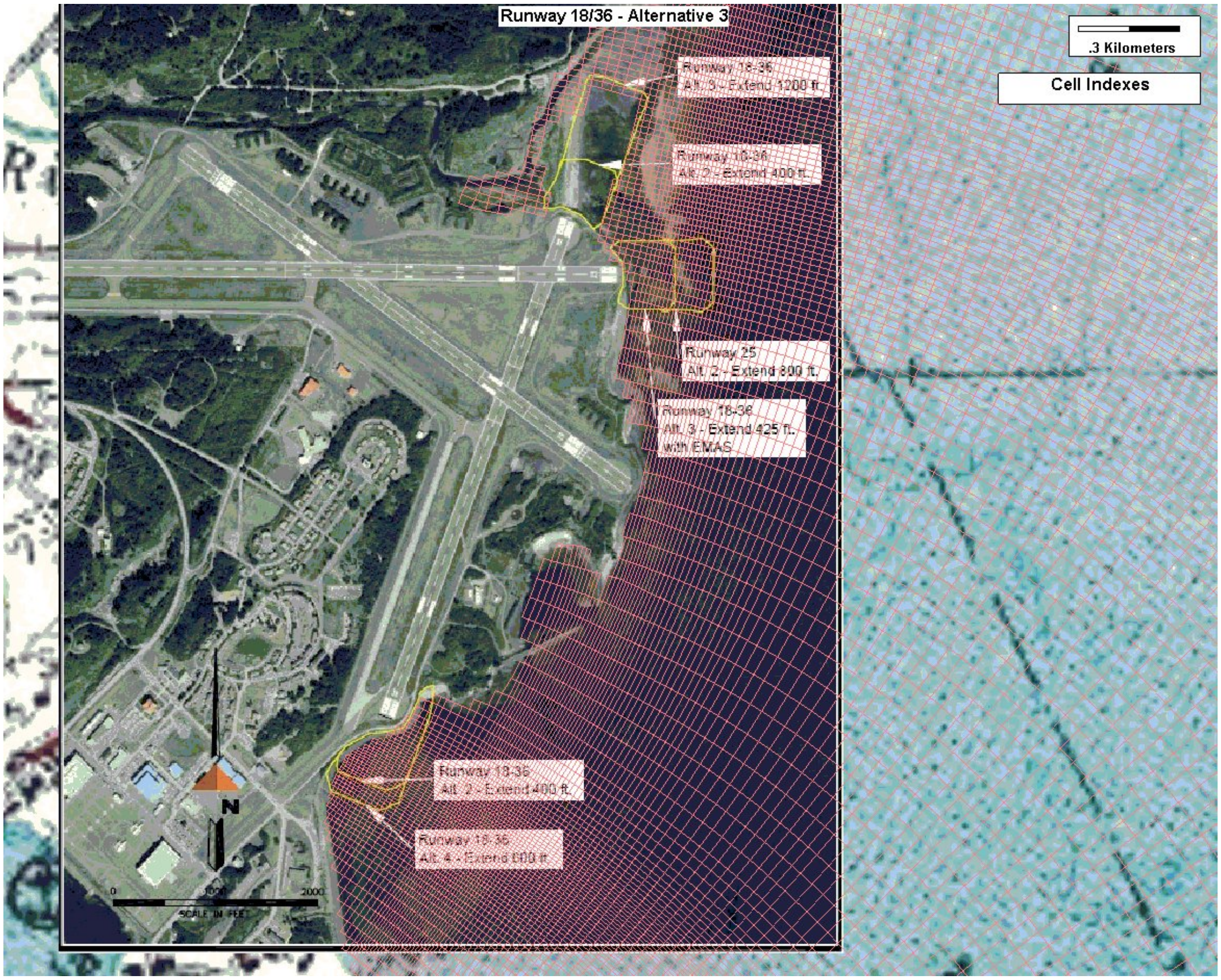

Figure 59 Runway 18/36 Alternative 3 model grid.

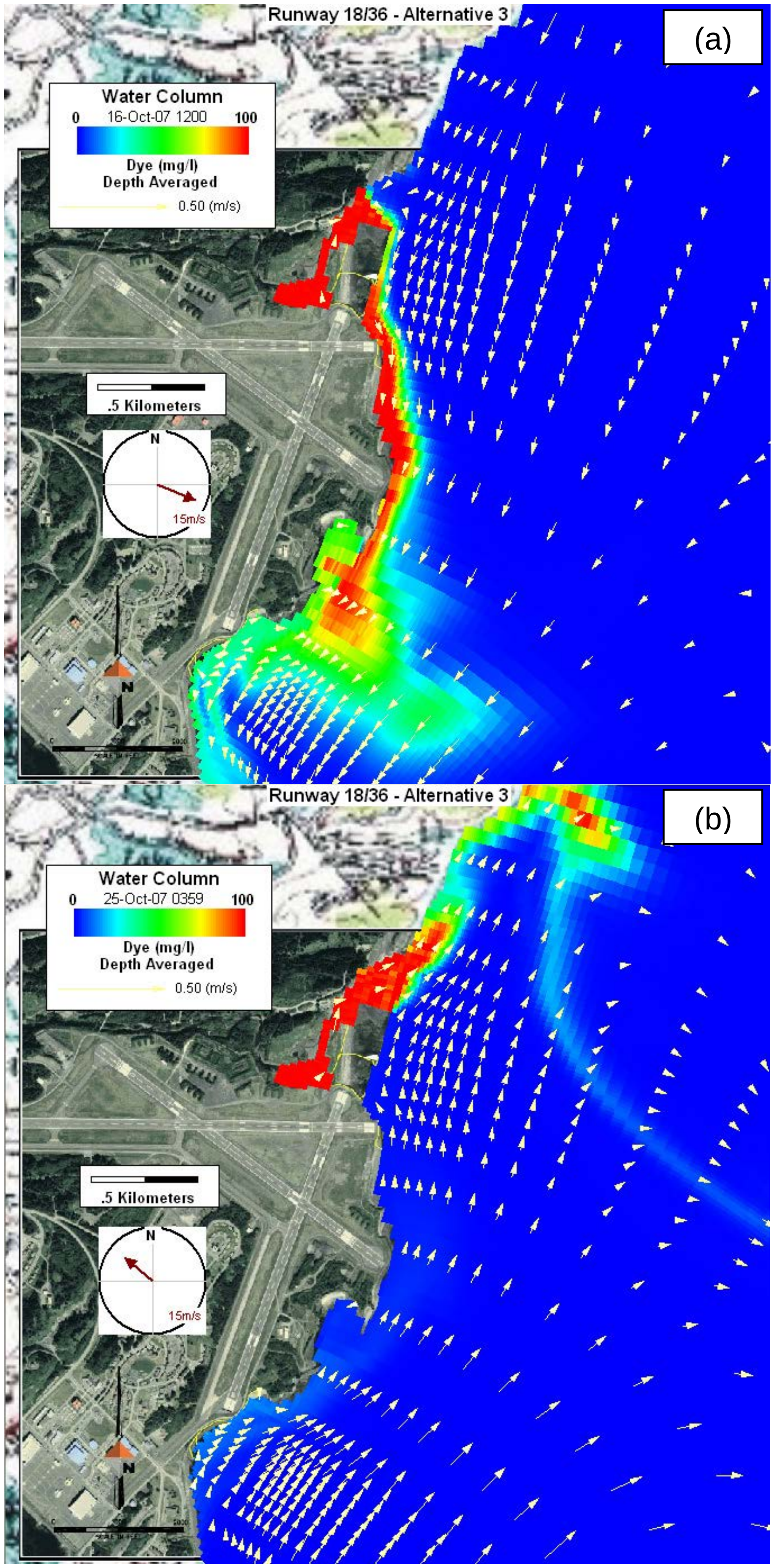

Figure 60 Runway 18/36 Alternative 3; Typical dye concentration patterns for (a) offshore winds and (b) onshore winds.

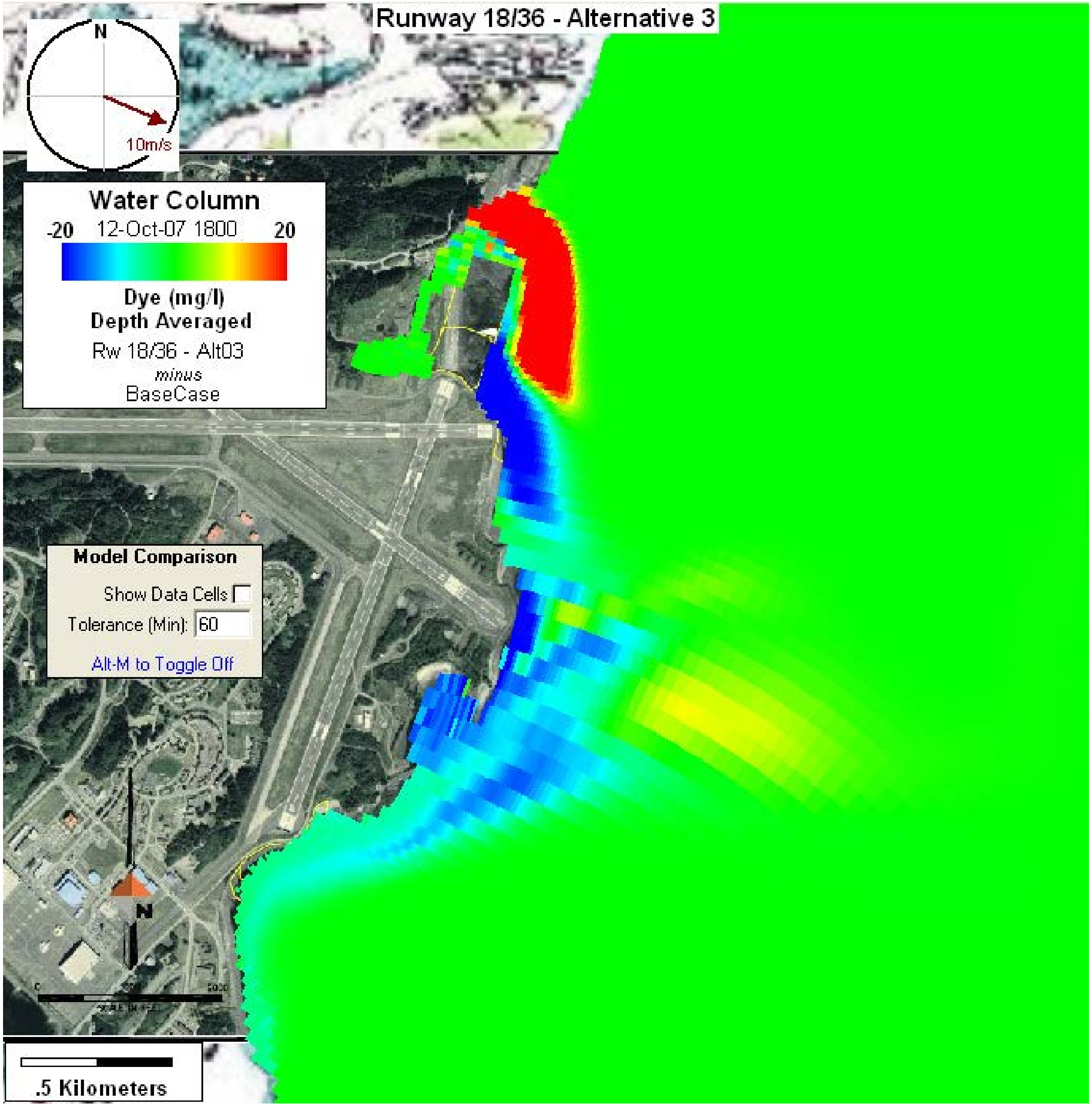

Figure 61 Runway 18/36 Alternative 3; Difference between dye concentrations of Alternative and Base Case.

Figure 62 shows the bed shear stress for the same times as shown for the Base Case in Figure 53. Figure 63 shows the difference between the bed sheer stress for Runway 18/36 Alternative 3 and the Base Case. Red areas show where the bed shear stresses are higher than the Base Case. Blue areas would have lower bed shear stresses than the Base Case.

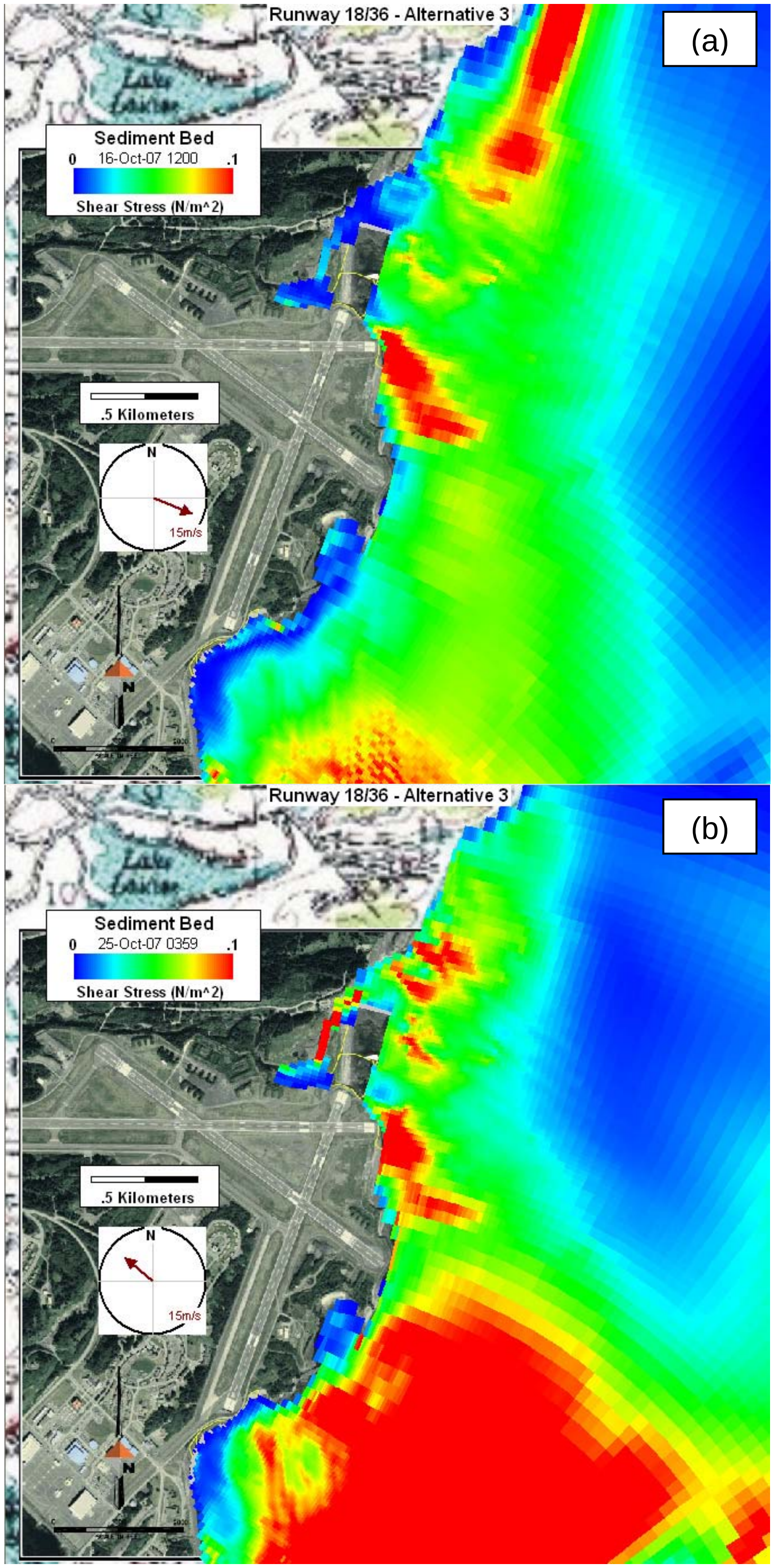

Figure 62 Runway 18/36 Alternative 3; Typical bed shear stress for (a) offshore winds and (b) onshore winds.

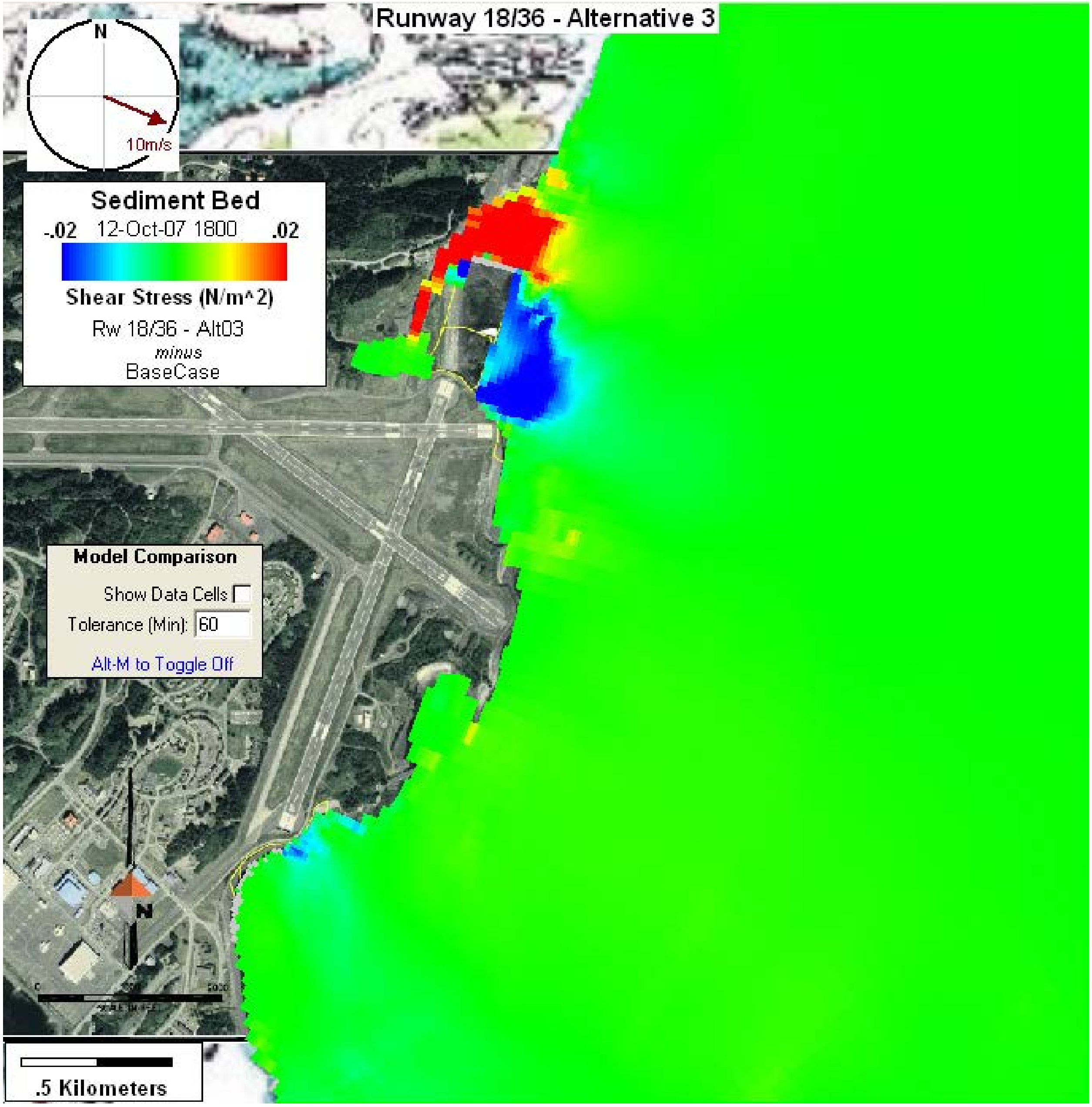

Figure 63 Runway 18/36 Alternative 3; Difference between bed shear stresses of Alternative and Base Case.

4.4.5 Runway 07/25 RSA Alternative 2

The *Runway 07/25 RSA Alternative 2* proposed to extend the Runway 07/25 RSA by 800 feet. In the areas of the extension, a number of cells were deactivated to represent the filled areas. The depth of the water, the elevation of the runway and the slope of the embankments were used to estimate the extents of the cells to deactivate. The Figure 64 shows the resulting grid for the area near the airport for *Runway 07/25 RSA Alternative 2.*

The revised model was run for the same time period as the Base Case model. Figure 65 shows the dye concentrations for this alternative for the same times as shown in Figure 52 for the Base Case. Figure 66 shows the difference between the dye concentration for Runway 07/25 Alternative 2 Case and the Base Case. Red areas show where the Buskin River water will have a higher concentration relative to the Base Case. Blue areas would have less river water mixed in to harbor waters.

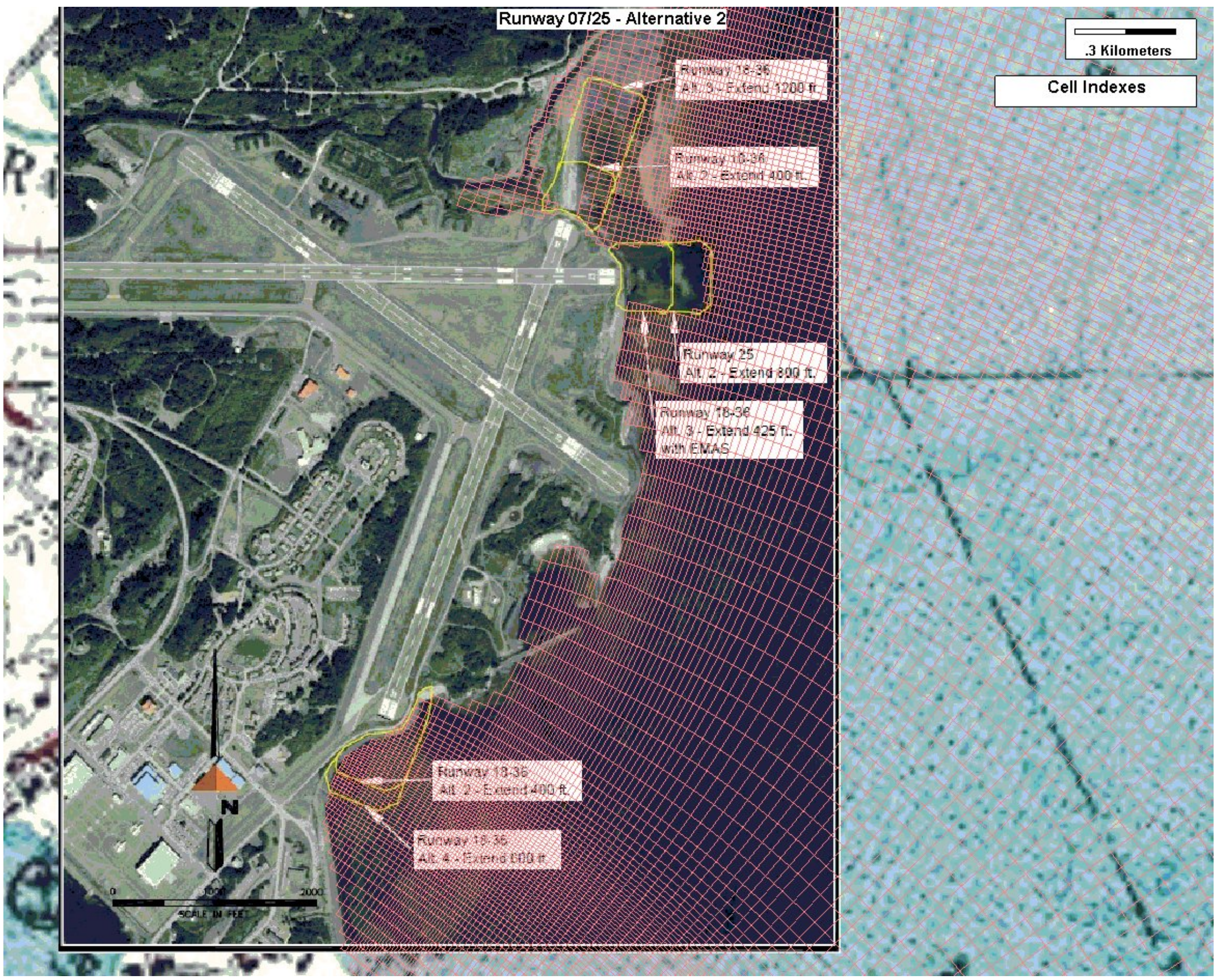

Figure 64 Runway 07/25 Alternative 2 model grid.

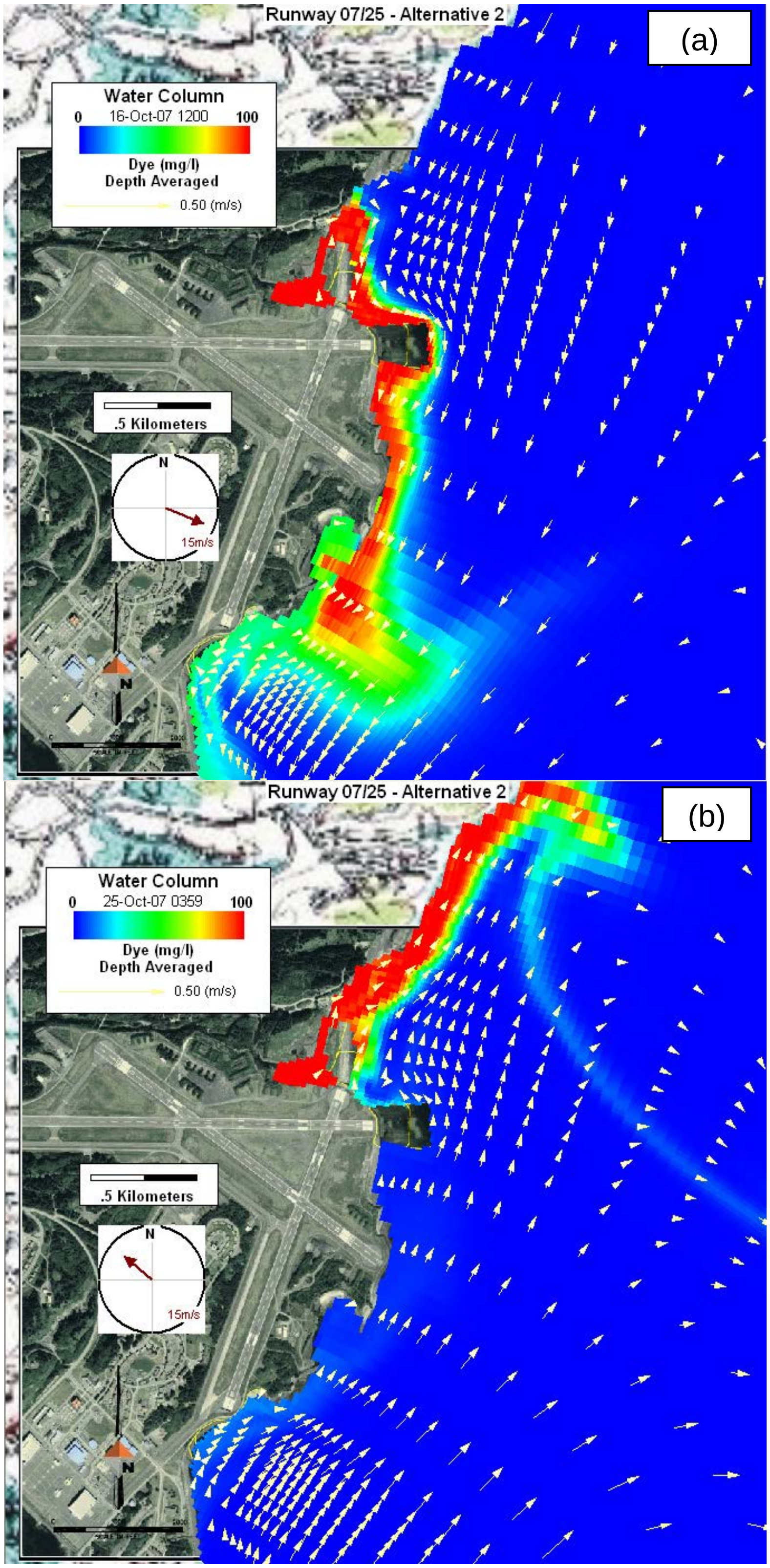

Figure 65 Runway 07/25 Alternative 2; Typical dye concentration patterns for (a) offshore winds and (b) onshore winds.

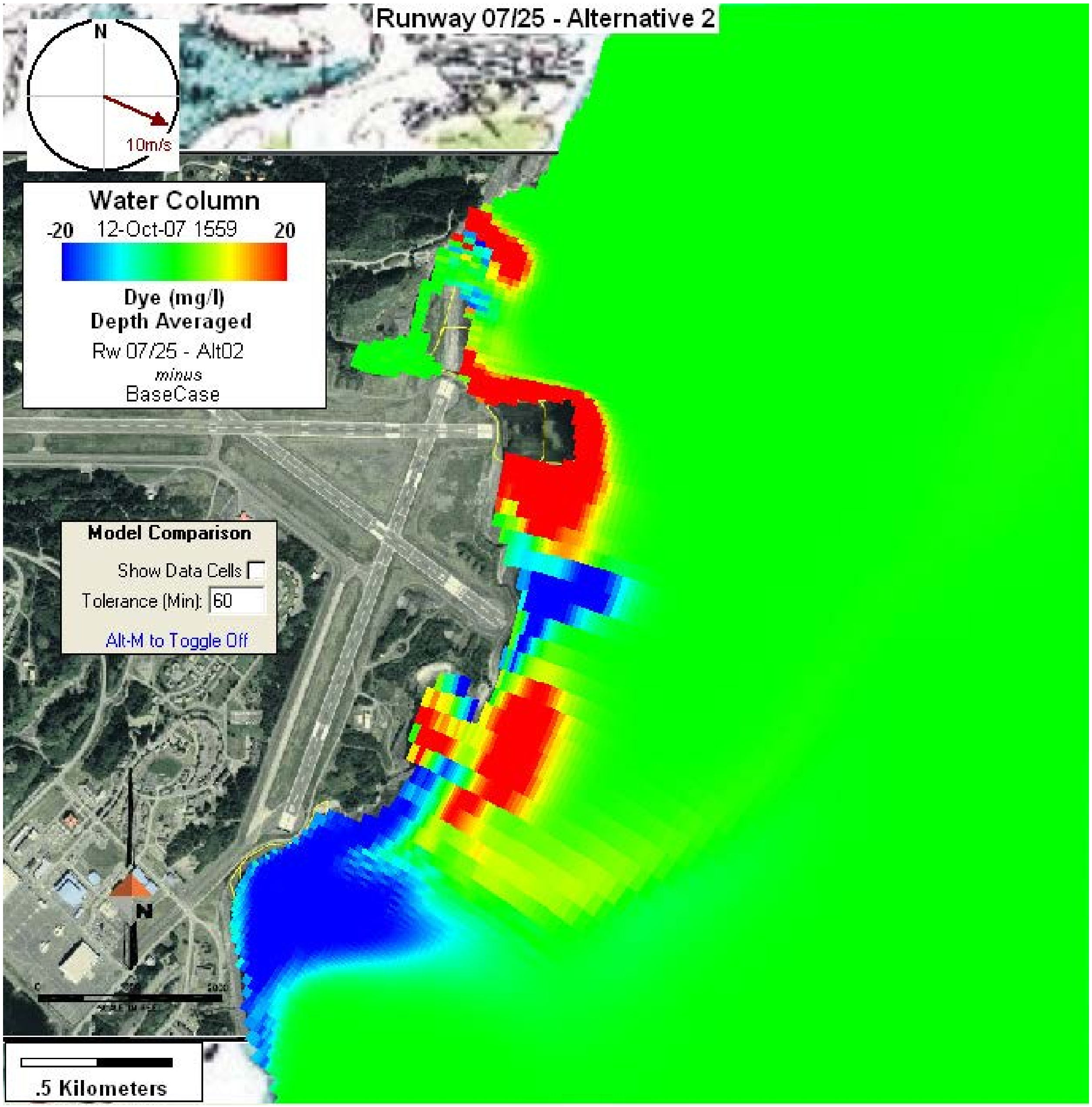

Figure 66 Runway 07/25 Alternative 2; Difference between dye concentrations of Alternative and Base Case.

Figure 67 shows the bed shear stress for the same times as shown for the Base Case in Figure 53. Figure 68 shows the difference between the bed sheer stress for Runway 07/25 Alternative 2 Case and the Base Case. Red areas show where the bed shear stresses are higher than the Base Case. Blue areas would have lower bed shear stresses than the Base Case.

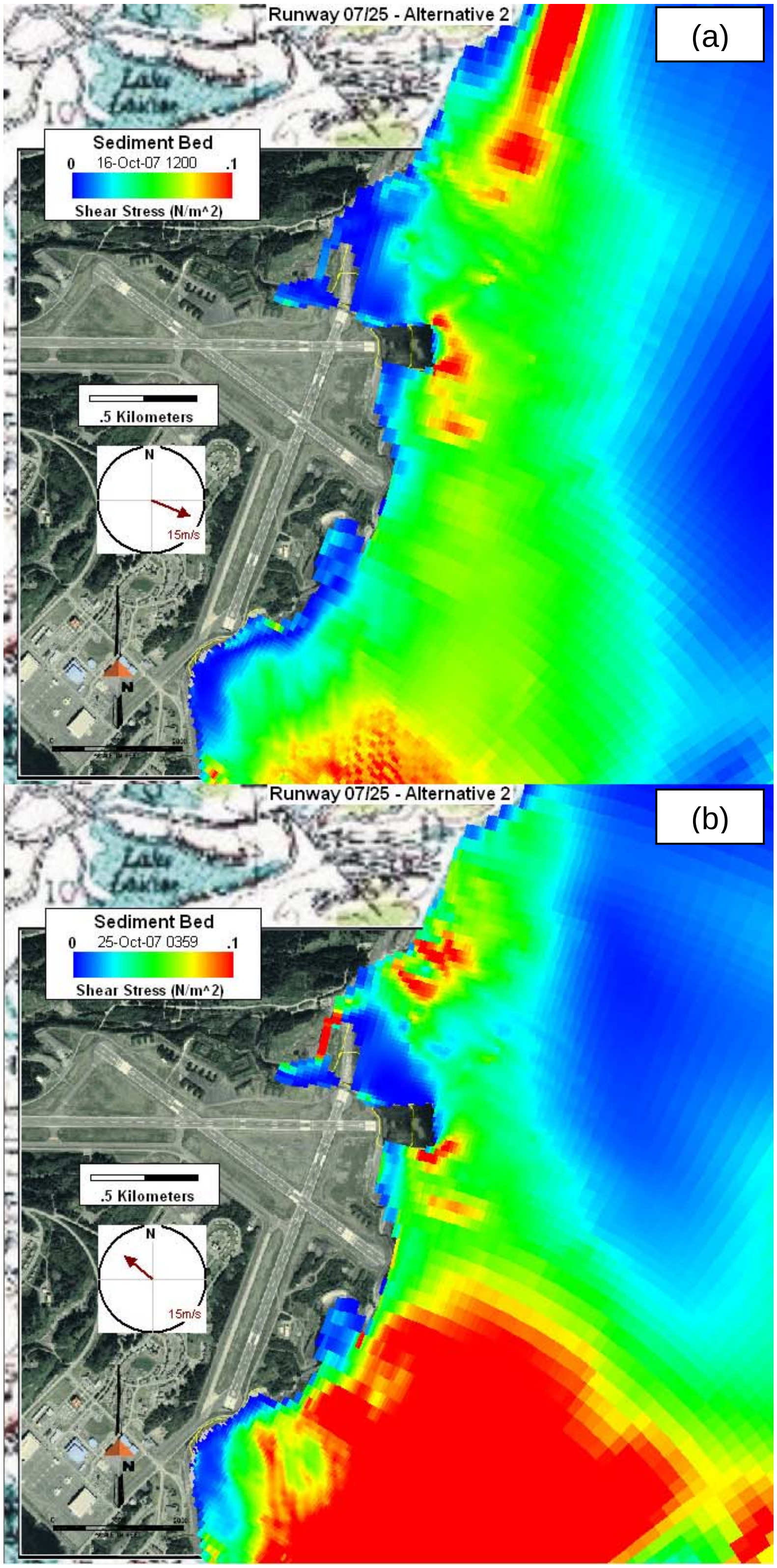

Figure 67 Runway 07/25 Alternative 2; Typical bed shear stress for (a) offshore winds and (b) onshore winds.

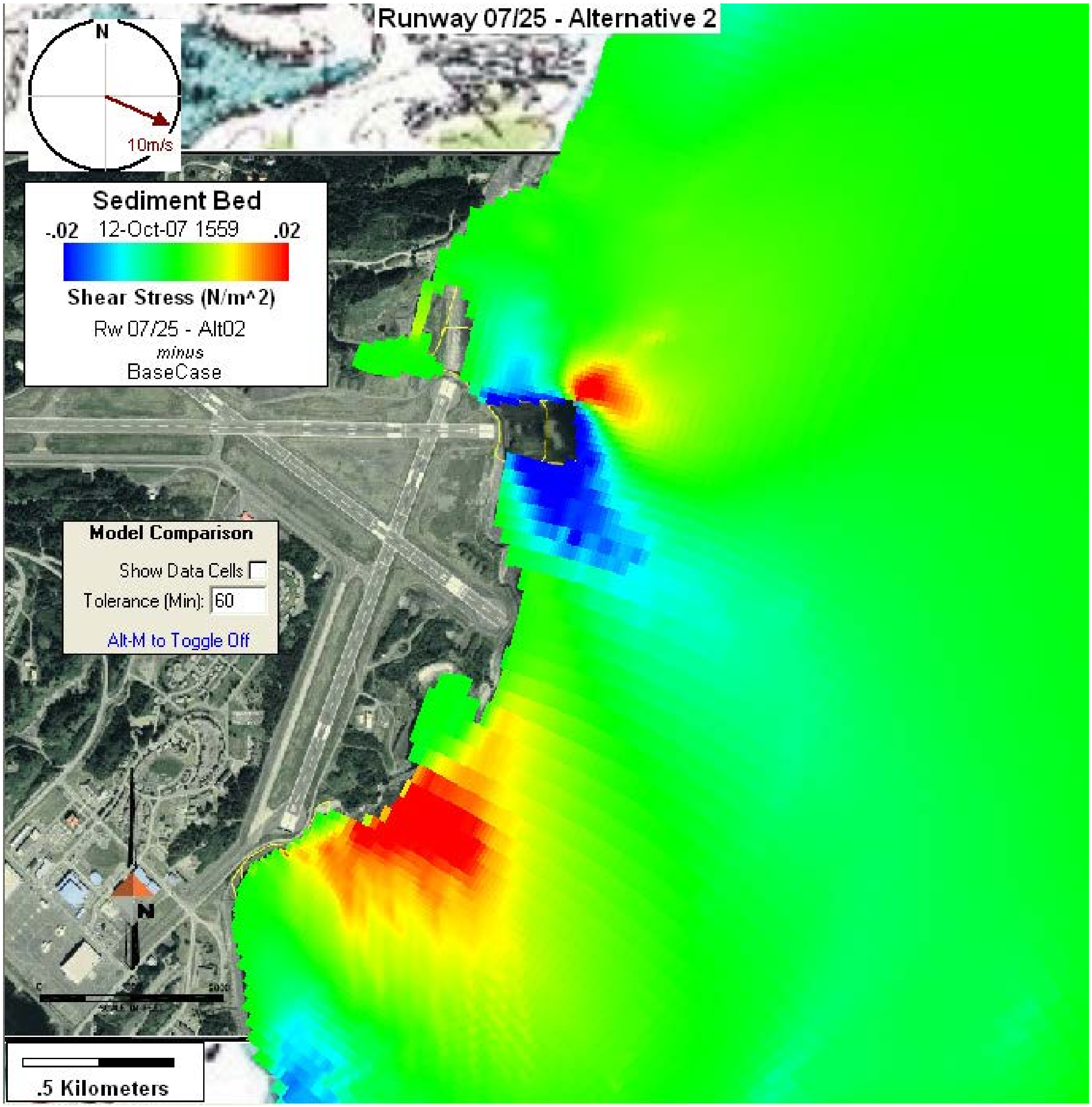

Figure 68 Runway 07/25 Alternative 2; Difference between bed shear stresses of Alternative and Base Case.

4.4.6 Combined Alternative

The *Combined Alternatives* option combines the maximum extension for both runways for all alternatives. Thus, Runway 07/25 was extended by 800 feet and Runway 18/36 was extended by 1,200 ft and 600 ft on north and south ends, respectively. In the areas of the extensions, cells were deactivated to represent the filled areas in a similar manner as described for the other alternatives. Figure 69 shows the resulting grid for the area near the airport for the *Combined Alternatives.*

The revised model was run for the same time period as the Base Case model. Figure 65 shows the dye concentrations for this alternative for the same times as shown in Figure 52 for the Base Case. Figure 66 shows the difference between the dye concentration for Runway 07/25 Alternative 2 Case and the Base Case. Red areas show where the Buskin River waters will have a higher concentration relative to the Base Case. Blue areas would have less river waters mixed in to harbor waters.

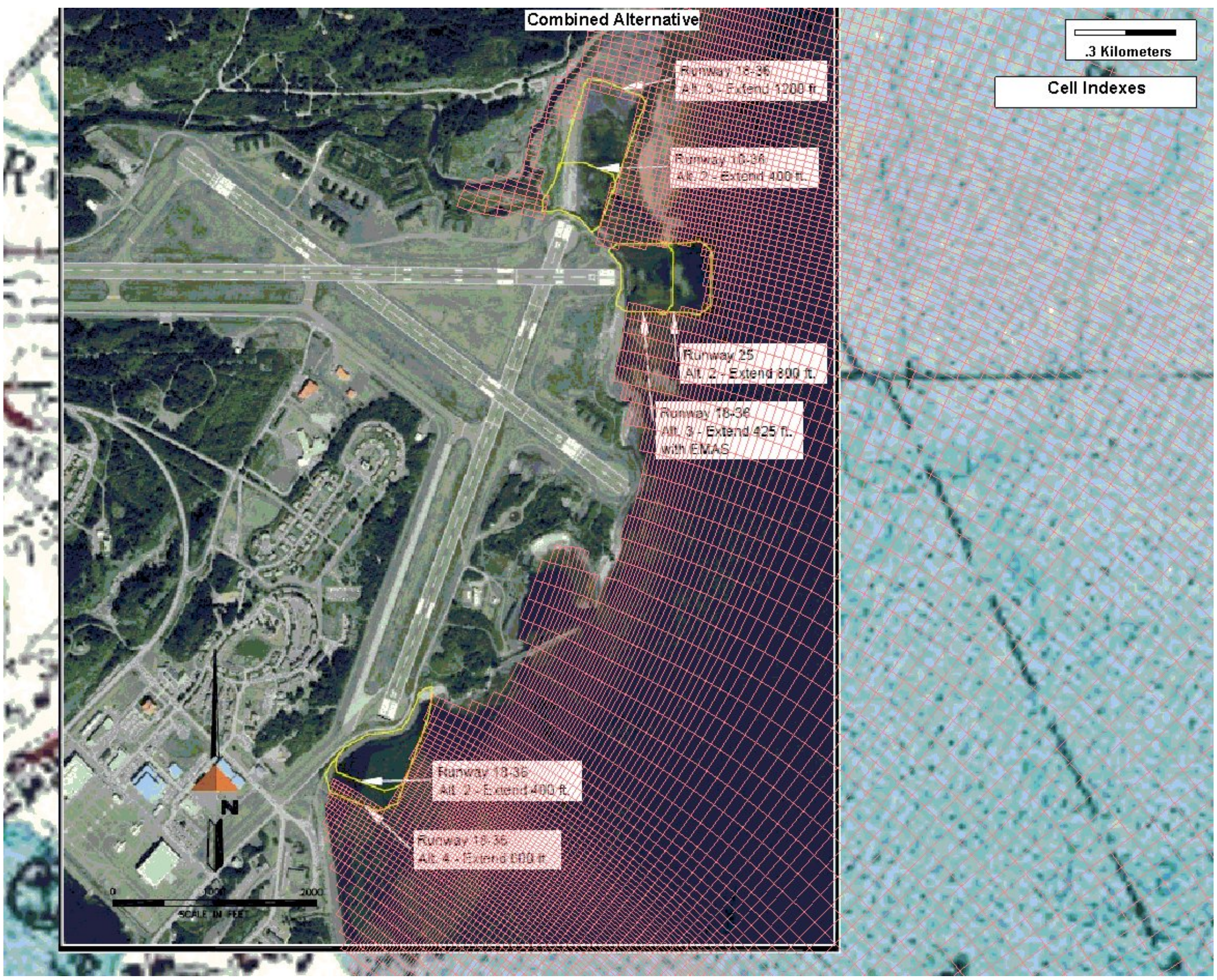

Figure 69 Combined Alternative model grid.

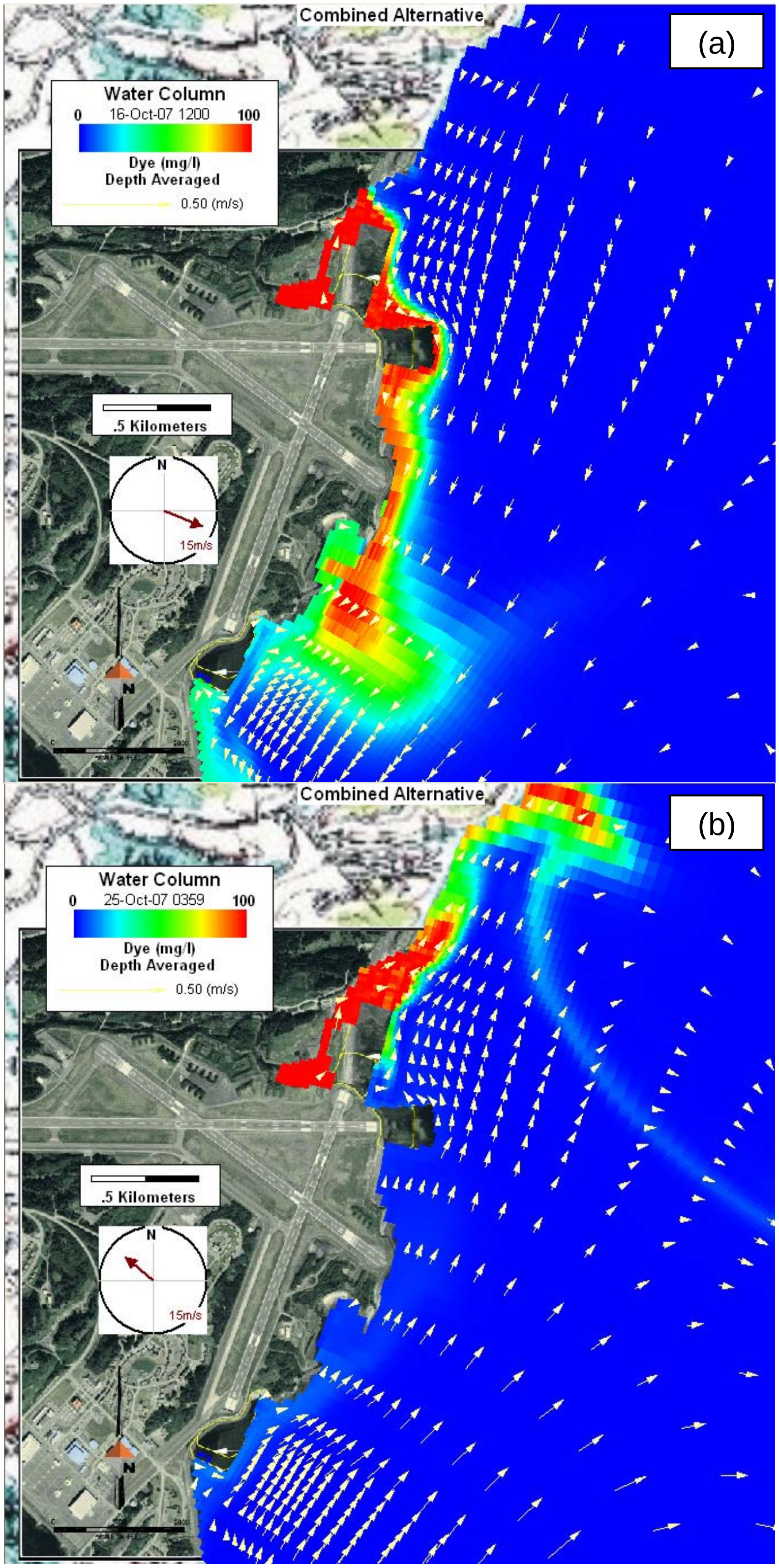

Figure 70 Combined Alternative; Typical dye concentration patterns for (a) offshore winds and (b) onshore winds.

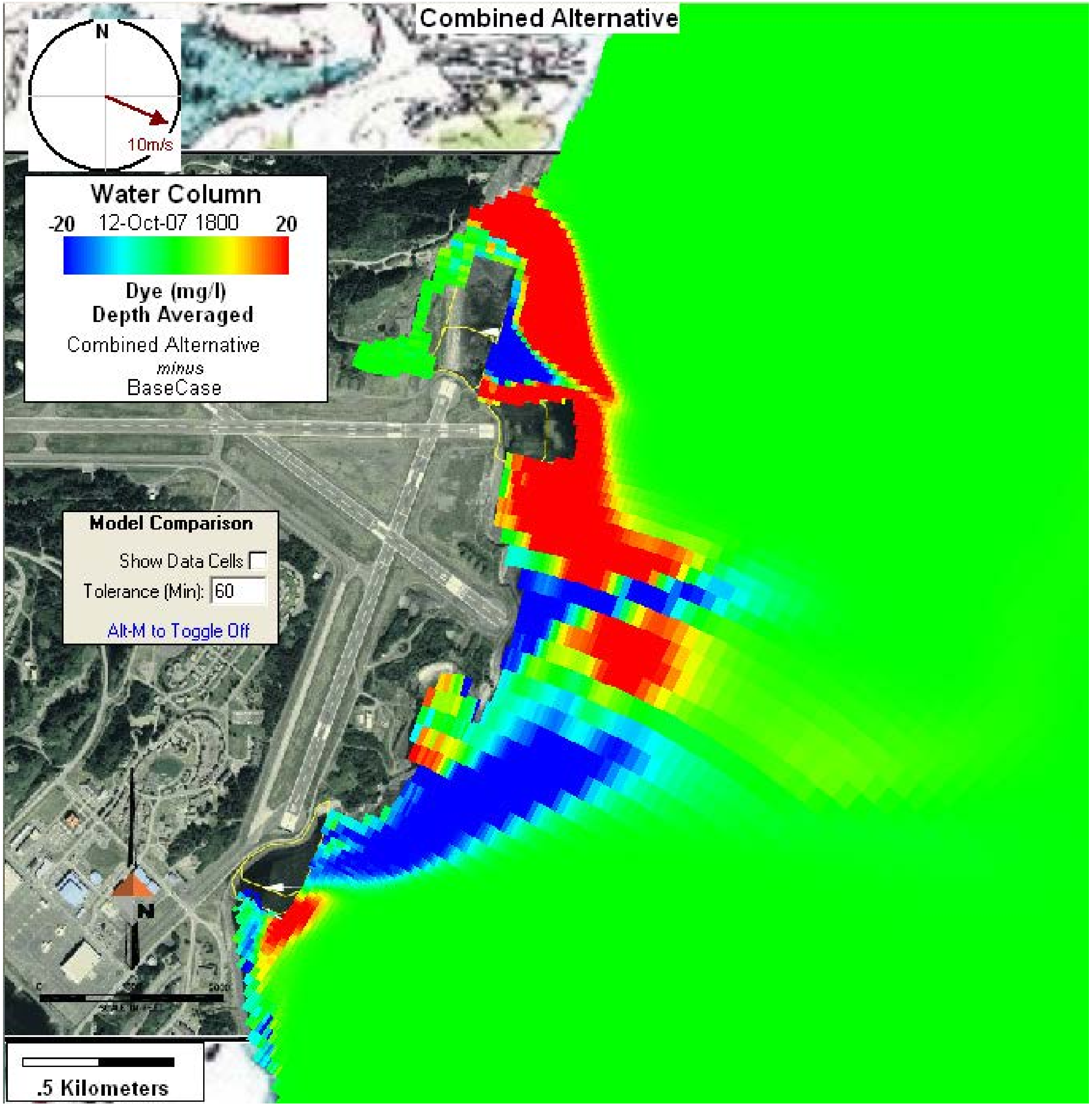

Figure 71 Combined Alternative; Difference between dye concentrations of Alternative and Base Case.

Figure 72 shows the bed shear stress for the same times as shown for the Base Case in Figure 53. Figure 73 shows the difference between the bed sheer stress for *Combined Alternative* and the Base Case. Red areas show where the bed shear stresses are higher than the Base Case. Blue areas would have lower bed shear stresses than the Base Case.

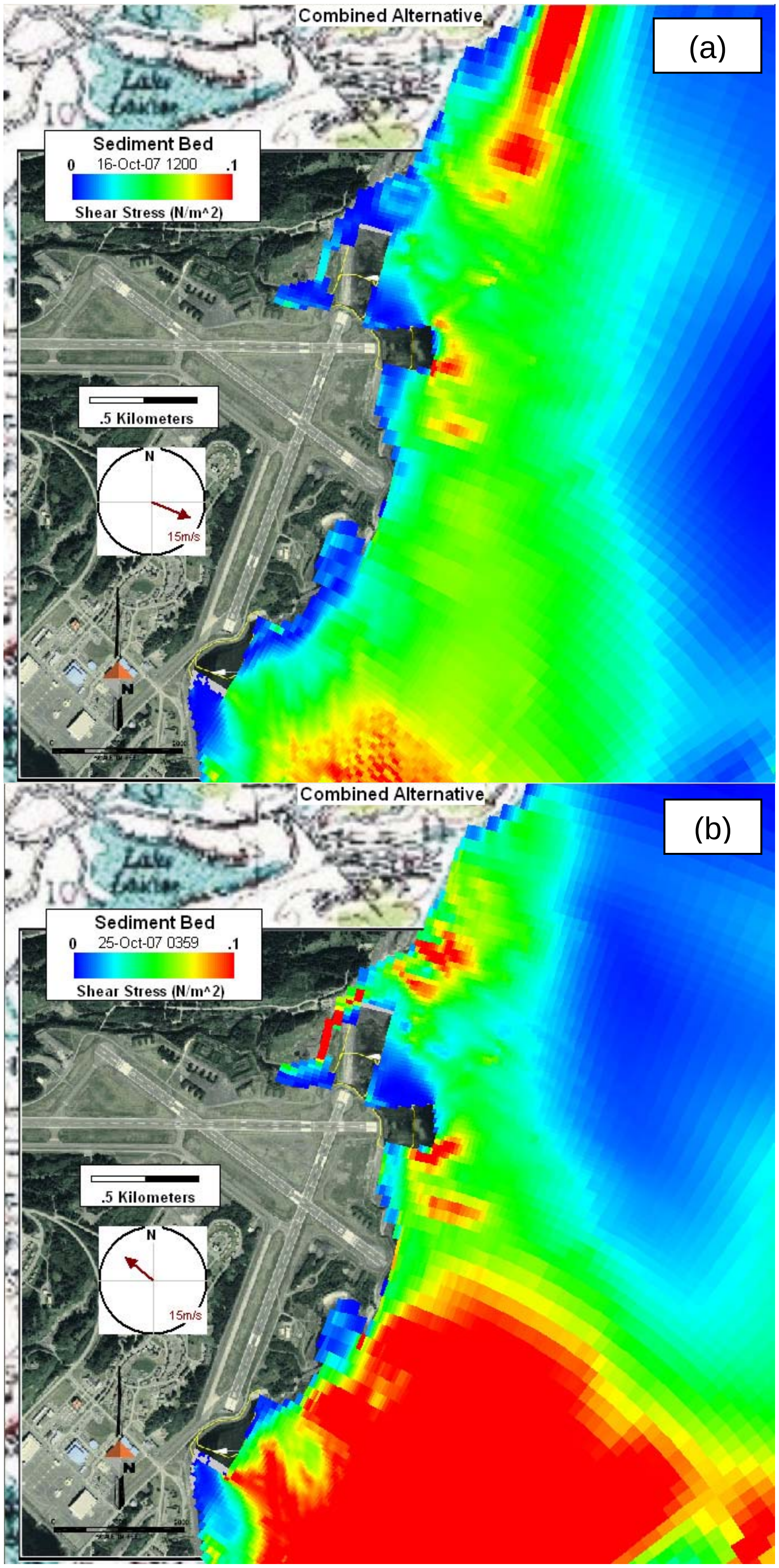

Figure 72 Combined Alternative; Typical bed shear stress for (a) offshore winds and (b) onshore winds.

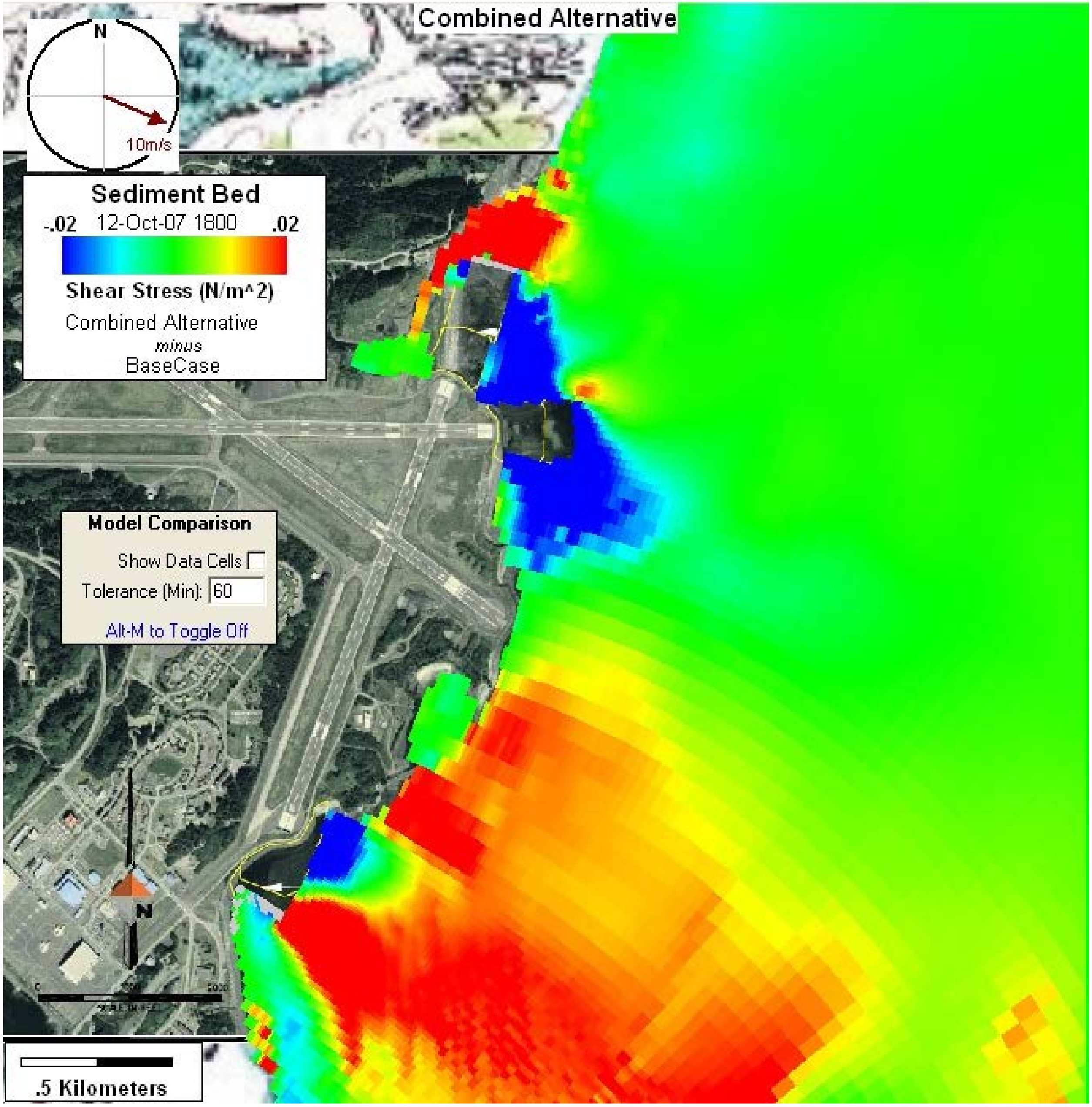

Figure 73 Combined Alternative; Difference between bed shear stresses of Alternative and Base Case.

4.4.7 Comparison of Alternatives

To compare the temporal changes in bed shear stress between the various alternatives, five representative points were selected. The locations of these points were selected after reviewing the 2D plan view animations of computed results. These points are shown in Figure 74 and referred to as P1, P2 and P3. P1 was used for Runway 18/36 Alternatives 2 and 3, P3 was used only for Runway 18/36 Alternative 2 and P2 was used only for Runway 07/25 Alternative 2. Two additional points (Figure 74) located near waste water treatment plant (WWTP) and IA-3 was also included in this time series analysis.

.

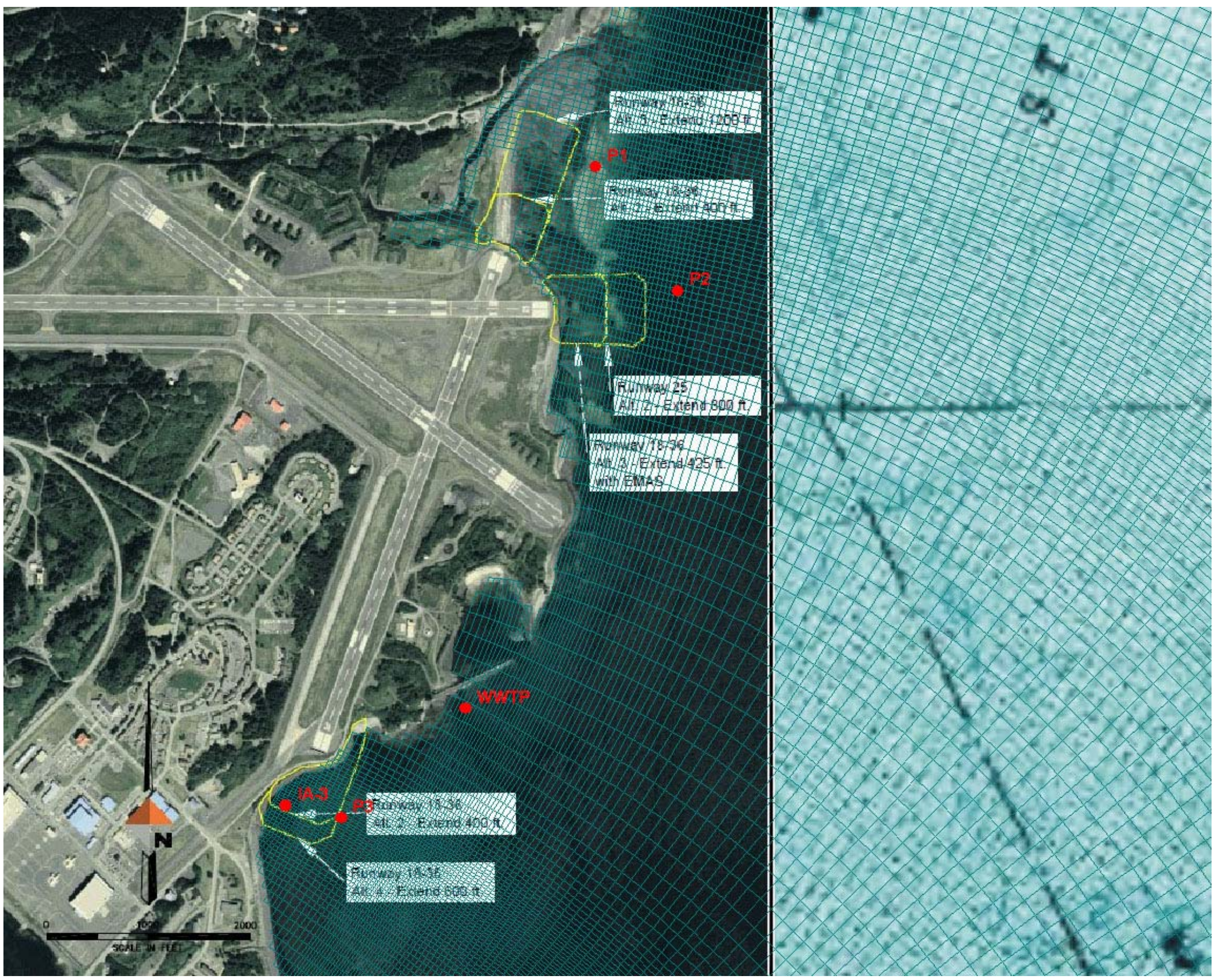

Figure 74 Location of selected representative points.

For the points P1, P2 and P3, the time series of bed shear stress for each of the alternatives were shown in Figures 75 to 78 together with the Base Case. This analysis shows that on average there is not a significant increase in bed shears with the runway extensions. However, bed shears after the implementation of a runway extension can spike up to 200% over the Base Case, depending on tide and wind conditions. P3 (*Runway 18/36 Alternative 2,* South end) exhibits the largest increase in bed shears and P1 (*Runway 18/36 Alternative 2,* North end) has the smallest.

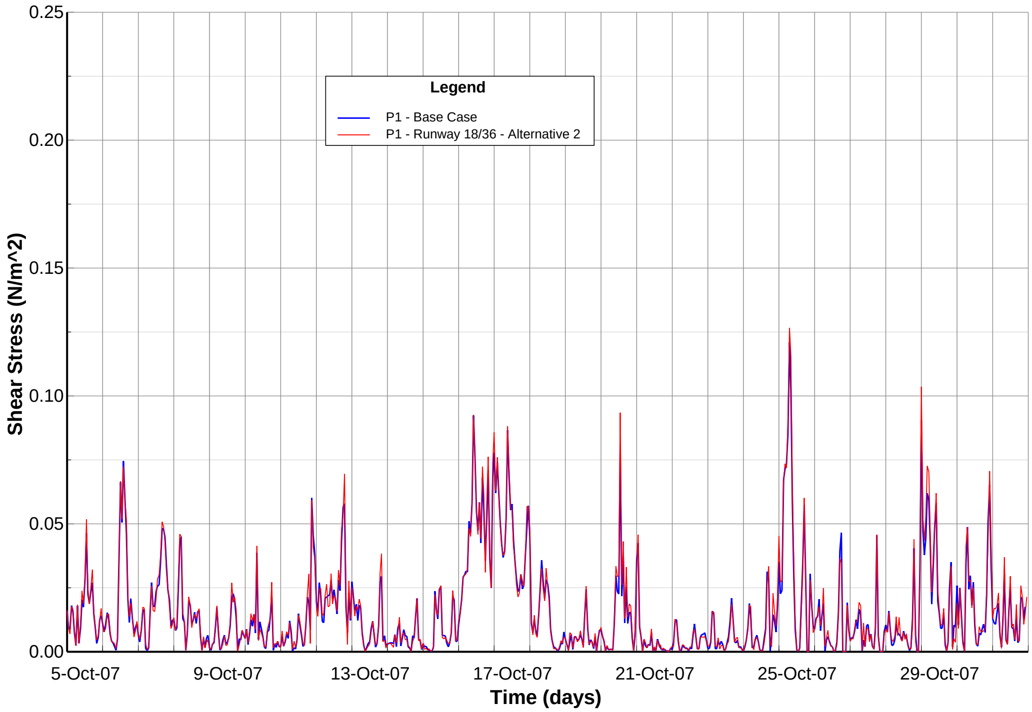

Figure 75 Shear stress at P1 during calculation period.

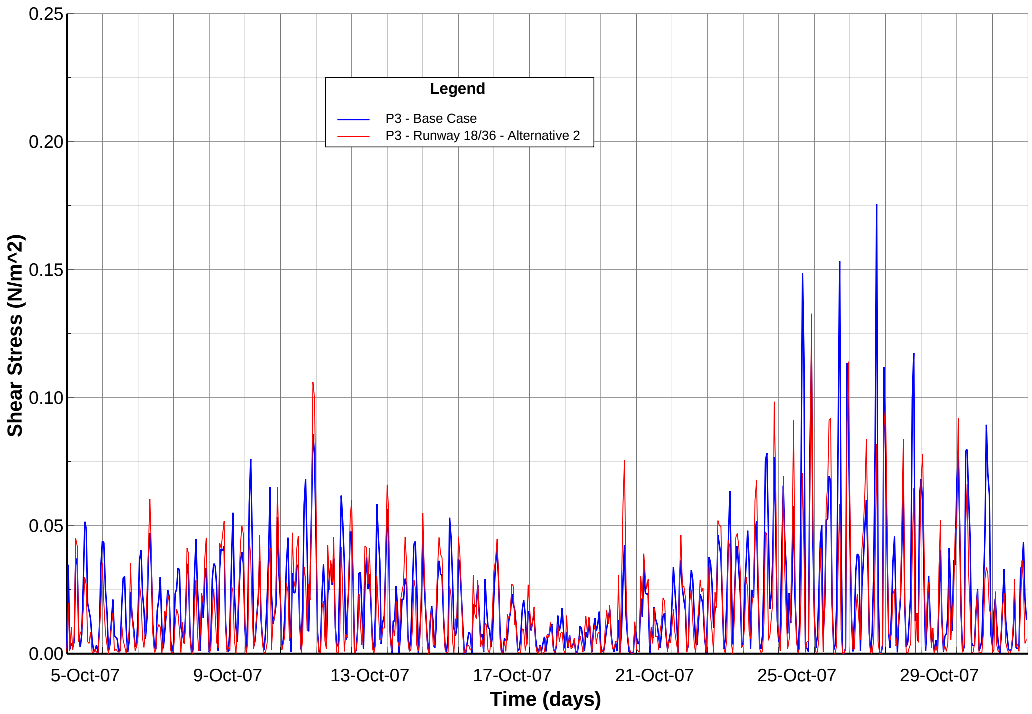

Figure 76 Shear stress at P3 during calculation period.

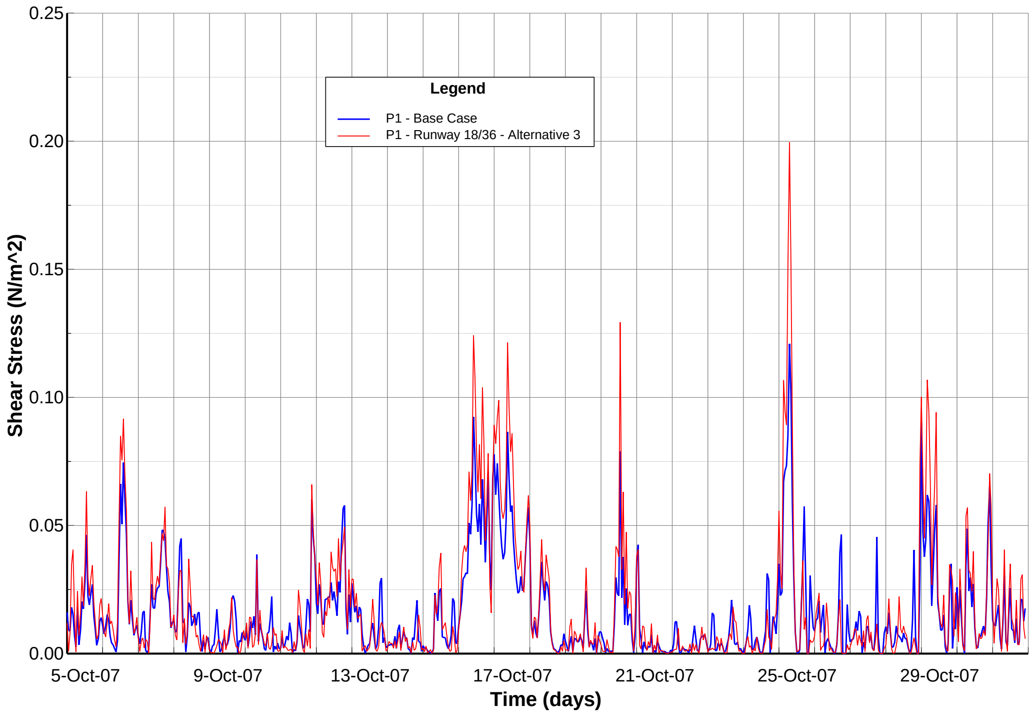

Figure 77 Shear stress at P1 during calculation period.

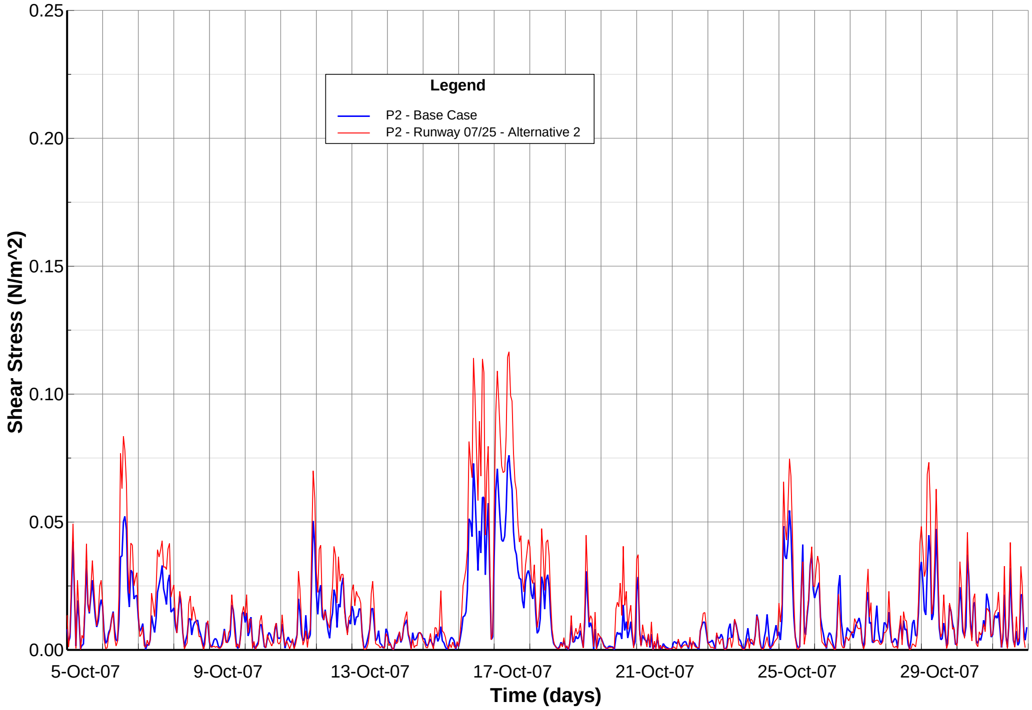

Figure 78 Shear stress at P2 during calculation period.

To address the bed shear impacts near two areas of concern (the points were requested by a commenter), two additional points were added to this time series analysis. The two locations, WWTP near the Kodiak Waste Water Treatment Plant and IA-3, are shown in Figure 74. The time series of bed shear stresses at these locations for the simulation period are shown in Figures 79 and 80. For IA-3, the extension of Runway 18/32 Alternative 2 significantly lowers the bed shears at that location. These areas that once had higher bed shear stresses but are now semi-protected by the runway extension will have more fine sediment deposition in the future, depending on the alternative selected.

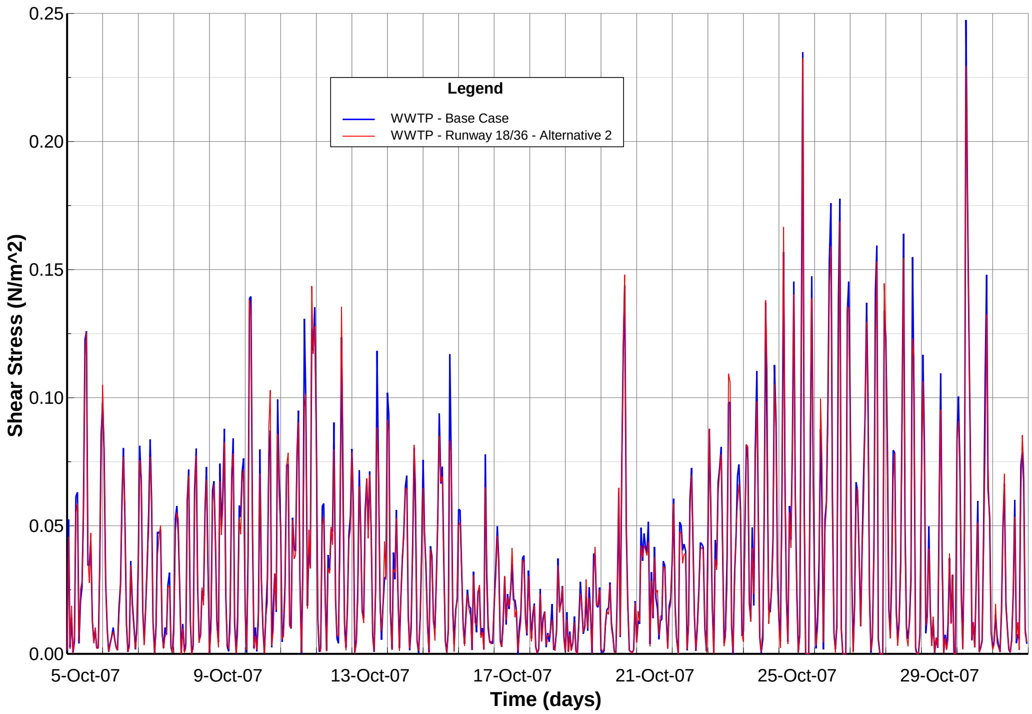

Figure 79 Shear stress at WWTP during calculation period.

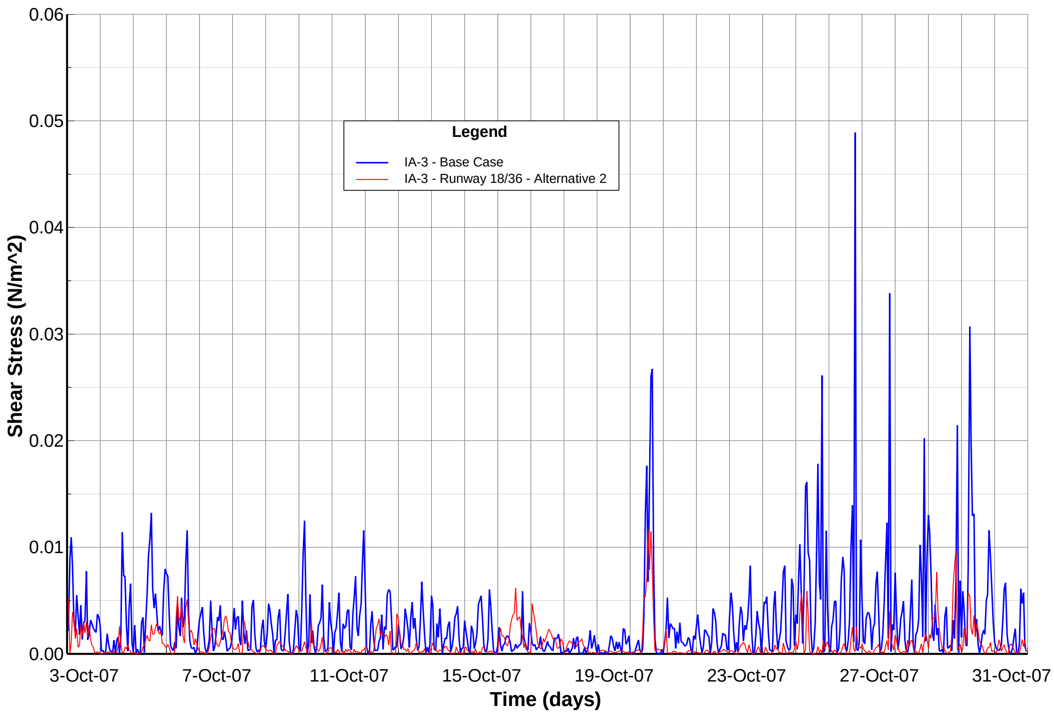

Figure 80 Shear stress at IA-3 during calculation period.

4.5 Wave Modeling

4.5.1 General

Wave consideration for the affected area should be of lesser concern than the circulation or water quality. The waves provide a tool for transporting sediments once they are delivered to the beach or to the near-shore via erosion or transport by rivers. Waves will certainly be important to the design of any of the facilities that will be considered to fulfill FAA requirements. Those will be addressed later in a separate report. The overall wave climate would also be important if the need for a sediment budget was required; that is not the case however. In this report, the wave analysis tools will be developed to address future concerns.

The waves will be described at two distinct levels. In both levels the wave model SWAN will be used. The first level considers a coarse grid development that will model the waves that can occur in the Gulf of Alaska and be directed toward the affected area. These are for the most part deepwater waves which are only affected by the water depth when they approach Kodiak Island. These are waves directed toward Chiniak Bay. The second level considers a smaller geographic area and investigates how the waves are affected as they propagate from Chiniak Bay into the affected area. Here they undergo refraction and shoaling and are significantly reduced in height and energy from their deepwater counterparts. SWAN will be configured to address this transformation. The framework for that effort, with a specific example, is discussed below.

SWAN is a robust wind wave model developed by the Delph Hydraulic Institute in the Netherlands. It is a third-generation model and heavily used by wave modelers for near-shore application. The "third-generation" implication is that SWAN now uses a more explicit and computing-intensive calculation of the quadruplet wave-wave interactions than the two previous generations had. The key concepts that make SWAN (acronym for Simulation WAves Nearshore) have been described well by Holthuijsen, (2007).

- It is a free, open-sourced application.
- It accounts for wave-current interaction and is based on the spectral action balance equation (similar to the spectral energy balance equation).
- It is formulated for both Cartesian and spherical co-ordinates to accommodate small and larger modeling areas, respectively. Both are used for this analysis.
- To accommodate the co-ordinates of some hydrodynamic flow models, it can be configured with curvilinear grids in place of the standard rectilinear grids.
- It has nesting capabilities to highlight areas within the coarse grid to require greater detail.

- The robustness includes the ability to solve complex time-dependent, two-dimensional spectral action balance equations to simple steady state, single dimension equations.
- Shoaling and breaking from bottom elevations and currents as well as refraction are accounted for explicitly and diffraction (from waves impinging on obstacles) is approximated.
- SWAN accounts for transmission through and reflection from obstacles.
- Dissipation is calculated from white-capping, bottom friction, and surf beating.
- The quadruplet wave-wave interaction is computed using the discrete-interaction approximation (DIA) of Hasselmann, *et.al.* (1985).
- Wave-induced setup is calculated exactly for the stationary, one-dimensional case and estimated for the more complex cases.

4.5.2 Coarse Grid

The first step in examining the waves in the affected area is to consider the waves generated in the Gulf of Alaska and directed westward. This is done with a coarse-grid model. The winds that will be used to calculate these waves are realistic wind speeds taken directly from the NOAA Buoy 46001. East winds of 25 meters per second (m/s) were used for illustration in this case. The maximum waves that could arrive at deepwater locations seaward of the affected area have not yet been determined.

For the initial grid a model domain equal to two degrees of longitude (150°-152°) in the horizontal direction and 1.5 degrees of latitude (57°-58.5°) in the vertical direction (Figure 81). At this latitude this gives a grid of about 64 n. m. wide by 90 n. m. high. The grid corners were centered on each two minutes of longitude and latitude. This produced 2,700 individual grids approximately 2,000 meters wide and 2,800 meters high.

For this grid and wind conditions, waves of about 7 meters high were produced on the west side of the grid in the deep waters of Chiniak Bay (Figure 82). These were then used as input into the waves that were propagated into the affected area. These were steady state waves that were limited by both wind speed and fetch.

4.5.3 Fine Grid

A fine grid was use to examine the transformation of the deepwater waves into the shallower water of the affected area. This included most of Chiniak Bay and its western extensions into St. Paul Harbor and Womens Bay (Figure 83). The domain for this analysis used 127 grids in the horizontal direction and 64 in the vertical. The total number of grids was 8,128 and they were square measuring 100 meters on each side.

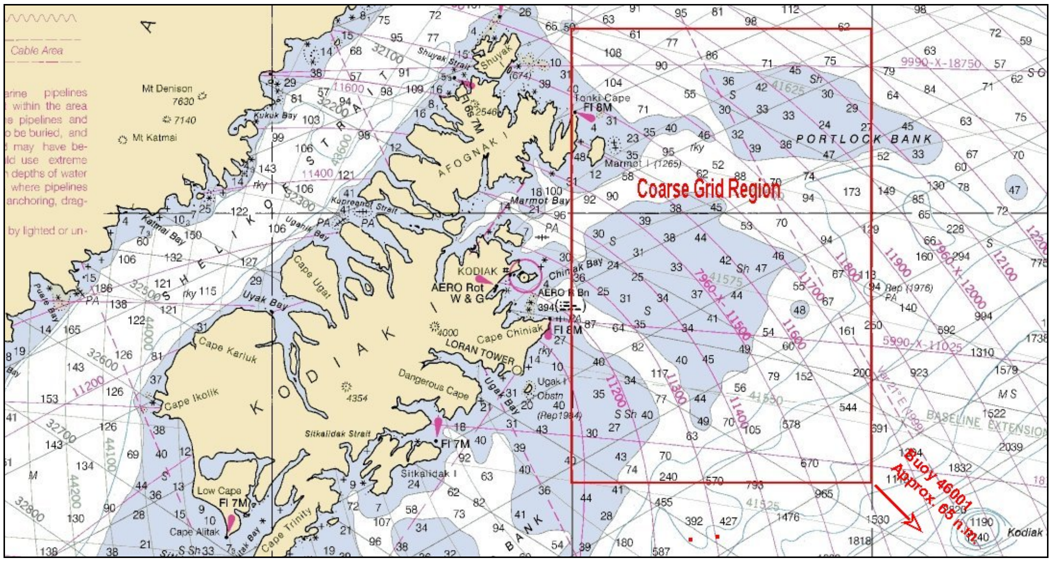

Figure 81 Outline of the domain used for the coarse grid wave modeling.

The 7 meter wave calculated using the coarse grid was used as input to the finer grid domain. The overall depth was also increased by adding a 3 meter tide across the entire domain. The waves were significantly reduced as they entered the shallower waters. Figure 84 shows the extent of this transformation. It appears that waves where any of the possible alternatives would occur are limited by the water depth to less than 2 meters (6.5 feet).

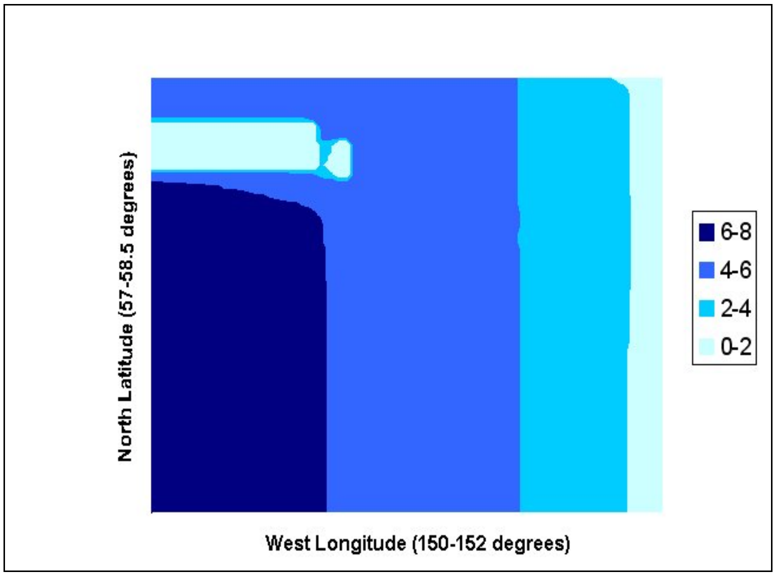

Figure 82 Wave heights (meters) for coarse grid domain.

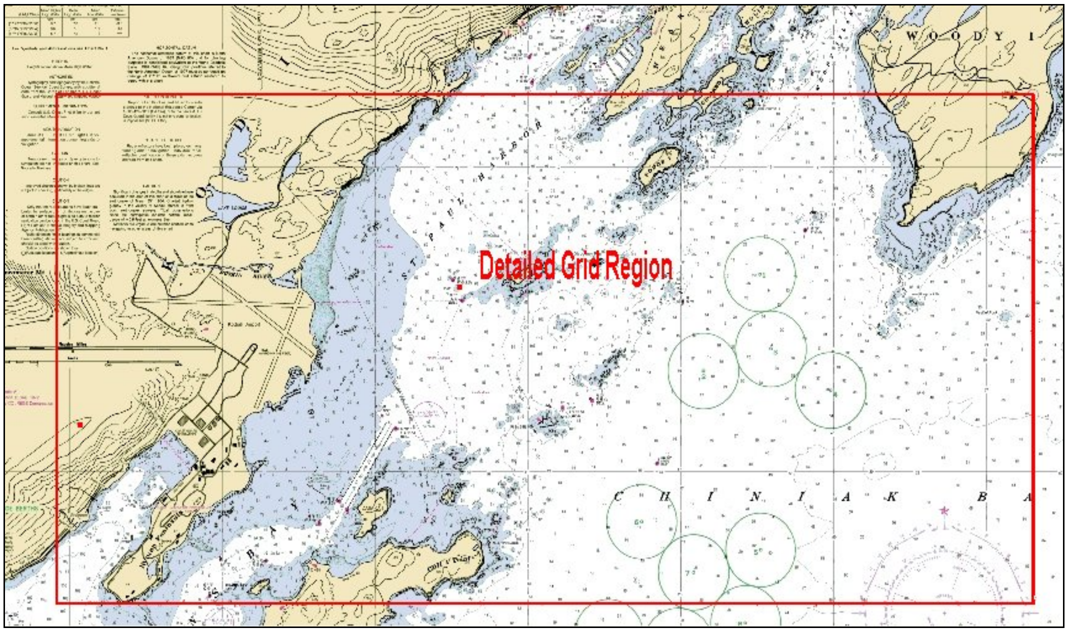

Figure 83 Outline of the domain used in the fine grid wave modeling.

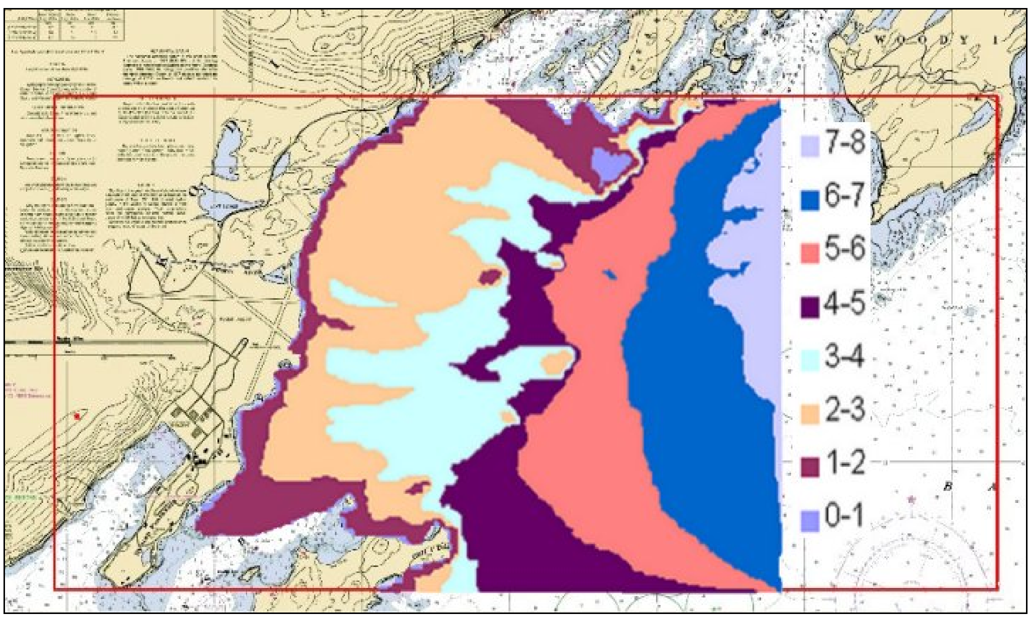

Figure 84 Wave heights (meters) for the fine grid domain.

Long period waves from the North Pacific feel he bottom in very deep water. This causes the waves to refract and attempt to align their crests parallel to the shorelines and nearshore bottom contours. In the shallow water of the project area the waves will lose much of the obliqueness relative to the shoreline,

4.6 Physical Changes Due to Alternatives

4.6.1 Introduction

Most shorelines described in Section 2 are clearly outside of the zone of influence from any of the RSA alternatives. As such, these shorelines are not anticipated to experience change in the coastal dynamic environment (wave size or frequency and sediment transport) or in the coastal physical description (sediment size distribution, beach slope or beach width). Such changes would normally be associated with wave sheltering or longshore sediment transport effects.

While the majority of the area will not experience any of these project-associated changes, the Buskin River area is an important exception. Here the proposed projects on the east end of runway 07/25 and on the north end of runway 18/36 can create significant changes to the wave activity and to sediment transport regime. Changes could occur in the vicinity of the Buskin River mouth, the barrier bar to the south and to the coastal area to the north. Both of the proposed RSA extensions will potentially shelter waves, block the natural flow of longshore sediments, and physically bury potential sources of transportable sediments.

The Buskin River has been migrating north since it was relocated in 1939-40 and perhaps only temporarily reversed that trend for a shore period following the 1964 Earthquake although there is a difference of opinion on that event (Section 2). The migration is slow relative to beaches with greater supplies of beach material and greater wave activity. On such beaches, the mouths of streams or inlets often migrate creating a barrier bar along their seaward side. At some point, flow conditions combined with flood and/or storm conditions cause a breakout toward the original location of the mouth. Compared to many river mouths located on sandy beaches, the Buskin River has a meager supply of sediments and is well protected from the waves that can move sediments strongly either to the north or south in this vicinity. Larger waves undergo a higher degree of refraction that causes their crests to line up nearly parallel to the shoreline. This reduces the directionality of these larger waves and further reduces longshore transport.

Vegetation has been established on the Buskin River barrier bar attesting to its stability. The vegetation ends near the northern end of the 1,200-foot fill being considered. For approximately half that distance, the vegetation is quite robust.

4.6.2 RSA Extensions on Runway 07/25

The beach and nearshore area on the east end of Runway 07/25 are shown in Figure 25. The possible alternatives for this runway (400 and 800 foot RSA extensions) are shown in Figure 54. The modeling has shown that with winds out of the north and east the Buskin River freshwater plume is to the south. While the water parallels the shore under the existing condition, the RSA extensions would cause the freshwater to be displaced further offshore.

In addition, the extensions would tend to shelter the coastline on its south side from waves from the north and conversely they could provide some protection to the barrier bar from waves out of the south. Figure 25 clearly shows a pronounced deposit of primarily gravel just south of the proposed RSA extensions. It is suspected that this is the site of a former mouth of the Buskin River (prior to its relocation to the north to reclaim land for the runway). These alternatives could bury some of these former deposits and isolate the remaining from entering the longshore transport process.

While either of these extensions might create a sediment deficiency on its north side, the extent of this deficiency is hard to assess. It appears that most of the more-easily transportable material from this deposit has already been moved to the north (perhaps used to help create the barrier bar) and has been contributing to the near shore sediments in the region of the present site of the Buskin River mouth. It is more likely that the barrier bar now owes its continued existence to the supply of near shore sediment directly offshore of it and on material supplied by the river itself. However, if these estimates are incorrect, then this deficiency could increase erosion on the barrier bar and slow its migration to the north. It could even erode into the barrier bar south of the present river mouth enough to weaken it to the point of contributing to a southern breakout. However, in our professional opinion, it is more likely that the loss of this sediment source will only cause a slower northward migration of the Buskin River mouth.

The potential erosion of the barrier bar and the northward migration of the river mouth would be slowed to a greater extent by the longer fill.

4.6.3 Northward RSA Extensions on Runway 18/36

The proposed RSA extensions of Runway 18/36 are shown, in relation to the barrier bar and the Buskin River mouth, in Figure 54. (Existing conditions are shown in Figure 26).

The RSA extension would be nearly parallel to the barrier bar; its west side is located on the east side of the bar. As such it would bury much of the barrier bar sediments and much of the near shore sediments. Currently these sediments contribute to the coastal processes of both onshore/off shore and the longshore transport.

In our professional opinion, onshore/off-shore and longshore transport near the barrier bar would be severely impacted by this alternative. Since the river mouth migration requires that sediments be supplied to the system, the main impact from these alternatives would likely slow or stop. Much of the present supply (perhaps most) probably comes from the barrier bar. The only persistent sediment supply, should one of these extensions be built, would likely be the river and the portion of the barrier bar that would remain exposed west of the fill.

If the supply from the south is maintained, the 18/36 structures would block sediments; it would probably take years for the northward sediment transport stream to re-establish on the outside of the fill. If RSA extensions were added to both runways, then the possible erosion of the barrier bar described above would likely be avoided because much of the bar would be buried and in our opinion the only additional impact due to this combination would be a further slowing or stopping of the river mouth migration.

It appears that the largest impact created by the 18/36 alternatives would be that the bar/near shore system would lose much of its sandy beach due to the RSA structure. Hundreds of lineal feet of beach would be buried and hundreds of feet of bay vista would disappear.

4.6.4 Southern RSA Extensions on Runway 18/36

The southward extension of runway 18/36 would have little impact as minimal sediment transport occurs in this area. A portion of the shoreline would be lost or would be replaced with riprap protection for the fill.

5. CONCLUSIONS

The Buskin River mouth has been migrating to the north since it was relocated for construction of the runways in 1939-40. The rate seems to have been steady but slow having migrated about 2,000 feet since its relocation. This migration is dependent on wave activity and sediment supply.

The RSA extensions on Runway 07/25 could reduce the sediment supply to the mouth of the Buskin River and thereby slow or stop its northward migration. The extensions could also severely reduce the northward-directed longshore wave thrust perhaps resulting in a net southward wave energy thrust which, when combined with its sediment-reduction impact, could cause the mouth to migrate south of its present position. These extensions could also cause the trajectory of the Buskin River freshwater plume to become displaced further offshore than in the existing condition when this plume is directed to the south (during ebb tides and southern winds).

The proposed RSA extensions to the north on Runway 18/36 would bury much of the beach and shallow nearshore portion of the barrier bar. The extensions would provide wave protection and eliminate much of the barrier bar as a sediment source, possibly slowing or stoping the northward migration of the Buskin River mouth. In addition, the extensions would provide a northern limit to any southern migration of the river mouth as no migration could proceed south of their northern-most footprint.

The impact of the southern extension of this structure is limited to replacing a few hundred feet of rock outcropping shoreline with RSA fill and a shoreline of armor rock further offshore. Little or no sediment is presently being transported along this area and that should not change.

No other coastal impacts or impacts to the freshwater plume of the Buskin River are anticipated from the proposed extensions.

6. REFERENCES

Bennett, A.F. 1976. Open boundary conditions for dispersive waves. J. Atmos. Sci. 32:176-182.

Bennett, A.F. and P.C. McIntosh. 1982. Open ocean modeling as an inverse problem: Tidal theory. J. Phys. Ocean. 12:1004-1018.

Blumberg, A.F. and L.H. Kantha. 1985. Open boundary condition for circulation models. J. Hydr. Engr. 111:237-255.

Blumberg, A.F. and G.L. Mellor. 1987. A Description of a Three-Dimensional Coastal Ocean Circulation Model. In: Three-Dimensional Coastal Ocean Models, *Coastal and Estuarine Sciences*, vol. 4, N. Heaps, ed., AGU, Washington, DC. p. 1-16.

Craig, Paul M. 2004. User's Manual for EFDC_Explorer: A Pre/Post Processor for the Environmental Fluid Dynamics Code. Dynamic Solutions, LLC, Knoxville, TN, April.

Edinger, J.E., D.K. Brady and J.C. Geyer. 1974. Heat Exchange and Transport in the Environment. Report No. 14, EPRI Publication No. 74-09-00-34. Prepared for Electric Power Research Institute, Cooling Water Discharge Research Project (RP-49), Palo Alto, CA.

Galperin, B., L.H. Kantha, S. Hassid, and A. Rosati. 1988. A quasi-equilibrium turbulent energy model for geophysical flows. J. Atmos. Sci. 45:55-62.

Hasselmann, S., K. Hasselmann, J.H. Allender and T.P. Barnett, 1985. Computations and parameterizations of the nonlinear energy transfer in a gravity wave spectrum, Part II: parameterization of the nonlinear transfer for application in wave models, J. Phys. Oceanogr. V. 15, No. 11, 1378-1391.

Hamrick, J.M., 1992. A Three-Dimensional Environmental Fluid Dynamics Computer Code: Theoretical and Computational Aspects. Special Report No. 317 in Applied Marine Science and Ocean Engineering, Virginia Institute of Marine Science, Gloucester Point, VA. 64 pp.

Hamrick, J.M., 1996. User's Manual for the Environmental Fluid Dynamics Computer Code. Special Report No. 331 in Applied Marine Science and Ocean Engineering, Virginia Institute of Marine Science, Gloucester Point, VA.

Holthuijsen, Leo H., 2007. *Waves in oceanic and coastal waters*, Cambridge University Press, The Edinburgh Building, Cambridge CB2 2RU, UK. 387pp.

Hood, Donald W. and Steven T. Zimmerman, 1987. *Gulf of Alaska: physical environment and biological resources*, Eds. U.S. Dept of Commerce and U.S. Dept. of the Interior, 655 pp.

Johnson, B.H., K.W. Kim, R.E. Heath, B.B. Hsieh, and H.L. Butler. 1993. Validation of three-dimensional hydrodynamic model of Chesapeake Bay. J. Hyd. Engrg. 119:2-20.

Lung, W.L. 2002. *Water Quality Modeling and Wasteload Allocations and TMDLs*. John Wiley & Sons, Inc., New York, NY, 333 pp.

Martin, James L. and Steven C. McCutcheon. 1999. Hydrodynamics and Transport for Water Quality Modeling. Lewis Publishers, CRC Press, Boca Raton, FL.

Mellor, G.L. and T. Yamada. 1982. Development of a turbulence closure model for geophysical fluid problems. Rev. Geophys. Space Phys. 20:851-875.

Park, K., A.Y. Kuo, J. Shen and J.M. Hamrick. 2000. A three-Dimensional Hydrodynamic - Eutrophication Model (HEM-3D): Description of Water Quality and Sediment Process Submodels (EFDC Water Quality Model). Special Report in Applied Marine Science and Ocean Engineering No. 327, School of Marine Science, Virginia Institute of Marine Science, College of William and Mary, Gloucester Point, VA.

Rosati, A.K. and K. Miyakoda. 1988. A general circulation model for upper ocean simulation. J. Phys. Ocean. 18:1601-1626.

Smolarkiewicz, P.K. and T.L. Clark. 1986. The multidimensional positive definite advection transport algorithm: Further development and applications. J. Comp. Phys. 67:396-438.

Smolarkiewicz, P.K. and W.W. Grabowski. 1990. The multidimensional positive definite advection transport algorithm: Nonoscillatory option. J. Comp. Phys. 86:355-375.

Smolarkiewicz, P.K. and L.G. Margolin. 1993. On forward-in-time differencing for fluids: extension to a curvilinear framework. Mon. Weather Rev. 121:1847-1859.

Solin, 1996. Overview of Surface-Water Resources at the U.S. Coast Guard Support Center Kodiak, Alaska, 1987-1989. U.S. Geological Survey, Open-File Report 96-463, p. 17.

Weingartner, Thomas, 2005. Physical and geological oceanography: coastal boundaries and coastal and ocean circulation, in: *The Gulf of Alaska: biology and oceanography*, Mundy, Phillip R., ed.,Exxon Valdez Oil Spill Trustee Council, Alaska Sea Grant College Program, UUF, 214 pp.

APPENDIX
ADCP locations and Data Examples

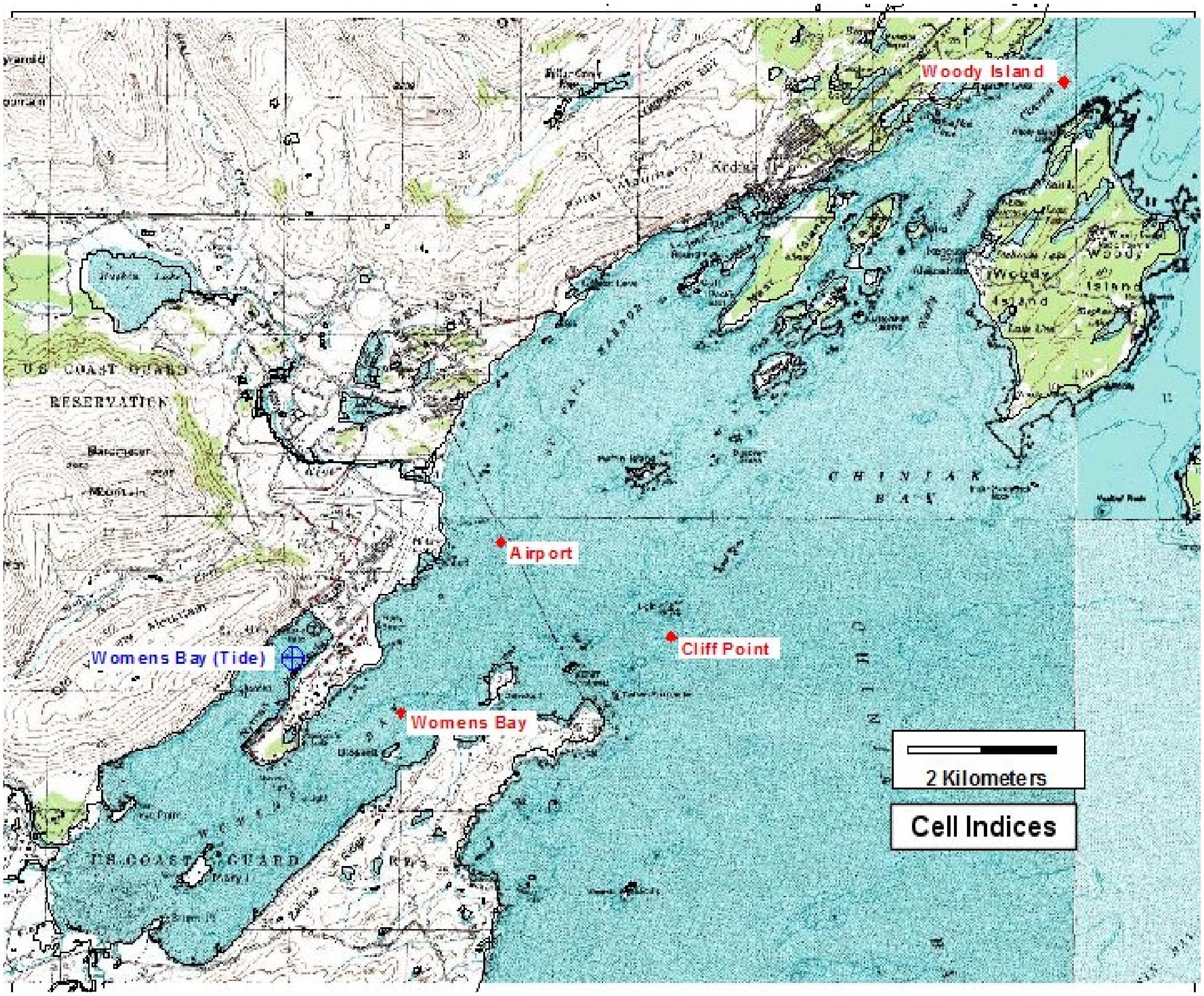

Figure A-1 Location of the Acoustic Doppler Current Profiler (ADCP) used for collecting current

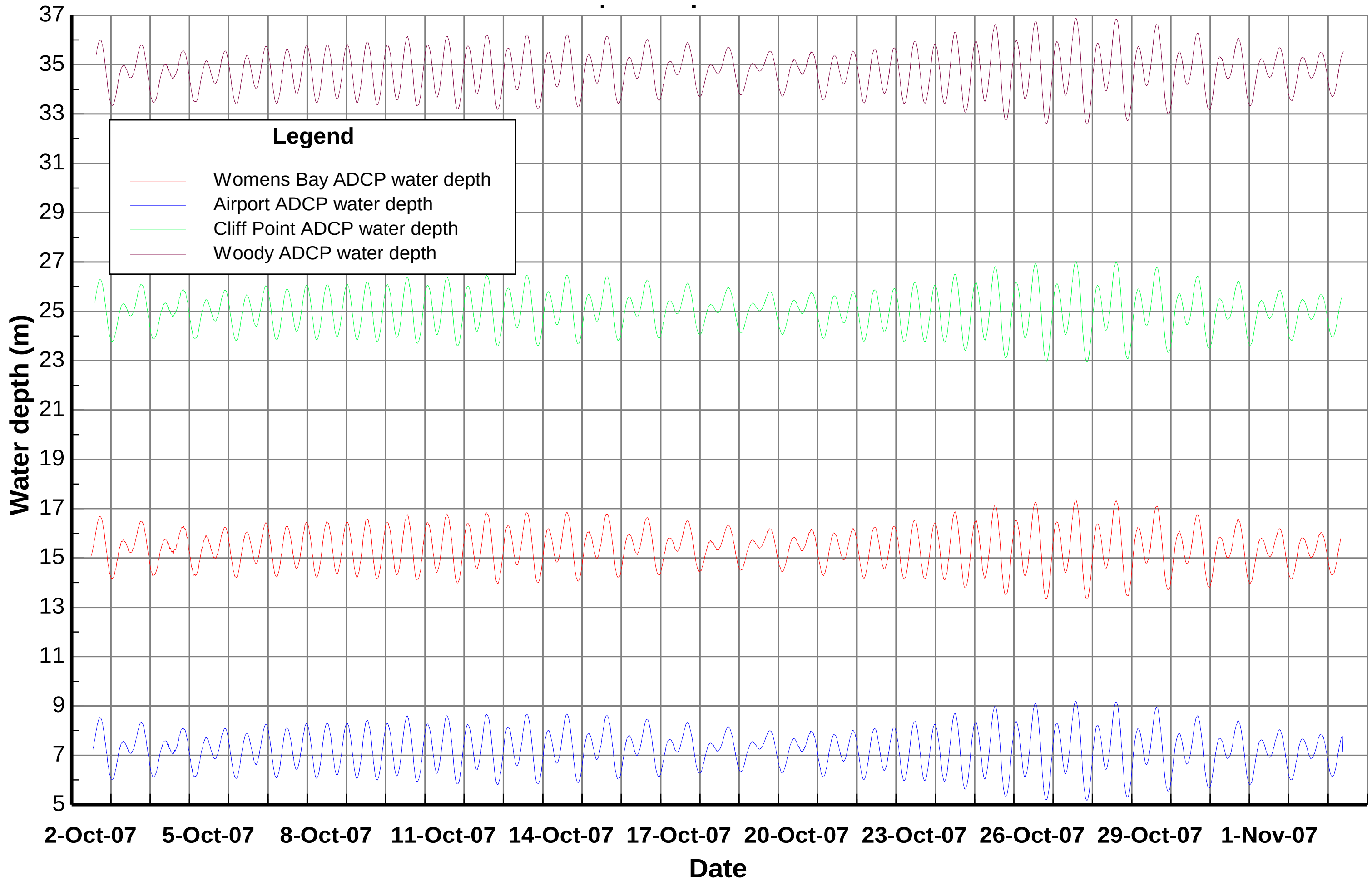

Figure A-2 ADCP water depths for the period of data collection.

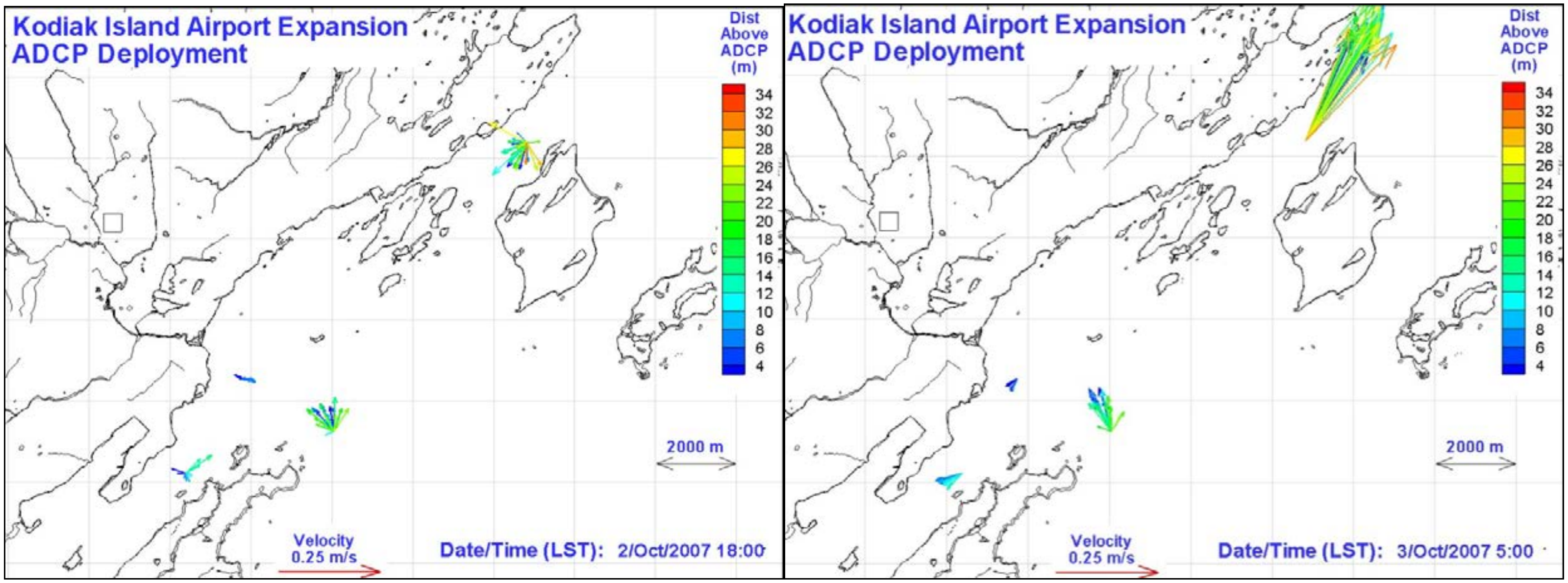

Figure A-3 ADCP velocities for two times. Velocities are colored by distance above the bottom mounted ADCP.

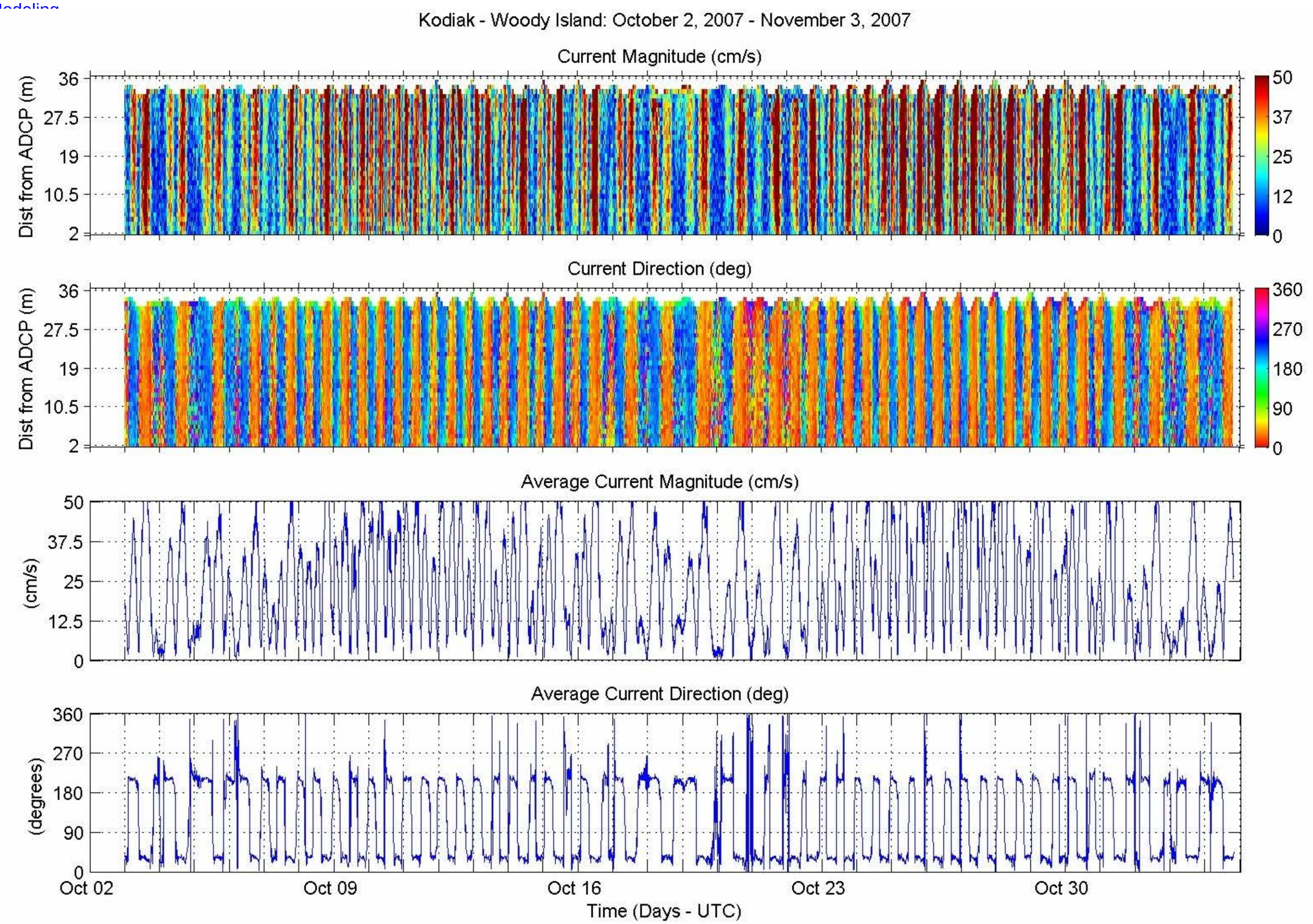

Figure A-4 Summary of ADCP velocities for the data collection period for Kodiak at Woody Island: Scale 50 cm/s.

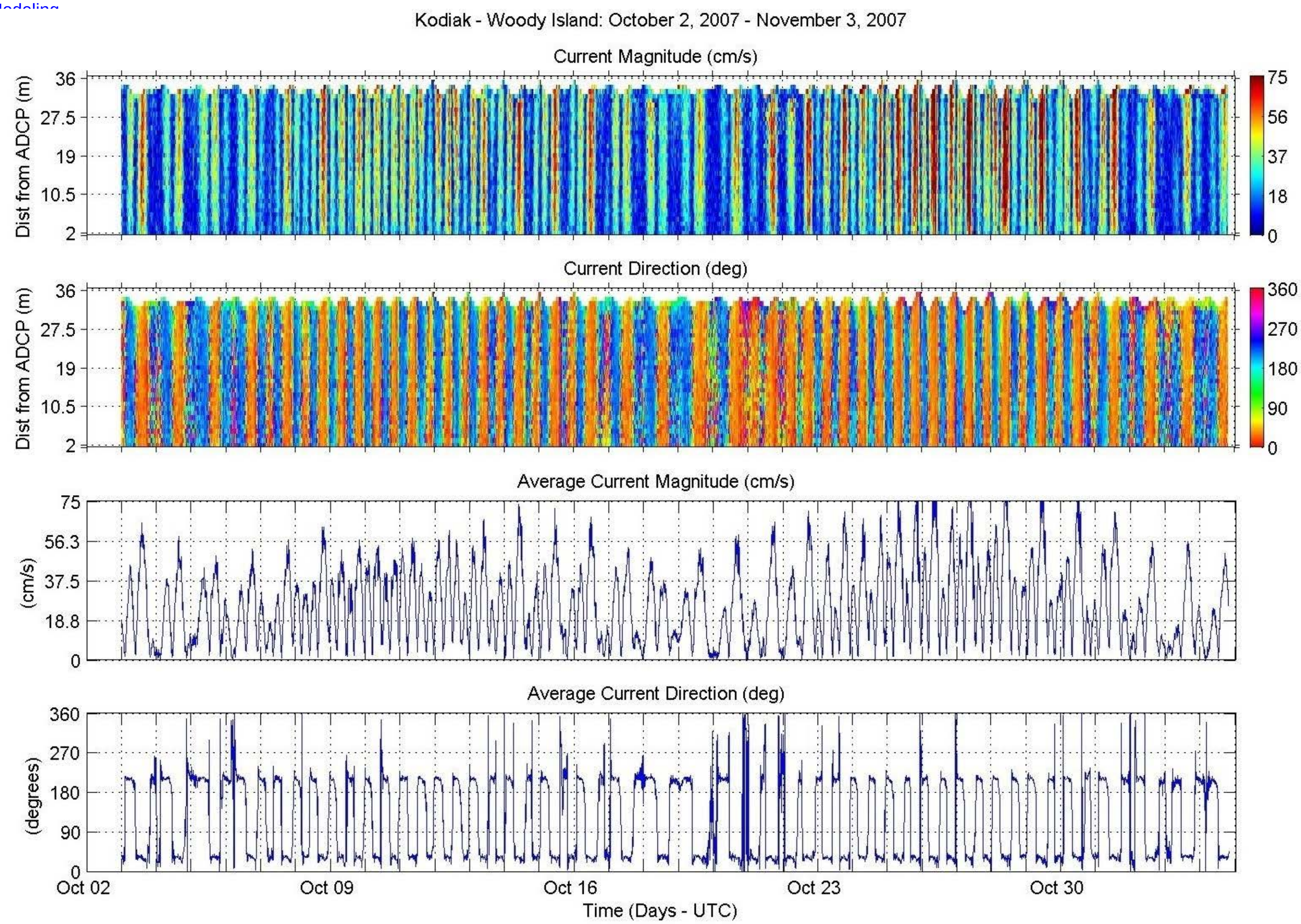

Figure A-5: Summary of ADCP velocities for the data collection period for Kodiak at Woody Island: Scale 75 cm/s.

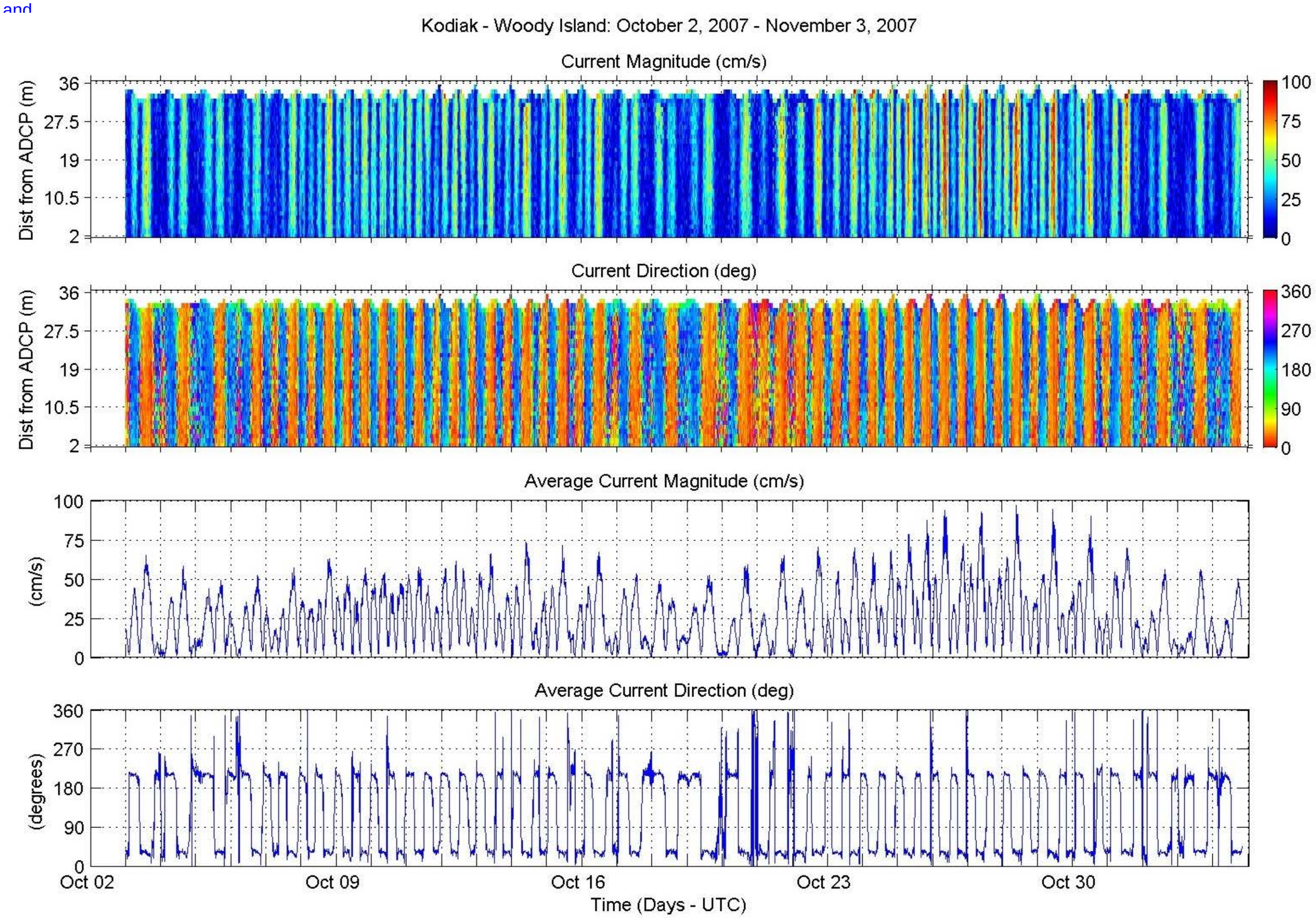

Figure A-6: Summary of ADCP velocities for the data collection period for Kodiak at Woody Island: Scale 100 cm/s.

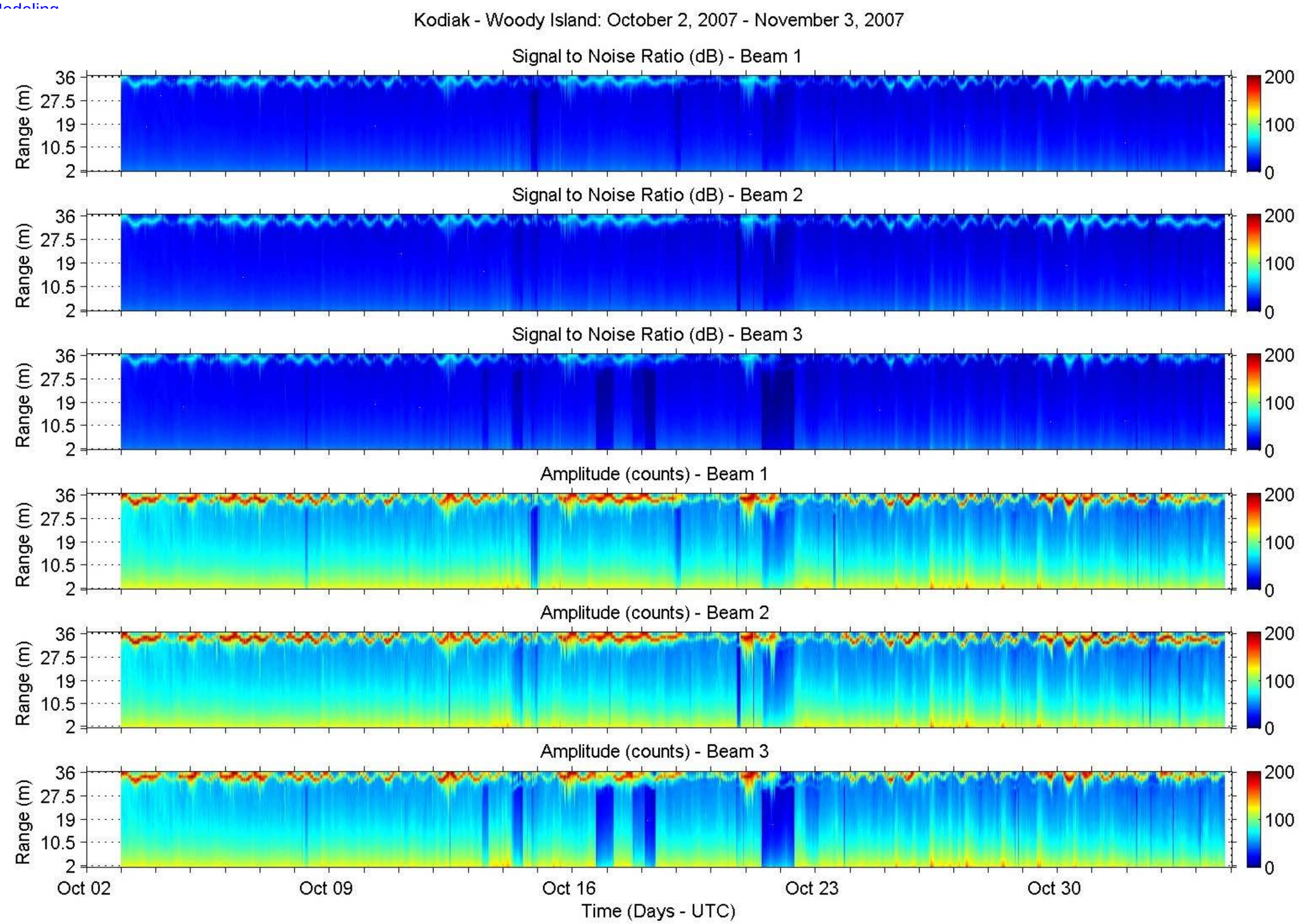

Figure A-7 Summary of ADCP signal-to-noise and amplitude for the data collection period for Kodiak at Woody Island.

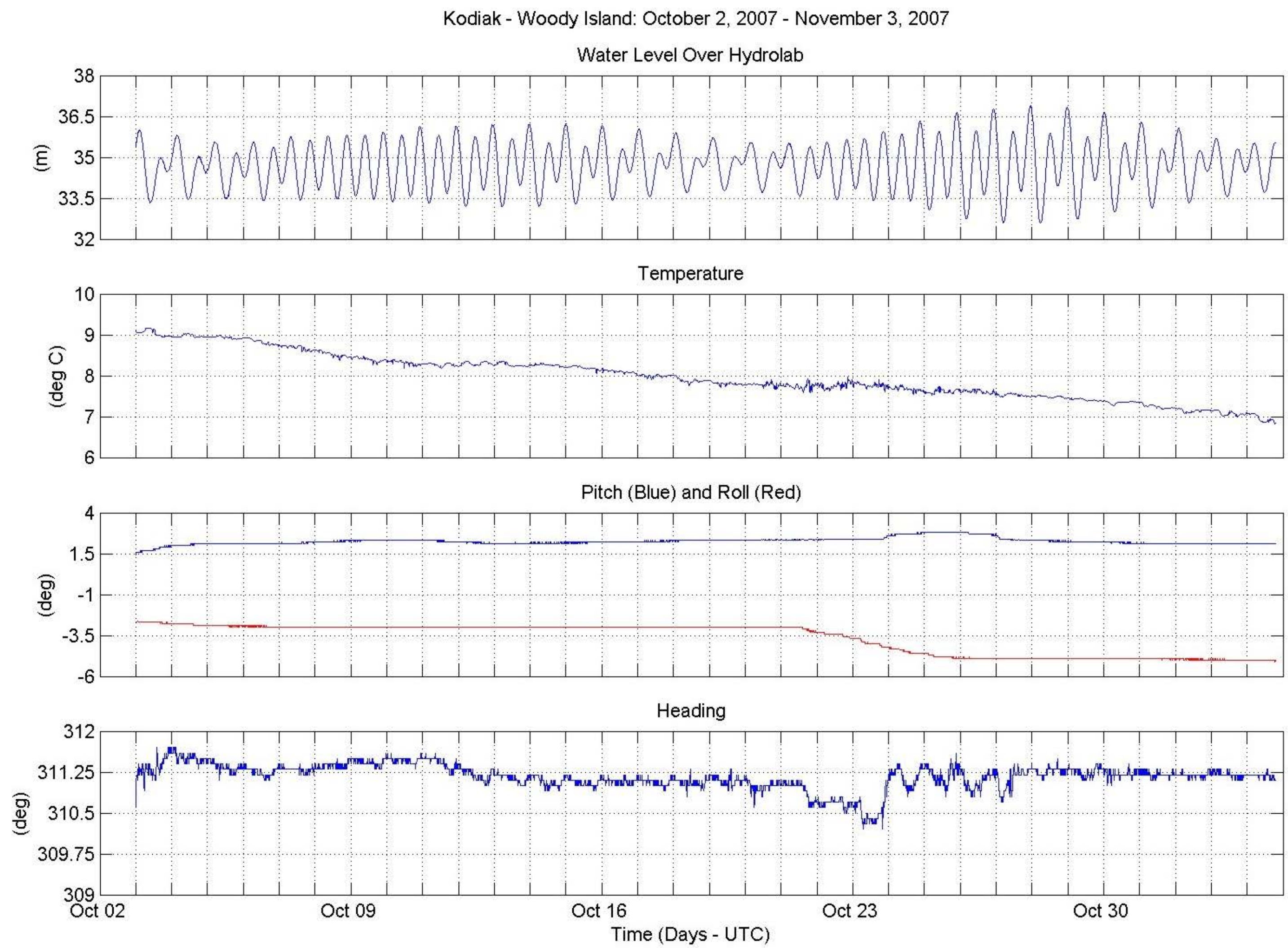

Figure A-8 Water level, water temperature, pitch, roll, and heading for Woody Island ADCP.

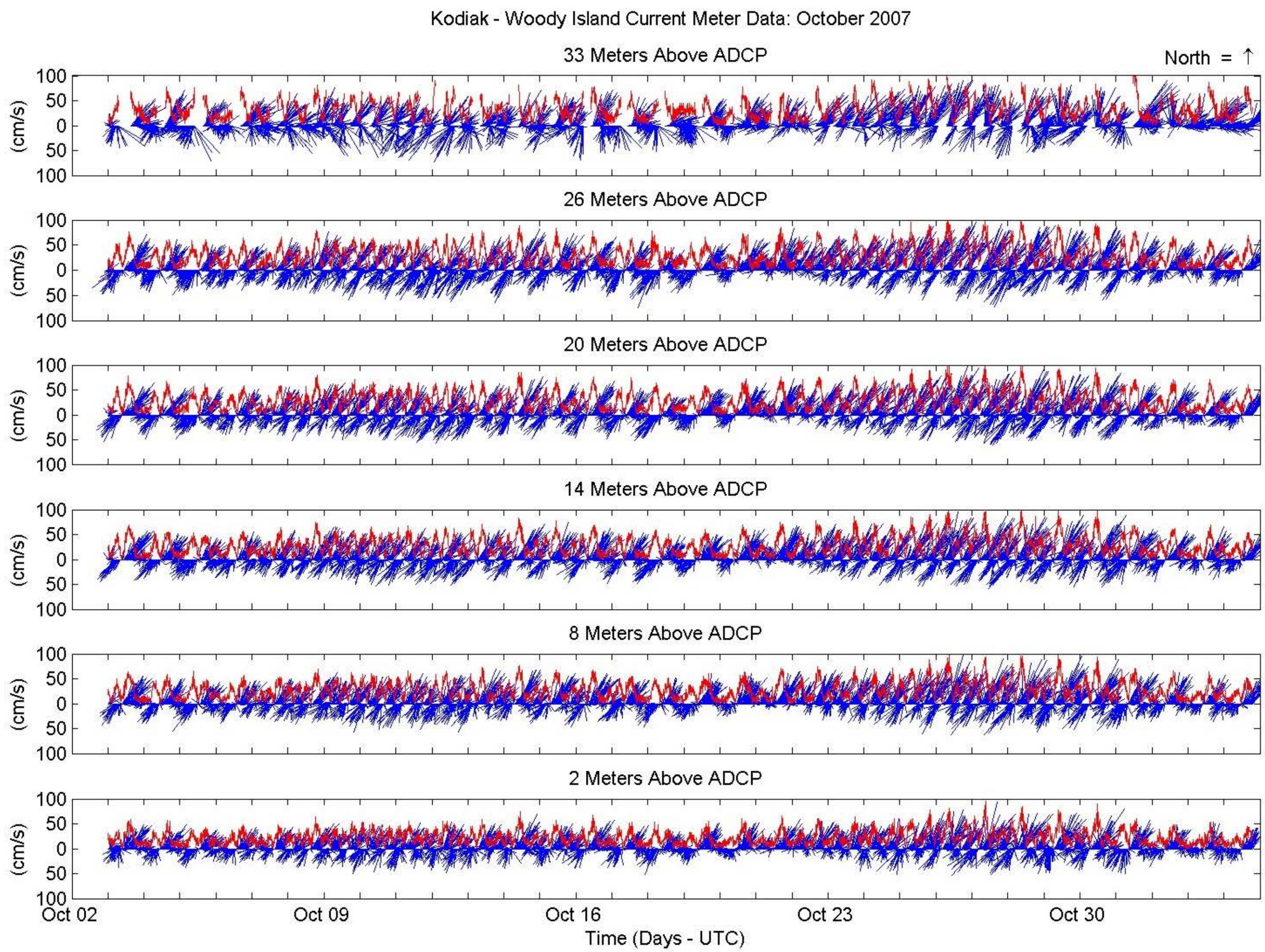

Figure A-9 Current meter vectors for October at Woody Island, Kodiak for various depths.

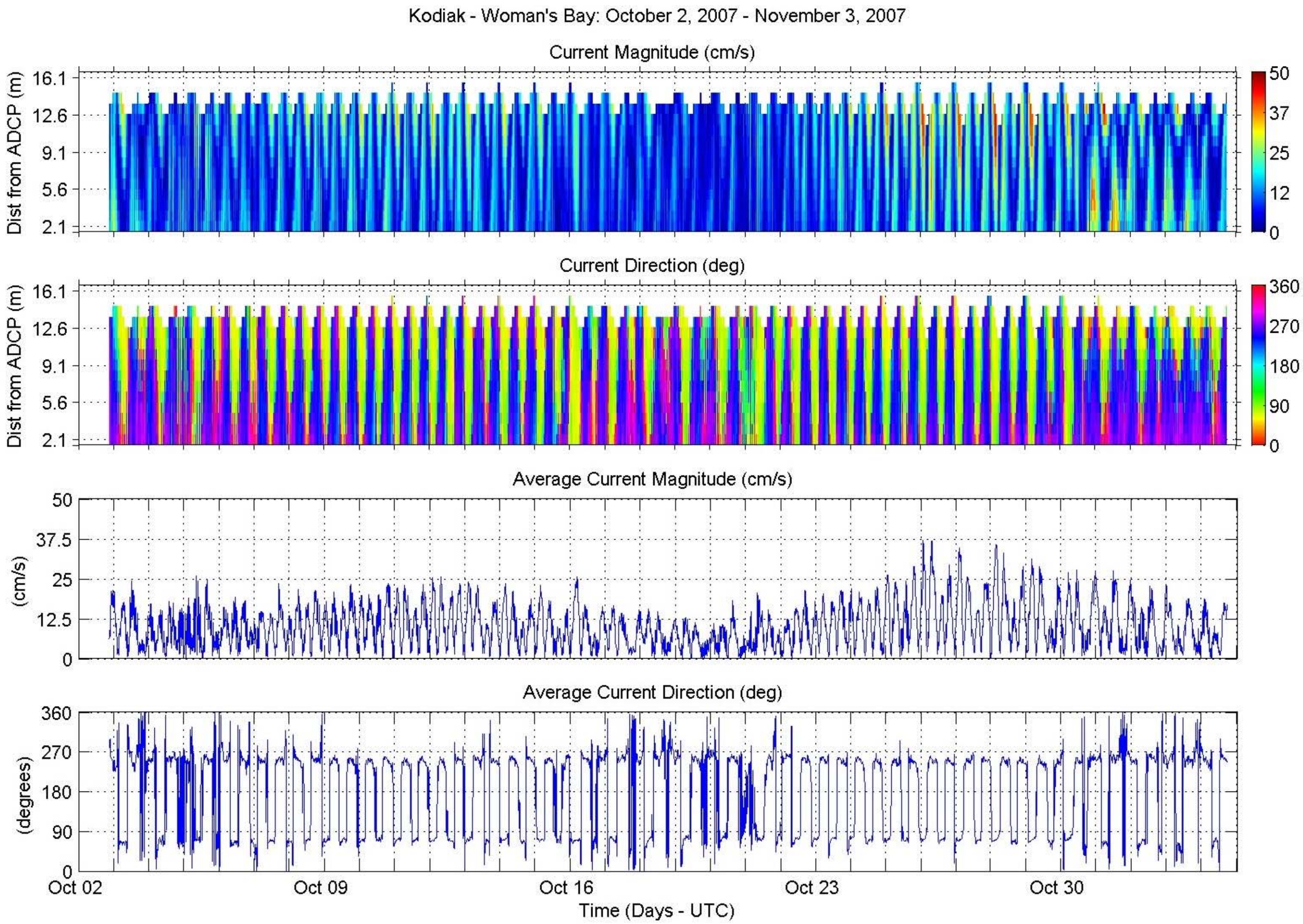

Figure A-10 Summary of ADCP velocities for the data collection period for Kodiak at Womens Bay: Scale 50 cm/s.

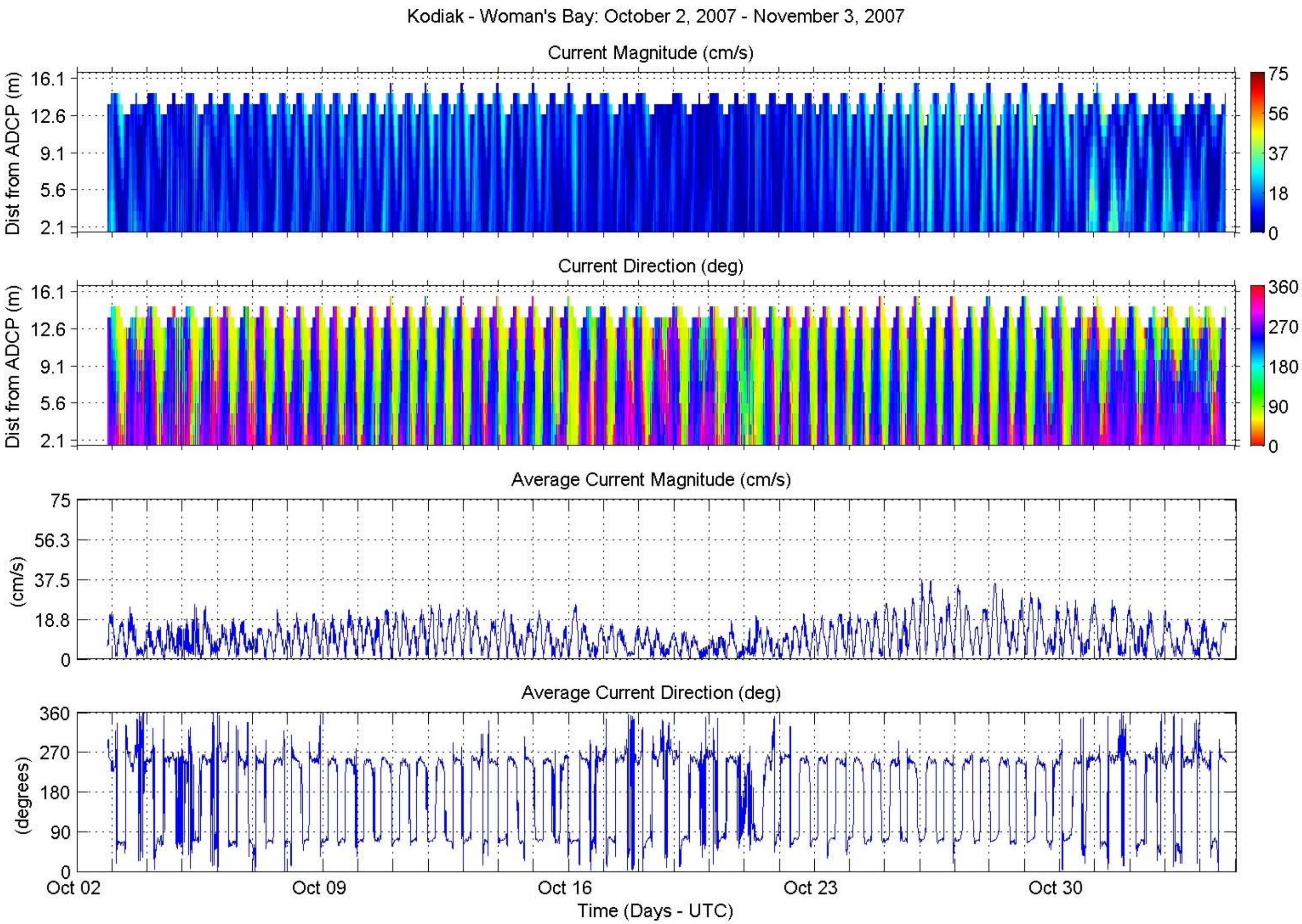

Figure A-11 Summary of ADCP velocities for the data collection period for Kodiak at Womens Bay: Scale 75 cm/s.

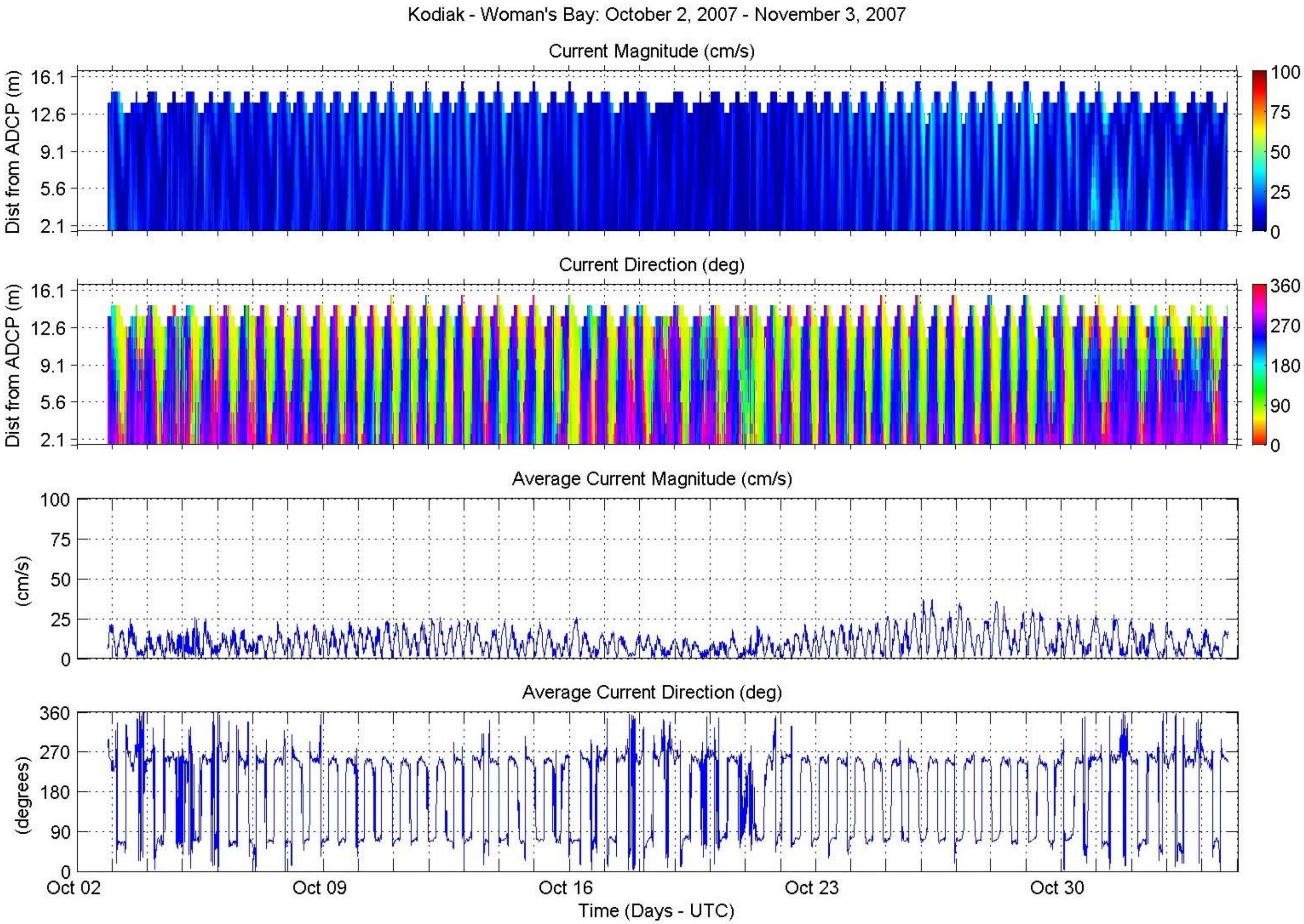

Figure A-12 Summary of ADCP velocities for the data collection period for Kodiak at Womens Bay: Scale 100 cm/s.

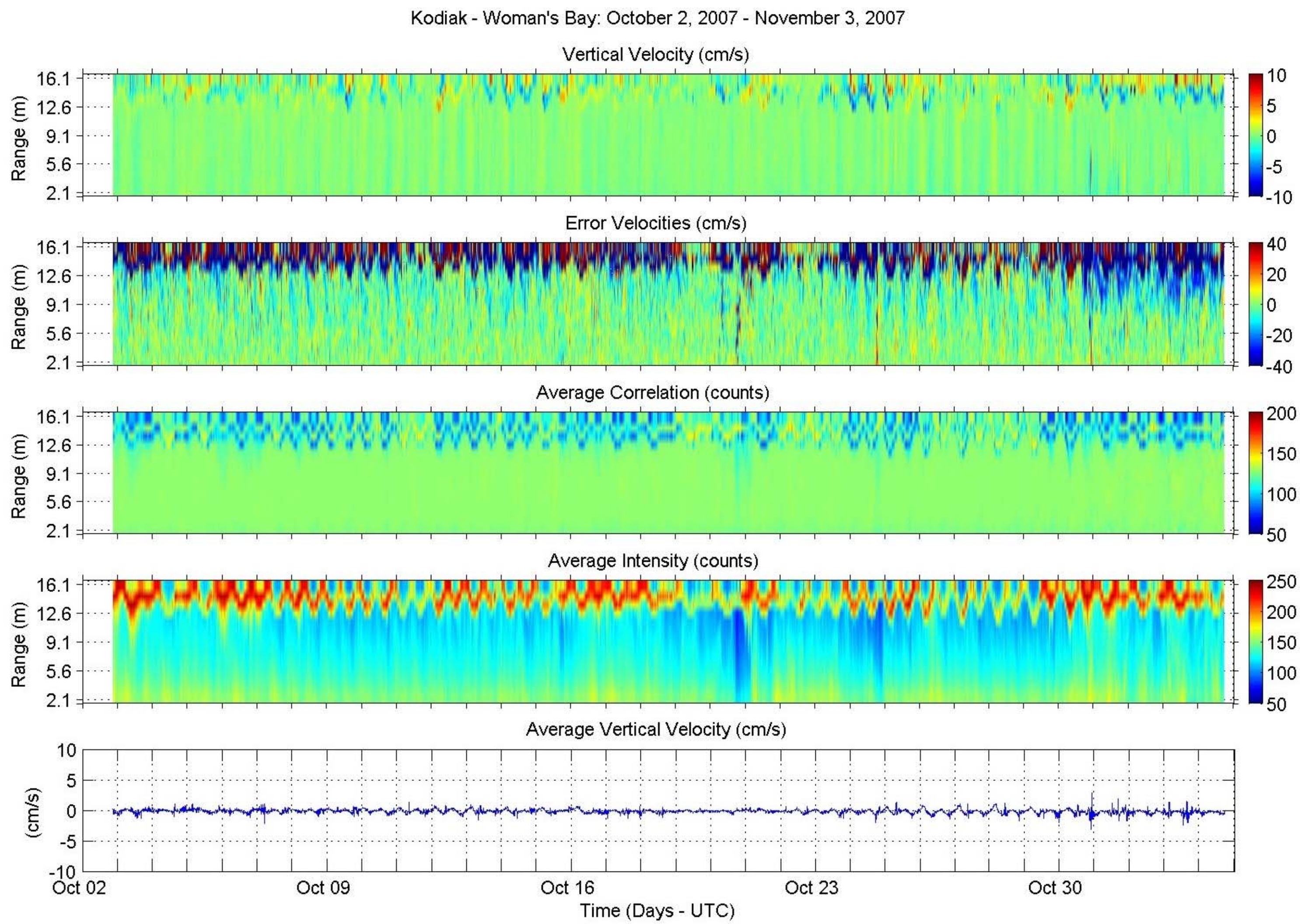

Figure A-13 Summary of ADCP average vertical velocities for the data collection period for Kodiak at Womens Bay.

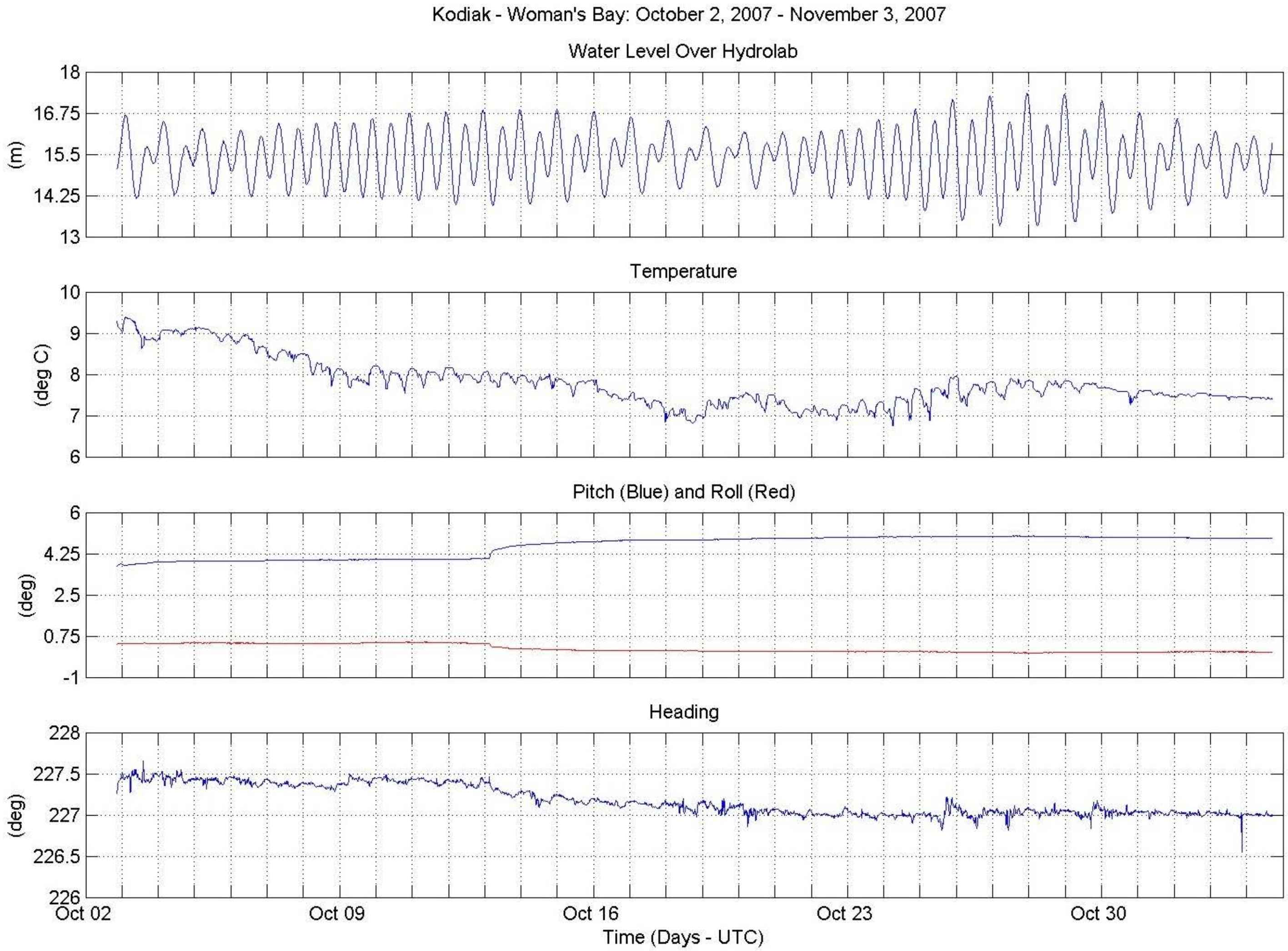

Figure A-14 Water level, water temperature, pitch, roll, and heading for Womens Bay ADCP.

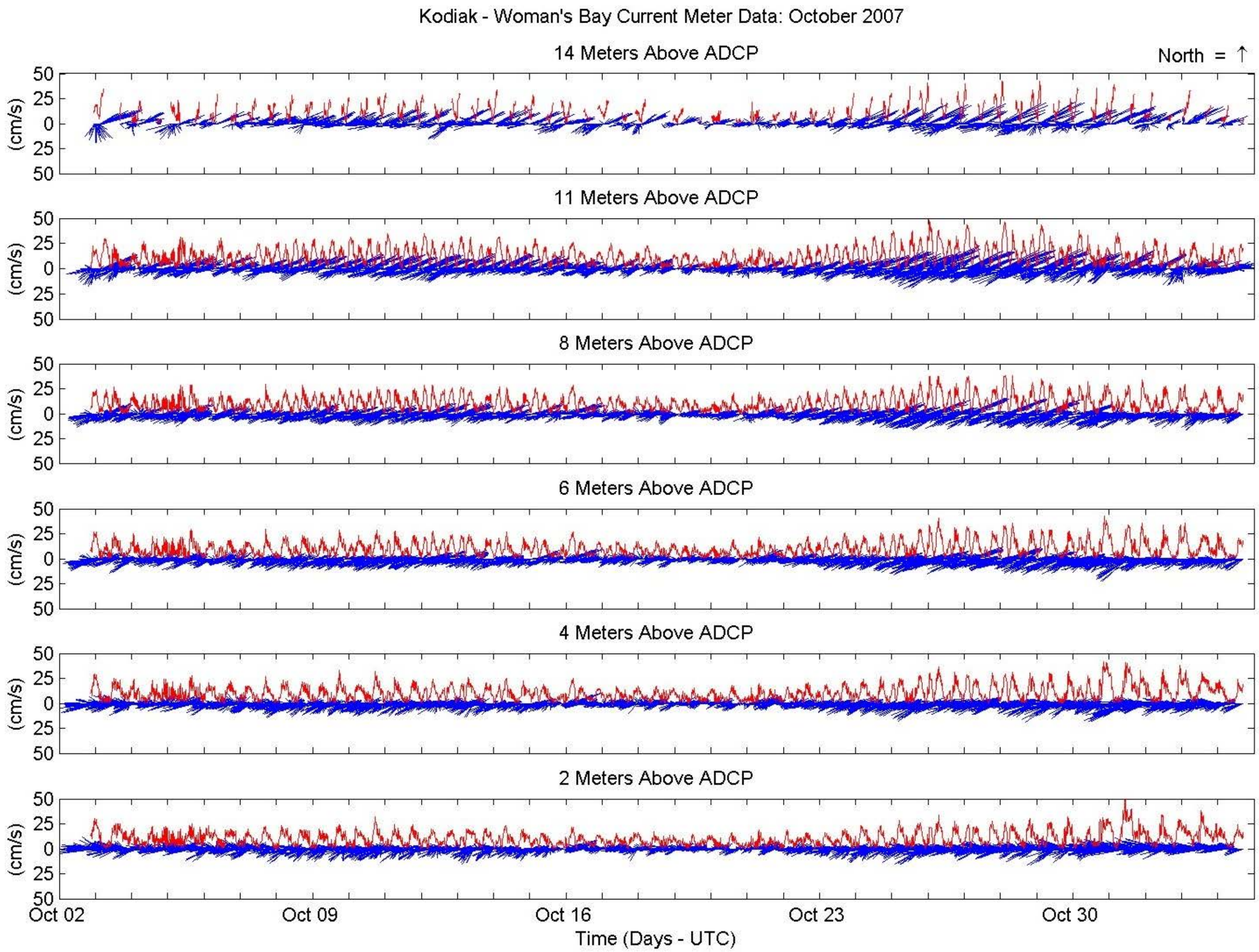

Figure A-15 Current meter vectors for October at Womens Bay, Kodiak for various depths.

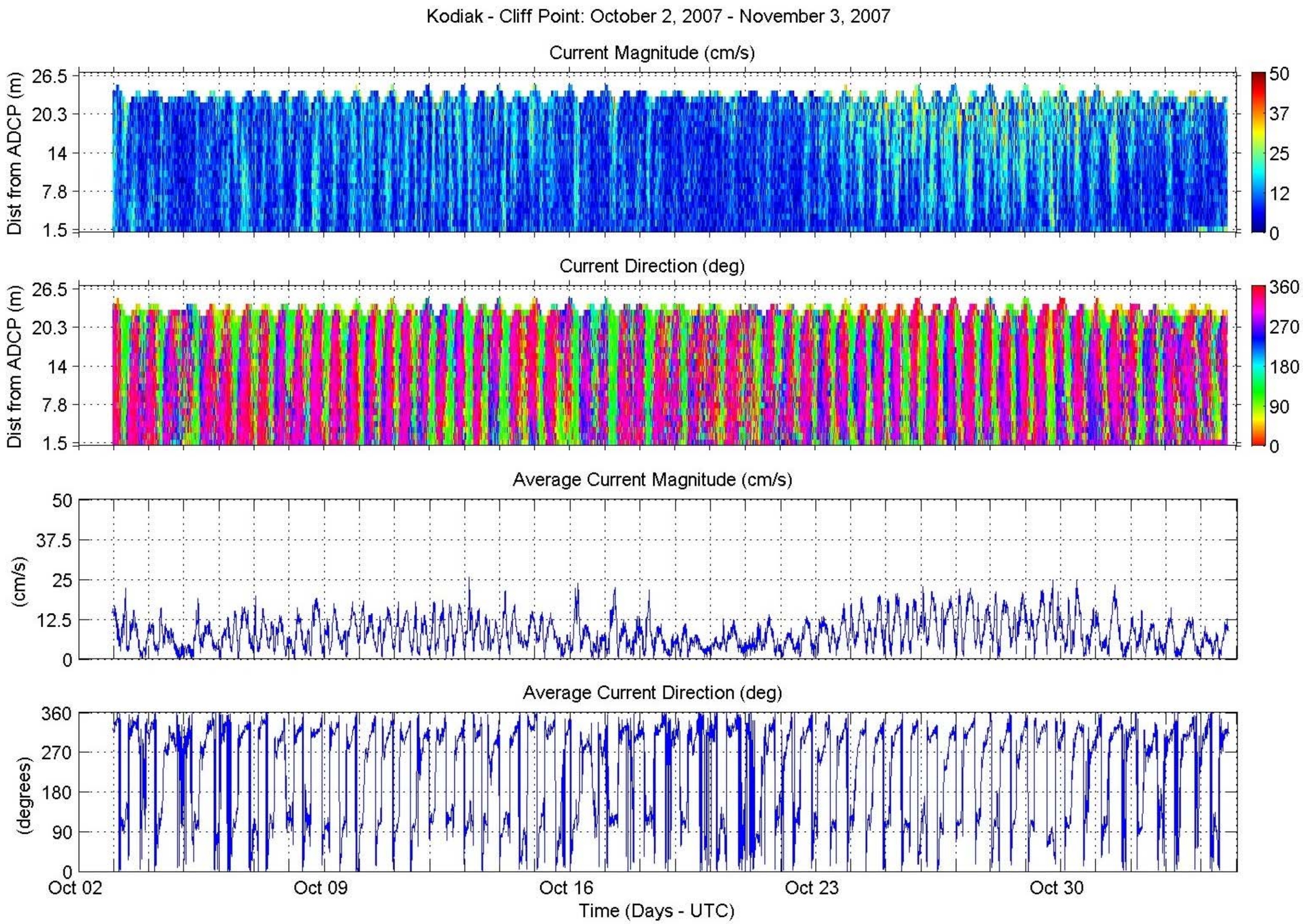

Figure A-16 Summary of ADCP velocities for the data collection period for Kodiak at Cliff Point: Scale 50 cm/s.

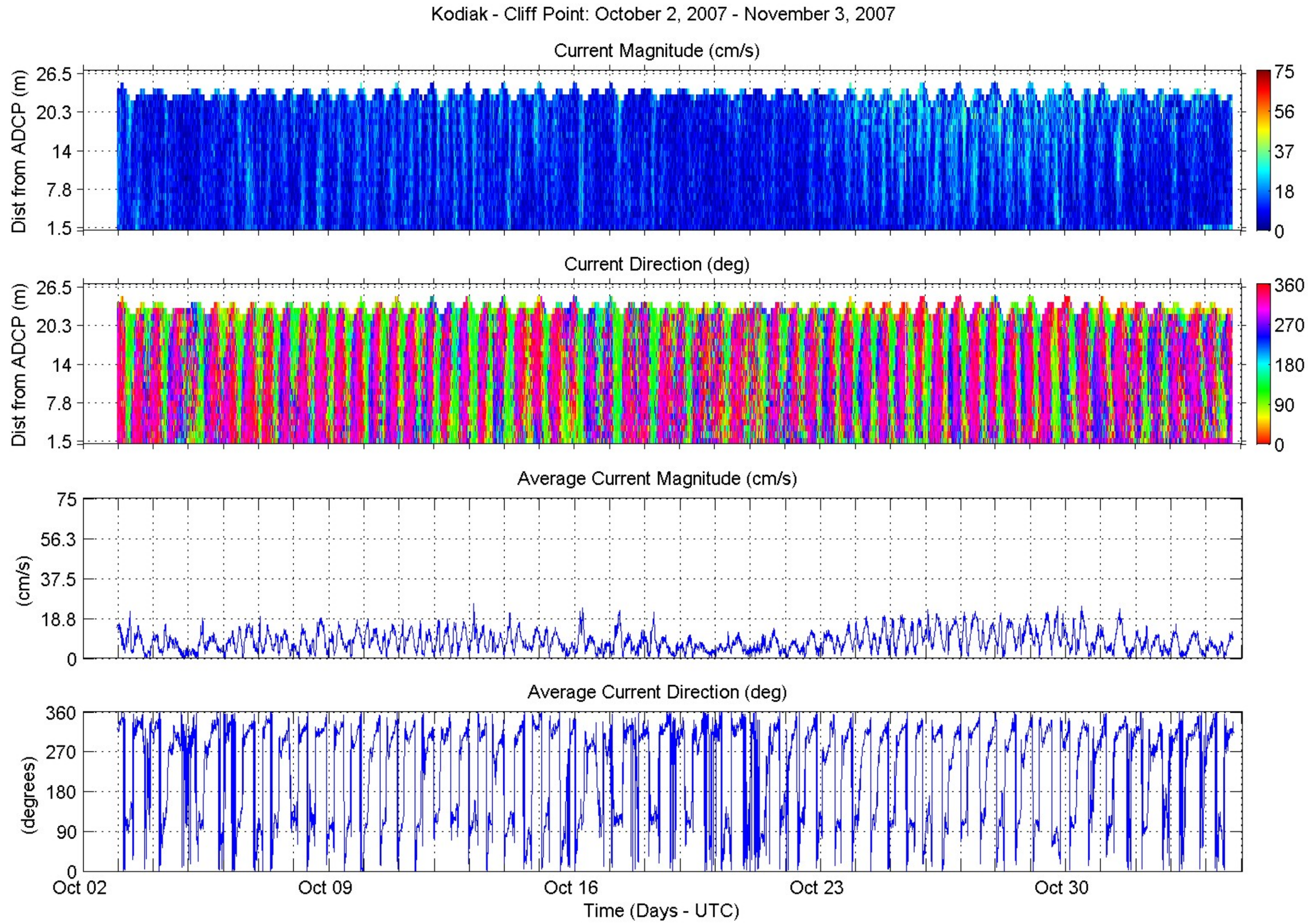

Figure A-17 Summary of ADCP velocities for the data collection period for Kodiak at Cliff Point: Scale 75cm/s.

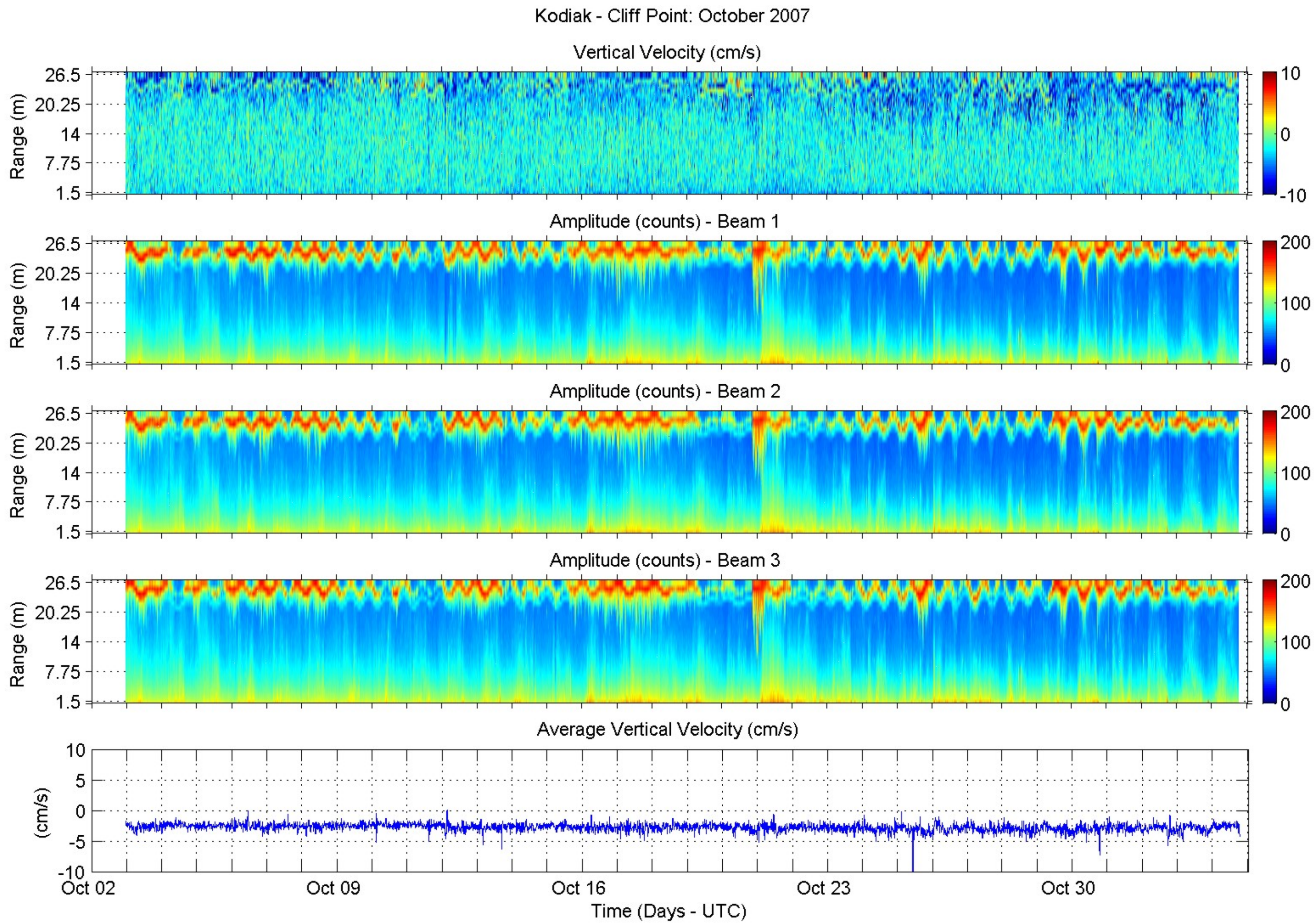

Figure A-18 Summary of ADCP average vertical velocities for the data collection period for Kodiak at Cliff Point.

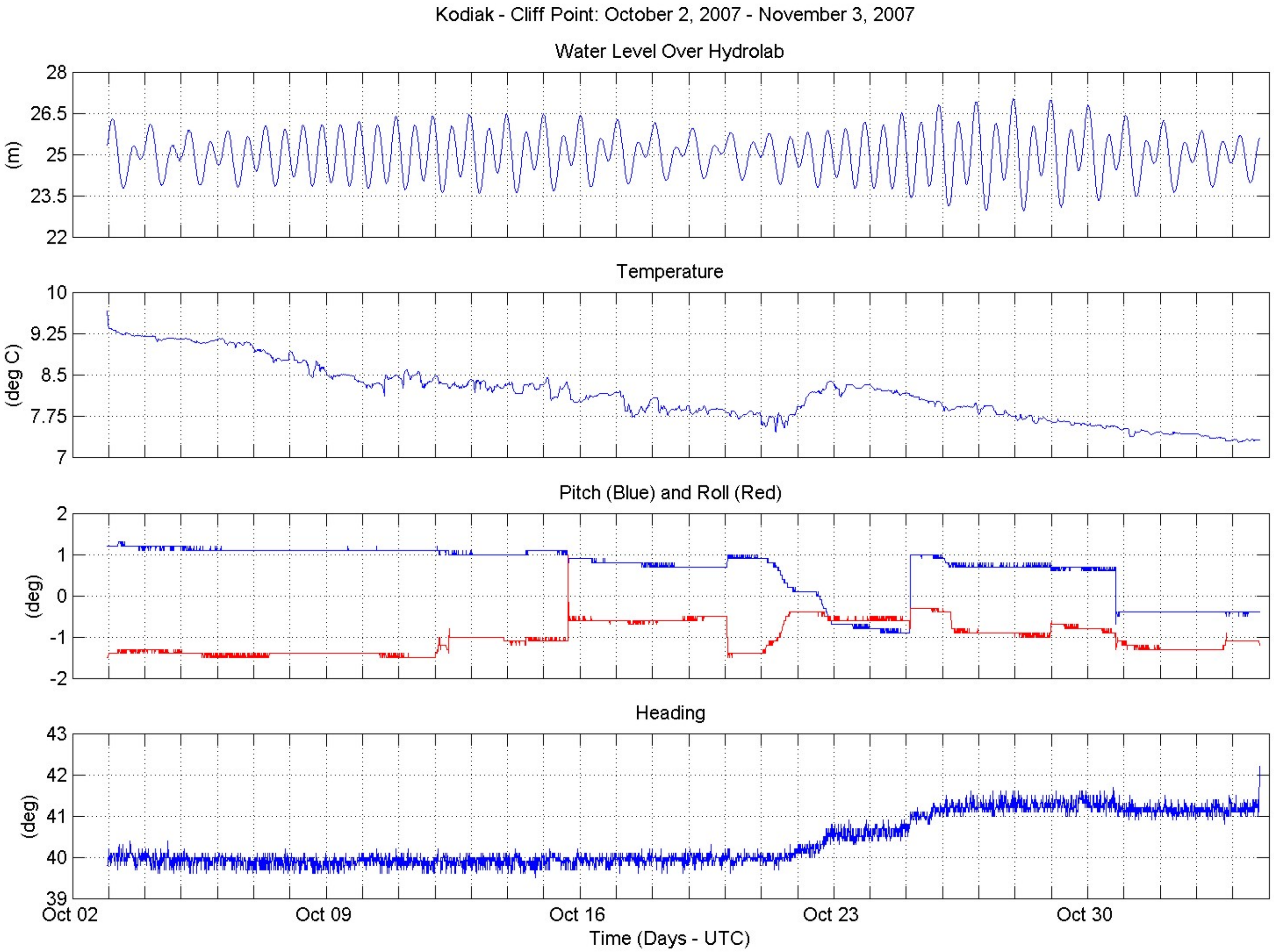

Figure A-19 Water level, water temperature, pitch, roll, and heading for Cliff Point ADCP.

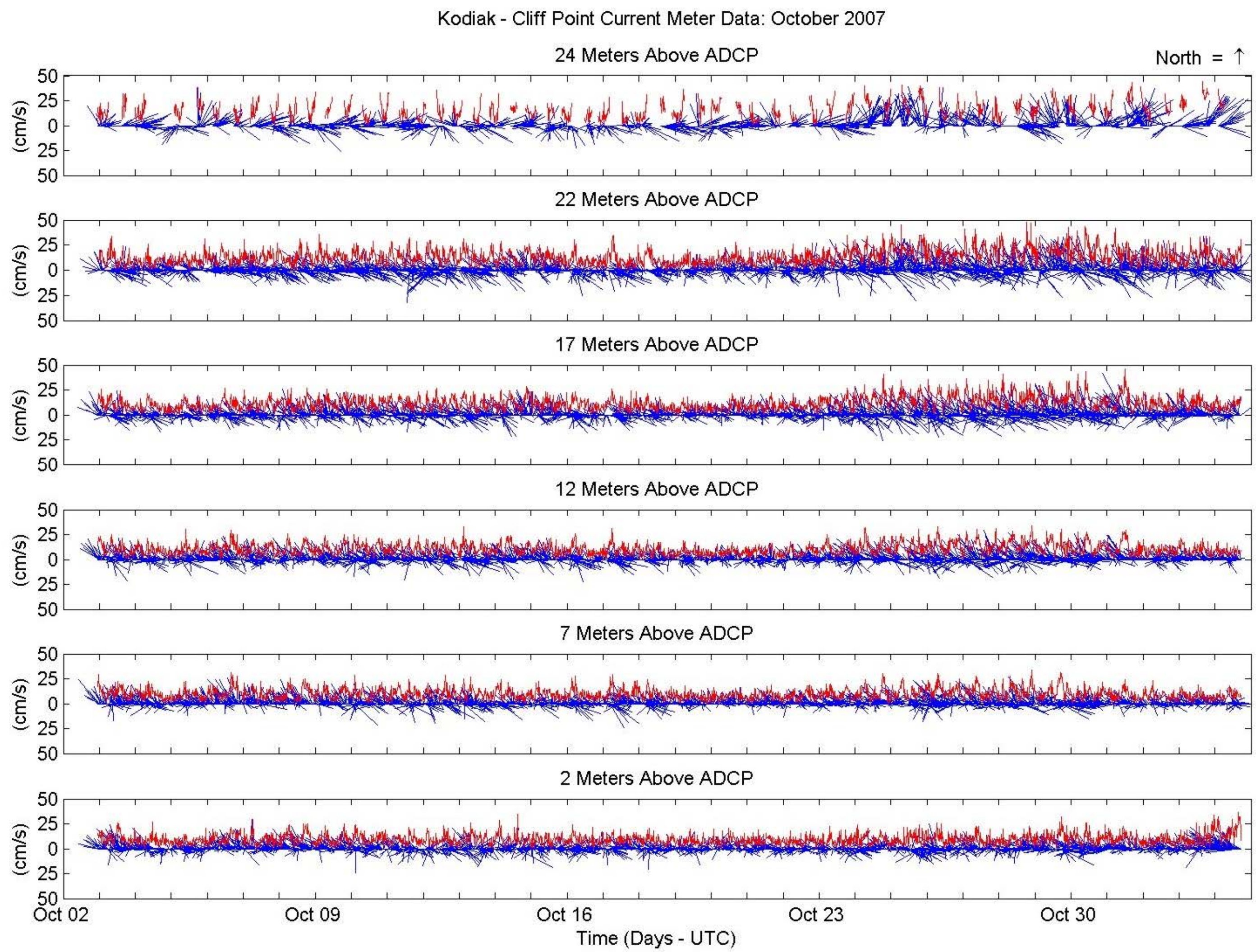

Figure A-20 Current meter vectors for October at Cliff Point, Kodiak for various depths.

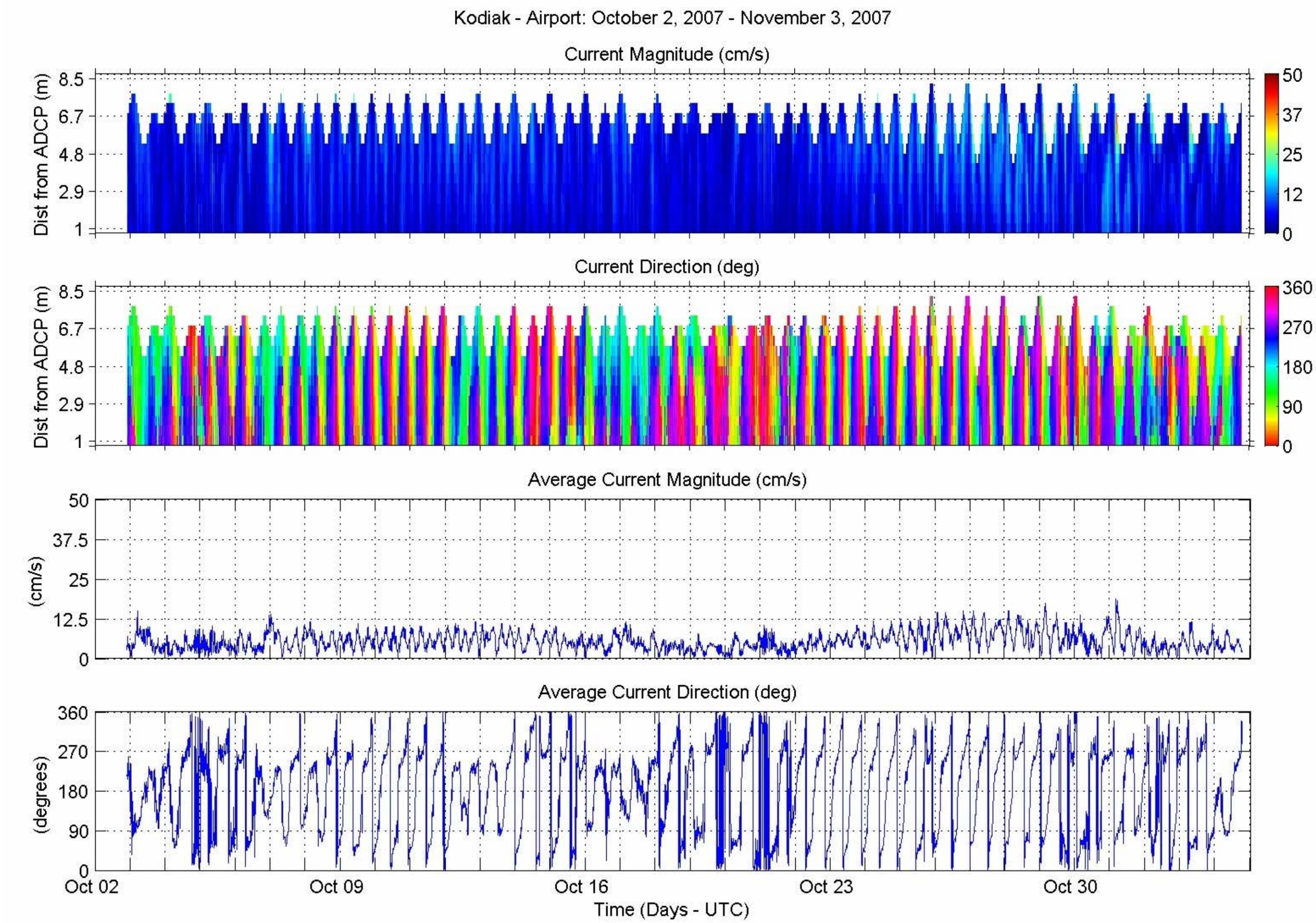

Figure A-21 Summary of ADCP velocities for the data collection period for Kodiak at airport site: Scale 50 cm/s.

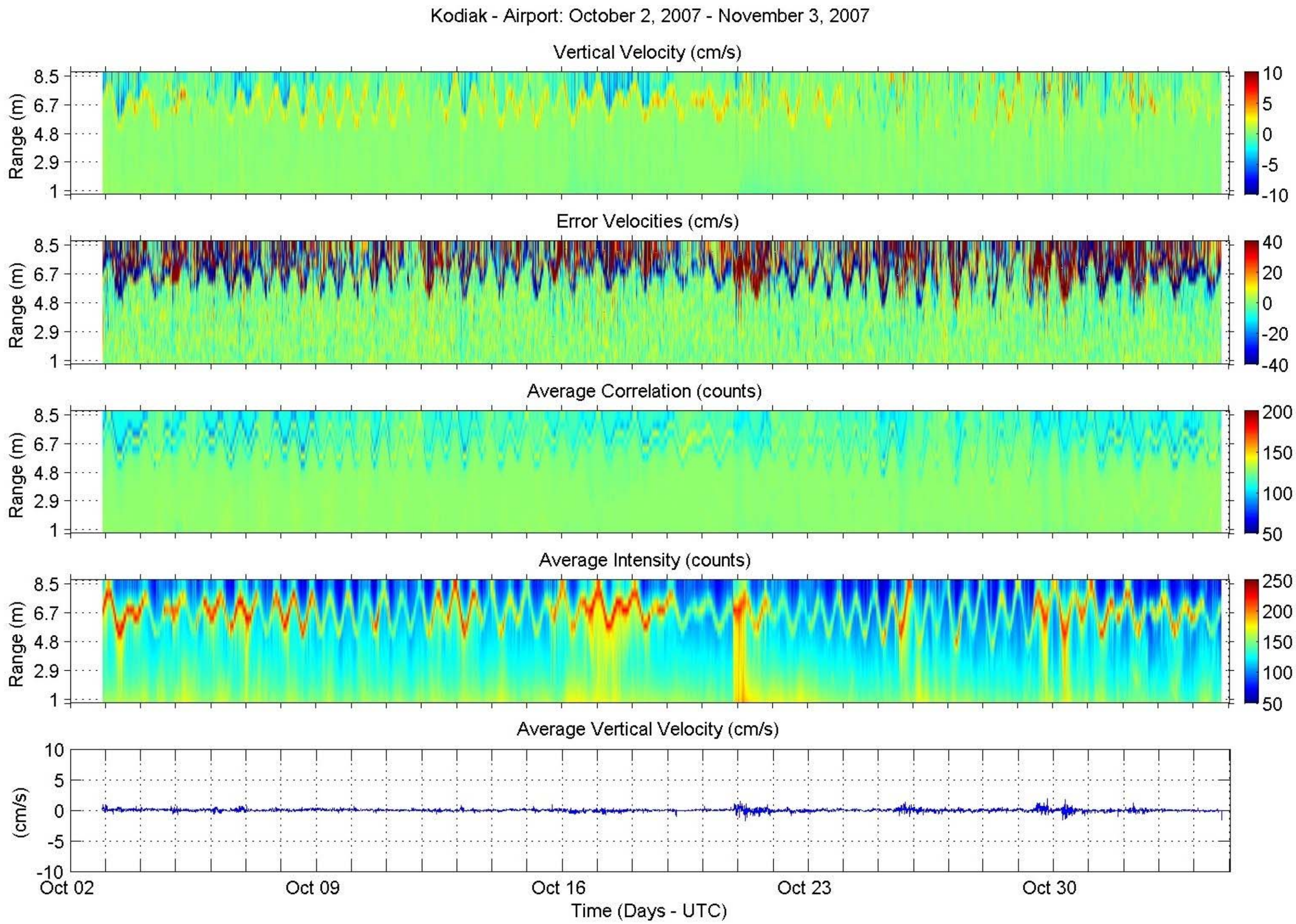

Figure A-22 Summary of ADCP average vertical velocities for the data collection period for Kodiak at airport site.

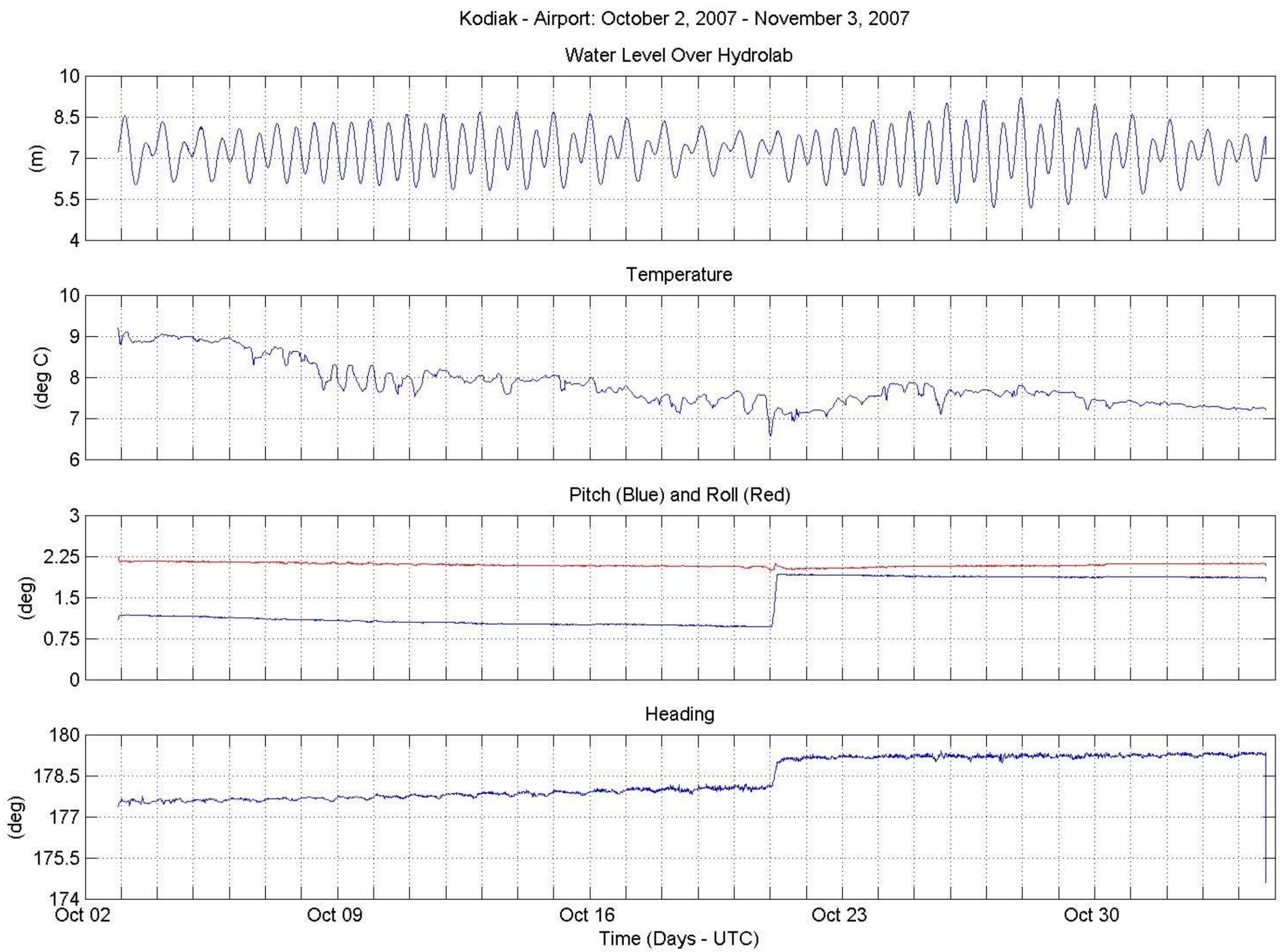

Figure A-23 Water level, water temperature, pitch, roll, and heading for airport site ADCP.

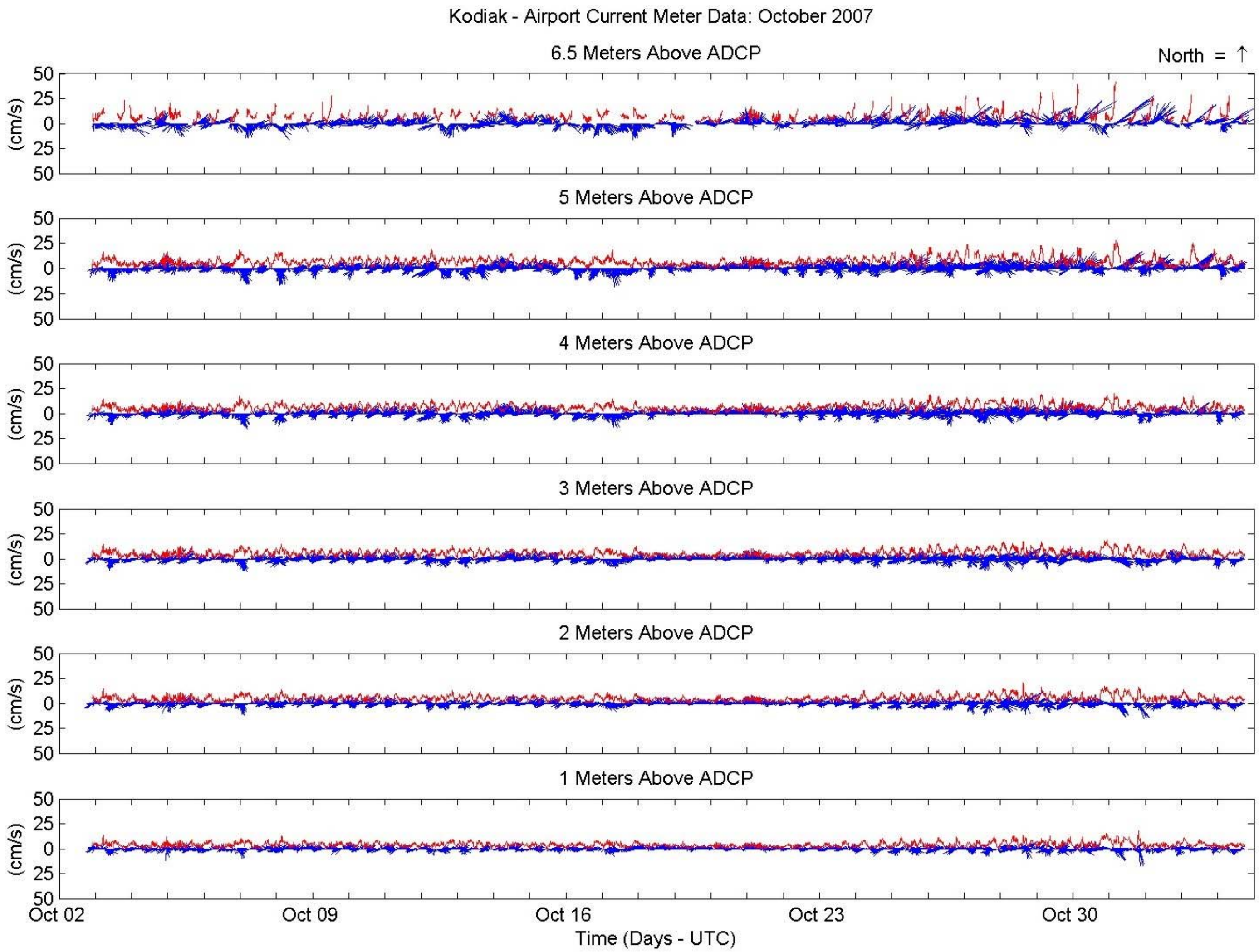

Figure A-24 Current meter vectors for October at airport site, Kodiak for various depths.

COASTLINE ENGINEERING
5900 Lynkerry Circle • Anchorage Alaska 99504 • (907) 338-6626

SUPPLEMENTAL COASTAL MODELING MEMO

Modeling information for 3 new alternatives is included herein.

Modeling of New Alternatives

The Buskin River contributes freshwater to the marine system within the project area. Other than biota that might not be tolerant to freshwater, no substances from the Buskin have been identified as toxic. Three additional alternatives were modeled to examine the extent that the salinities in the project area are lowered even for short time durations. To examine the latest alternative, the computer model was run in the 3-dimensional mode. It was suggested that this would provide a higher degree of realism to the outcomes. The final result is then presented as the vertically-averaged salinity. The new alternatives are presented below.

- RW 7/25 extended 1,000 feet to the east and RW 18/36 extended 600 feet to both the north and south
- RW 7/25 extended 600 feet to the east and RW 18/36 extended 300 feet to both the north and south
- RW 7/25 extended 600 feet to the east and RW 18/36 extended 600 feet to the south

For comparison, the base case was also run in the 3-D mode.

Each alternative is shown below in a separate frame as it appears in the modeling grid.

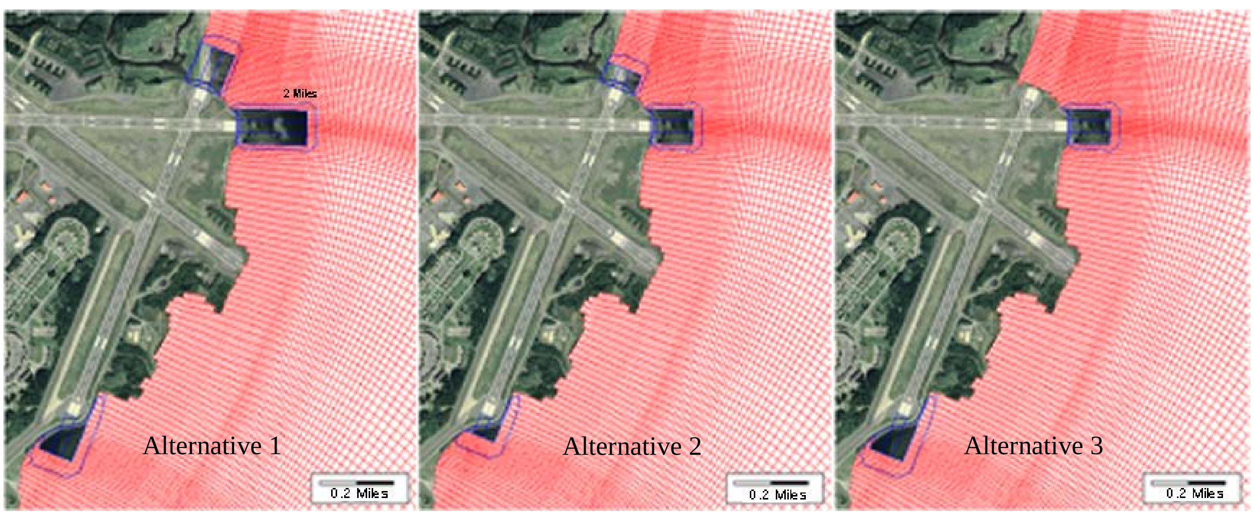

Each of these alternatives was modeled with the 3-D model and the geographic extent of the vertically-averaged salinity was documented. The tidal, current, and wind conditions were the same as those used in the earlier modeling. The discharge from the Buskin River was assumed to be fresh (salinity = 0 parts per thousand—ppt) and the ambient salinity was assumed to be 35 ppt. This is higher than the true ambient water salinity, but the exact value should not affect the results of this comparison. We are primarily looking at the dilution of the ambient waters not their precise value.

The following figure represents the model results superimposed on a Google image. The various alternatives are also shown on that image. Each extension shows a short and a long version which will be shown separately in following images.The image shows three sets of four lines. The three sets are at progressively further distances from the shore and represents salinity contour lines of 20, 25, and 30-ppt with the furthest from shore being the largest salinity—30 ppt. Within each set one of the lines represents the existing condition and each of the other three represents one of the alternatives.

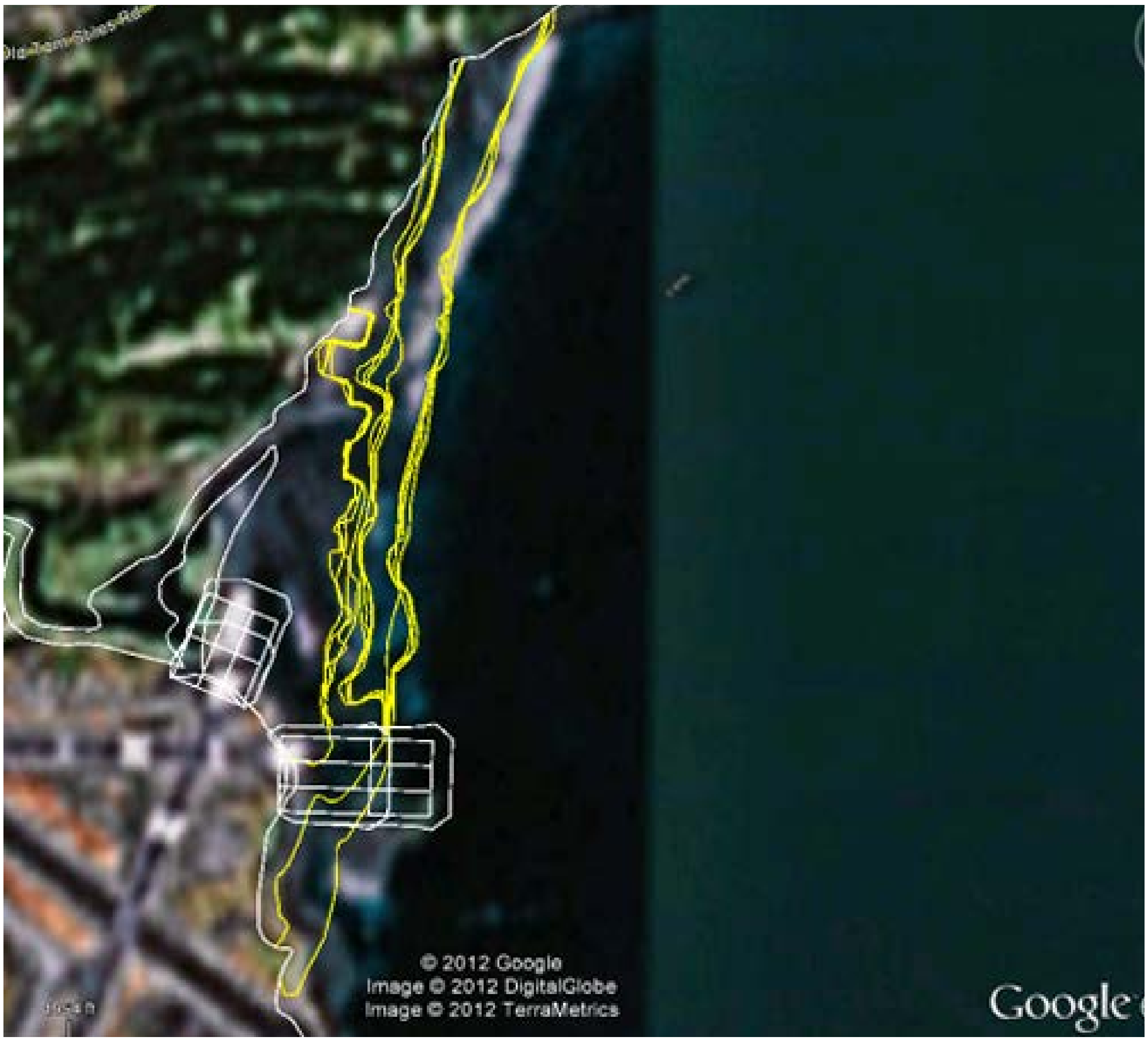

Figure 1 This shows a Google image of the 3 sets of salinity contours (20, 25, and 30 ppt) for the existing conditions plus the 3 alternatives described above.

It is immediately clear that each of the alternatives creates only a minor change in the distribution of these three salinity contours in comparison to the contour for the existing condition. The three contours for the existing condition are the ones that appear to go through some or all of the eastward extension of RW 7/25. These contours will be examined individually in the following sections for each alternative.

Existing Condition

In this case there are no extensions off the ends of any runways. The maximum areal extent for the Buskin River discharge modeled during May (215 cfs) is shown in Figure 2.

Figure 2 Maximum extent of the 20, 25, and 30 ppt salinity contours during the modeled period for the existing condition.

The effect of the Buskin River freshwater as represented by a reduction in salinity is seen nearly 2,000 feet south of RW 7/25.

Alternative 1—RW 7/25 Extended 1,000 Feet to the East and RW 18/36 Extended 600 Feet to Both the North and South

Figure 3 Maximum extent of the 20, 25, and 30 ppt salinity contours during the modeled period for Alternative 1.

For this alternative no significant freshwater extends beyond the RW 7/25 extension. The southern extension from RW 36 is not shown to increase the resolution in the area affected by the Buskin River freshwater.

Alternative 2—RW 7/25 Extended 600 Feet to the East and RW 18/36 Extended 300 Feet to Both the North and South

Figure 4 Maximum extent of the 20, 25, and 30 ppt salinity contours during the modeled period for Alternative 2.

As with Alternative 1, no significant freshwater extends south of the RW 7/25 extension.

Alternative 3—RW 7/25 Extended 600 Feet to the East and RW 18/36 Extended 600 Feet to the South

Figure 5 Maximum extent of the 20, 25, and 30 ppt salinity contours during the modeled period for Alternative 3.

As with the previous 2 alternatives, no significant freshwater from the Buskin River is seen south of the RW 7/25 extension.

Conclusion

Three additional extension alternatives have been investigated through modeling. The model was run in the 3-D mode using 3 distinct layers each representing a third of the water depth; therefore, if the water was 3 feet deep each layer would be 1 foot deep, and if the water was 6 feet deep then each layer would be 2 feet deep.

The extent is represented by salinity contour lines that show the maximum distance from the mouth of the Buskin River during the 31-day modeling duration. The contour lines are the vertically averaged salinity as determined by averaging the values for each of the three layers at each grid node.

The mixing occurs quickly as the Buskin River water enters the marine water in the project area. The contours were based on the assumption that the marine water has a salinity of 35 parts per thousand. However, the actual marine water is diluted by freshwater runoff along much of the Alaskan coast and is between 32 and 33 ppt. The contours can be thought of as differential differences rather than absolute values. So the 30 ppt contour can be visualized as the point where the salinity would be 5 ppt less than the original marine water value and the 20 ppt line would represent a difference of 15 ppt less.

It is clear from the figures that no significant amount of freshwater is present south of any of the eastward extensions on RW 7/25. Minor amounts of freshwater color effects could be found south, but the vertically averaged salinity would be only slightly less than the original marine water. Since winds are responsible for much of the water transport in the project area, there could be significant differences in salinity between the top and bottom of the water column.